



This document was produced
by scanning the original publication.

Ce document est le produit d'une
numérisation par balayage
de la publication originale.

GEOLOGICAL SURVEY OF CANADA
ECONOMIC GEOLOGY REPORT 38

THE MINERALOGY AND GEOCHEMISTRY OF THE HEMLO GOLD DEPOSIT, ONTARIO

D.C. Harris



Energy, Mines and
Resources Canada

Énergie, Mines et
Ressources Canada

Canada

THE ENERGY OF OUR RESOURCES

THE POWER OF OUR IDEAS

GEOLOGICAL SURVEY OF CANADA
ECONOMIC GEOLOGY REPORT 38

**THE MINERALOGY AND GEOCHEMISTRY
OF THE HEMLO GOLD DEPOSIT,
ONTARIO**

D.C. Harris

1989

© Minister of Supply and Services Canada 1989
Available in Canada through
authorized bookstore agents and other bookstores
or by mail from

Canadian Government Publishing Centre
Supply and Services Canada
Ottawa, Canada K1A 0S9

and from

Geological Survey of Canada offices:

601 Booth Street
Ottawa, Canada K1A 0E8

3303-33rd Street N.W.,
Calgary, Alberta T2L 2A7

A deposit copy of this publication is also available for reference
in public libraries across Canada

Cat. No. M43-38/1989E
ISBN 0-660-13269-9

Price subject to change without notice

Cover description:

Aerial view looking west of the Hemlo gold mines adjacent to Trans-Canada Highway #17. Photo taken in 1985 by George Patterson, Ministry of Northern Development and Mines, Thunder Bay. Inset: Photograph of a regular-stibnite-rich boudinaged quartz vein specimen from the Page-Williams mine.

Critical readers:

R.I. Thorpe
E.M. Cameron

Original manuscript submitted—1988-11-07
Final version approved for publication—1989-02-01

CONTENTS

1	Abstract/Résumé
2	Summary/Sommaire
6	Introduction
6	Size and grade of the Hemlo Deposit
7	Regional geology
8	Samples and methods of investigation
8	Mineralogy
8	General mineralogy
16	Detailed ore mineralogy
16	Pyrite
17	Molybdenite
17	Sphalerite
18	Gold minerals
19	Pyrrhotite
19	Chalcopyrite
19	Galena
19	Stibnite
20	Tetrahedrite and Tennantite
20	Arsenic minerals
21	Mercury minerals
21	Thallium minerals
22	Sulphosalt minerals
22	Telluride minerals
22	Rare ore minerals
23	Sparse ore minerals
23	Oxide mineralogy
23	Rutile
23	Barian tomichite
24	Hemloite
24	Magnetite, hematite, ilmenite, chromite
24	Lewisite
25	Gangue mineralogy
25	Detailed gangue mineralogy
25	Barite
25	Feldspar
26	Micas
26	Accessory gangue minerals
27	Geochemical features
27	Mineral distribution
27	The David Bell mine
34	The Golden Giant mine
45	The Page-Williams mine
62	The Page-Williams "C" zone
63	The Golden Sceptre Resources property
64	Alteration
64	Origin of mineralization
68	Acknowledgments
68	References

Tables

- 10 1. The minerals in the main Hemlo gold deposit
- 19 2. Specimens containing aurostibite
- 28 3. Elemental listing of minerals and their relative abundance in the Hemlo deposit
- 28 4. Distribution of elements in four drill cores from the Hemlo deposit

Appendices

- 71 A. Microprobe analyses of minerals in the Hemlo gold deposit
- 83 B. Location of drill core specimens collected from the Hemlo deposit
- 84 C. Geochemical data

Figures

- 7 1. Location map for the Hemlo deposit.
- 8 2. Aerial view looking west of the Hemlo gold mines.
- 9 3. Geological map of the Hemlo area.
- 12 4. Vertical longitudinal section showing the property boundaries, the ore zones and location of the sampled drill holes.
- 13 5. Vertical longitudinal section showing the distribution of the mercury minerals.
- 14 6. Vertical longitudinal section showing the distribution of barite.
- 15 7. Electron backscattered images of zoned barian microcline feldspar.
- 16 8. (a). Photograph of a polished specimen showing the banded nature of the pyrite-rich ore. (b). Photomicrograph of coarse anhedral pyrite in silicate matrix. (c). Photomicrograph of coarse anhedral pyrite associated with molybdenite and rutile in silicate matrix. (d). Photomicrograph of ore containing pyrite partially replaced by pyrrhotite, magnetite and molybdenite.
- 17 9. (a). Photomicrograph of a molybdenite-rich specimen with anhedral coarse pyrite. (b). Photomicrograph of slightly oriented molybdenite flakes with fine grained pyrite in a quartz-microcline-muscovite matrix.
- 18 10. Profile of mercury contents in sphalerite across the ore zone within drill hole W70.
- 18 11. Photomicrograph of native gold rimmed with native arsenic.
- 20 12. (a). Photomicrograph of coarse stibnite with fine inclusions of realgar adjacent to a parapirotite grain that contains inclusions of coarse aurostibite and fine native antimony. (b). Radial cluster of native arsenic grains in quartz.
- 24 13. (a). Photomicrograph of barian tomichite with aligned molybdenite flakes in a silicate matrix. (b). Photomicrograph of barian tomichite with alteration rim of titanite in contact with coarse stibnite and pyrite.
- 25 14. Photograph of a polished slab of barite-rich ore from the Golden Giant orebody.
- 29 15 - 77. Plots of mineral distribution and elemental data for various drill holes.
- 65 78. Photomicrograph of filaments or veinlets of native gold in hessite in contact with fractured pyrite.
- 65 79. Electron backscattered image of barian microcline showing also fine inclusions of barite and pyrite interstitial to the microcline grains.

THE MINERALOGY AND GEOCHEMISTRY OF THE HEMLO GOLD DEPOSIT, ONTARIO

Abstract

The Hemlo gold deposit, discovered in 1982, is located near the northeast shore of Lake Superior, 35 km east of Marathon, Ontario, adjacent to Trans-Canada Highway 17. The deposit is of Archean age and occurs at the contact of felsic metavolcanics and pelitic metasediments. It consists of several mineralized zones, of which the main zone extends for a length of 2900 m, for a distance of 2500 m down-dip and ranges in thickness from 3 to 45 m. This zone contains at least 80 million tonnes of ore with an average grade of 7.7 g/t Au. Three properties covering portions of the deposit are in production, i.e. from east to west, the David Bell mine, the Golden Giant mine and the Page-Williams mine.

The gold ore is substantially enriched in Mo, V, As, Sb, Hg, Tl and Ba and contains a diverse assemblage of minerals. A total of 81 minerals have been identified in the deposit, of which three are new species, named criddleite, vaughanite and hemloite. Also, the Hemlo deposit is the first Canadian locality for several other minerals. Native gold is the principal gold mineral. It occurs as free grains, between 1 and 20 μm , in gangue and is mercury-rich, with as much as 26.9 wt. % Hg. The ore zone is pyrite-rich and is characterized by the presence of molybdenite, green vanadian muscovite, a V-Sb-W-bearing rutile, barian microcline and in places, major barite. The principal mercury minerals, cinnabar and aktashite; the thallium minerals routhierite and parapierrroite and the arsenic mineral realgar are restricted to the central portion of the deposit. Telluride minerals are rare. Other common ore minerals are stibnite, tetrahedrite-tennantite, mercury-bearing sphalerite (up to 29.5 wt. % Hg), several sulphosalts of the lead sulphantimonide variety and arsenopyrite. Tomichite, a rare oxide mineral previously known only in the "green leader" gold lodes at Kalgoorlie, Western Australia is a sparse mineral in the ore. Barite is a major constituent in both the Golden Giant and Page-Williams orebodies, with some parts containing up to 70%. In some barite-rich sections, angular fragments of ore are contained within the baritic matrix and only where sufficient ore fragments are present is the rock of ore grade. Barian microcline is the second major barium mineral.

Potassic alteration is evident throughout the deposit and has produced abundant barian microcline, and white mica that is most abundant in the felsic rocks, but which is also developed in the sedimentary rocks adjacent to the ore. Structural studies by other investigators have suggested that the gold-bearing rocks occupy the most intensely deformed, central portion of a large scale, wide ductile zone of oblique thrusting closely related to the Lake Superior shear. The ore minerals were formed from hydrothermal fluids that may in part be related to the shear zone.

Résumé

Le gisement aurifère d'Hemlo, découvert en 1982, est situé à proximité de la rive nord-est du lac Supérieur, à 35 km à l'est de Marathon (Ontario), près de la Transcanadienne (route 17). Le gisement est d'âge archéen et se trouve au contact de roches métavolcaniques felsiques et de roches métasédimentaires pélitiques. Il se compose de plusieurs zones minéralisées. La principale fait 2900 m de long, soit 2500 m en aval-pendage; son épaisseur varie de 3 m à 45 m. Cette zone contient au moins 80 millions de tonnes de minerai d'une teneur moyenne en Au de 7,7 g/t. Trois propriétés occupant des parties du gisement sont actuellement exploitées; il s'agit, de l'est à l'ouest, des mines David Bell, Golden Giant et Page-Williams.

Le minerai d'or est très riche en Mo, V, As, Sb, Hg, Tl et Ba et contient une association variée de minéraux. On a pu identifier 81 minéraux dans le gisement, dont trois sont de nouvelles espèces, à savoir la criddleite, la vaughanite et l'hémloïte. En outre, le gisement d'Hemlo est le gîte canadien le plus important pour plusieurs autres minéraux. L'or natif est le minerai d'or principal. Il se présente sous forme de grains libres, de 1 μm à 20 μm , contenus dans une gangue riche en mercure dont la teneur peut atteindre 26,9 % en masse. La zone minéralisée est riche en pyrite et est caractérisée par la présence de molybdénite, de muscovite verte vanadiée, de rutile riche en V-Sb-W, de microcline barytique et, par endroits, de grandes quantités de barytine. Les principaux minerais de mercure, le cinabre et l'aktashite, ceux de thallium, la routhiérite et la parapierrroite, et celui d'arsenic, le réalgar, sont confinés à la partie

centrale du gisement. Le gisement renferme très peu de tellurures. Les autres minéraux de base sont la stibine, la tétraédrite-tennantite, la sphalérite riche en mercure (jusqu'à 29,5 % de Hg en masse), plusieurs sulphosels de la variété sulpho-antimoniure de plomb et l'arsénopyrite. La tomichite, oxyde rare repéré auparavant uniquement dans les filons aurifères du "filon guide vert" à Kalgoorlie, dans l'ouest de l'Australie, se manifeste en petites quantités. La barytine est un constituant important des deux corps minéralisés de Golden Giant et de Page-Williams qui par endroits en renferment jusqu'à 70 %. Dans certaines sections riches en barytine, des fragments anguleux de minerai se trouvent dans une gangue barytique, et la roche ne présente de teneur commerciale qu'aux endroits où des fragments de minerai sont présents en quantités suffisantes. La microcline barytique est le deuxième minerai de baryum en importance.

L'altération potassique est manifeste dans tout le gisement et a produit beaucoup de microcline barytique et du mica blanc abondant surtout dans les roches felsiques, mais présent aussi dans les roches sédimentaires contiguës au minerai. Des études structurales effectuées par d'autres chercheurs semblent indiquer que les roches aurifères occupent la partie centrale, la plus fortement déformée, d'une grande et large zone ductile de charriage oblique étroitement liée au cisaillement du lac Supérieur. Les minéraux métalliques ont été formés à partir de fluides hydrothermaux qui peuvent être en partie associés à la zone de cisaillement.

SUMMARY

The main ore zone of the Hemlo gold deposit is a single orebody that contains at least 80 million tonnes at 7.7 g/t Au. The deposit is currently being mined as three properties which are, from east to west, the David Bell mine, the Golden Giant mine and the Page-Williams mine. The ore zone is enriched in Mo, Sb, As, Hg, Tl, V and Ba. Within the ore zone, 53 ore minerals have been identified of which two have been accepted as new minerals, i.e. criddleite and vaughanite; 8 oxide minerals of which one has been accepted as a new mineral, i.e. hemolite, and 28 gangue minerals. In addition, several minerals represent the first Canadian occurrence, namely routhierite, parapirotite, aktashite, tvalchrelidzeite, galkhaite, cafarsite and barian tomichite. Native gold is the principal gold mineral, with trace amounts of gold occurring as aurostibite. Electron-microprobe analysis of the native gold reveals that it is mainly a gold-mercury-rich alloy with minor silver and contains as much as 26.9 wt. % Hg. The ore zone is characterized by the presence of molybdenite, V-Sb-W-bearing rutile and green vanadian muscovite. Pyrite is the most abundant sulphide, with the Golden Giant orebody averaging 8 wt. %. The other ore minerals account for less than 1% of the deposit and are fine grained and generally difficult to recognize. The principal mercury minerals are cinnabar and aktashite, the principal thallium minerals are routhierite and parapirotite and the principal arsenic mineral is réalgar. These minerals are closely associated and are confined to the central portion of the deposit. Within this zone are boudinaged quartz veins as much as 30 cm in width that extend from surface to the lower limits of the deposit. These quartz veins are enriched in réalgar, with coarse stibnite, cinnabar, thallium minerals, native antimony and native arsenic, and frequently contain native gold with rims of native arsenic. Sphalerite is minor, but widespread, and it contains as much as 29.5 wt. % Hg. This is the

SOMMAIRE

La principale zone minéralisée du gisement aurifère d'Hemlo est constituée d'un seul corps minéralisé qui renferme au moins 80 millions de tonnes d'une teneur en Au de 7,7 g/t. Le gisement est actuellement exploité dans trois propriétés soit, de l'est à l'ouest, les mines David Bell, Golden Giant et Page-Williams. La zone minéralisée est riche en Mo, Sb, As, Hg, Tl, V et Ba. À l'intérieur de cette zone, on a pu identifier 53 minéraux métalliques dont deux nouveaux soit la criddleite et la vaughanite; huit oxydes, dont un a été accepté comme nouveau minéral (l'hémolite), et 28 minéraux de gangue. En outre, plusieurs minéraux ont été repérés pour la première fois au Canada, à savoir la routhiérite, la parapirotite, l'aktashite, la tvalchrelidzéite, la galkhaïte, la cafarsite et la tomichite barytique. L'or natif est le principal minéral d'or; le métal précieux est aussi présent en traces sous forme d'aurostibite. L'analyse à la microsonde électronique de l'or natif révèle que ce dernier est principalement constitué d'un alliage riche en or et en mercure avec une faible quantité d'argent, et qu'il renferme jusqu'à 26,9 % de Hg en masse. La zone minéralisée est caractérisée par la présence de molybdénite, de rutile riche en V-Sb-W et de muscovite vanadiée verte. La pyrite est le sulfure le plus abondant et atteint une teneur moyenne de 8 % en masse dans le corps minéralisé de Golden Giant. Les autres minéraux métalliques comptent pour moins de 1 % du gisement; ils sont à grain fin et sont généralement difficiles à reconnaître. Les principaux minerais de mercure, soit le cinabre et l'altashite, ceux de thallium, soit la routhiérite et la parapirotite et celui d'arsenic, le réalgar, sont étroitement associés et se trouvent confinés à la partie centrale du gisement. Dans cette zone, on trouve des veines de quartz boudinées qui atteignent 30 cm de large et qui s'étendent de la surface jusqu'aux limites inférieures du gisement. Ces veines sont riches en réalgar et renferment sous forme grossière de la stibine, du cinabre, des minerais de thallium, de l'antimoine natif; on y trouve en outre, souvent, de l'or natif auréolé d'arsenic natif. La sphalérite se manifeste en faibles quantités, mais est largement répandue et renferme jusqu'à 29,5 % de Hg en masse. La documentation publiée sur la sphalérite ne fait état que d'une seule teneur plus élevée en mercure. La stibine est le principal minéral d'antimoine et se reconnaît facilement dans les échantillons que l'on peut

second highest mercury content recorded in the literature for sphalerite. Stibnite is the principal antimony mineral and is readily visible in hand specimens. Several sulphosalts of the lead sulphantimonide variety have been identified, of which zinkenite is the most common and widespread. Tetrahedrite and tennantite are both widespread and are the principal silver-bearing minerals. Tennantite is more common in the lower levels of the Page-Williams mine, particularly in the northwest down-plunge extension. This portion of the deposit is mineralogically different, in that sphalerite (with low to not detected mercury), galena (nearly absent in other parts of the deposit), chalcopyrite, native gold (with as much as 29.1 wt. % Ag) and tellurides (altaite, calaverite and petzite, which are nearly absent throughout the deposit), are the principal ore minerals.

The principal oxide mineral in the deposit is rutile and within the main ore zone, it contains as much as 5.6 wt. % V_2O_3 , 6.5 wt. % Sb_2O_3 and 3.2 wt. % WO_2 . The V-Sb-W-bearing rutile appears to define the ore zone. A search of the literature has failed to find a reference to the substitution of V, Sb and W in rutile. Barian tomichite is the second most common oxide mineral, although it is sparse and occurs mainly within the core of the deposit. Tomichite is a rare mineral that was first reported from the "green leader" gold lodes at Kalgoorlie, Western Australia associated with green vanadian muscovite (Nickel, 1977).

The ore host rock in the eastern portion of the deposit (the David Bell mine) and in the upper levels of the adjacent Golden Giant mine is a biotite-rich schist and/or felsic, quartz-feldspar porphyritic rock. Within this portion of the deposit, plagioclase, tremolite and hornblende occur in narrow intervals. These rocks pass transitionally into a muscovite schist and/or feldspathic rock to the west and down-dip. The feldspathic rock contains barite as a major constituent, with associated quartz, barian microcline (with as much as 9.5 wt. % BaO), muscovite, green vanadian muscovite (with as much as 8.5 wt. % V_2O_3) and sparse albite. Carbonates are sparse in the deposit. Kyanite and staurolite are present in the metasedimentary hanging wall rocks and within parts of the ore zone. The presence of these minerals has led some researchers to suggest an amphibolite facies of metamorphism for the deposit. Feldspar porphyry sills (dykes?) and intermediate to mafic dykes have intruded the ore.

Barite, as noted above, is a major constituent in the feldspathic rock that occurs principally within the Page-Williams mine and the lower levels of the Golden Giant mine. It is nearly absent in the eastern portion of the deposit. In places, the barite-rich ore has a fragmental nature with ore-bearing siliceous fragments contained within a barite matrix. Barite is most abundant in the central portion of the deposit where the ore widths are as much as 45 m, and some intervals contain as much as 70% barite. Barite occurs interstitial to the silicate

manipuler. On a pu identifier plusieurs sulphosels de la variété sulpho-antimoniure de plomb, dont la zinkénite est le plus commun et le plus répandu. La tétraédrite et la tennantite sont toutes deux répandues et constituent les principaux minéraux argentifères. La tennantite se retrouve plus fréquemment dans les niveaux inférieurs de la mine Page-Williams, particulièrement dans le prolongement nord-ouest en aval-pendage. Cette partie du gisement est minéralogiquement différente, car la sphalérite (avec une teneur faible à non détectée de mercure), la galène (presque absente dans d'autres partie du gisement), la chalcopyrite, l'or natif (contenant jusqu'à 29,1 % d'Ag en masse) et les tellurures (l'altaïte, la calavérite et la petzite, qui sont presque absentes ailleurs partout dans le gisement), y constituent les principaux minéraux métalliques.

Le principal oxyde du gisement, soit le rutile renferme, en masse, jusqu'à 5,6 % de V_2O_3 , 6,5 % de Sb_2O_3 et 3,2 % de WO_2 dans la zone minéralisée principale. Le rutile riche en V-Sb-W semble délimiter la zone minéralisée. Une recherche bibliographique n'a pas permis de trouver de référence se rapportant à la substitution du V, du Sb et du W dans le rutile. La tomichite barytique est l'oxyde le plus commun après la rutile, bien qu'elle soit peu abondante et qu'elle se manifeste surtout au sein du noyau du gisement. La tomichite est un minéral rare qu'on a signalé pour la première fois dans des filons d'or du "filon guide vert" de Kalgoorlie, dans l'ouest de l'Australie, où il est associé à une muscovite vanadiée verte (Nickel, 1977).

La roche hôte du minerai, dans la partie est du gisement (la mine David Bell) et dans les niveaux supérieurs de la mine Golden Giant contiguë est un schiste riche en biotite ou une roche porphyrique, de nature felsique, à quartz et feldspath. Dans cette partie du gisement, on rencontre un plagioclase, de la trémolite et de la hornblende au sein d'intervalles étroits. Ces roches passent latéralement et d'une façon progressive à un schiste à muscovite ou à une roche feldspathique à l'ouest et en aval-pendage. La roche feldspathique renferme de la barytine comme composant principal, associée à du quartz, à de la microcline barytique (contenant jusqu'à 9,5 % de BaO en masse), à de la muscovite, à de la muscovite verte vanadiée (renferment jusqu'à 8,5 % de V_2O_3 en masse) et à un peu d'albite dispersée. Les roches carbonatées sont peu abondantes dans le gisement. On trouve de la cyanite et de la staurolite dans les roches métasédimentaires du toit et dans certaines parties de la zone minéralisée. D'après certains chercheurs, le présence de ces minéraux semble indiquer que le métamorphisme dans le gisement a atteint le faciès des amphibolites. Des filons-couches (dykes?) de porphyres feldspathiques et des dykes de nature neutre à mafique ont pénétré le minerai.

La barytine, comme il a été signalé antérieurement, constitue un composant important de la roche feldspathique qui occupe une place prépondérante dans la mine Page-Williams et dans les niveaux inférieurs de la mine Golden Giant. Elle est presque absente dans la partie est du gisement. Par endroits, le minerai riche en barytine est de nature détritique, et une matrice de barytine renferme des débris siliceux métallifères. Dans la partie centrale du gisement, la barytine domine et le minerai qui atteint, à cet endroit, des largeurs de 45 m renferme des intervalles où la barytine atteint la teneur de 70 %. Celle-ci occupe la position interstitielle par rapport aux minéraux silicatés, renferme très peu de minéraux métalliques et semble diluer le minerai alors qu'elle contribue en partie à en augmenter l'épaisseur.

minerals, contains very few ore minerals and appears to dilute the ore while contributing in part to the extra thickness.

Potassic alteration is evident throughout the deposit and has produced abundant microcline and white mica, both within the main ore zone and in the surrounding rocks. This alteration is most intense in the Page-Williams mine and the Golden Giant mine, but is seldom obvious in the wall rocks of the David Bell mine, although Burk et al. (1986) reported that these minerals display a spatial correlation with most of the ore zone. The footwall contact in most of the Page-Williams and Golden Giant mines is defined by a quartz-eye muscovite schist. Walford et al. (1986) and Muir (1986) related Au-Mo mineralization to potassic feldspathization of the host rocks and, although this alteration is strongest in the felsic rocks, it is also developed in the sedimentary rocks adjacent to the main ore zone. Hugon (1986) demonstrated that the gold-bearing rocks occupy the most intensely deformed, central portion of a large scale, wide ductile zone of oblique thrusting. Petrofabric analysis supports the hypothesis that the mineralizing event occurred subsequent to the attainment of peak amphibolite metamorphism. The occurrence of cinnabar, realgar, tetrahedrite, stibnite, arsenopyrite, sphalerite and native arsenic in a kyanite-bearing muscovite schist in drill hole W104 and their textural relationships with the kyanite as noted in this study, tend to support Hugon's observations that the ore minerals formed after peak metamorphism. The close association of gold with molybdenite, green vanadian muscovite, V-Sb-W-bearing rutile and the potassic alteration that has resulted in the formation of barian microcline in spatial association with ore, and the mineralogical similarities of the main zone to the stratigraphically lower gold-bearing zones all suggest that potassium metasomatism was an integral part of the ore-forming process.

The intense tectonic deformation of the deposit, together with its complex suite of minerals, makes Hemlo a unique gold deposit. It is interesting to compare some of the mineral assemblages to other worldwide occurrences. Thallium minerals are sparse in the Hemlo deposit, but these minerals are rare species. Two localities already discussed in the paper are the Allchar deposit, Yugoslavia and the Jas Roux (Hautes Alpes) in France. Other occurrences are the Carlin gold deposit, Nevada where lorandite, $TlAsS_2$ and carlinite, Tl_2S occur with realgar and orpiment in barite veinlets cutting carbonaceous limestone of Tertiary Age (Radtke et al., 1974; Radtke and Dickson, 1975); at the Rambler mine, Wyoming where lorandite is associated with realgar, orpiment, pyrite and barite (Rogers, 1912) and at the famous Lengenbach locality at Binnatal, Switzerland where the Tl-As-S minerals lorandite and imhofite; the Pb-Tl-As-S minerals, hutchinsonite, hatchite and wallisite occur with a variety of sulphosalt and sulphide minerals replacing dolomite beds. Weissberg (1969) has found thallium, gold, arsenic, antimony and mercury in

L'altération potassique est manifeste dans tout le gisement et a donné naissance à d'importantes quantités de microcline et de mica blanc, à la fois dans la zone minéralisée principale et dans les roches avoisinantes. Cette altération est plus intense dans les mines Page-Williams et Golden Giant, et rarement évidente dans les roches encaissantes de la mine David Bell, bien que Burk et coll. (1986) aient signalé que ces minéraux font preuve d'une corrélation spatiale avec la majeure partie de la zone minéralisée. Le contact du mur de la majeure partie des mines Page-Williams et Golden Giant est défini par un schiste à muscovite et à quartz ocellé. Walford et coll. (1986) et Muir (1986) ont associé la minéralisation en Au et Mo à la feldspathisation potassique des roches hôtes et, bien que cette altération soit la plus poussée dans les roches felsiques, elle se manifeste aussi dans les roches sédimentaires contiguës à la zone minéralisée principale. Hugon (1986) a montré que les roches aurifères occupent la partie centrale la plus fortement déformée d'une grande et large zone ductile de charriage oblique. La pétrographie structurale appuie l'hypothèse selon laquelle la minéralisation est postérieure au maximum du métamorphisme à faciès des amphibolites. La présence de cinabre, de réalgar, de tétraédrite, de stibine, d'arsénopyrite, de sphalérite et d'arsenic natif dans un schiste à muscovite riche en cyanite, dans le trou de sonde W104, ainsi que les relations structurales de ces minéraux avec cette dernière, comme on l'a fait remarquer dans la présente étude, ont tendance à appuyer les travaux de Hugon qui prétend que les minéraux métalliques se sont formés après le maximum de la phase de métamorphisme. L'association étroite d'or à de la molybdénite, à de la muscovite verte vanadiée, à du rutile riche en V-Sb-W et à l'altération potassique qui a eu comme résultat la formation de microcline barytique associée dans l'espace avec le minerai, ainsi que les ressemblances minéralogiques de la zone principale avec les zones aurifères, stratigraphiquement inférieures, laissent toutes supposer que le métasomatisme potassique faisait intégralement partie du processus de formation du minerai.

La déformation tectonique intense du gisement, ainsi que le série complexe de minéraux qui l'accompagne, font d'Hemlo un gisement aurifère unique. Il est d'ailleurs intéressant de comparer certaines associations minérales avec d'autres manifestations semblables dans le monde. Les minerais de thallium sont peu abondants dans le gisement d'Hemlo, mais il s'agit d'espèces rares. Deux emplacements, étudiés dans le présent document, sont le gisement d'Allchar en Yougoslavie et celui de Jas Roux (Hautes Alpes) en France. On peut aussi mentionner le gisement aurifère de Carlin, au Nevada, qui se caractérise par la présence de lorandite, $TlAsS_2$ et de carlinite, Tl_2S , accompagnées de réalgar et d'orpiment dans des veinules de barytine traversant un calcaire carbonneux d'âge tertiaire (Radtke et coll., 1974; Radtke et Dickson, 1975); la mine de Rambler, au Wyoming, où la lorandite est associée à du réalgar, à de l'orpiment, à de la pyrite et à de la barytine (Rogers, 1972); et l'emplacement célèbre de Lengenbach à Binnatal, en Suisse, où les minerais de Tl-As-S sont de la lorandite et de l'imhofite; les minerais de Pb-Tl-As-S, à savoir la hutchinsonite, la hatchite et la wallisite, se manifestent en association avec divers sulfosels et sulfures remplaçant des lits de dolomite. Weissberg (1969) a trouvé du thallium, de l'or, de l'arsenic, de l'antimoine et du mercure dans des calcaires de précipitation de sources chaudes, le long de la marge est de la zone volcanique de Taupo en Nouvelle-Zélande. La comparaison des minerais de mercure, de thallium, d'arsenic et d'antimoine, qui se trouvent au sein de la partie central du gisement d'Hemlo, avec les calcaires de précipitation de sources

hotspring precipitates along the eastern margin of the Taupo volcanic zone, New Zealand. In comparing the mercury, thallium, arsenic and antimony minerals within the central portion of the Hemlo deposit with the New Zealand hotspring precipitates, an origin of mineralization from geothermal fluids is a strong probability as suggested by Goldie (1985), although no recognizable siliceous sinter has been found at Hemlo.

There is a close relationship between vanadium and gold at Hemlo. The occurrence of green vanadian mica, commonly referred to as roscoelite, has been reported with gold-telluride deposits in Colorado, Montana, Oregon and California, U.S.A. The famous "green leader" gold ore at Kalgoorlie, Western Australia contains a green vanadian muscovite and the rare mineral, tomichite. These two minerals also occur at Hemlo. It is not suggested that the vanadium and gold share a common origin, but that their transport and deposition most likely occurred under the same conditions. The source of the vanadium is unknown, but, to date, no systematic geochemical study of the rocks in the area has been undertaken.

The thermal stability of some minerals in the deposit indicate a relatively low temperature of ore deposition. Thermochemical data of Craig and Barton (1973) show that the upper stability of realgar is 265°C, cinnabar 345°C and orpiment 175°C. Barton's (1971) studies on the Fe-Sb-S system suggest that the assemblage pyrite+aurostibite is stable only at low temperatures (below about 125°C, but the uncertainties are large). Based on hydrothermal study of the ZnS-HgS system by Tauson and Abramovich (1980), the critical temperature for decomposition of solid solutions with the sphalerite structure has been estimated semiempirically at about 330°C. It would appear that the upper temperature range for the Hemlo ore deposition is about 300°C.

Earlier genetic models for the deposit favoured a syngenetic origin (Quartermain, 1985; Cameron and Hattori, 1985, Valliant and Bradbrook, 1986), but recent studies support an epigenetic origin of mineralization with the ore minerals being deposited from hydrothermal fluids in a structurally controlled zone that may, in part, be closely related to the Lake Superior shear zone.

However, a number of points remain unresolved. First, Cameron and Hattori (1985) show that the isotopic composition of the pyrite indicates clearly that it was derived from a fluid that contained both sulphide and sulphate and that the isotopic composition of the pyrite is strongly correlated with the gold grade. Mineralogical studies show no correlation between gold grade and pyrite. Second, barium is a component of the ore-forming fluids that resulted in the formation of barian microcline, but the barite itself appears to be later than the ore. Hence, what is the origin of the barite? Third, the timing of the mineralization is uncertain. Observations by Kuhns et al. (1986) on the

chaudes en Nouvelle-Zélande, établit qu'il est fort probable que la minéralisation se soit formée à partir de fluides géothermiques comme l'a proposé Goldie (1985), bien qu'aucun tuf siliceux reconnaissable n'ait été trouvé à Hemlo.

Il existe une relation étroite entre le vanadium et l'or à Hemlo. La présence de mica vert vanadié, connu généralement sous le nom de roscoélite, a été signalée dans des gisements d'or et tellurés au Colorado, au Montana, dans l'Oregon et en Californie, aux États-Unis. Le célèbre minerai d'or du "filon guide vert" de Kalgoorlie, dans l'ouest de l'Australie, contient une muscovite verte vanadiée et le minéral rare, la tomichite. Ces deux minéraux se manifestent également à Hemlo. On n'émet pas l'hypothèse que le vanadium et l'or ont une origine commune, mais bien que leur transport et leur sédimentation se soient produits très vraisemblablement dans les mêmes conditions. La source du vanadium est inconnue, mais, à ce jour, aucune étude géochimique systématique des roches de la région n'a été effectuée.

La stabilité thermique de certains minéraux du gisement atteste de la présence d'une température relativement faible au moment de la mise en place du minerai. Les données thermochimiques de Craig et de Barton (1973) montrent que les températures maximales de stabilité du réalgar, du cinabre et de l'orpiment sont respectivement de 265°C, 345°C et 175°C. Les études de Barton (1971) sur le système Fe-Sb-S semblent indiquer que l'association pyrite + aurostibite n'est stable qu'aux basses températures (au-dessous d'environ 125°C, mais les incertitudes sont grandes). D'après une étude hydrothermique du système ZnS-HgS par Tauson et Abramovich (1980), la température critique de décomposition de solutions solides ayant la structure de la sphalérite a été estimée d'une façon semi-empirique à environ 330°C. Il semble que la température maximale au moment de la mise en place des minerais d'Hemlo ait été d'environ 300°C.

Les premiers modèles génétiques du gisement soutenaient une origine syngénétique (Quartermain, 1985; Cameron et Hattori, 1985, Valliant et Bradbrook, 1986), mais des études récentes appuient une origine épigénétique de la minéralisation, et les minéraux métalliques auraient été déposés à partir de fluides hydrothermaux dans une zone à contrôle structural qui peut en partie être étroitement liée à la zone de cisaillement du lac Supérieur.

Il reste toutefois un certain nombre de points non résolus. Premièrement, Cameron et Hattori (1985) montrent que la composition isotopique de la pyrite indique nettement que celle-ci s'est formée à partir d'un fluide qui contenait des sulfures et des sulfates et que cette composition est en corrélation très étroite avec la concentration d'or. Des études minéralogiques montrent qu'il n'existe aucune corrélation entre la concentration d'or et la pyrite. Deuxièmement, le baryum est un composant des fluides qui sont à l'origine du minerai et qui ont donné naissance à de la microcline barytique, mais la barytine elle-même semble s'être formée plus tard que le minerai. Quelle est donc l'origine de la barytine? Troisième, le moment où la minéralisation s'est produite demeure incertain. D'après des observations faites par Kuhns et coll. (1986) sur le corps minéralisé de Golden Giant, la principale minéralisation s'est produite avant le dernier degré maximum conservé de métamorphisme ou en même temps que celui-ci. Un argument en faveur de cette théorie est la présence locale de cyanite et de sillimanite accompagnant l'or, ainsi que l'absence de rétro-morphose importante ou constante dans les unités associées au minerai. On

Golden Giant orebody, suggests that major mineralization occurred prior to or synchronous with the last preserved highest grade of metamorphism. One argument to support this view is the local occurrence of kyanite and sillimanite with gold, and no significant or consistent retrograde metamorphism of ore-related units. The association of gold with kyanite and sillimanite was also noted in this study, but associated with the gold are cinnabar and realgar. It is unlikely these minerals can be preserved in the amphibolite grade facies of metamorphism. Structural analysis by Hugon (1986) suggests that the mineralizing event is syntectonic and occurred after peak metamorphic conditions were established. Fourth, what is the relationship of the gold-molybdenite-telluride style of mineralization that occurs in fractures within the Page-Williams "C" zone and west onto the Golden Sceptre Resources property with the main ore zone that is more massive and foliated?

a en outre remarqué dans cette étude l'association de l'or avec de la cyanite et de la sillimanite, mais l'or est associé aussi à du cinabre et du réalgar. Il est peu probable que ces minéraux puissent être conservés dans la phase métamorphique correspondant au faciès des amphibolites. D'après une analyse structurale de Hugon (1986), la minéralisation est syntectonique et s'est produite après la phase de métamorphisme maximal. Quatrièmement, quelle relation y a-t-il entre, d'une part le style de minéralisation d'or, molybdénite et tellurure qui se produit dans des fractures à l'intérieur de la zone "C" de la mine Page-Williams et à l'ouest, sur la propriété de Golden Sceptre Resources, et d'autre part la zone minéralisée principale qui est plus massive et plus schisteuse?

INTRODUCTION

The Hemlo gold deposit is near the northeast shore of Lake Superior, 35 km east of Marathon, Ontario adjacent to Trans-Canada Highway (Highway 17) at latitude 48° 40' N and longitude 86° 00' W (Fig. 1). The main deposit consists of several mineralized zones which extend 2900 m in length, 1300 m in vertical height and range in thickness from 3 to 45 m. Three properties, covering portions of this single large deposit, have been brought into production within the last few years. They are, from east to west, the David Bell mine (formerly named the Teck-Corona mine) of Teck-Corona Operating Corporation, the Golden Giant mine of Hemlo Gold Mines Inc. (formerly Noranda Inc.) and the Page-Williams mine of LAC Minerals Ltd. (Fig 2). The Page-Williams mine was brought into production by LAC Minerals Ltd., but by court decision rendered in 1986 and upheld by the Supreme Court of Canada in August 1989 was awarded to Corona Corporation who have renamed it the Williams mine. The 3000 t/d mill at the Golden Giant mine was commissioned in March 1985, the David Bell mine poured its first gold on May 29, 1985, and the Page-Williams mine commenced mining operations in December 1985 from an open pit within the "A" zone.

SIZE AND GRADE OF THE HEMLO DEPOSIT

The total of published reserves for the Hemlo deposit is approximately 80 million tonnes at 7.7 g/t Au distributed as follows: The David Bell mine, 7.6 million tonnes grading

12 g/t Au (Burk et al., 1986); the Golden Giant mine, 22 million tonnes grading 8.5 g/t Au, 0.10% Mo and 1.5 g/t Ag (Kuhns et al., 1986); and the total reserves for the "A", "B" and "C" zones of the Page-Williams mine, 47 million tonnes grading approximately 6 g/t Au (Walford et al., 1986). Of the three zones within the Page-Williams mine, the "B" zone is the down-dip extension of the "A" zone and these two zones, when considered together, are known as the "main" zone which is the western extension of the Golden Giant mine. The "C" zone is geographically distinct and is several hundred metres west of the "main" zone. The "A" zone contains 3 million tonnes grading 6.21 g/t Au, the "B" zone contains 40 million tonnes grading 6.45 g/t and the "C" zone contains 3.9 million tonnes grading 3.98 g/t Au (Valliant and Bradbrook, 1986).

The Teck-Corona mine was renamed the David Bell mine in 1987 after preparation of this report had begun thus many designations in this publication appear with the symbol TC (Teck-Corona). The Golden Giant mine is designated as GG and the Page-Williams mine as W.

This publication describes the mineralogy of the main Hemlo gold deposit, the distribution of the various minerals and some geochemical characteristics of the ore zones. The study was carried out by reflected light and transmitted light microscopy, quantitative and qualitative electron-microprobe analysis and geochemical analysis.

REGIONAL GEOLOGY

The Hemlo gold deposit is located within the Hemlo-Heron Bay greenstone belt (Muir, 1982a, 1982b, 1983), a sequence of Archean metasedimentary and volcanic rocks (Fig 3). This belt, in turn, is part of the east-trending, Schreiber-White River section of the Shebandowan-Wawa subprovince of the Superior Province of Ontario. To the west near Heron Bay, the greenstone belt is divided into two lithologically and metallogenetically distinct sequences. The southerly and stratigraphically lower Playter Harbour sequence of predominantly iron-rich tholeiitic basalts hosts molybdenite and Cu-Zn sulphide occurrences in the Heron Bay area (Muir, 1982b). The northerly and stratigraphically overlying Heron Bay sequence of calc-alkaline intermediate to felsic volcanic, volcanoclastic and sedimentary rocks hosts several gold occurrences, including the Hemlo orebodies and several barite occurrences located 10 km east of Marathon (Patterson, 1986). Rocks of the Heron Bay sequence have been folded into a broad, east-trending, doubly-plunging synform called the "Hemlo" synform. The axis of the Hemlo synform is, in part, coincident with the Heron Bay-Black River fault, a major northeast-trending fault zone with which a number of subsidiary splay faults are associated (Brown et al., 1985). Late Archean granitoid plutons have intruded these supracrustal metamorphic rocks, and include the Gowan Lake quartz monzonite to the north, the Heron Bay

granodiorite to the southwest, and the Cedar Lake and Cedar Creek granodiorites to the north of the Hemlo deposit. The late Archean Pukaskwa granodioritic gneissic complex forms the southern limit of the greenstone belt. The greenstone belt is truncated to the west by the Proterozoic Port Coldwell alkalic complex, and to the east and north by Archean (or Kenoran) granitoid intrusions and migmatites.

The Hemlo gold deposit is located along and near contacts between rocks of metasedimentary and felsic metavolcanic-volcanoclastic origins in the lower part of the Heron Bay Group along the south limb of the Hemlo synform. The rocks in the main deposit strike at 110° to 115° and dip 60° to 70° northeast. The rocks hosting the deposit and those in the immediate vicinity are highly deformed and Hugon (1986) has demonstrated that the deposit lies within a major ductile fault, 1 m to 10 m wide, which is itself the most highly strained component of a regional scale, oblique thrust zone. For a more detailed description of the general geology, lithology, and structural elements of the region, the reader is referred to the published works of Muir (1985, 1986), Muir and Elliott (1987) and Patterson (1986); and for more detailed descriptions of the local geology of the mine properties, the published works of Burk et al. (1986), Kuhns et al. (1986), Valliant and Bradbrook (1986), Walford et al. (1986), Hugon (1986) and Muir (1986).

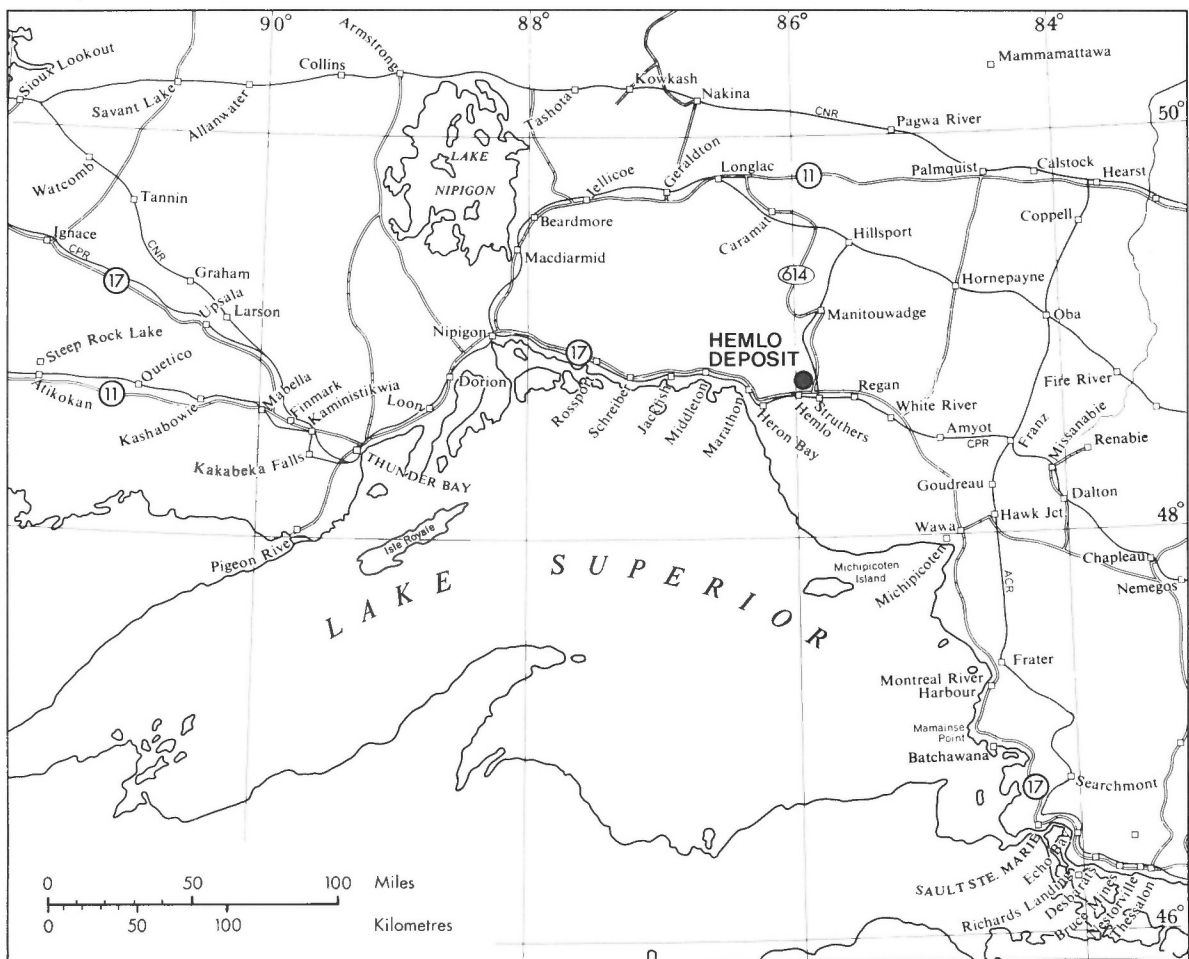


Figure 1. Location map for the Hemlo deposit.

SAMPLES AND METHODS OF INVESTIGATION

In 1983 a mineralogical study of the main ore zone and other related mineralized zones, was initiated to determine: (a) the mineral assemblages and compositions, (b) textural relationships (c) spatial distribution within the deposit, and (d) the effects of metamorphism and deformation on the minerals. It was anticipated that such a study would aid in the planning of ore beneficiation and could also contribute to a conceptual model for the genesis of the ore.

Split drill core samples were selected at 1-m intervals or less, from 25 drill holes (Fig 4). These samples are representative of the gold mineralization on the three properties that make up the Hemlo deposit. A polished section was prepared from each sample and polished thin sections were prepared for samples from six drill holes: TC218W and TC234 from the David Bell mine, GG20, GG23 and GG37Y from the Golden Giant mine and W70 from the Page-Williams mine. The locations of the drill core samples are listed in Appendix B. More than 900 polished sections and 110 polished thin sections have been examined. The sections were initially examined with a petrographic microscope to identify the constituent minerals, insofar as possible, by their optical properties, but most identifications were based on energy dispersive

electron microprobe analyses, quantitative wavelength dispersive analyses using a CAMEBAX microprobe and/or by X-ray powder diffraction techniques. The minerals present, their compositions and relative abundances were documented and then correlated with available gold assay and geochemical data. Initial studies indicated a diverse mineral assemblage and significant compositional ranges for many phases. As part of a geochemical and isotopic study (Cameron and Hattori, 1985), whole rock chemical analyses were determined for samples from drill holes TC218W, TC236, GG14W, GG20 and W70 and these analyses are listed in Appendix C.

MINERALOGY

General mineralogy

Preliminary data on the mineralogy of the Hemlo gold deposit were reported by Harris (1984, 1986a,b,c). The minerals identified within the main ore zone are listed in Table 1. Based on frequency of occurrence in the samples examined, the minerals have been classified as common, less common and least common. Since the main ore zone contains such diverse mineral assemblages and also is mineralogically zoned, this classification is not applicable to every part of the deposit. Also, the Golden Giant and the Page-Williams



Figure 2. Aerial view looking west of the Hemlo gold mines. Moose River separates the David Bell mine from the Golden Giant mine. Photo by George Patterson, Ontario Ministry of Northern Development and Mines, Thunder Bay.

orebodies have the thickest ore widths, thus more samples were selected from these orebodies, and therefore the classification is somewhat biased towards these areas of the deposit. Further, many of the minerals listed in Table 1 only occur in the central portion of the deposit. Ore minerals, other than pyrite, account for less than 1 per cent of the deposit, and are usually fine grained and difficult to recognize. Therefore, quantitative measuring techniques utilizing image analysis methods were not attempted. The simplified mineral formula (Fleischer, 1987) and chemical composition or elemental characteristics of each mineral at Hemlo are also listed in Table 1, but more details on many of these minerals are presented below.

The mineralogical studies reveal that the best indicator of the main gold-bearing zone is the presence of molybdenite and a light to dark grass-green-coloured vanadial muscovite. The former is widespread and high concentrations of molybdenite usually indicate high gold contents. Paragenetically, molybdenite and native gold appear to have been among the earlier minerals to form in the deposit. The vanadial muscovite occurs principally within the central portion of the deposit, rarely being present in the eastern portion of the David Bell orebody and in the northwestern down-plunge extension of the Page-Williams orebody. A plot onto a vertical

longitudinal section of the minerals present within each drill hole throughout the deposit shows that the mercury minerals, cinnabar and aktashite, and the principal arsenic mineral, realgar, are confined to the central part of the deposit (Fig 5). Within this zone are boudinaged quartz veins up to 30 cm in width that outcrop in the Page-Williams "A" orebody and extend to at least the lower limits of the Golden Giant orebody. These quartz veins are enriched in realgar, with coarse stibnite, cinnabar, the thallium minerals routhierite and parapierrhotite, native gold frequently rimmed with native arsenic, native antimony and several other rare minerals. Sphalerite is present throughout the deposit, generally as a minor component. It is unique in composition in that it contains as much as 29.5 wt. % Hg. Native gold is the principal gold mineral and contains as much as 26.9 wt. % Hg. In most native gold grains, mercury content is higher than silver. Auostibite is the second most important gold-bearing mineral and occurs mainly within the biotite-rich zones in the eastern portion of the Golden Giant orebody and down-dip within the western portion of the David Bell orebody. Stibnite is the principal antimony mineral although several lead sulphantimonides occur in minor amounts. It is widely distributed and coarse stibnite occurs along the periphery of and within the boudinaged quartz veins.

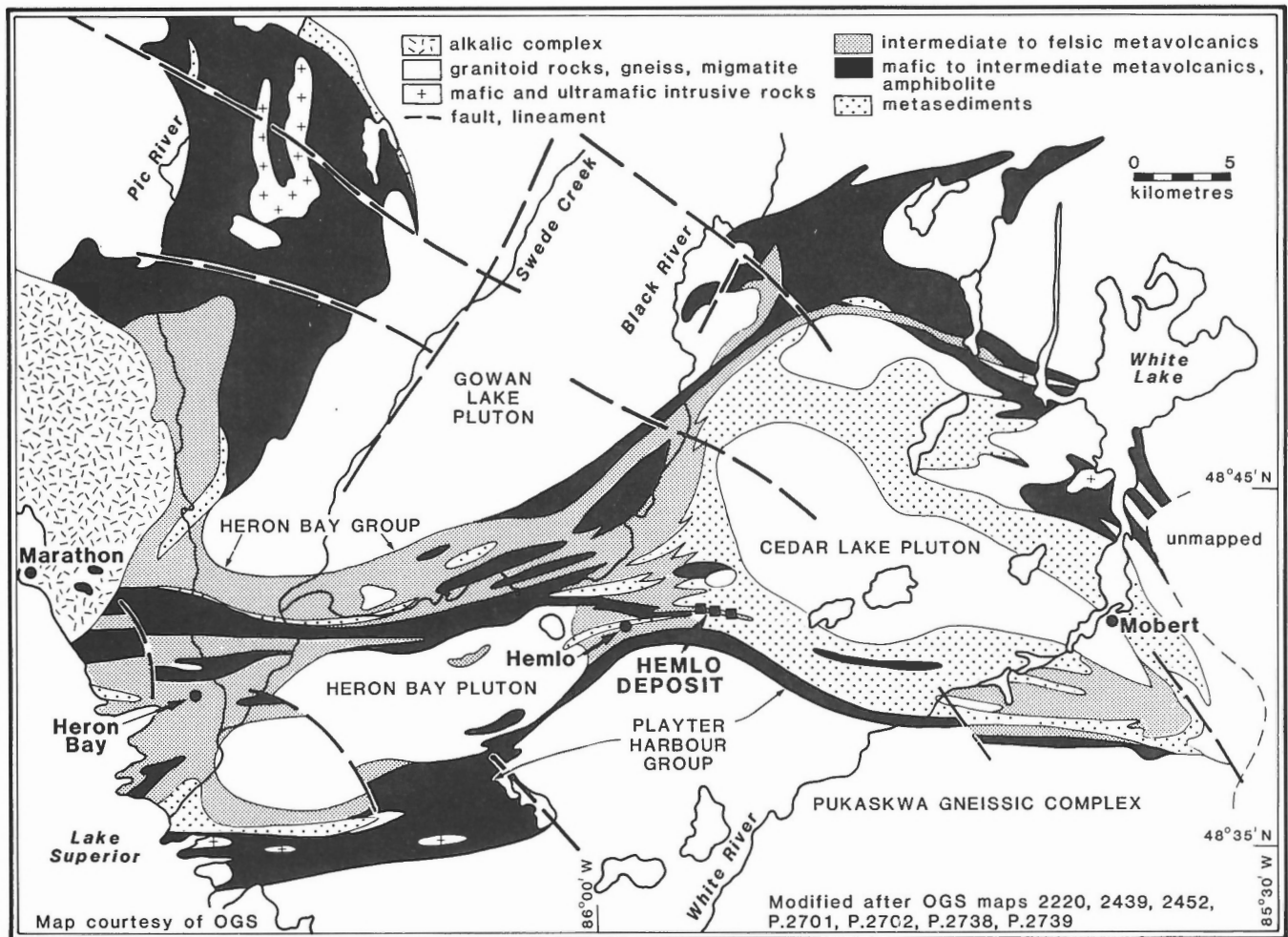


Figure 3. Geological Map of the Hemlo area by T. Muir (Map courtesy Ontario Geological Survey.)

Table 1. The minerals in the Hemlo gold deposit. The formula listed for each mineral is the most representative for that species in the deposit.

ORE MINERALS		
Common species	Simplified formula	Hemlo
Native Gold	Au	Hg 0.0-26.9, Ag 0.0-29.1
Pyrite	FeS ₂	FeS ₂
Molybdenite	MoS ₂	MoS ₂
Sphalerite	ZnS	Hg 0.0-29.5, Fe 0.0-1.9
Arsenopyrite	FeAsS	FeAsS
Stibnite	Sb ₂ S ₃	As 0.0-4.8
Tetrahedrite	(Cu,Ag,Hg,Fe,Zn) ₁₂ Sb ₄ S ₁₃	Hg 0.0-18.6, Ag 0.0-8.9
Tennantite	(Cu,Ag,Hg,Fe,Zn) ₁₂ As ₄ S ₁₃	Hg 0.0-15.2, Ag 0.0-8.3
Zinkenite	Pb ₆ Sb ₁₄ S ₂₇	As 0.0-11.5
Realgar	AsS	Sb 0.0-0.5
Cinnabar	HgS	HgS
Less common species	Simplified formula	Hemlo
Aktashite	Cu ₆ Hg ₃ As ₄ S ₁₂	Cu ₆ Hg ₃ (As,Sb) ₄ S ₁₂
Aurostibite	AuSb ₂	AuSb ₂
Chalcopyrite	CuFeS ₂	CuFeS ₂
Pyrrhotite	Fe _{1-x} S	Fe _{1-x} S
Galena	PbS	PbS
Native Antimony	Sb	As 0.0-1.3
Berthierite	FeSb ₂ S ₄	Mn 0.0-13.4
Bourmonite	PbCuSbS ₃	As 0.0-6.0
Boulangerite	Pb ₅ Sb ₄ S ₁₁	As 2.4-5.8
Native Arsenic	As	As
Gersdorffite	NiAsS	Fe 1.4-14.9
Parapierrrotite	Tl(Sb,As) ₅ S ₈	TlSb ₅ S ₈
Routhierite	TlHgAsS ₃	CuTlHg ₂ (As _{1.4} Sb _{0.6})S ₆
Altaite	PbTe	PbTe
Twinnite	Pb(Sb,As) ₂ S ₄	Pb(Sb _{1.2} As _{0.8})S ₄
Orpiment	As ₂ S ₃	Sb 0.0-5.0
Geocronite	Pb ₁₄ (Sb,As) ₆ S ₂₃	Pb ₁₄ (Sb _{3.0} As _{3.0})S ₂₃
Least common species	Simplified formula	Hemlo
Native Silver	Ag	Ag
Chalcostibite	CuSbS ₂	CuSbS ₂
Jamesonite	Pb ₄ FeSb ₆ S ₁₄	Pb ₄ FeSb ₆ S ₁₄
Gudmundite	FeSbS	FeSbS
Ullmannite	NiSbS	NiSbS
Coloradoite	HgTe	HgTe
Melonite	NiTe ₂	NiTe ₂
Baumhauerite	Pb ₂ As ₄ S ₉	Pb ₂ (As _{2.2} Sb _{1.8})S ₉
Seligmannite	PbCuAsS ₃	PbCu(As _{5.2} Sb _{4.8})S ₃
Dufrenoyite	Pb ₂ As ₂ S ₅	Pb ₂ (As _{1.1} Sb _{0.9})S ₅
Calaverite	AuTe ₂	AuTe ₂
Pararealgar	AsS	not analyzed
Stibarsen	SbAs	SbAs
Breithauptite	NiSb	NiSb
Clausthalite	PbSe	PbSe
Cubanite	CuFe ₂ S ₃	CuFe ₂ S ₃
Wurtzite	(Zn,Fe)S	Fe _{4.8} Hg _{6.2}
Galkhaite	(Cs,Tl)(Hg,Cu,Zn) ₆ (As,Sb) ₄ S ₁₂	-
Tvalchrelidzeite	Hg ₁₂ (Sb,As) ₈ S ₁₅	Hg ₁₂ (Sb _{4.7} As _{3.3})S ₁₅
New species	Simplified formula	
Criddleite	TlAg ₂ Au ₃ Sb ₁₀ S ₁₀	
Vaughanite	TlHgSb ₄ S ₇	
Unnamed species		
Antimony-rich routhierite		
Manganese-rich berthierite		
AgSbTe ₂		

Table 1 (continued)

OXIDE MINERALS		
Common species	Simplified formula	Hemlo
Rutile	TiO ₂	(Ti,Sb,V,W)O ₂
Barian Tomichite	(V,Fe) ₄ Ti ₃ AsO ₁₃ (OH)	Ba _{0.5} Ti ₂ (V,Fe) ₅ (As ₂) _{0.5} O ₁₃ (OH)
Less common species	Simplified formula	Hemlo
Magnetite	Fe ₃ O ₄	Fe ₃ O ₄
Ilmenite	FeTiO ₃	Mn 4.7
Least common species	Simplified formula	Hemlo
Hematite	Fe ₂ O ₃	(Fe,V) ₂ O ₃
Chromite	FeCr ₂ O ₄	Fe ₅₆ Zn ₄₅ Al ₉₉ Cr ₉₅ V ₀₄ O ₄
Lewisite	(Ca,Fe,Na) ₂ (Sb,Ti) ₂ O ₇	Ca _{1.1} (Fe,Mn) ₀₆ Ti _{1.25} As _{1.2} Sb _{1.47} O _{6.05}
New species	Simplified formula	
Hemloite	(Ti,V,Fe,Al) ₁₂ (As,Sb) ₂ (O,OH) ₂₄	
SILICATE MINERALS, etc.		
Common species	Simplified formula	Hemlo
Quartz	SiO ₂	SiO ₂
Muscovite	KAl ₂ (Si ₃ Al)O ₁₀ (OH,F) ₂	
Vanadian Muscovite	K(Al,V) ₂ (Si ₃ Al)O ₁₀ (OH,F) ₂	V ₂ O ₃ up to 8.5
Biotite	K(Mg,Fe ⁺³) ₃ (Al,Fe ⁺³)(Si ₃ O ₁₀ (OH,F) ₂	
Phlogopite	KMg ₃ Si ₃ AlO ₁₀ (OH,F) ₂	
Microcline	KAlSi ₃ O ₈	KAlSi ₃ O ₈
Barian Microcline	KAlSi ₃ O ₈	BaO up to 16.6
Barite	BaSO ₄	SrO up to 7.2
Titanite	CaTiSiO ₅	V ₂ O ₃ up to 14.2
Less common species	Simplified formula	Hemlo
Plagioclase	(Na,Ca)Al ₂ Si ₃ O ₈	An ₀ -An ₉₀
Anhydrite	CaSO ₄	CaSO ₄
Calcite	CaCO ₃	CaCO ₃
Scheelite	CaWO ₄	CaWO ₄
Apatite	-	-
Clinozoisite	Ca ₂ Al ₃ (SiO ₄) ₃ (OH)	-
Zoisite	Ca ₂ Al ₃ (SiO ₄) ₃ (OH)	-
Zircon	ZrSiO ₄	-
Amphibole	-	Tremolite,Actinolite,Hornblende
Tourmaline	-	var. dravite
Least common species	Simplified formula	Hemlo
Fluorite	CaF ₂	-
Cafarsite	Ca ₆ (Ti,Fe,Mn) ₆₋₇ (AsO ₃) ₁₂ ·4H ₂ O	Ca ₆ (Ti,Mn,V,Fe) ₇ (AsO ₃) ₁₂ ·xH ₂ O
Ferberite	FeWO ₄	Fe ₆₇ Mn ₁₈ Mg ₁₅ WO ₄
Monazite	(Ce,La,Nd,Th)PO ₄	(Ce,La,Nd,Th)PO ₄
Allanite	(Y,Ce,Ca) ₂ (Al,Fe) ₃ (SiO ₄)(OH)	(Ca,RE) ₂ (Al,Fe) ₃ (SiO ₄)(OH)
Stilbite	Zeolite Group	not analyzed
Chlorite	Chlorite Group	-
Vanadian grossular	Ca ₃ Al ₂ Si ₃ O ₁₂	Ca _{3.1} Al _{1.2} V _{0.8} Si _{2.9} O ₁₂
Vesuvianite	Ca ₁₀ Mg ₂ Al ₄ (SiO ₄) ₅ (Si ₂ O ₇) ₂ (OH) ₄	not analyzed

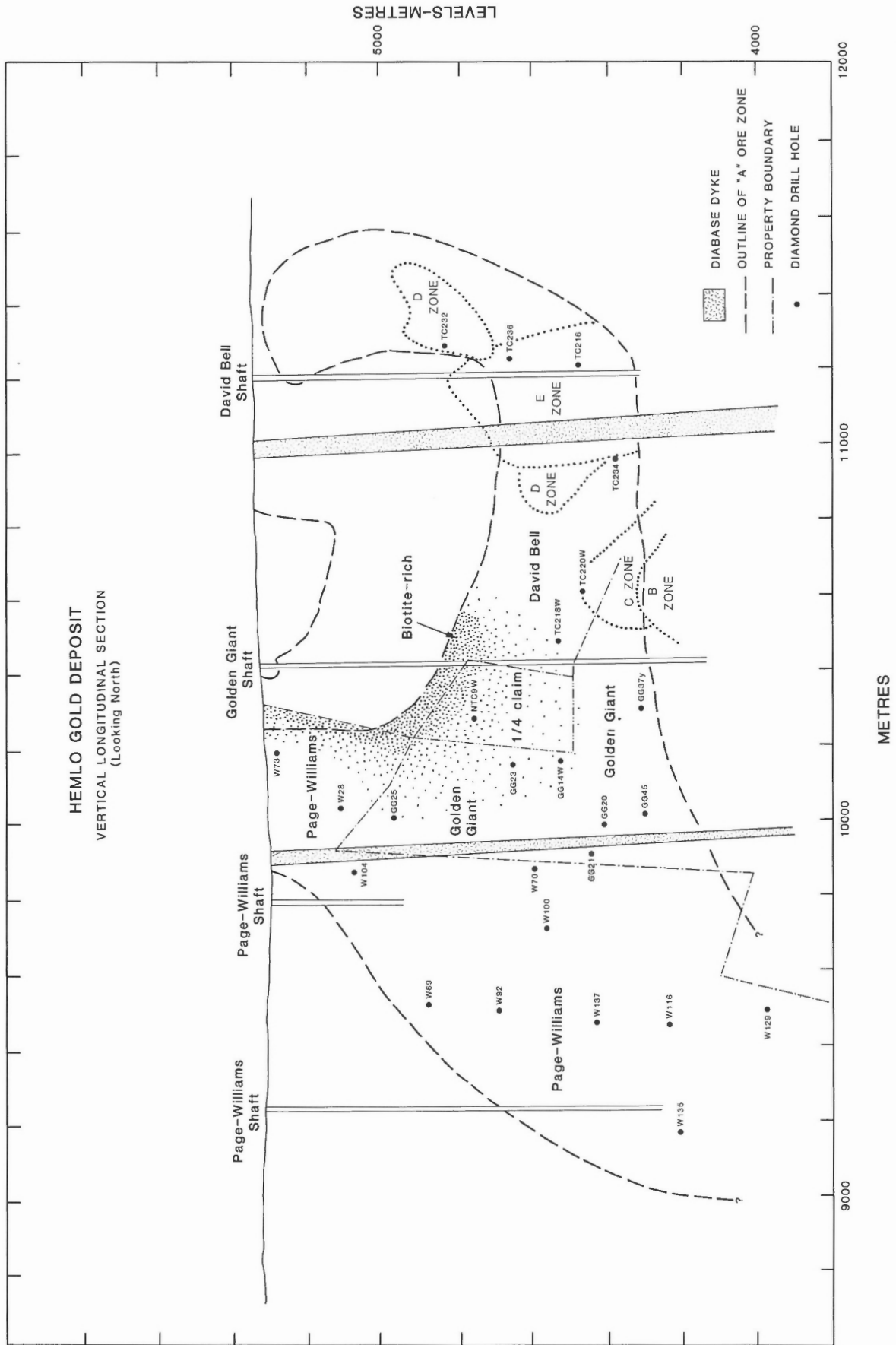


Figure 4. Vertical longitudinal section showing the property boundaries, the ore zones and location of the sampled drill holes.

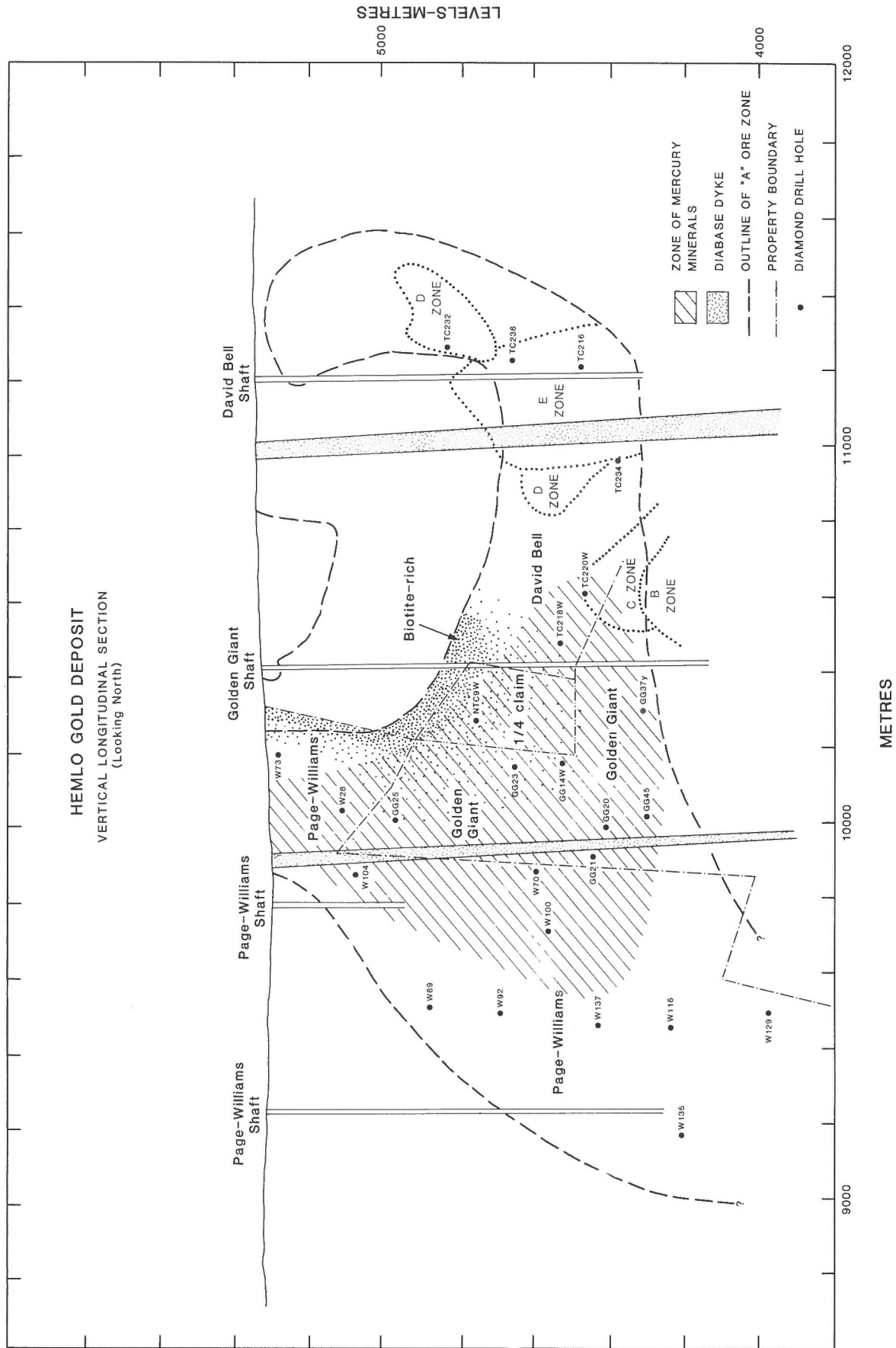


Figure 5. Vertical longitudinal section showing the distribution of the mercury minerals.

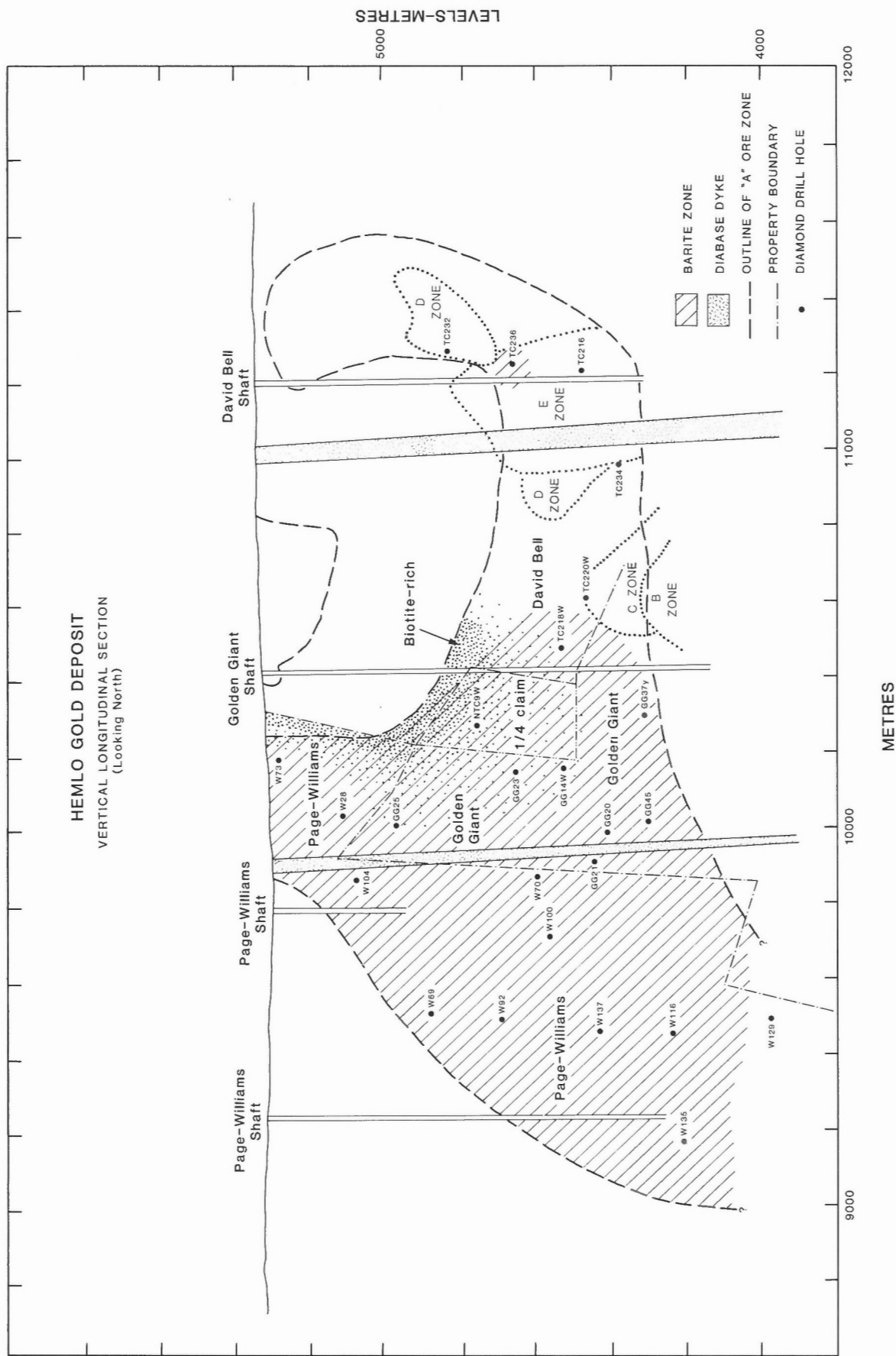
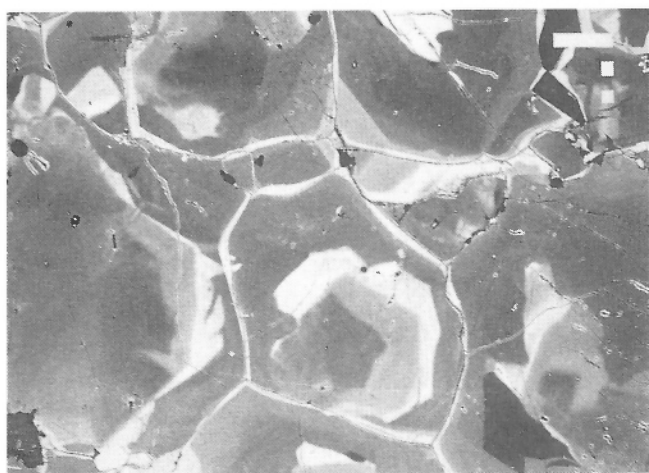


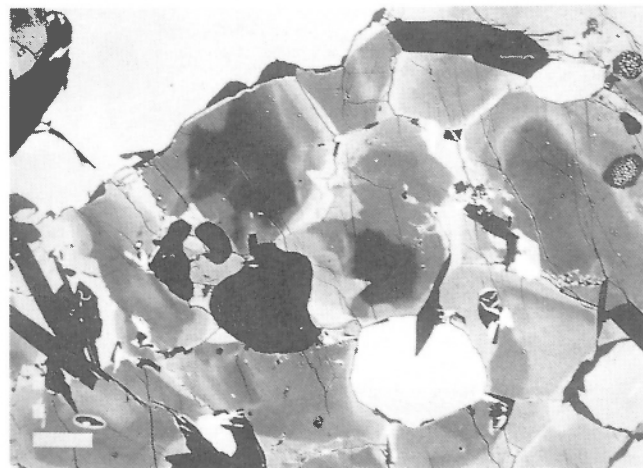
Figure 6. Vertical longitudinal section showing the distribution of the barite.

Tetrahedrite and tennantite are both widespread and are the principal silver-bearing minerals. Tellurides are rare in the deposit, occurring principally within the northwest down-plunge extension of the Page-Williams orebody below the zone of mercury minerals. This portion of the deposit is mineralogically different in that sphalerite (with low to not detected mercury), galena (nearly absent in other parts of the deposit), chalcopyrite, pyrite, molybdenite and native gold (with high silver contents) are the main ore minerals. The principal oxide mineral in the deposit is rutile and this has been found to contain as much as 5.6% V_2O_3 , 6.5% Sb_2O_3 and 3.2% WO_2 . Barian tomichite, the second most common oxide mineral, occurs principally within the core of the central portion of the deposit. Tomichite is a rare oxide mineral that was first reported from the "green leader" gold lodes at Kalgoorlie, Western Australia (Nickel and Grey, 1979). Magnetite, ilmenite and chromite are sparse, with magnetite occurring mainly in the hanging wall and in parts of the David Bell orebody and the biotite-rich zones in the

Golden Giant orebody. The common gangue minerals in the deposit are quartz, muscovite, phlogopite, barian feldspar and barite. In parts of the eastern portion of the deposit, biotite, plagioclase, tremolite and hornblende occur as principal constituents within narrow drill core intersections. Important mineralogical features of the gangue are the abundance of barite, the near absence of carbonate, and the presence of grass-green vanadian muscovite and barium-bearing microcline. Barite is a major constituent in both the Page-Williams and the Golden Giant orebodies, but is rarely present in the David Bell orebody (Fig 6). It occurs in massive zones within the central part of the deposit, with some areas containing up to 70 per cent. In some barite-rich sections, angular fragments of ore groundmass are contained within the baritic matrix. The barite, in part, appears to dilute the ore while contributing to the extra thicknesses. Barite is present in rock units situated below the ore zone on the Page-Williams property and there is a barite-rich horizon 25 km west of the deposit. The stratigraphic relations



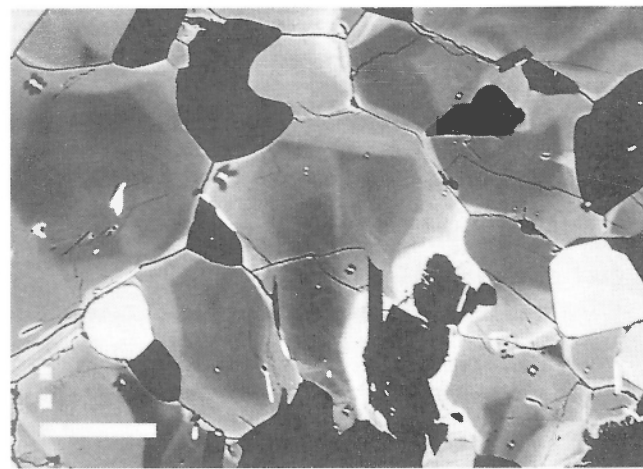
W70 737.4



GG37Y 1040.2



GG37Y 1040.2



GG37Y 1040.2

Figure 7. Electron backscattered images of zoned barian microcline. The lightest grey areas contain higher barium contents. The white areas are pyrite and the black areas quartz and mica. The labels represent the drill hole and metres depth. The scale bar is 100 μ m.

between the Hemlo barite and that to the west are unknown, but there are differences. The most notable features of the barite in the deposit are the degree of recrystallization that has resulted in coarser and the occasionally bladed crystals with a whiter colour (Patterson, 1986). Microcline is very common and is generally barium-rich, with as much as 9.5 wt. % BaO in the ore zones and as much as 17.0 wt. % BaO in rare specimens collected from the immediate hanging wall rock. The feldspar grains range from some with rhythmic zoning to others with irregularly distributed barium contents (Fig 7). The paragenetic position of the barian microcline is uncertain, but it appears to have been formed by potassium-rich hydrothermal fluids that are considered to have been closely associated with formation of the deposit.

Detailed ore mineralogy

Pyrite

Pyrite is the most abundant sulphide and its banded nature gives the ore a stratified appearance (Fig. 8a). The pyrite content of the deposit ranges from 5 to 20%, averaging 8% in the Golden Giant orebody (Brown et al., 1985). Pyrite occurs in two modes; principally as coarse subhedral to anhedral deformed aggregates, not exceeding 3 mm in maximum dimension, which are concentrated in "layers or lenses" up to 1 m thick, and less commonly as fine grained euhedral grains less than 200 µm in size which are disseminated throughout the silicate groundmass (Fig. 8b,c,d). Inclusions within the pyrite grains are sparse and, when present,

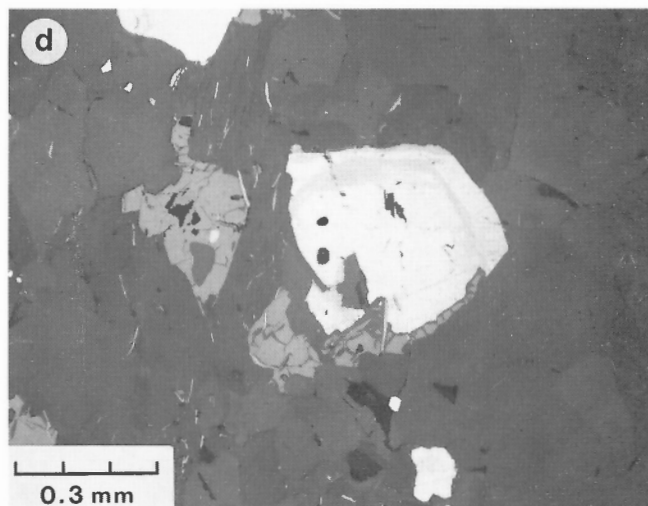
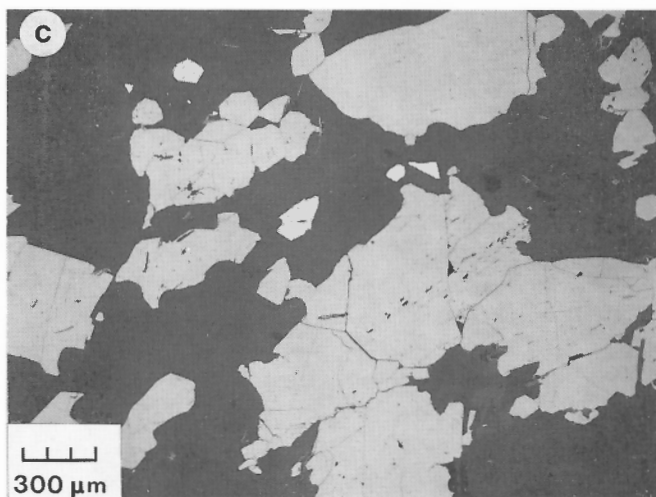
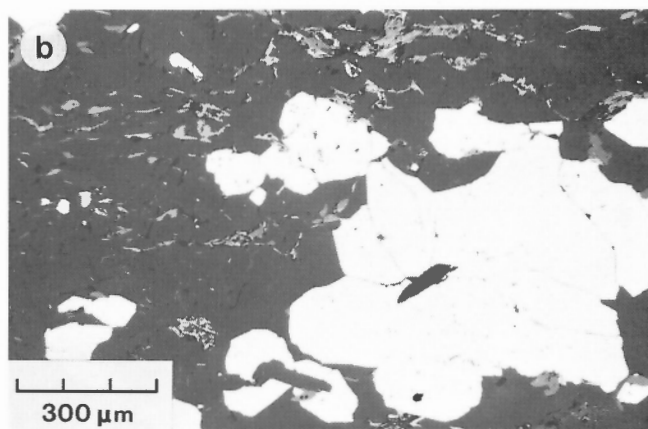
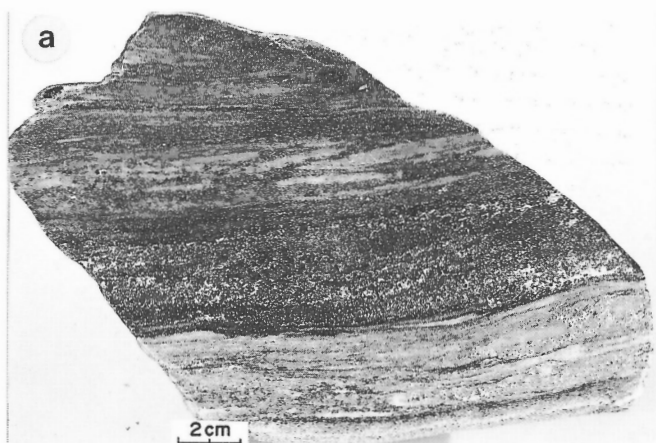


Figure 8(a). Polished specimen showing the banded nature of the pyrite-rich ore. **(b).** Photomicrograph of coarse anhedral pyrite in silicate matrix. GG23, 651.8m. **(c).** Photomicrograph of coarse anhedral pyrite associated with molybdenite and rutile in silicate matrix. GG25, 347.6m. **(d).** Photomicrograph of ore containing pyrite partially replaced by pyrrhotite, magnetite and molybdenite. TC234, 903.6m.

consist mainly of molybdenite, rutile, sphalerite and, rarely, pyrrhotite and native gold. The coarser pyrite grains show the effects of subsequent deformation of the ore, and have been modified in shape and are aligned parallel to the dominant foliation in the ductile shear zones. There is no relationship between pyrite contents and gold assay values, in fact massive pyrite zones generally have lower gold values.

Molybdenite

Molybdenite the second most abundant sulphide, is widespread throughout the deposit. It occurs principally in association with the silicate minerals, is also found as isolated inclusions within pyrite and, less frequently, within the barite-rich portions of the deposit. The molybdenite consists of blades oriented parallel to the foliation of the ore, as fine-grained individual euhedral crystals in the quartz-rich zones and as deformed platy masses (Fig. 9a,b). The occurrence of molybdenite along the foliation and schistosity planes of the muscovite schist, which tends to cleave very readily, imparts a distinct bluish tint to hand specimens from this lithology. The presence of molybdenite can be used as an indicator for gold-bearing zones. The molybdenite itself, however, is generally free of gold inclusions, with only

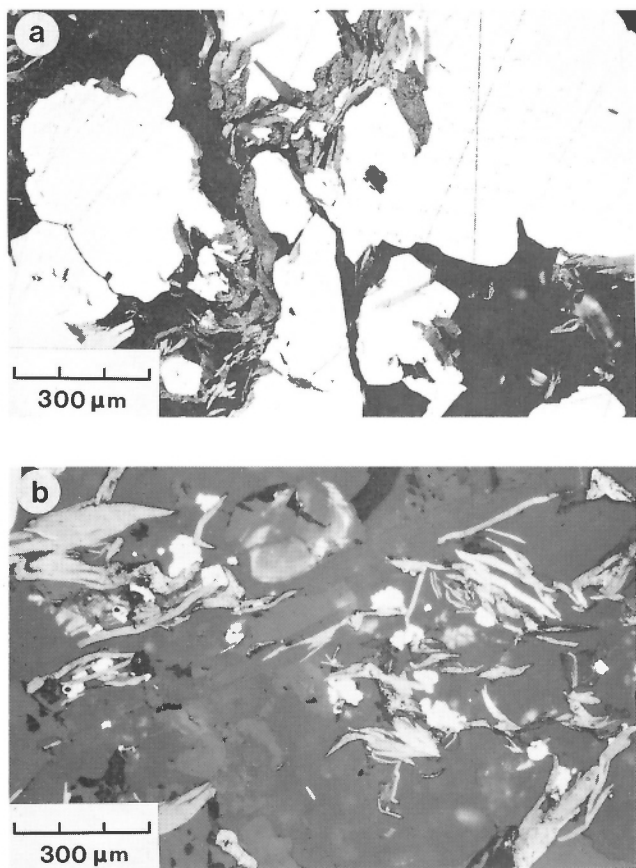


Figure 9(a). Photomicrograph of molybdenite-rich specimen with coarse anhedral pyrite. W135, 1191.2m (GSC 204385) **(b).** Photomicrograph of slightly oriented molybdenite flakes with fine-grained pyrite in a quartz-microcline-muscovite matrix. W70, 754.4m (GSC 204385-D).

rare blebs of native gold (less than 2 µm) occurring as inclusions within the molybdenite flakes and interstitial to the molybdenite masses.

The molybdenite content in the Golden Giant orebody has been reported to average 0.16%, with a range of 0.03 to 0.40% (Brown et al., 1985). A circuit has been included in the mill to recover molybdenite, although recoveries are less than the 60% expected (Tintor, 1986). Up to the end of 1987, neither the David Bell nor the Page-Williams mills were attempting to recover molybdenite.

Sphalerite

Sphalerite is a minor constituent in the deposit, but in some individual specimens it is a major component. It occurs mainly as irregular grains, less than 400 µm in size, interstitial to the silicate gangue minerals. Sphalerite also forms coarse grains or masses as much as 3 mm in size in a few drill core samples from holes W129 and W135 in the Page-Williams orebody and as coarser masses as much as 1 cm in diameter in realgar-stibnite-quartz-rich samples from the underground workings in the Golden Giant mine. Sphalerite has an unusually high mercury content. Electron microprobe analyses are listed in Table A.1 (Appendix A). Initially, analyses for Cd, In and Mn were attempted, but as these elements were not detected, they were not subsequently determined. The presence of mercury-bearing sphalerite is a characteristic feature of the Hemlo ore and the highest value of 29.5 wt. % Hg for sample TC220W, 923.8m is the second highest recorded in the literature. A mercury-rich sphalerite containing 38 wt. % Hg was reported by Gruzdev (1975) from the Galkhaya mercury-antimony deposit, USSR. Other mercury-rich sphalerites have been reported by Vasil'yev and Lavrent'yev (1969), with one specimen from the oxidation zone of the Belo-Osipovskoye mercury deposit, USSR containing 15.6 wt. % Hg, and more recently by Barbanson et al. (1985) from Cabezon de la Salarea, Santander, Spain where sphalerite is present with 15 wt. % Hg without visible included cinnabar and with as much as 27 wt. % Hg when it includes visible cinnabar. Microprobe analyses and back-scattered electron imaging reveals no inclusions of cinnabar in the Hemlo sphalerite, although cinnabar is present in the deposit. The analyses show that the mercury occurs as an isomorphous substitution for zinc and X-ray powder diffraction studies show an increase in unit-cell parameters. Experiments by Tauson and Abramovich (1980) on the phase relations in the ZnS-HgS system by hydrothermal synthesis at 200-280°C and about 1000 atm. showed that the unit-cell parameter as a function of the HgS content can be expressed by the equation:

$$a = 5.409 + 0.00442 \text{ mol. \% HgS}$$

The unit-cell parameter for the most mercury-rich sphalerite (29.5 wt. % Hg) in sample TC220W, 923.8m, as determined using a 114.6mm Debye-Scherrer camera, is 5.479(1)Å°, equivalent to a calculated value of 26.7wt. % Hg. This is in reasonable agreement with the analyzed mercury content.

Sphalerite is rather sparse in the David Bell and Golden Giant orebodies (the lack of analyses reflects this in Table A.1), but is more abundant in the Page-Williams orebody.

Sphalerite in drill hole W70 occurs throughout the width of the ore zone and microprobe analyses reveal an increase in mercury contents towards the centre of the ore zone (Fig. 10). Sphalerites in drill holes W135, W129, W116 and W137, which are located within the northwest down-plunge extension of the Page-Williams orebody and outside the zone of mercury minerals (Fig. 5), contain from the detection limit (less than 0.4 wt. %) to a maximum of 1.6 wt. % Hg. In this part of the deposit, the ore is more galena-rich, with some tellurides, chalcocopyrite and native gold with high silver contents.

The colour of the mercury-bearing sphalerite is virtually identical to that of the iron-poor variety and ranges from honey yellow to pale yellow to colourless. Since the amount of mercury substituting for zinc in the sphalerite appears to have no effect on its colour, microprobe analyses are essential to determine the mercury contents. Even though certain parts of the deposit contain high mercury-bearing sphalerites, the mineral is not a major source of mercury within the deposit.

Gold minerals

Gold minerals identified in the main deposit are native gold, aurostibite, calaverite, petzite and criddleite. *Native gold*, the principal gold-bearing mineral, occurs as free grains, generally between 1 and 20 μm in size, along quartz-feldspar grain boundaries; as inclusions in, or rimmed with, native arsenic (Fig. 11), cinnabar, stibnite, tetrahedrite, sulphosalts, chalcocopyrite and aurostibite; as grains in contact with pyrite, as a filling constituent in fractures in pyrite grains; and very rarely as inclusions within the pyrite. The average grain size of native gold is visually estimated to be approximately 15 μm . Megascopically visible native gold is rare in drill core but is more common, although sparse, in samples from the underground workings. Microprobe analyses of native gold grains larger than 10 μm are given in Table A.2. The analyses, listed in this table for each sample, represent the average of several spots on one or more grains in a given polished section in which there is very little variation in composition. For polished sections with several grains with different compositions, the individual analyses are presented. The analyses indicate that the native gold in the deposit is a gold-mercury-rich alloy with minor silver. Native gold grains with mercury

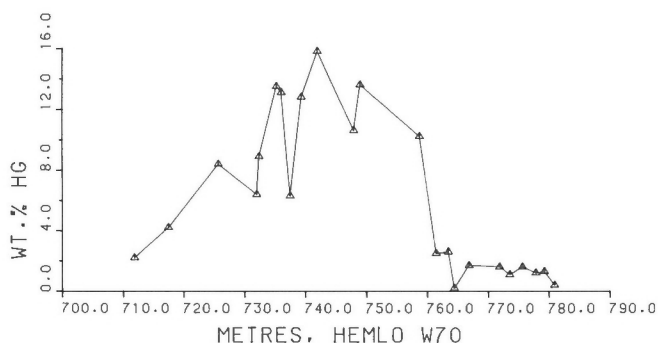


Figure 10. Profile of mercury contents in sphalerite across the ore zone within drill hole W70. Mercury analyses by electron microprobe of sphalerite in polished sections.

values of 26.9 wt. % were found in sample TC220W, 923.8 m. No systematic variation in mercury contents of gold grains is apparent throughout the deposit. The average composition of native gold in the David Bell orebody is 83.6% Au, 11.6% Hg, 4.6% Ag (8 polished sections); in the Golden Giant orebody it is 89.1% Au, 6.5% Hg, 3.9% Ag (15 polished sections); in the Page-Williams orebody it is 85.4% Au, 5.7% Hg, 7.0% Ag (52 polished sections). The higher silver contents within the Page-Williams orebody reflect the analyses for mercury-poor native gold grains from the northwest down-plunge extension where the average composition is 87.0% Au, 9.1% Ag, 1.1% Hg (12 polished sections from drill holes W135, W129, W116 and W137). This part of the deposit lies outside the zone of mercury minerals (Fig. 5) and its mineral assemblage is of a more base-metal-rich nature with associated telluride minerals. Optically, there is no distinct difference in the colour of the native gold to indicate its mercury content, thus microprobe analysis is essential. Some visible gold occurs within zones that contain highly fractured and boudinaged quartz veins and within pods of quartz which are enriched in a mineral assemblage of realgar, cinnabar and stibnite. These boudinaged veins occur principally within the central mercury-rich portion of the deposit (Fig. 5). Higher gold assays were obtained from the biotite-rich eastern portion of the Golden Giant orebody and the western portion of the David Bell orebody, and particularly in sparse zones where tremolite is a dominant gangue mineral. The occurrence and association of the native gold grains suggest some remobilization as a result of later tectonic deformation of the deposit, but the gold appears to be restricted to its original zones.

The native gold in the Hemlo deposit is the first reported mercury-rich gold alloy in a Canadian gold deposit. Recently, Healy and Petruk (1989) have reported a Au-Ag-Hg alloy in the volcanogenic massive sulphide ore from the Trout Lake deposit in Flin Flon, Manitoba. In this deposit, the average composition of the alloy is Ag 49.2, Au 38.7, Hg 11.0 wt. %,

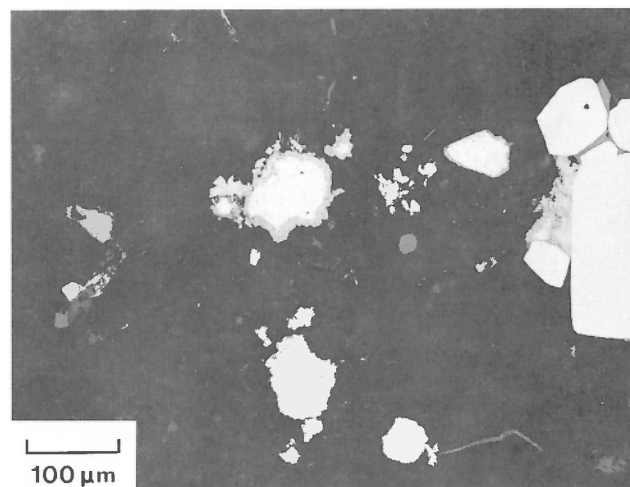


Figure 11. Photomicrograph of native gold rimmed with native arsenic. The white euhedral grains are pyrite. A few molybdenite flakes occur in the silicate matrix. Specimen from the Golden Giant orebody.

but there is a large range in the proportions of the three elements, Ag (17.34 to 76.47 wt. %), Au (1.62 to 79.86 wt. %) and Hg (1.29 to 30.87 wt. %). Other worldwide occurrences of mercury-rich gold have been reported from a gold-antimonide deposit in Kazakhstan (Naz'mova and Spiridonov, 1979) that contains 2.9 to 14.8 percent Hg and from a middle to late Carboniferous mercury-antimony deposit of the Zeravshan-Gissar antimony-mercury belt in southern Tienshan, Soviet Central Asia (Vershkovskaya et al., 1984) that contains as much as 7 to 10 per cent Hg. A mercury-containing Au-Ag alloy that has a composition close to $Au_{0.45}Ag_{0.24}Hg_{0.10}$ has been reported by Nysten (1986) from a Precambrian volcanogenic mercury-rich sulphide deposit in Northern Sweden (Langsele). Oberthur and Saager (1986) have reported native gold particles with as much as 5.9 wt. % Hg from the Proterozoic Witwatersrand placer deposits of South Africa and recently, Shikazono and Shimizu (1988) have reported the first find of mercurian gold in Japan from the middle Miocene epithermal Tsugu gold-antimony vein deposit. The gold contains up to 8.5 wt. % Hg. Because of the paucity of microprobe analyses of native gold grains in massive sulphide deposits, it is possible that mercury-bearing gold is more common than presently known. However, it would appear that the Hemlo occurrence is the first major gold deposit in the world that contains principally mercury-rich gold.

The second important gold-bearing mineral is *aurostibite*, and in places, the mineral accounts for a significant portion of the gold content. It is nearly impossible to accurately estimate the amount of aurostibite present on the basis of polished sections, but lower gold recoveries are encountered for those parts of the deposit where the mineral occurs, since the gold contained in aurostibite is largely unrecovered in the cyanide treatment of the ore. The locations where aurostibite has been identified are given in Table 2. These are chiefly within the biotite-rich zones in the eastern portion of the Golden Giant orebody and the western portion of the David Bell orebody as defined by drill holes GG14, GG23, GG25 and TC220W. Aurostibite occurs generally as grains less than 20 μm in gangue, in contact with pyrite, as intergrowths with stibnite, rimming native gold or rimmed by criddleite. Commonly associated minerals are native antimony, gudmundite, berthierite, parapierrrotite and chalcostibite. A common indicator of the presence of aurostibite in a polished section are the minerals, native antimony, gudmundite and berthierite. Based on equilibrium studies in the Fe-Sb-S system, Barton

Table 2. Specimens containing aurostibite

DDH	metres
TC236	673.9, 677.0
TC220W	923.8
TC216	876.3
GG14	903-910 (composite)
GG21	821.45, 823.5
GG23	646.4, 647.0, 647.7, 651.6
GG25	323.4, 324.9, 324.95, 327.0, 328.2, 328.6, 329.2, 330.0, 331.5, 332.5
W70	758.6
W92	642.9, 643.8, 644.5, 645.1

(1971) reported that these three minerals are clearly stable only under conditions of relatively low sulphur activity and that the assemblage pyrite and aurostibite is stable only at low temperatures, possibly below about 125°C, although the uncertainties are too large for this to be a useful point on the geothermometric scale.

Less common gold-bearing minerals are *calaverite*, *petzite* and *criddleite*. Calaverite and petzite were only identified in drill hole W137, 971.2 in association with coloradoite, hessite, an unnamed $AgSbTe_2$, native arsenic, tennantite, realgar and native gold. *Criddleite*, is a new gold-bearing mineral with the formula $TlAg_2Au_3Sb_{10}S_{10}$; it has been identified in four drill holes, namely GG23, 651.6; GG25, 324.9; W92, 642.9 and W70, 758.6. The mineral commonly forms lath-like, tabular or anhedral grains (20-30 μm) usually surrounding and penetrating aurostibite. The name and data have been accepted by the Commission on New Minerals and Mineral Names, IMA and a complete description of the mineral has been reported by Harris et al. (1988).

Pyrrhotite

Pyrrhotite is rare within the central portion of the deposit, but it accompanies pyrite in the hanging wall rocks and in thin zones within the David Bell orebody and parts of the Golden Giant orebody. In places, the modal content of pyrrhotite exceeds that of pyrite. In the hanging wall, pyrrhotite is associated with pyrite and magnetite, frequently as a replacement along fractures in pyrite (Fig. 8d). Pyrrhotite, sometimes with associated chalcopyrite, commonly occurs as small inclusions in pyrite.

Chalcopyrite

Chalcopyrite is not a major ore mineral in the deposit, except for parts of the northwest down-plunge extension of the Page-Williams orebody where it occurs with sphalerite, galena and pyrite. In the remainder of the deposit, it was frequently observed in polished section, but in trace amounts.

Galena

Galena was only identified in five drill holes in the deposit, namely W73, W92, W129, W135 and W137. Of these, only W135 contained other than trace amounts. Galena in this hole occurs throughout the lower two-thirds of the ore zone, with samples from a depth of 1183.3 m containing sphalerite, altaite and galena as the major ore minerals. Even in this case, these minerals account for less than one per cent of the area of the polished section.

Stibnite

Stibnite is the most abundant of the antimony minerals and is readily visible in hand specimens in which it occurs as fine disseminations and coarser masses concentrated along the periphery of and within boudinaged quartz veins and in realgar-sphalerite-quartz-rich samples. The most common form of stibnite is as radiating acicular crystals in quartz and occasionally in vugs. Microprobe analyses (Table A.3) show that as much as 4.8 wt. % As occurs in solid solution in the stibnite, but most grains contain no arsenic. Fine inclusions

of realgar (Fig. 12a) were noted in some of the more arsenic-rich grains. Stibnite-rich samples are generally higher in gold content and grains of visible gold were frequently found in these samples. Minerals commonly associated with stibnite are various sulphosalt minerals and tetrahedrite.

Tetrahedrite and tennantite

Tetrahedrite and tennantite are both widespread in the deposit and are the principal silver-bearing minerals. Tetrahedrite is more common in the David Bell mine, the Golden Giant mine and the upper levels of the Page-Williams mine, whereas tennantite is more common in the lower levels of the Page-Williams mine, particularly the northwest down-plunge extension. Microprobe analyses (Table A.4) show that the minerals are variable in composition and may contain as much as 18.6 wt.% Hg and as much as 10.9 wt.% Ag. The minerals are rarely visible in hand specimen and seldom exceed 300 μm in maximum dimensions.

Arsenic minerals

The most abundant arsenic mineral is *realgar*. It is readily visible in hand specimens as it imparts a reddish to yellowish orange colour to the drill core. In the boudinaged quartz veins, realgar forms coarse irregular masses interstitial to fractured quartz and as concentrations along the edges of the veins. In some specimens, the colour of realgar is more yellowish, similar to the colour of orpiment and pararealgar, which are also present in the deposit. Realgar is restricted to the central portion of the deposit within the Golden Giant and Page-Williams orebodies and its distribution is nearly coincident with that of mercury minerals (Fig. 5). Trace amounts of realgar and native arsenic were identified in holes W92 and W137, which are slightly to the west of the area defined by the mercury minerals. Microprobe analyses of realgar indicate antimony contents are undetectable to 0.6 wt.%, but the tendency for the microprobe beam to physically react with the realgar causing a pit meant that only the coarsest grains could be analyzed with an expanded beam. In some specimens *native arsenic* occurs as clusters of crystals (Fig. 12b), frequently associated with realgar, and in parts of the Golden Giant orebody native arsenic occurs rimming native gold (Fig. 11). In yet other specimens, native arsenic and native antimony are found together, sometimes in association with aurostibite, berthierite, stibnite and gudmundite. *Orpiment* is rare and microprobe analysis for the one grain analyzed, gave 5.0 wt.% Sb. *Pararealgar* was identified by X-ray in one specimen, GG20,877.9, although it is probably more common as its colour is yellow to orange-yellow and a common mode of occurrence of pararealgar is as replacements of realgar (Roberts et al., 1980). Also, the composition of pararealgar is identical to realgar (AsS), therefore the yellow to orange-yellow colour noted for many "realgar" grains could indicate the presence of pararealgar. *Arsenopyrite* is moderately abundant in the deposit and in places it is a major ore mineral. It occurs as euhedral to subhedral crystals that range from less than 10 to 200 μm in size. It is most abundant in the hanging wall rocks where it is the principal arsenic mineral, rare in the David Bell orebody, more common in the Golden Giant orebody, particularly

in the biotite-rich zones, and is finely disseminated throughout the Page-Williams orebody. The mineral seldom contains inclusions, but in places it was observed as intergrowths with pyrite. Arsenopyrite is not a significant arsenic-containing mineral in the ore zones. *Gersdorffite* (NiAsS) was identified in several drill holes. It occurs mainly in the David Bell orebody and the biotite-rich portions of the Golden Giant orebody. It is present as subhedral to euhedral 10 to 50 μm grains, isolated in gangue and in contact with pyrite grains. Microprobe analyses are given below.

Location		Ni	Fe	As	S
GG21,855.0		22.3	13.1	43.0	18.9
GG23,651.6		27.0	7.7	45.2	19.6
W92,667.7	Gr.1	34.0	1.4	44.2	19.8
	Gr.2	20.3	14.9	42.6	21.1

Co,Sb were not detected

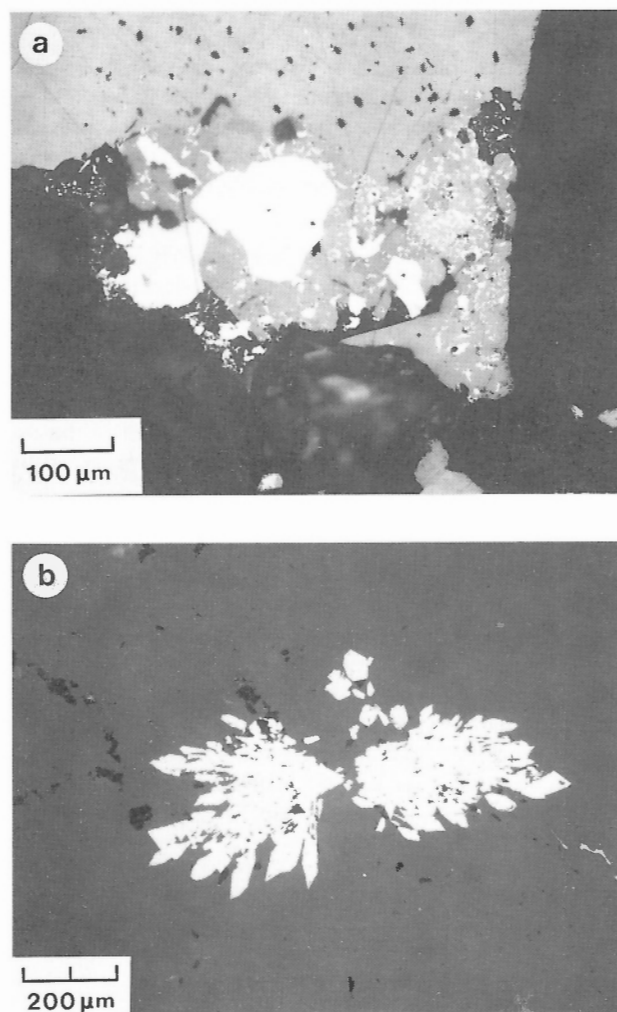


Figure 12(a). Photomicrograph of coarse stibnite with fine inclusions of realgar adjacent to a parapierrhotite grain that contains inclusions of coarse aurostibite and fine native antimony. GG25, 324.9m **(b)** Radial cluster of native arsenic grains in quartz. This form of native arsenic was frequently observed in the realgar-rich boudinaged quartz veins. GG25, 324.95m.

Mercury minerals

The major and most abundant mercury minerals are *cinnabar* (HgS) and *aktashite* ($\text{Cu}_6\text{Hg}_3(\text{As},\text{Sb})_4\text{S}_{12}$). These minerals are located principally in the central, thickest part of the deposit (Fig. 5). Cinnabar is more abundant in the upper levels and aktashite in the lower levels of the deposit. Cinnabar is most common in the "A" zone and upper parts of the "B" zone of the Page-Williams orebody and the upper levels of the Golden Giant orebody. Samples of sericite schist from the open pit on the Page-Williams orebody contain visible cinnabar, principally along the schistosity planes, and this imparts a reddish surface to some specimens. Cinnabar also occurs in the realgar-rich boudinaged quartz veins, but, due to the abundance of reddish coloured realgar, it is not as readily visible. In the boudinaged quartz veins it occurs along and around the fractured quartz, indicating remobilization or later deposition. Down-dip within the central part of the deposit, cinnabar is less common and aktashite is the principal mercury mineral. Microprobe analyses of aktashite are listed in Table A.5. Aktashite is a rare mineral, specific to polymetallic antimony-mercury deposits where it is associated with realgar-orpiment ores in zones of antimony-mercury mineralization. The mineral was first reported by Vasil'ev (1968) from the Aktash mercury deposit, Gornyi Altai, where it is associated with quartz, pyrite, calcite, sphalerite, stibnite, chalcostibite, mercurian tetrahedrite, tennantite, luzonite, enargite, chalcopyrite, cinnabar, dickite and orpiment. A second occurrence has been reported from the Gal-Khay (Yakutiya) arsenic-antimony-mercury deposit by Gruzdev et al. (1972a) and a third occurrence has been reported from Jas Roux (Hautes-Alpes), France by Mantienne (1974). At Jas Roux, the aktashite-bearing mineral assemblage is similar to those in Siberia. At Jas Roux, aktashite occurs with realgar, orpiment, wakabayashilite, stibnite, pyrite, greigite and metacinnabar as veinlets in quartz and calcite metasomatites in Triassic rocks. Recently, Spiridonov et al. (1983) reported an antimonian aktashite from the Chauvay mercury deposit, Soviet Central Asia, which contains as much as 13.46 per cent Sb. The chemical composition of this antimonian aktashite established the formula as $\text{Cu}_6\text{Hg}_3(\text{As},\text{Sb})_4\text{S}_{12}$ which is in better agreement with the formula, $\text{Cu}_6\text{Zn}_3\text{As}_4\text{S}_{12}$, for isostructural nowackiite. The Hemlo deposit is the first reported Canadian locality for aktashite. In polished section the mineral is very similar to the tetrahedrite-tennantite minerals and, until the mineral was X-rayed, it was tentatively identified as a mercury-rich tennantite. Aktashite ranges in grain size from 10 to 300 μm .

Thallium minerals

Routhierite, (TlHgAsS_3), *parapierrrotite*, (TlSb_5S_8), *vaughanite*, ($\text{TlHgSb}_4\text{S}_7$) (a new mineral) and an unnamed thallium-bearing mineral have been encountered in the deposit. There is a close spatial association between the mercury and thallium minerals. In this regard, the realgar-cinnabar-rich quartz veins that occur within the central portion of the deposit, as defined by the zone of mercury minerals (Fig. 5), are common hosts for the thallium minerals. Routhierite is the most common thallium mineral,

parapierrrotite is less abundant, vaughanite and the unnamed mineral rare. This is the first reported occurrence of routhierite and parapierrrotite in Canada. *Parapierrrotite* is a rare mineral, originally described by Johan et al. (1975) from the Allchar deposit, Macedonia, Yugoslavia. The Allchar occurrence is famous because several new thallium minerals have been discovered there. Metallogenic studies of the Allchar district by Ivanov (1963) has shown an antimony-rich central zone surrounded by a Tl and As secondary zone which in turn is bordered by a belt with no metallic minerals, but characterized by an intense development of silicification and dolomitization. The mineralizations are linked to tuff and andesite melts. At Hemlo, parapierrrotite has been found in several drill holes and is recognized by its deep cherry-red internal reflections that are more apparent with oil immersion lenses. Grains of the mineral seldom exceed 200 μm in maximum dimensions and occur in isolation in the silicate gangue, in contact with routhierite, chalcostibite, aurostibite and criddleite. Microprobe analyses are given in Table A.6 and indicate that parapierrrotite is essentially identical in composition to its ideal formula, TlSb_5S_8 , with very little substitution of As for Sb.

Routhierite, TlHgAsS_3 was first described by Johan et al. (1974) from Jas Roux (Hautes-Alpes), France where it is associated with pierrotite, stibnite, smithite, sphalerite, realgar, orpiment, pyrite, laffittite and barite. At this occurrence, the mineralization was preceded by an intense metasomatic silicification of Triassic carbonate rocks which resulted in the formation of microcrystalline chert, as well as hydrothermal quartz, barite and fluorite. Mantienne (1974) concluded that the Jas Roux mineralization, of epithermal nature, is not genetically related to felsic rocks, but implies a relationship to an ancient geothermal zone associated with a deep suture. The description of routhierite by Johan et al. (1974) showed the presence of Tl, Ag, Cu, Hg, Zn, As, Sb, and S and gave the formula $(\text{Tl},\text{Cu},\text{Ag})(\text{Hg},\text{Zn})(\text{As},\text{Sb})\text{S}_3$, or a composition of the type MHgAsS_3 with Tl as the dominant element in the M position. Routhierite in reflected light is bluish white, weakly pleochroic, weakly anisotropic with red internal reflections. In the Hemlo deposit, it occurs as anhedral grains, up to 300 μm across, that are commonly associated with pyrite, stibnite, realgar, cinnabar, parapierrrotite, molybdenite, sphalerite and tetrahedrite-tennantite. The microprobe analyses (Table A.7) of the Hemlo routhierite show that copper is an essential constituent and that some grains contain antimony in excess of arsenic, even within the same polished section. X-ray single crystal studies of grains from sample W70, 738.9 m confirmed the identity of this mineral with type routhierite in that it has a tetragonal symmetry and cell dimensions of $a = 9.986(5)$, $c = 11.348(8)\text{\AA}$, very comparable to those previously reported for the mineral. The data obtained from the Hemlo routhierite indicate that the theoretical formula for routhierite should be redefined as $\text{CuTlHg}_2\text{As}_2\text{S}_6$. The grains in which antimony exceeds arsenic represent the antimony analogue of routhierite which, based on the standard rules of mineralogical nomenclature, could be considered as a new species. However, due to insufficient material to properly characterize

the mineral to meet the requirements of the Commission on New Minerals and Mineral Names, the mineral is referred to as an antimony-rich routhierite. *Vaughanite* is a new thallium-bearing mineral with the formula $\text{TlHgSb}_4\text{S}_7$. The mineral occurs as a 400 μm grain in sample GG25, 324.9 m in association with stibnite, pääkkönenite, realgar, native arsenic and parapirotite. The name and data have been accepted by the Commission on New Minerals and Mineral Names, IMA and a complete description of the mineral has been reported by Harris et al. (1989). An unnamed thallium-bearing mineral with the formula $\text{Pb}_2\text{Tl}_5(\text{Sb,As})_{24}\text{S}_{43}$ occurs as a 100 μm grain in quartz in contact with pyrite in sample W100, 784.2 m. Other minerals in the polished section are routhierite, sphalerite, aktashite, stibnite, parapirotite and realgar. More grains must be isolated before characterization of this mineral can be completed.

Sulphosalt minerals

Sulphosalt minerals in the ore are mainly of the lead sulphantimonide variety, and consist of zinkenite, boulangerite, twinnite, geocronite, dufrenoyite, jamesonite, baumhauerite, chalcostibite, berthierite, bournonite and seligmannite. The identities of the minerals have been based on their microprobe compositions and, where possible, on X-ray powder diffraction. The formulas derived from the microprobe analyses (Tables A.8 and A.9) are in general agreement with their ideal formulas and, where deviations occur, the difference is probably due to errors in analyses resulting from the minute grain sizes or the presence of impurities. *Zinkenite* is the most widespread and is only absent in the northwest down-plunge extension of the Page-Williams orebody defined by drill holes W116, W129, W135 and W137. The analyses listed in Table A.8 represent a very small number of the samples in which zinkenite occurs. The minerals *boulangerite*, *baumhauerite*, *twinnite*, *dufrenoyite* and *geocronite* are rare and their locations are essentially as given in Table A.8. *Chalcostibite* is rare and the composition of the mineral in the four drill holes is close to its ideal formula of CuSbS_2 , with no evidence of substitution of arsenic for antimony. *Bournonite* was only identified in the Page-Williams orebody where it occurs in six drill holes. Microprobe analysis shows that arsenic has readily substituted for antimony in most of the grains analyzed, to the extent that arsenic slightly exceeds antimony in atomic proportions in grains from sample W100, 818.0 m. Based on the accepted mineral nomenclature, the arsenic analogue of bournonite is *seligmannite*. *Berthierite* is the second most widespread sulphosalt. It has been identified in 11 drill holes, namely TC236, TC220W, GG20, GG21, GG23, GG25, GG37Y and GG45, W73, W104 and W100. It is most abundant in drill hole GG25 where it is the major sulphosalt in samples from 324.0 to 331.5 m. Commonly associated minerals are aurostibite and native antimony. Quantitative microprobe analyses for some berthierite grains are listed in Table A.9 whereas most berthierite grains were identified by their energy dispersion spectra and optical characteristics. The analyses of berthierite (Table A.9) indicates substitution of manganese for iron with grains in sample GG20, 884.8 containing 4.7 wt. % Mn and those in samples W100, 784.2 to 784.7 m indicating total replacement of iron by manganese, leading to the formula $\text{Mn}_{1.0}\text{Sb}_{1.98}\text{As}_{0.1}\text{S}_{4.09}$.

A weak powder pattern of the mineral indicates it is not structurally related to berthierite, but compositionally it is the Mn-analogue, and thus a new mineral species. Further work is underway on this mineral. *Jamesonite* is very rare and was identified in three drill holes, GG14 (composite sample), TC220W, 926.3 and W73, 33.8.

Telluride minerals

Telluride minerals are rare and the most abundant tellurides were encountered in narrow zones or seams in drill hole W137. The tellurides identified and their locations are as follows:

Mineral	Formula	Location
Clausthalite	PbTe	TC234,902.5
Melonite	NiTe_2	W135,1176.3
Hessite	Ag_2Te	W137,971.2
Calaverite	AuTe_2	W137,971.2
Petzite	Ag_3AuTe_2	W137,971.2
Coloradoite	HgTe	W70,718.6,722.9,735.1,758.6, 770.6; W135,1180.3; W137,971.2; W100,819.8; GG20,888.1
Altaite	PbTe	W135,1173.4,1177.5,1180.3,1 182.6-1184.95
Unnamed	AgSbTe_2	W137,971.2

The unnamed AgSbTe_2 is a new mineral, but sufficient material for its characterization is not available. This is the second reported occurrence of the mineral, as it was previously reported from the Mattagami Lake mine, Matagami area, Quebec (Thorpe and Harris, 1973).

Rare ore minerals

A few minerals have been identified in the deposit that are known from a very limited number or worldwide localities, and for which the Hemlo deposit constitutes the first reported locality in Canada. These minerals are as follows:

Mineral	Location
Galkhaite	TC218W,774.25; W100,784.2
Tvalchrelidzeite	W104,249.1
Pääkkönenite	GG25,324.9
Cafarsite	GG21,863.5

Galkhaite (Hg,Cu,Zn,Tl,Fe)₆(Cs,Tl)(As,Sb)₄S₁₂ has been tentatively identified in two drill holes. Its identification is based on a powder diffraction pattern and a microprobe analysis of one grain in polished section W100, 784.2 m that gave a composition $\text{Hg}_{3.9}\text{Cu}_{0.9}\text{Zn}_{0.7}\text{Tl}_{0.7}\text{Cs}_{0.3}\text{As}_{2.7}\text{Sb}_{0.6}\text{S}_{12}$. *Galkhaite* is a rare mineral, having been previously reported from the Gal Khaya deposit, Yakutia; the Khaydarkan deposit, Kirgizia (Gruzdev et al., 1972b) and the Getchell mine, Humboldt County, Nevada (Botinelly et al., 1973). Chen and Szymanski (1981, 1982) reported on the structure and chemistry of galkhaite and showed that the mineral contains Cs, not reported in the previous publications. *Tvalchrelidzeite* ($\text{Hg}_{12}(\text{Sb,As})_8\text{S}_{15}$) is rare and its identity is based on a microprobe analysis that gave Hg 65.1, As 6.9, Sb 15.4, S 12.7 wt. % or a formula of $\text{Hg}_{12}(\text{Sb}_{4.7}\text{As}_{3.4})_8\text{S}_{14.6}$, very

close to its ideal formula. Attempts to verify its identity by x-ray were not successful. *Pääkkönenite* (Sb_2AsS_2) was identified on the basis of a microprobe analysis that gave Sb 62.4, As 21.7, S 16.2, equivalent to $\text{Sb}_{1.96}\text{As}_{1.11}\text{S}_{1.93}$. The mineral occurs as acicular crystals less than 100 μm long within the recently described mineral vaughanite in sample GG25,324.9. *Cafarsite*, a rare Ca-Ti-Fe-Mn arsenate mineral was only identified in drill core GG21,863.5. It occurs as dark reddish brown irregular grains as large as 1 mm across that are associated with molybdenite, pyrite, tennantite, sphalerite and green vanadian muscovite. Cafarsite was first described by Graeser (1966) from Monte Leone-Decke in dolomitic rocks at Binnatal, Switzerland and a second occurrence was reported by Graeser and Roggiani (1976) from around Pizzo Cervandone on the Swiss-Italian border. The genesis of cafarsite is explained as the result of the <<remobilization>> of an old (Hercynian) Cu-As-ore deposit in the centre of the area. The formula of type cafarsite, based on a new chemical analysis and a crystal structure determination by Edenharter et al.(1977) is $(\text{CaO})_8(\text{Ti,Fe})_{6.5}\text{O}_{10}(\text{As}_2\text{O}_3)_6 \cdot 2\text{H}_2\text{O}$. Microprobe analysis of the Hemlo material showed significant amounts of V and Mn, therefore cafarsite specimens from the Swiss and Italian localities were obtained from S. Graeser for comparison. Results of the microprobe analyses are as follows:

	Hemlo	Italy	Switzerland
CaO	17.9	17.6	17.6
FeO	2.3	7.9	8.2
MnO	6.3	2.6	5.1
TiO ₂	11.5	13.4	11.5
Al ₂ O ₃	0.7	0.0	0.0
V ₂ O ₃	4.7	0.0	0.0
As ₂ O ₃	53.3	55.2	54.5
Total	96.7	96.7	97.9
Atomic proportions = 60 cations			
Ca	15.97	15.94	15.78
Fe	1.57	5.56	5.75
Mn	4.42	1.86	3.60
Ti	7.22	8.47	7.22
Al	0.73	—	—
V	3.14	—	—
As	26.94	28.17	27.64

Based on the microprobe analyses, the Hemlo cafarsite represents a Mn-rich variety with a significant vanadium content. Crystal structure studies are currently underway to determine the site occupancy of the various cations in order to determine the proper nomenclature for the Hemlo material.

Sparse ore minerals

Ullmannite (NiSbS) is present in six drill holes, of which five are in the David Bell and the Golden Giant orebodies. The mineral is sparse and occurs as 10–20 μm inclusions in pyrrhotite. *Gudmundite* (FeSbS) is rare and occurs in samples from the Golden Giant orebody in association with berthierite and aurostibite. Other well characterized minerals of worldwide distribution occur sparsely in the Hemlo deposit. These minerals and their locations are listed below.

Mineral	Location
Native silver	W129,1447.4; GG20, 909.5; NTC9W, 577.4
Cubanite	W100,819.8
Breithauptite	TC220W,925.7
Stibarsen	W92,639.5,640.0; W104,249.1; GG25,324.9,325.7,331.5,332.5
Wurtzite	hand specimen Page-Williams open pit

Oxide Mineralogy

Rutile

Rutile is widespread and occurs as subhedral to anhedral grains up to 2 mm in maximum dimensions, with most grains averaging less than 200 μm . In hand specimen, rutile appears as black submetallic crystals with some well developed faces. In polished sections with crossed nicols, some rutile grains exhibit cyclic twinning, but most show no twinning and appear as single crystals. Partial to nearly complete replacement by titanite is common. Microprobe analyses reveal that the rutiles within the gold-bearing zones are unique in that they contain as much as 5.6% V_2O_3 , 6.5% Sb_2O_3 and 3.2% WO_2 . The V, Sb and W contents of rutiles were determined for most of the drill holes and profiles of these elements for drill holes in the Golden Giant and the Page-Williams orebodies are presented later. Microprobe analyses of rutile in the David Bell orebody are listed in Table A.10. This is the first reported case of isomorphous substitution of V and Sb in rutiles.

Barian tomichite

Barian tomichite is the second most common oxide mineral, but it only occurs within the central portion of the deposit. Tomichite is a rare oxide mineral that was first reported from the "green leader" gold lodes at Kalgoorlie, Western Australia (Nickel, 1977; Nickel and Grey, 1979). Hemlo is the second reported locality in the world and the association of barian tomichite here with green vanadian muscovite is the same as for the lodes at Kalgoorlie. The Hemlo barian tomichite occurs as anhedral to subhedral tabular grains ranging from 50 μm to 3 mm in maximum dimensions (Fig. 13a,b). In hand specimens, tomichite is black with a metallic to submetallic luster, conchoidal fracture and a black streak. In polished section, its reflectance colour is grey in air and it is weakly to moderately anisotropic. It has been identified in drill holes GG14W, GG20, GG21, GG23, W70 and W100 and some common minerals within the same sections, although not always in contact with barian tomichite, are pyrite, molybdenite, stibnite, native arsenic, sphalerite, zinkenite, aktashite, tetrahedrite and vanadian muscovite, in a matrix of quartz, barian microcline and, sometimes barite. Microprobe analyses (Table A.11) reveal that the Hemlo tomichite is a barian variety that contains between 2.9 and 7.3% BaO and 1.2 to 10.0% Sb_2O_3 , unlike the Kalgoorlie tomichite which contains no barium and 0.95 to 1.44 Sb_2O_3 . X-ray single crystal studies on the Hemlo barian tomichite show that it has similar unit-cell parameters to those for

Kalgoorlie tomichite (i.e. $a = 7.10$, $b = 14.22$, $c = 5.04\text{\AA}$, $\beta = 104.9^\circ$), but with a different space group, A2/m. Its powder diffraction pattern is practically indistinguishable from that of barium-free tomichite. A crystal structure refinement of the barian tomichite and comments on its relationship to derbylite and tomichite have been reported by Grey et al. (1987).

Hemloite

A previously unknown oxide mineral, named *hemloite*, occurs in drill hole W70, 746.8m. In reflected light, it is lighter grey than barian tomichite and slightly darker grey than rutile. It has a distinct powder pattern and, based on a crystal structure study, the unit cell parameters are $a = 7.158$, $b = 7.552$, $c = 16.014\text{\AA}$, $\alpha = 89.06^\circ$, $\beta = 104.33^\circ$,

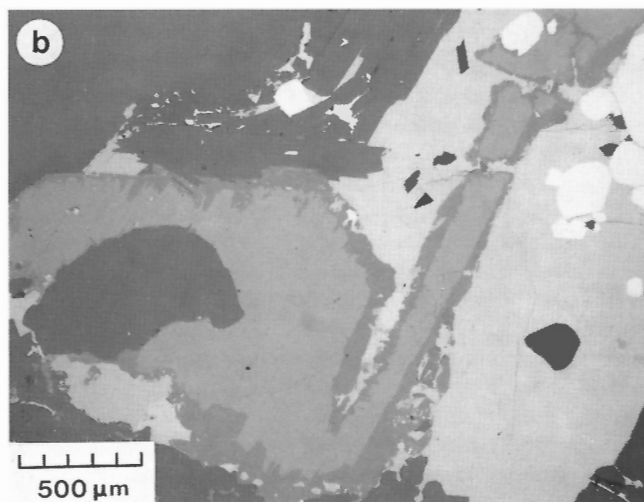
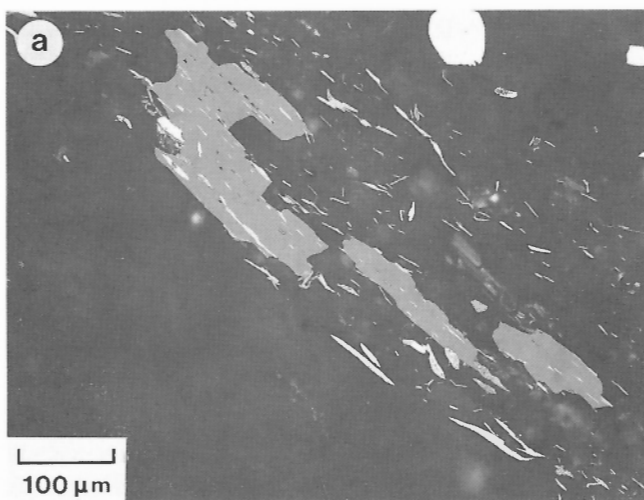


Figure 13(a). Photomicrograph of barian tomichite with aligned molybdenite flakes in a silicate matrix. W70, 735.1m. **(b).** Photomicrograph of barian tomichite (medium grey) with alteration rim of titanite (dark grey) in contact with coarse stibnite (light grey) and pyrite (white). W70, 735.1m.

$\gamma = 84.97^\circ$, space group $P\bar{1}$ with an ideal formula $(\text{As,Sb})_2(\text{Ti,V,Fe,Al})_{12}\text{O}_{23}(\text{OH})$. The mineral name and the above proposed formula have been accepted by the Commission on New Minerals and Mineral Names, International Mineralogical Association. A full description of the mineral is reported elsewhere (Harris et al., 1989).

Magnetite, hematite, ilmenite and chromite

These minerals are sparse in the deposit. *Magnetite* occurs in places within the hanging wall rocks where it is found in association with and rimming pyrite that has been partially replaced by pyrrhotite (Fig. 8d) and as isolated grains within several parts of the ore zones, particularly in the biotite-rich zones. Samples with magnetite as a major constituent were found in drill hole TC234 at a location near the thick diabase dyke that cuts the David Bell orebody. *Hematite* was only identified in one polished section from drill hole GG45, 1108.6m. Another V-Fe-oxide phase with a hematite-like powder pattern occurs in drill hole GG14W, 879.45m. It occurs as a platy crystal consisting of two minerals, a vanadium-rich hematite core with composition V_2O_3 40.6 wt.%, Fe_2O_3 54.2 wt.%, TiO_2 3.3 wt.%, Cr_2O_3 1.4 wt.%, equivalent to $\text{Fe}_{1.06}\text{V}_{.84}\text{Ti}_{.06}\text{Cr}_{.03}\text{O}_{3.01}$ and a rim of an iron-rich karelianite having a composition V_2O_3 50.7 wt.%, Fe_2O_3 38.3 wt.%, TiO_2 4.0 wt.%, Cr_2O_3 1.8 wt.%, equivalent to $\text{V}_{1.11}\text{Fe}_{.78}\text{Ti}_{.08}\text{Cr}_{.03}\text{O}_{3.05}$. *Ilmenite* is sparse in the gold-bearing zones. It was frequently noted in the metasedimentary hanging wall rocks and occasionally in the feldspar porphyry sills that have intruded the ore. Most ilmenite grains show no variation from the ideal formula, but samples from the hanging wall of drill hole TC218W, 745.9m contain 4.7 wt.% MnO and others in the ore zone at TC220W, 926.3 contain 7.2 wt.% MnO. *Chromite* is rare and was only identified in two drill holes, namely TC220W, 926.3m and W92, 663.5, 664.65, 667.7, 670.3m. Microprobe analyses as listed below shows that it is a zinc-bearing variety.

Microprobe Analyses of Chromite

	FeO	Cr ₂ O ₃	ZnO	Al ₂ O ₃	V ₂ O ₃	MnO	MgO
TC220W,926.3	17.4	45.4	17.6	15.7	—	2.1	0.4
W92, 667.7	18.7	33.9	17.0	23.9	2.1	0.8	0.6

Lewisite

A mineral tentatively identified as *lewisite* is present in samples from drill holes GG20, 888.1m, W28, 189.5m and TC220W, 926.3m. The mineral occurs as moderately coarse (up to 400 μm) honey-yellow anhedral grains. Microprobe analyses as listed below reveal that the mineral in samples GG20, 888.1m and W28, 189.5m is essentially a Ca-Ti-Sb-oxide whereas that in sample TC220W, 926.3m is a Ca-Ti-Sb-W-oxide and, judging from the low analytical totals, it probably also contains H₂O. A single crystal study of a grain from sample GG20, 888.1 shows that the mineral is cubic with $a = 10.25\text{\AA}$, space group Fd3m and possesses a pyrochlore structure, probably of the stibiconite subgroup. Based on the composition and on X-ray powder data that are

very close to those of lewisite, the mineral is possibly lewisite. Electron backscattered images of the grain in polished section TC220W, 926.3 reveal varying degrees of alteration or replacement and for this reason further studies were not undertaken. On the basis of its composition, this grain has been also tentatively identified as lewisite.

Microprobe Analyses of Lewisite

Sample	CaO	MnO	FeO	TiO ₂	Sb ₂ O ₃	As ₂ O ₃	WO ₃	Totals
GG20,888.1	15.9	0.9	0.2	25.4	54.6	3.0	—	100.0
W28, 189.5	16.2	0.	0.5	27.1	49.7	5.5	—	99.7
TC220W,926.3	13.4	1.1	1.1	25.5	37.8	0.8	10.3	90.0
	13.0	1.1	1.0	26.8	36.4	0.7	10.1	89.1
	14.3	0.9	1.1	27.6	31.7	0.7	11.8	88.1

Atomic Proportions based on 4 Cations

	Ca	Mn	Fe	Ti	Sb	As	W	O
GG20,888.1	1.10	0.05	0.01	1.25	1.47	0.12	—	6.05
W28,189.5	1.11	0.04	0.03	1.30	1.31	0.21	—	6.06
TC220W,926.3	1.06	0.07	0.07	1.41	1.15	0.04	0.20	6.40
	1.03	0.07	0.06	1.49	1.11	0.03	0.19	6.46
	1.13	0.06	0.07	1.53	0.96	0.03	0.22	6.47

Gangue mineralogy

The non-opaque minerals are listed in Table 1. The gangue minerals in the deposit are quartz, muscovite, phlogopite, microcline and barite, although in parts of the eastern portion of the deposit, biotite, plagioclase, tremolite and hornblende occur as major constituents within narrow drill core intersections. Some important characteristics of the gangue are the near absence of carbonates, the abundance of barite in the central portion of the deposit, the close correlation of green vanadian muscovite with the gold contents and the presence of barian microcline. Kyanite and staurolite are present in the metasedimentary hanging wall rocks and within parts of the ore zone. The occurrence of these minerals has led some researchers to suggest an amphibolite-facies metamorphic grade for the deposit (Quartermain, 1985; Kuhns, 1986; Burk et al., 1986).

The ore zone within the central portion of the deposit contains four rock types: (1) feldspar porphyry sills and intermediate to mafic barren dykes that have intruded the ore; (2) a feldspathic rock that comprises the major portion of the thicker parts of the ore unit; (3) a biotite-rich rock; and (4) a muscovite schist. The feldspathic rock, although commonly brecciated, usually has a sharp, locally sheared, contact with the footwall quartz-eye muscovite schist, and gold grades of this feldspathic rock in the Page-Williams orebody range from 6 to 20 g/t Au (Walford et al., 1986). The feldspathic rock in many places passes transitionally into a muscovite schist or biotite-rich rock, both to the east of the Golden Giant orebody and west of the Page-Williams orebody.

Detailed gangue mineralogy

Barite

Barite is a major constituent in both the Golden Giant and the Page-Williams orebodies. It occurs in massive zones principally within the feldspathic brecciated ore, as thin fracture fillings, and disseminated. The fracture-controlled barite usually constitutes 5% to 15% of the rock, with some areas containing up to 70%. In some barite-rich sections, angular fragments of ore are contained within the baritic matrix and only where sufficient ore fragments are present is the rock of ore grade (Fig. 14). Barite occurs in places throughout the complete width of the ore zone, but in the case of the east orebody of the David Bell mine, it is nearly absent (Fig. 6). Barite has also been identified in rock units situated below the ore zone on the Page-Williams property (McIlveen, 1983). Microprobe analyses of barite from 7 samples in drill holes W135 and 12 samples in W70 gave an average SrO value of 0.95 wt. % with a variation from 0.5 to 7.2 wt. %. In polished sections, the barite is interstitial to the silicate minerals and, except for some pyrite grains, it contains few ore minerals. This indicates that the barite formed later than the principal hydrothermal fluids that deposited the exotic suite of ore minerals. In the central part of the deposit where the ore is as much as 45 m thick, barite is most abundant and appears to dilute the ore while contributing in part to the extra thickness, in contrast to the 5 m thickness of the ore zone in the David Bell mine where barite is nearly absent. Where the ore zone within the David Bell mine thickens to 10 m, next to the Golden Giant orebody, barite becomes a major gangue constituent.

Feldspar

Feldspar is a major gangue mineral throughout the deposit. Feldspars include microcline, barian microcline and, less commonly, plagioclase. Microprobe analyses of feldspars in those samples for which polished thin sections were prepared are given in Table A.12. Most microcline is barium-rich and contains up to 9.5 wt. % BaO in the ore zones and up to 16.6 wt. % BaO in rare specimens collected from the

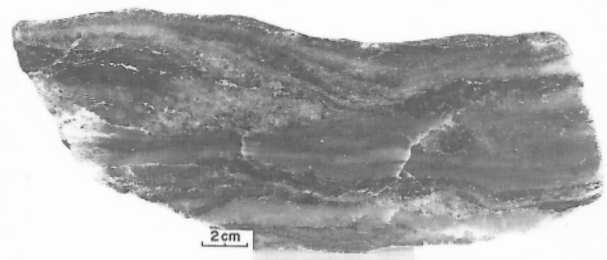


Figure 14. Photograph of a polished slab of barite-rich ore from the Golden Giant orebody. The barite shows a distinct flow texture enclosing ellipsoidal ore-bearing siliceous fragments. (GSC 204588-A)

immediate hanging wall rock. The barium content of microcline in the ore zone is very variable and, as shown in the electron backscattered images (Fig. 7), feldspar grains range from some with rhythmic zoning to others with irregularly distributed barium contents. Microprobe analyses of barian microcline have been obtained for most drill holes and the data are presented later in the section on mineral distribution. The paragenetic position of the microcline is uncertain, but it appears to have formed from the same potassium-rich hydrothermal fluids that contributed to the alteration of the rocks that now constitute the ore zones. The barian microcline lacks sericitic alteration attesting to its origin from the fluids that caused potassic alteration, including deposition of microcline in the felsic rocks and adjacent sediments. Barian microcline is the second most abundant barium-bearing species after barite, and in some "layers" it is the principal barium mineral. In thin section, some of the microcline grains are readily distinguished by their characteristic cross-hatch twinning, whereas other grains show no twinning. In this study, microprobe analysis of their barium contents was carried out to establish that the feldspars consist of the barium microcline. *Plagioclase* feldspars are less common in the deposit, and albite is the dominant species. In certain "layers", plagioclase of An₉₀ composition has been noted. The abundance of plagioclase feldspar is greatest within the David Bell orebody.

Micas

Micas are widespread and sericite, muscovite, green vanadian muscovite and biotite - phlogopite varieties are present. Sericitic alteration associated with the mineralization is developed adjacent to the feldspathic ore and is particularly extensive in the footwall. Sericite is widespread in the muscovite schist ore nearest the hanging wall in the Page-Williams orebody and constitutes most of the ore recovered from the open pit in the "A" orebody. Within the feldspathic ore, muscovite and vanadian muscovite are the most abundant micas. The vanadian muscovite, previously reported as roscoelite (Quartermain, 1985), is easily recognized by its light to dark grass-green colour. The intensity of the green colour increases with increasing vanadium contents. The name roscoelite is inappropriate for the green mica at Hemlo since roscoelite requires at least 15% V₂O₃ and a 1M muscovite structure (Heinrich and Levinson, 1955). The green mica at Hemlo contains no more than 8.5% V₂O₃ and X-ray studies show that it possesses the 2M muscovite structure, hence it is a *vanadian muscovite*. The vanadian muscovite has only been identified in the ore-bearing zones and, like molybdenite, it is spatially associated with gold mineralization. *Biotite* and *phlogopite* are the principal micas in the biotite-rich host rock that forms the eastern and western edges of the Page-Williams "A" orebody, the eastern half of the Golden Giant orebody and the western part of the David Bell orebody. Biotite also occurs as thin layers within the feldspathic rock that contains most of the ore in the Page-Williams orebody and lower levels of the Golden Giant orebody. The biotite-rich rocks contain most of the aurostibite found in the deposit. Microprobe analyses of the micas from eleven drill holes are listed in Table A.13. The Fe, V and Ba contents

of micas in four drill holes, namely GG20, GG23, W70 and W116 are presented later to show the relationship of these elements to the mineralogical and geochemical zonation within the ore zone. Chromium is not present in most of the micas, and others contain less than 0.3 wt.% Cr₂O₃, although one muscovite in drill hole TC236, 688.4 m contains 0.9 wt.% Cr₂O₃. The barium contents in the micas range from not detected to 6.9 wt.% BaO. Those that contain barium are principally the green vanadian muscovite, although there is no positive correlation between Ba and V values. The micas that occur outside the ore zone were not investigated in this study.

Accessory gangue minerals

Titanite or sphene, amphiboles of the hornblende and tremolite-actinolite varieties, zoisite, clinozoisite, apatite, zircon and tourmaline are the most common accessory gangue minerals. *Titanite* occurs throughout the deposit, generally as grains less than 40 μm that have formed by partial to nearly complete replacement of rutile. Coarser grains up to 2 mm across were noted in zones rich in tremolite and calcite. The mineral ranges from pink to greenish-yellow in colour, is homogeneous in composition and, in reflected light under the ore microscope, some grains exhibit even anisotropism whereas others consist of clusters of randomly oriented crystals. Microprobe analyses of titanite from a few selected drill holes are listed in Table A.14. The analyses show that titanite grains in the deposit have vanadium contents ranging from undetectable to as much as 14.2 wt.% V₂O₃. X-ray powder diffraction study of a grain containing 8.5 wt.% V₂O₃ (sample W70, 730.5m) revealed no detectable differences in its unit cell dimensions. *Amphiboles* are sparse, occurring generally within narrow zones, in which they are major constituents. In composition, they range from hornblende to tremolite-actinolite and occur in association with the biotite schists, generally in the David Bell and the Golden Giant orebodies. *Tourmaline* is irregularly distributed in the deposit and was observed within the footwall quartz-eye muscovite schist, in the ore zone in association with quartz veins and quartz-rich areas, in isolated layers within muscovite schists and in some biotite-rich zones. Tourmaline crystals as much as 1 by 5 cm in size in a quartz-rich sample associated with pyrite, vanadian muscovite and molybdenite were noted in samples from the underground workings of the Golden Giant mine. Also, an unusual zone within the Page-Williams orebody (drill core W70, 758.6m) contains a well foliated tourmaline-biotite schist with well developed crystals up to 1 by 5 mm in size. Microprobe analyses of some tourmalines (Table A.15) indicate they are the dravite variety. *Garnet* is rare in the ore zone, but Walford et al. (1986) reported an almandine garnet occurring with hornblende in sedimentary rocks within the hanging wall and footwall to the ore. In this study, a garnet was identified in one sample GG20, 879.6 and a microprobe analysis gave CaO 35.3, MnO 0.3, Al₂O₃ 11.7, Fe₂O₃ 0.2, V₂O₃ 13.5, SiO₂ 35.6 wt.% which indicates it is a vanadian grossular. *Zoisite* and *clinozoisite* were noted in several drill holes in quartz-rich areas containing calcite and biotite, in amphibole-rich zones and in the biotite schists. Microprobe analyses of some zoisite/clinozoisite grains are listed in Table A.16.

Carbonates are sparse in the ore zone, but in places, particularly within the tremolite-rich zones and in some quartz-rich areas that may represent remnants of boudinaged quartz veins, calcite is a major constituent. *Anhydrite* was noted in a few samples in which it occurs as fracture fillings or in fine intergrowths with barite.

GEOCHEMICAL FEATURES

The results of geochemical and isotopic studies of four drill holes from the deposit were reported by Cameron and Hattori (1985) and the characteristics of trace element dispersion halos in the hanging wall and footwall of the Golden Giant orebody have been reported by Kuhns (1986). The data from these studies, together with the mineralogical observations from this study, show that the ore zone is enriched in Mo, As, Sb, Hg, Tl, V and Ba. Table 3 presents a listing of the minerals found in the ore zone with an estimate of their relative contribution to the abundances of Au, Mo, Sb, As, Hg, Tl, V and Ba. Tl contents were reported by Cameron and Hattori (1985) for 32 samples from drill hole W70 of the Page-Williams orebody and these yielded a median value of 42 ppm and a maximum value of 350 ppm Tl. The maximum values for other elements in drill hole W70 over one metre intervals are: Mo 4000 ppm, As 1000 ppm, Sb 2000 ppm, Hg 77 ppm, Zn 620 ppm, V 3200 ppm, Ba 29.2 wt. %, B 430 ppm, Sr 1400 ppm (data from LAC Minerals geochemical report). Base metals such as Cu, Pb and Zn are generally low, but concentrations in selected drill core samples were as much as 890 ppm Cu in GG20, 888.1m, 88 ppm Pb in GG20, 888.1m and 3220 ppm Zn in GG14W, 885.3m. Mineralogical studies of these samples show that the high Cu values in GG20 are due to major tetrahedrite and minor chalcopyrite, the Pb values in GG20 are due to lead sulphosalts, and the Zn in GG14W is due solely to the presence of sphalerite. Compositional data from four drill holes through the deposit and its host rocks were published by Cameron and Hattori (1985). These data are reproduced in Table 4 and show that the ore zone and footwall are highly enriched in Mo, Hg and Sb. V is also enriched in the ore zone, being present primarily as green vanadian muscovite. Footwall alteration is characterized by low Mg, Mn and Ca and relatively high K values. Tourmaline, which occurs in both the footwall rocks and the ore zone, indicates that boron was either added to the rocks or was concentrated locally. Another general feature of the ore is the rather low carbonate content, but local concentrations of calcite have been identified in association with tremolite, clinozoisite and titanite within parts of the David Bell mine and, rarely, in the Golden Giant and Page-Williams orebodies. Significant concentrations of Ba as barite and barian microcline occur within the Page-Williams and the Golden Giant orebodies and parts of the David Bell orebody (Fig. 6). Analyses of drill core gave as much as 46.9 wt.% BaO in TC218W, 53.1 wt.% BaO in GG14W and 43.3 wt.% BaO in GG20. Graphite was reported by Brown et al.(1985) to occur in the Golden Giant orebody, but it was never detected in the numerous drill core samples from the orebody analyzed in this study. Silver concentrations are generally less than 3 ppm, with local concentrations as high as 200 ppm. The principal silver-bearing

mineral is tetrahedrite-tennantite. Microprobe analyses of the native gold grains (Table A.2) show that mercury is in excess of silver, except for grains in samples from the northwest down-plunge extension of the Page-Williams orebody that are more silver-rich. Kuhns (1986) reported that data from the Golden Giant ore indicate an average Au:Ag ratio of 6.6 and an average Au:Hg ratio of 0.58. The low Au:Hg ratio reflects the abundance of mercury minerals in the ore.

MINERAL DISTRIBUTION

The mercury minerals, namely cinnabar and aktashite, as well as realgar, are confined to the central portion of the deposit (Fig. 5). However, these minerals may be more widespread since drill core sampling indicated that in places they occur in millimetre-wide zones along fractures, and may thus not have been recognized during the sampling of all the drill holes. Barite, on the other hand, is more widespread, occurring throughout both the Page-Williams and the Golden Giant orebodies and within parts of the David Bell orebody (Fig. 6). Since Figures 5 and 6 illustrate the spatial distribution of these minerals as projected onto the vertical longitudinal section, the data fail to illustrate the spatial distribution from the hanging wall to the footwall of the ore zone. To illustrate these features, X-Y plots of all the minerals versus their depth location are presented. These X-Y plots represent the minerals identified in each polished and/or polished thin section and serve to illustrate the true spatial distribution within the ore zone. An X-Y plot has been prepared for each drill hole examined and these clearly reveal that the spatial distribution of the minerals within each drill hole and from one drill hole to the next is very heterogeneous. The only opaque minerals that appear to be uniformly present throughout the deposit are pyrite, rutile and molybdenite. The other minerals occur in various assemblages within zones or intervals that, in combination with other characteristics, give a stratified appearance to the deposit. The zones are of variable width and limited horizontal extension around each drill hole. When available, the gold assays, geochemical data and microprobe analyses of the rutiles, micas and feldspars are given for correlation with the mineral plots.

The David Bell mine

The orebody of the David Bell mine (formerly named Teck-Corona) is the eastern portion of the main Hemlo deposit and covers five tabular ore zones, (Fig. 4) designated the "A", "B", "C", "D" and "E" zones (Burk et al., 1986). Three zones are parallel to, and are within 50 m of either the upper or lower contacts of the quartz-porphyritic felsic rock. Because of the low density of drill hole intersections for certain areas of the deposit, the areal extents of some of the zones are not well known.

The "A" zone forms the eastern extension of the main mineralized zone in the Hemlo deposit and contains approximately 90% of the reserves of the David Bell mine or 105 t of gold. East of the central diabase dyke, the zone is generally 2-3 m thick, locally increasing to 6 m in thickness, and has an average grade of 12 g/t Au. West of the dyke, the

Table 3. Elemental listing of minerals and their abundance in the Hemlo gold deposit

	Major	Minor	Trace
Gold	Native gold	Aurostibite	Criddleite Calaverite Petzite
Molybdenum	Molybdenite	-	-
Antimony	Stibnite Zinkenite Tetrahdrite	Native antimony Boulangerite Bournonite Chalcostibite Gudmundite Berthierite Aurostibite Rutile (up to 6.5 Sb ₂ O ₃) Twinnite Parapirotite	Jamesonite Stibarsen Breithauptite Tvalchrelidzeite Lewisite Ullmannite Geocronite
Arsenic	Realgar	Orpiment Native arsenic Gersdorffite Barian tomichite Arsenopyrite Routhierite Aktashite Tennantite	Seligmannite Dufrenoyite Pararealgar Baumhauerite Cafarsite Stibarsen Geocronite
Mercury	Cinnabar Aktashite	Tetrahdrite (up to 18.6) Tennantite (up to 15.2) Native gold (up to 26.9) Sphalerite (up to 29.5) Routhierite	Tvalchrelidzeite Coloradoite
Thallium	Parapirotite Routhierite	-	Vaughanite Criddleite Galkhate
Vanadium	Muscovite (up to 8.5 V ₂ O ₃) Rutile (up to 5.6 V ₂ O ₃)	Barian tomichite Titanite (up to 14.2 V ₂ O ₃)	Cafarsite Grossular Hematite
Barium	Barite Microcline (up to 16.6 BaO)	Muscovite (up to 2.0 BaO)	Barian tomichite

Table 4. Distribution of elements in four drill cores from the Hemlo Deposit *Data from Cameron and Garreis(1980)

	HANGING- WALL META- SEDIMENTS (Median)	SERICITE SCHIST (Median)	---ORE ZONE--- MASSIVE BARITE (Median)	FOOTWALL METASEDIMENTS (Median)	ARCHEAN* SHALES (Mean)
NO.SAMPLES	18	42	29	27	406
ENRICHED					
Mo ppm(1)	7	935	1550	7	2.2
Sb ppm(3)	3.7	126	65	8	1.2
Hg ppm(3)	1.1	9	16	2.2	0.15
V ppm(1)	50	470	148	26	130
As ppm(3)	100	170	64	19	46
Ag ppm(2)	0.1	1.0	1.0	0.4	0.4
Ba % (5)	0.10	0.40	33.4	0.26	0.055
S % (6)	1.2	6.0	10.4	1.1	0.66
DEPLETED					
Mn ppm(1)	177	20	< 10	61	700
Ni ppm(1)	15	16	10	5	127
Cu ppm(1)	17	21	10	2	66
Cr ppm(4)	28	30	< 10	11	133
Co ppm(1)	14	15	22	10	35
Zn ppm(1)	57	61	122	43	323
Pb ppm(1)	10	8	6	18	26
Al ₂ O ₃ % (4)	15.7	9.7	2.1	16.3	16.9
TiO ₂ % (4)	0.40	0.39	0.24	0.27	0.73
MgO % (4)	1.3	0.49	0.10	0.82	3.3
Na ₂ O % (4)	2.0	0.74	0.16	2.0	2.5
CaO % (4)	2.9	0.42	0.11	1.4	2.1
CO ₂ % (6)	0.16	0.14	0.12	0.14	1.1
NEUTRAL					
Rb ppm(4)	45	48	14	83	91
Sr ppm(1)	460	170	250	348	199
K ₂ O % (4)	1.5	3.5	1.1	4.2	2.7
SiO ₂ % (4)	64.0	58.6	28.7	68.1	58.0
Fe ₂ O ₃ % (4)	3.6	8.4	2.2	1.5	7.6
P ₂ O ₅ % (4)	0.13	0.12	0.02	0.09	0.16
Analytical methods: (1) Emission - ICP, (2) AAS, (3) AAS-hydride, (4) XRF, (5) NAA, (6) Wet chemical					

ore thickness and grade increase gradually towards the west and down-dip adjacent to the Golden Giant orebody to a thickness of 10.5 m and an ore grade of more than 40 g/t Au. The zone cuts across the highly deformed conglomerate at a low angle. West of the central diabase dyke, the up-dip margin of the ore underlies the conglomerate, while to the east and down-dip, it overlies the conglomerate. Burk et al. (1986) reported that there is a broadly antipathetic relationship between areas where the conglomeratic unit is thickest and where the ore zone is thickest. It appears that in this part of the deposit, the ore-forming processes which resulted in the "A" zone operated most effectively in areas where the conglomerate was relatively thin or absent. However, observations based on the samples examined in this study show that both "ore" and barite thicken to the west towards the Page-Williams property.

The "B" zone is within the quartz-porphyrific felsic unit, approximately 20 m stratigraphically below the base of the main "A" zone. It has a very limited extent on the property. The mineralized zone is in sharp contact with muscovite-rich, quartz-porphyrific felsic rock on the hanging wall side, but the footwall is gradational with laminated muscovite-biotite-quartz schist. The "B" zone is hosted by schistose rock that is distinguished from the surrounding quartz-porphyrific felsic unit by its banded texture and lack of quartz phenocrysts.

The "C" zone, or lower zone as it is sometimes referred to, contains approximately 500 000 tonnes of ore on the property.

The "D" zone comprises two tabular bodies of disseminated mineralization occurring 10 to 20 m above the "A" Zone in the eastern portion of the property. Thickness of

the ore zones is approximately 2 m, and grade is in the range of 5 to 17 g/t Au. Various lithological units host the mineralization, including fine grained, biotitic and chloritic schist west of the central diabase, and quartzfeldspathic rock and highly strained conglomerate east of the dyke.

The "E" zone forms an oblong body up to 4 m thick within the highly deformed conglomerate unit and is located chiefly to the east of the central diabase. The mineralization is disseminated in a quartz-muscovite schist and laminated quartzfeldspathic rock.

Drill hole TC232, the most easterly hole examined on the property, intersected two zones, the upper "D" zone at approximately 486 to 488 m, and the lower main "A" zone at approximately 502 to 505 m. The minerals present and their distribution are shown in Figure 15. No gold minerals were detected in the samples collected. The two zones are very similar mineralogically, consisting of pyrite with minor to trace amounts of chalcopyrite, pyrrhotite, molybdenite, gerdorffite and magnetite. Most of the chalcopyrite and pyrrhotite occur as inclusions in pyrite. In the upper "D" zone, anhydrite occurs as coarse grains in quartz-feldspar veins that appear to have formed late in the deformational history. The most conspicuous minerals in the upper quartzfeldspathic rock are inclusions of brownish-red titanite and pale olive green clinozoisite. At 489.0 m, the host rock is mainly a chlorite schist. The lower main "A" zone consists of alternating layers of muscovite and phlogopite schists, with minor quartz stringers. At the base of the zone, the muscovite schist contains a few euhedral pale brown tourmaline crystals, calcite and millimetre-thick molybdenite-rich seams. The failure to detect gold minerals would suggest that the gold is not evenly distributed throughout the zones, but occurs within thin molybdenite-rich seams.

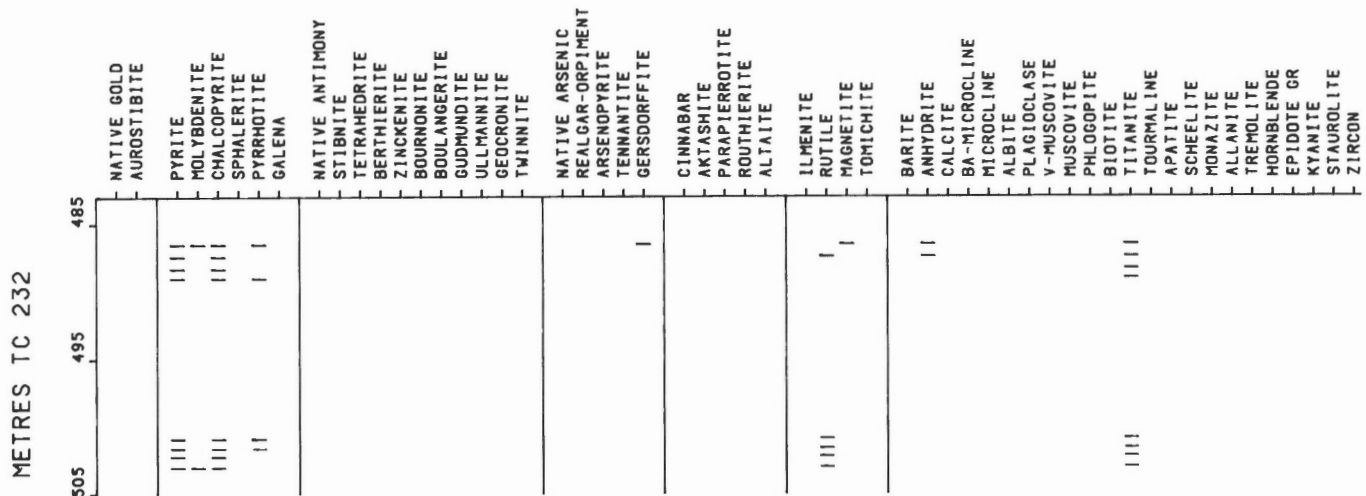


Figure 15. Plot of mineral distribution versus depth across the ore zone within drill hole TC232.

Drill hole TC236 is slightly down-dip from TC232 and also intersected two mineralized zones, the upper "D" or "E" zone at 674 to 678 m and the main "A" zone at 683 to 690 m. The minerals present and their distribution are shown in Figure 16. The main feature of the "D" or "E" zone is the presence of aurostibite in association with minor to trace amounts of berthierite, stibnite, native antimony, pyrrhotite, pyrite, arsenopyrite, molybdenite and sphalerite. No native gold was detected, but too little aurostibite was found to account for the gold assays. At 677.0 m the mineral chalcocite was identified. In most sections, pyrrhotite exceeds pyrite in abundance. The host rock is chiefly a phlogopite-biotite schist with some calcite as thin stringers. The main "A" zone contains native gold, pyrite, molybdenite, and stibnite, with trace amounts of tetrahedrite, chalcopyrite, zinkenite, ullmannite and sphalerite with a mercury content of 24.1 wt. %. At 685.9 m the host rock is a muscovite schist with some tourmaline. At 688.4 m the matrix is characterized by layers of dark green mica containing 0.9 wt. % Cr₂O₃ and 2.0 wt. % BaO. Vanadium was not detected in this mica. Towards the footwall contact at 689.9 m, major barite and minor anhydrite are present.

Drill hole TC216 near the down-dip limits of the "A" zone east of the central diabase dyke intersects two ore zones, the "E" zone at 849.0 to 853.0 m and the lower "A" zone at 874.0 to 877.2 m. The minerals and their distribution are shown in Figure 17. The "E" zone is pyrite-rich and contains fine grained (<5 μm) native gold with minor to trace amounts of molybdenite, chalcopyrite, sphalerite, stibnite, pyrrhotite, tetrahedrite, arsenopyrite, ullmannite and gersdorffite. The main "A" zone is also pyrite-rich with traces of molybdenite, chalcopyrite, pyrrhotite and sphalerite. Native gold, the principal gold mineral, occurs as <10 μm inclusions in gangue, although aurostibite is present at 876.3 m as <3 μm grains in gangue. Pyrrhotite and chalcopyrite occur principally as inclusions in pyrite. The host rock for the upper "E" zone is a sugary to massive felsic rock containing molybdenite, which imparts a bluish colour to the quartz, and traces of vanadian muscovite (2.8% V₂O₅, 6.9% BaO). The pyrite is distributed interstitially to the quartz and the rock has a strongly deformed character. The host rock for the lower main "A" zone is very similar and contains vanadian muscovite (1.9% V₂O₅, 2.1% BaO) and abundant barian microcline at 875.3 m that has as much as

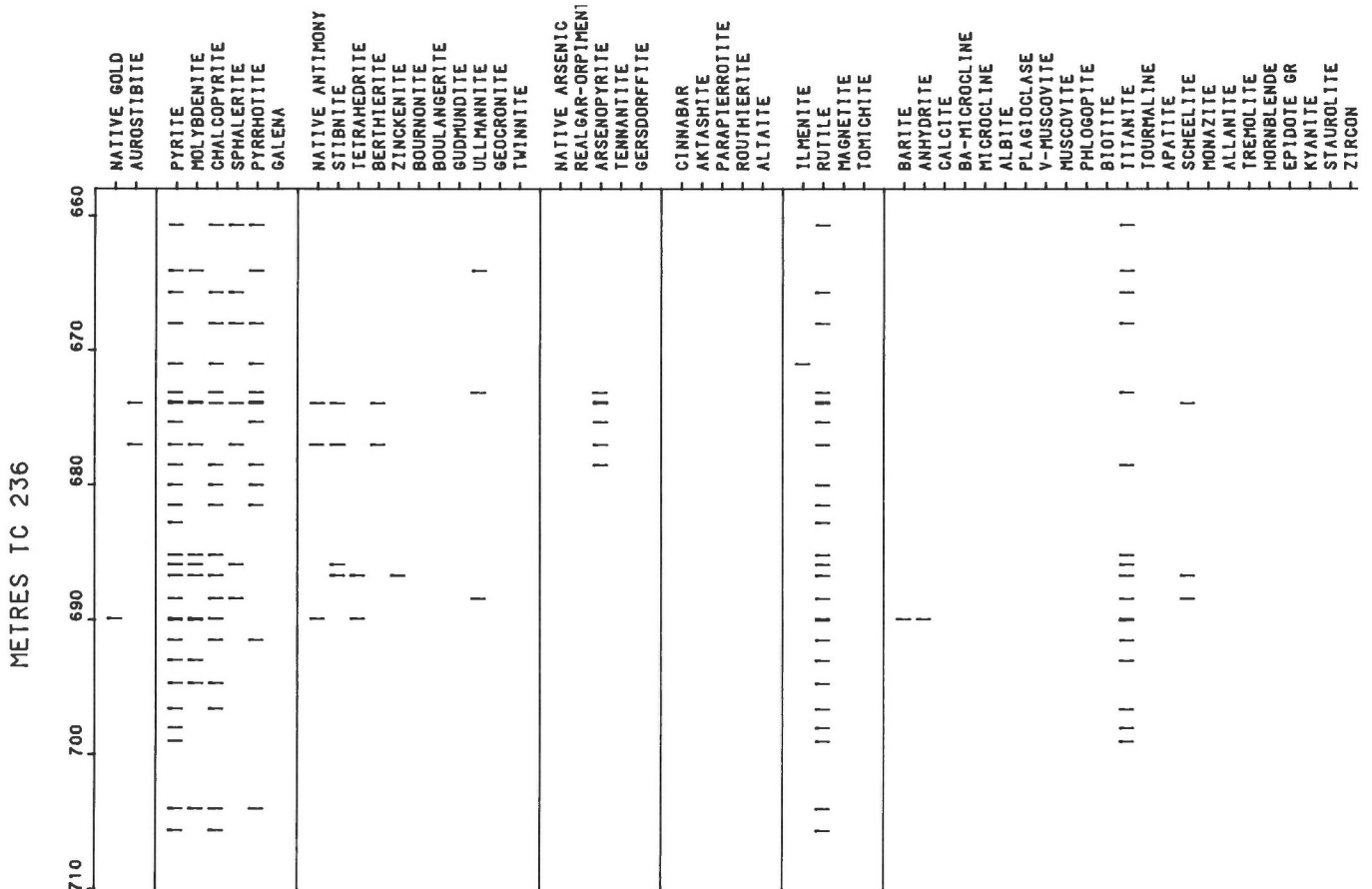


Figure 16. Plot of mineral distribution versus depth across the ore zone within drill hole TC236.

9.5% BaO. The major differences between the two zones is the presence of barian microcline within the lower zone near the footwall contact.

Drill hole TC234 is immediately west of the central diabase and intersects the main "A" zone at approximately 902 to 906 m. The minerals and their distribution are presented

in Figure 18. The main "A" zone contains coarse pyrite, in places partly altered to pyrrhotite and magnetite, fine grained native gold and traces of chalcocopyrite, molybdenite, gersdorffite, ullmannite and tetrahedrite. One small grain of clausthalite was identified in a section at 902.5 m. The gangue minerals consist of barian microcline with BaO contents from

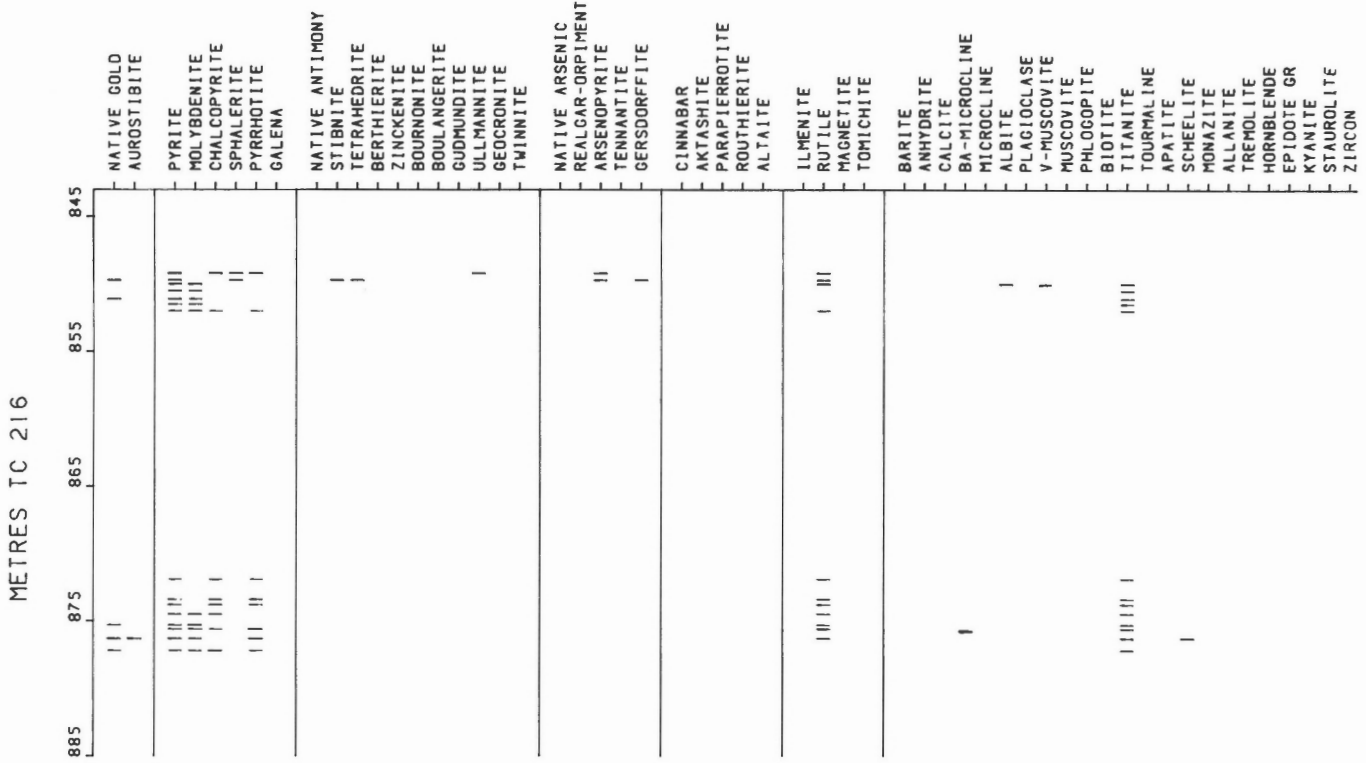


Figure 17. Plot of mineral distribution versus depth across the ore zone within drill hole TC216.

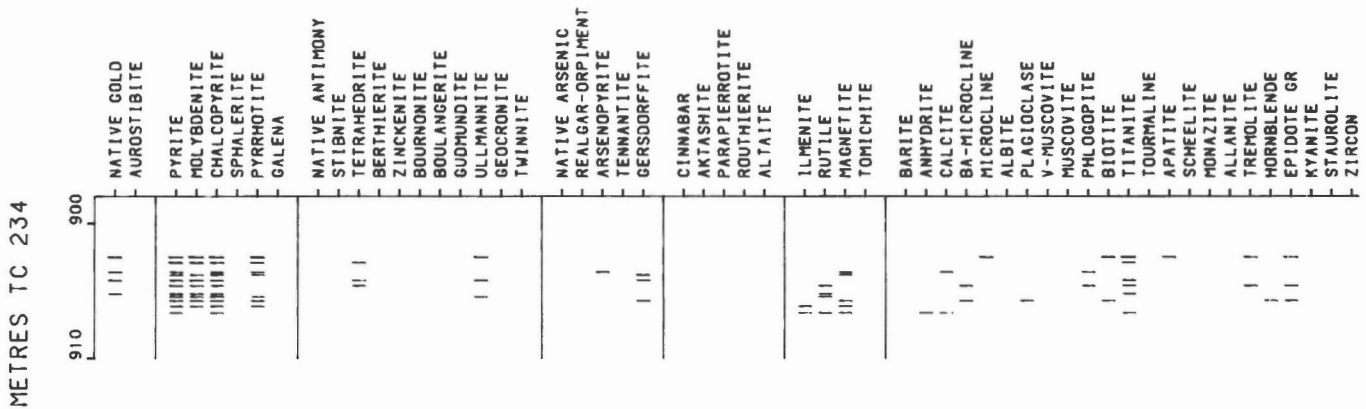


Figure 18. Plot of mineral distribution versus depth across the ore zone within drill hole TC234.

0.5 to 2.4 wt. %, actinolite-tremolite, hornblende, clinozoisite, calcite-dolomite, biotite, minor plagioclase (An₁₄), and traces of anhydrite and chlorite. This zone is characterized by the abundance of ferromagnesian minerals, biotite-rich layers, alteration of pyrite to pyrrhotite and magnetite, carbonate, and clinzoisite with minor plagioclase. Zones containing similar mineral assemblages occur within the Golden Giant orebody along the eastern contact with the fragmental unit.

Drill hole TC220W intersected two zones, namely the main "A" zone and the lower "C" zone. Samples were only studied from the "A" zone at 923 to 928 m. The minerals and their distribution are presented in Figure 19. This location represents the eastern limits of the zone of mercury minerals and realgar within the Hemlo deposit. The opaque minerals are pyrite, molybdenite, native gold, aurostibite, native antimony, berthierite, stibnite, tetrahedrite, zinkenite, bournonite, boulangierite, gudmundite, ullmannite, geocronite, twinnite, native arsenic, realgar-orpiment, arsenopyrite, tennantite, gersdorffite, cinnabar, aktashite, papierrotite, routhierite, altaite, ilmenite, rutile, magnetite, tomichite, barite, anhydrite, calcite, ba-microcline, microcline, albite, plagioclase, v-muscovite, muscovite, phlogopite, biotite, titanite, tourmaline, apatite, scheelite, monazite, allanite, tremolite, hornblende, epidote gr, kyanite, staurolite, zircon

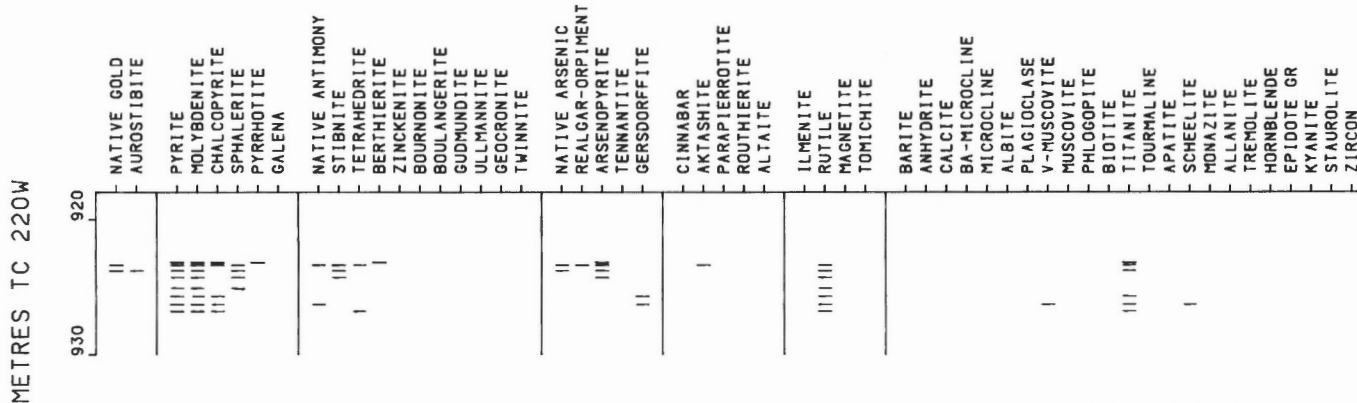


Figure 19. Plot of mineral distribution versus depth across the ore zone within drill hole TC220W.

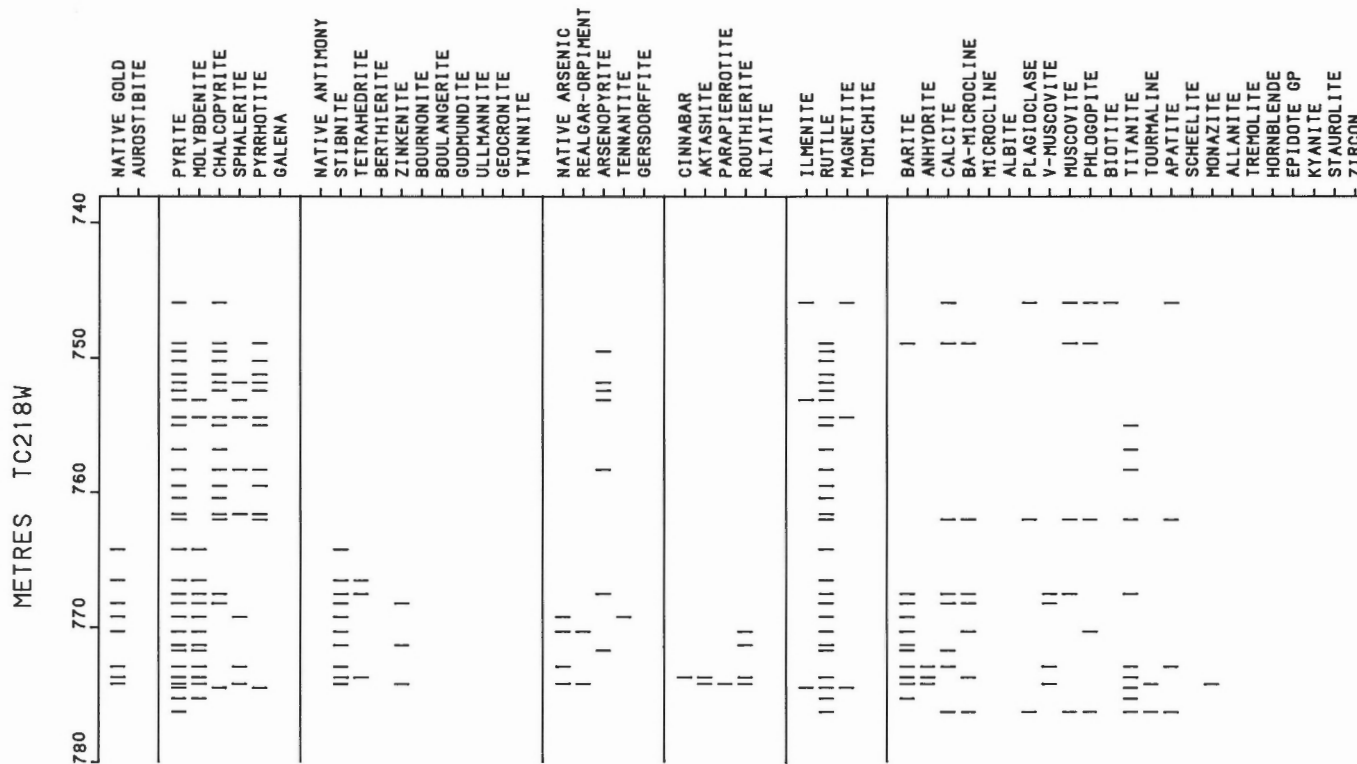


Figure 20. Plot of mineral distribution versus depth across the ore zone within drill hole TC218W.

breithauptite. The native gold grains contain as much as 26.9 wt. % Hg and the sphalerite grains contain as much as 29.5 wt. % Hg, the highest mercury contents that were detected for these minerals in the deposit. Rare accessory minerals in sample 926.3 m are scheelite in coarse grains that are rimmed with ferberite and zincian chromite (an analysis is listed under chromite description). Microprobe analysis of the scheelite gave CaO 20.0, WO₃ 78.7 wt.% and of the ferberite FeO 17.5, MgO 2.2, MnO 4.6, WO₃ 76.0 wt.%. The host rock consists of thin layers of mica that has a deep-chloritic-green colour without detectable V₂O₅ and Cr₂O₃, but with 1.2 % BaO, which is partly intergrown with biotite. Sample 923.45 m contains a coarse fragment of quartz that is rich in coarse stibnite, yellow sphalerite and minor realgar. The quartz is similar to the boudinaged stibnite-realgar-rich quartz veins that are common in the Golden Giant and Page-Williams orebodies. Most of the host rock is a muscovite schist with wavy layers of pale to dark green vanadian muscovite, both disseminations and layers of phlogopite-biotite, and traces of tourmaline.

Drill hole TC218W represents some of the highest gold grades encountered in the David Bell orebody, with 1 m inter-sections containing as much as 100 g/t Au. The average grade over 11.3 m from 763.8 to 775.1 is approximately 28 g/t Au and this part of the orebody contains the thickest ore. Burk et al. (1986) reported that a drill hole in the same area intersected 10.5 m of ore grading more than 40 g/t Au. The minerals and their distribution are presented in Figure 20. Sampling of this hole commenced at 745.9 m, which is 18 m above the main ore zone. At this location the host rock is a fine grained biotite schist that represents the hanging wall metasedimentary rocks. Lower in the drill hole, the first evidence of alteration is the appearance of a pyrite-rich feldspathic to muscovite schist with layers or zones of biotite-phlogopite. Within this rock at 748.9 m, trace amounts of barite and barian microcline containing as much as 17 wt. % BaO were noted, and at 753.5 to 754.0 m trace amounts of molybdenite are present, but without economic gold

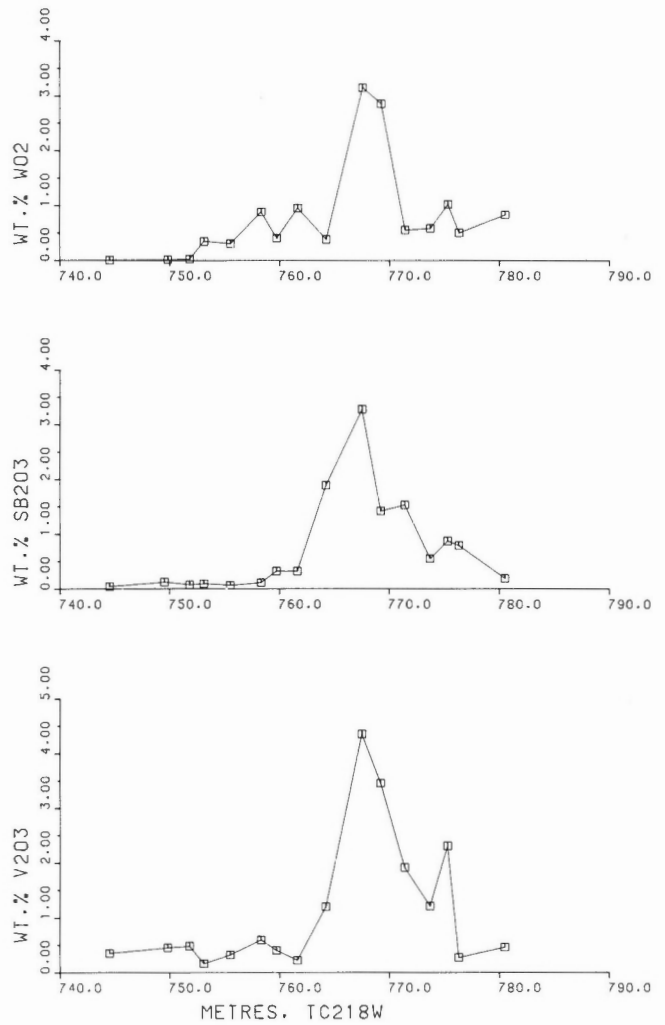


Figure 21. Plot of V₂O₅, Sb₂O₃ and WO₂ contents of rutile across the ore zone within drill hole TC218W.

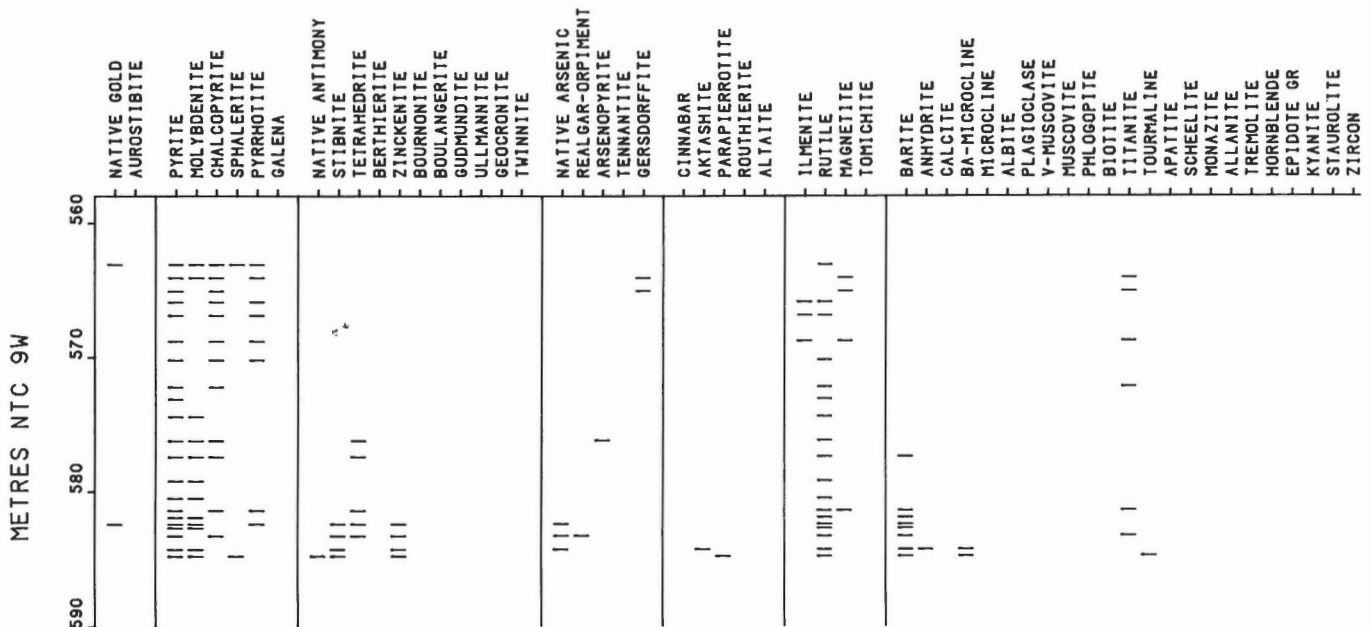


Figure 22. Plot of mineral distribution versus depth across the ore zone within drill hole NTC9W.

values. The main ore zone extends from 763.8 to 775.1 m (this intersection does not represent a true width for the zone because it is uncorrected for the drill hole angle) and is characterized by the presence of abundant molybdenite, vanadian muscovite (Table A.13), barian microcline (Table A.12), V-Sb-W-bearing rutile (Fig. 21), and, in the case of the footwall portion of the zone, abundant barite. The ore minerals consist of stibnite, native gold containing as much as 19.3 wt. % Hg (Table A.2), mercury-bearing sphalerite with as much as 27.5 wt. % Hg (Table A.1), the mercury minerals cinnabar and aktashite, the thallium minerals routhierite and parapierrrotite, and trace amounts of native arsenic and realgar. The footwall contact is distinguished by a well foliated quartz-eye muscovite schist with minor to trace amounts of biotite-phlogopite and tourmaline.

Drill hole NTC9W is within a block of ground known as the 1/4 claim (50% David Bell mine / 50% Golden Giant mine). Golden Giant's shaft is located within this block of ground and the ore is mined from this shaft. The minerals present and their distribution are presented in Figure 22. The gold-bearing zone extends from 563.0 m to 584.9 m with a hanging wall zone one metre thick containing approximately 4 g/t Au and a footwall zone from 581.6 to 584.9 m containing approximately 10 g/t Au. Between these two zones, the rock contains anomalous gold values that average approximately 1 g/t. The host rock consists principally of biotite-hornblende-quartz-feldspar and biotite-quartz-feldspar schists that enclose a quartz-feldspar porphyry sill and feldspar porphyry quartz monzonite fragments. These lithologies represent Unit 4 as described by Kuhns et al. (1986). Unit 4 on the Golden Giant property pinches out down-dip and to the west. The unit is dark grey to black, medium grained, strongly foliated and compositionally banded. Even though parts of Unit 4 contain anomalous gold values throughout much of its extent, it hosts considerable amounts of ore within the central part of the deposit. The footwall ore zone at 581.6 to 584.9 m is characterized by the presence of vanadian muscovite, V-Sb-W-bearing rutile, barite, minor barian microcline, stibnite, zinkenite, sphalerite with 17.3 wt. % Hg, native arsenic, realgar, aktashite and parapierrrotite. Barite also occurs above the footwall ore zone within the biotite-hornblende-quartz-feldspar schist that is anomalous in gold. The rutile compositions define the gold-rich ore zones (analyses below). Both the upper zone at 563.1 m and the lower zone at 582.4 to 584.8 m contain rutile with high vanadium contents. Antimony, on the other hand, shows a decrease in these two zones. The lower zone is also characterized by the presence of vanadian muscovite and barian feldspar. Unit 4 is apparently the main ore-bearing horizon and the degree of alteration by the ore-forming fluids appears to have determined the width and grade of the gold zones. Where the ore forming fluids have resulted in extensive potassic alteration with the formation of vanadian muscovite, barian microcline, V-Sb-W-rutile and various Sb, As and Hg minerals, the zones contain gold of economic importance. The sharp footwall contact is a strongly foliated, thinly layered, white to yellowish-grey quartz-muscovite-feldspar schist (Unit 3, Kuhns et al., 1986).

Microprobe Analyses of Rutile in Drill Hole NTC9W

Metres	TiO ₂	V ₂ O ₃	Sb ₂ O ₃	WO ₂	Fe ₂ O ₃
563.1	96.7	1.7	0.5	0.6	—
565.9	95.9	0.6	1.2	0.7	0.7
570.2	96.7	—	1.1	—	0.8
572.2	96.5	0.4	1.0	0.6	0.7
574.4	96.6	0.4	1.4	0.4	0.8
576.2	96.1	0.4	1.2	0.5	0.8
577.4	96.3	0.3	1.4	0.4	0.8
579.2	95.1	0.2	1.1	0.8	1.2
581.2	95.6	—	1.0	0.3	1.0
582.4	97.2	0.9	0.7	0.4	—
583.3	96.9	1.4	0.1	0.2	—
584.3	96.8	1.3	0.7	0.2	—
584.8	96.4	0.7	0.8	—	—

The Golden Giant mine

The Golden Giant orebody represents the central portion of the deposit, bordered on the east by the David Bell orebody, and on the west and up-dip by the Page-Williams orebody. Seven drill holes were selected for study. The orebody increases in thickness towards the west and attains maximum true widths of approximately 40 m in the vicinity of drill hole GG21 (Fig. 4). A second zone, the Lower Mineralized Zone, is 2-5 m thick and is located 40-80 m stratigraphically below the main orebody (Brown et al., 1985). The principal ore host in the upper levels and eastern portion of the deposit is a biotite-rich rock which passes transitionally into a muscovite schist and/or feldspathic rock to the west and down-dip (Fig. 4). This rock unit is referred to as Unit 4 by Kuhns et al. (1986).

Drill hole GG25 represents the uppermost levels in the Golden Giant mine and is adjacent to the Page-Williams boundary that defines the down-dip extension of the "A" orebody. The orebody extends from 322.6 to 354.85 m in this hole, for a true width of 23.6 m. The minerals and their distribution are presented in Figure 23. The upper part of the ore zone from 322.6 to 333.0 m consists of a foliated biotite schist with minor amounts of hornblende, chlorite, barite, anhydrite and calcite. The ore minerals are aurostibite, native gold, native antimony, berthierite, molybdenite, pyrrhotite, native arsenic, arsenopyrite and variable amounts of stibnite, tetrahedrite and zinkenite. The sample at 324.9 m contains the recently named gold mineral, criddleite, that is associated with native gold, aurostibite, chalcostibite, realgar, cinnabar, native antimony and native arsenic in a boundinaged quartz vein. Barite occurs throughout this zone as a minor constituent, whereas rutile is absent. This zone contains the highest gold grades. At 333.1 m to 337.0 m, the biotite schist grades to a muscovite schist with dominant green vanadian muscovite, rutile and minor barite. The ore minerals are characterized by native gold, stibnite, native arsenic, realgar and traces of cinnabar, aktashite and parapierrrotite. The interval 338 to 341 m consists mainly of a biotite-feldspar porphyry sill that contains no mineralization. From 342 to 350 m the host is principally a muscovite schist with some tourmaline, phlogopite and coarse pyrite.

METRES-HEMLO GG25

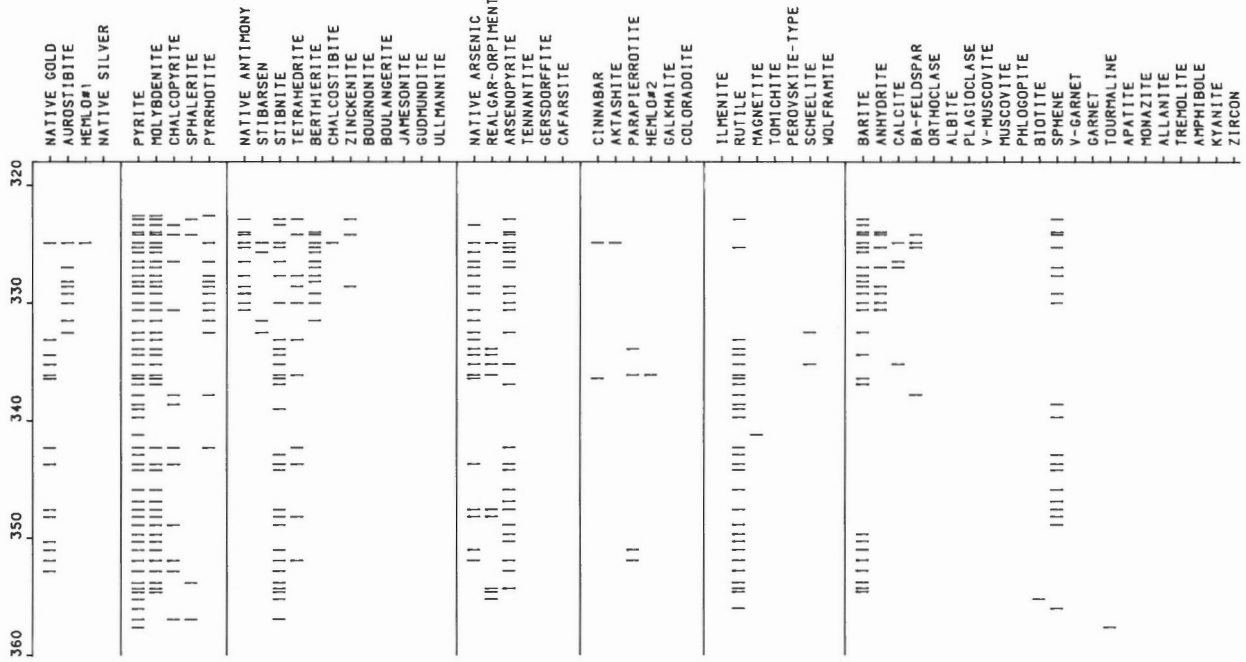


Figure 23. Plot of mineral distribution versus depth across the ore zone within drill hole GG25.

METRES GG 23

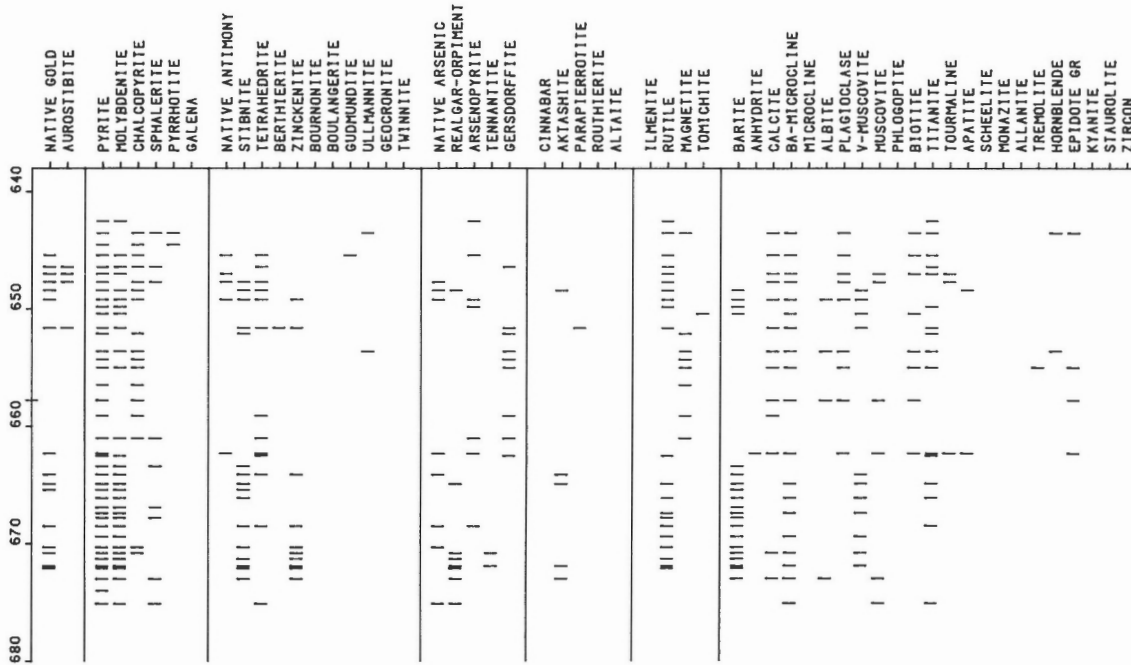


Figure 24. Plot of mineral distribution versus depth across the ore zone within drill hole GG23.

Included in this zone are narrow tremolite-rich bands. The gold grades are variable, with native gold, stibnite, molybdenite and pyrite the main ore minerals. The lower portion of the ore zone from 350 to 355 m, which, in part, has a fragmental texture and is barite-rich. The ore minerals are essentially identical to those in the previous zone. The footwall contact is sharp and is characterized by a strongly foliated quartz-eye muscovite schist with some tourmaline.

Drill hole GG23 is approximately 400 m down-dip from GG25 close to the western boundary of the 1/4 claim. The ore zone extends from 642.3 to 673.4 m or a true width of 23.72 m. The minerals and their distribution are presented in Figure 24, which represents data obtained from both polished sections and polished thin sections. The gold assay data are plotted in Figure 25. The stratigraphy is very similar to that of GG25, with the upper portion of the ore zone from above the hanging wall to 662.3 m consisting of biotite schist which contains hornblende, tremolite, plagioclase (albite to An₄₃), chlorite, barian microcline and epidote. Within this unit are seams of green vanadian muscovite interlayered with biotite which it appears to have partially replaced. The FeO, V₂O₃ and BaO contents of the muscovite and biotite are shown in Figures 26 and 27, respectively. It is of interest to note that a biotite at 650.4 m contains 1.5 wt. % V₂O₃. The lower portion of the ore zone from 663.4 to the footwall at 673.4 m is barite-rich and in places this portion has a fragmental texture and contains barian microcline, quartz, muscovite and pale green vanadian muscovite. The barium contents of the microcline throughout the ore zone are shown in Figure 28. The ore minerals in the upper, lower-grade

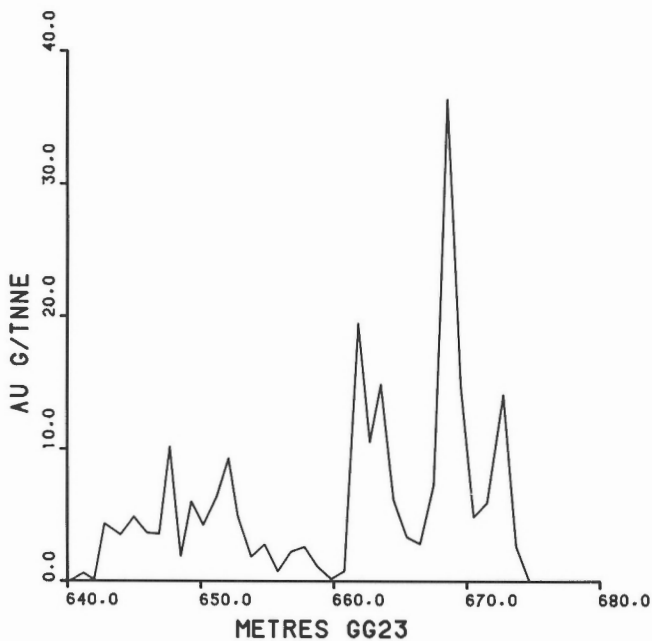


Figure 25. Profile of gold assay data across the ore zone within drill hole GG23.

portion consist of both native gold and aurostibite, with minor native antimony, stibnite, tetrahedrite, native arsenic and rare aktashite and parapirotite. The lower, higher-grade zone contains no aurostibite, and stibnite and zinkenite are the main antimony minerals, realgar is the main arsenic mineral and rare parapirotite is present. Rutile throughout the ore zone contains V, Sb and W (Fig. 29). The sharp footwall contact is marked by a well foliated muscovite schist containing barian microcline.

Drill hole GG14W is approximately 150 m down-dip from drill hole GG23. Specimens from this drill hole were selected for geochemical analyses and isotopic study of the pyrite and barite by Cameron and Hattori (1985). The hole intersected the main ore zone at 866.0 to 887.0 m, where it has a true width of 19.89 m, and a lower mineralized zone at approximately 934 to 938 m. The gold grades are variable in the

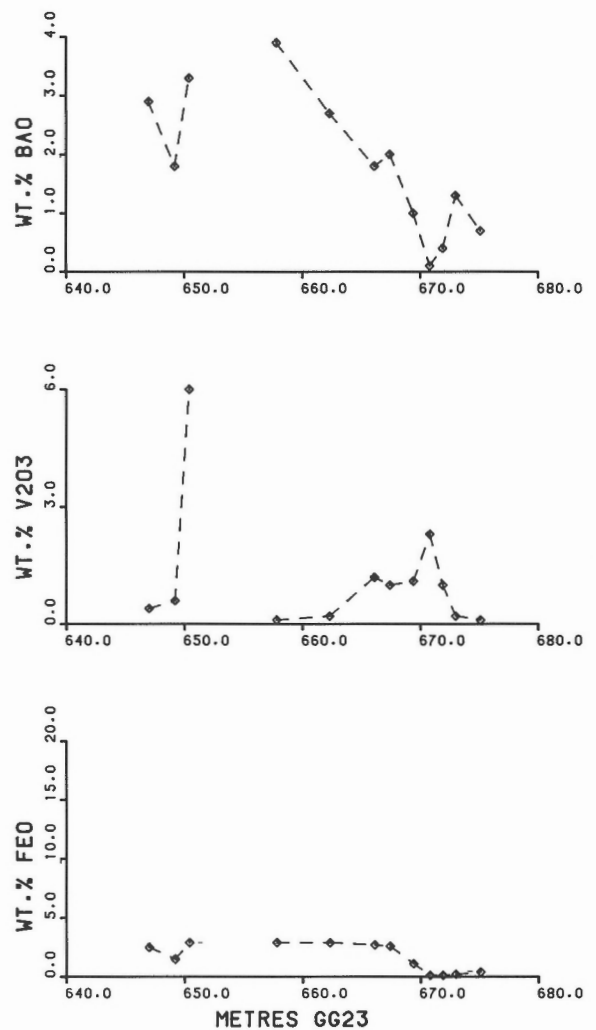


Figure 26. Plot of FeO, V₂O₃ and BaO contents of muscovite across the ore zone within drill hole GG23.

lower mineralized zone, and a maximum assay grade of 9.2 g/t over a 1.5 m interval was obtained. The minerals and their distribution are presented in Figure 30, with geochemical profiles of the elements Au, Mo, V, Sb and BaO across the main ore zone presented in Figure 31. A specimen examined from the metasedimentary hanging wall at 855.8 m consists of a kyanite-bearing muscovite schist with some tourmaline. The contact of the ore zone at 866.3 m is characterized by a biotite schist grading to a dark green vanadium-bearing muscovite schist at 867.3 m, which in turn grades to a barite-bearing feldspathic rock at 873 m that contains wisps of pale green vanadian muscovite. The footwall at 887 m is characterized by a muscovite schist. As shown in the mineral plot, the ore minerals from 866 to 880 m consist mainly of native gold, molybdenite, stibnite and traces of native arsenic, realgar and aktashite. The lower portion of this zone to the footwall contact at 887 m contains native gold, molybdenite and minor to trace amounts of sphalerite, tetrahedrite, zinkenite and native arsenic. Microprobe

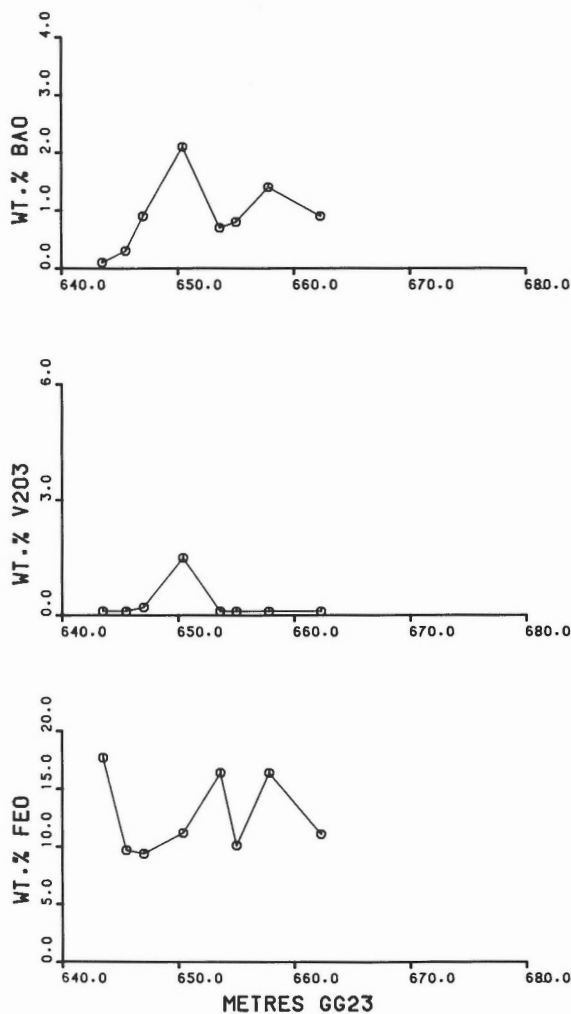


Figure 27. Plot of FeO, V₂O₃ and BaO contents of phlogopite-biotite across the ore zone within drill hole GG23.

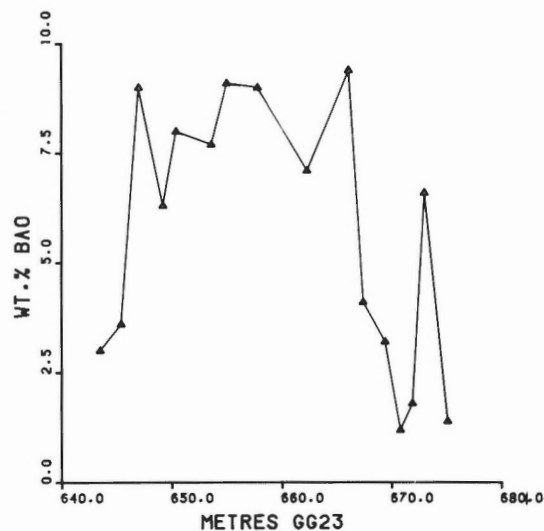


Figure 28. Plot of BaO contents of microcline across the ore zone within drill hole GG23.

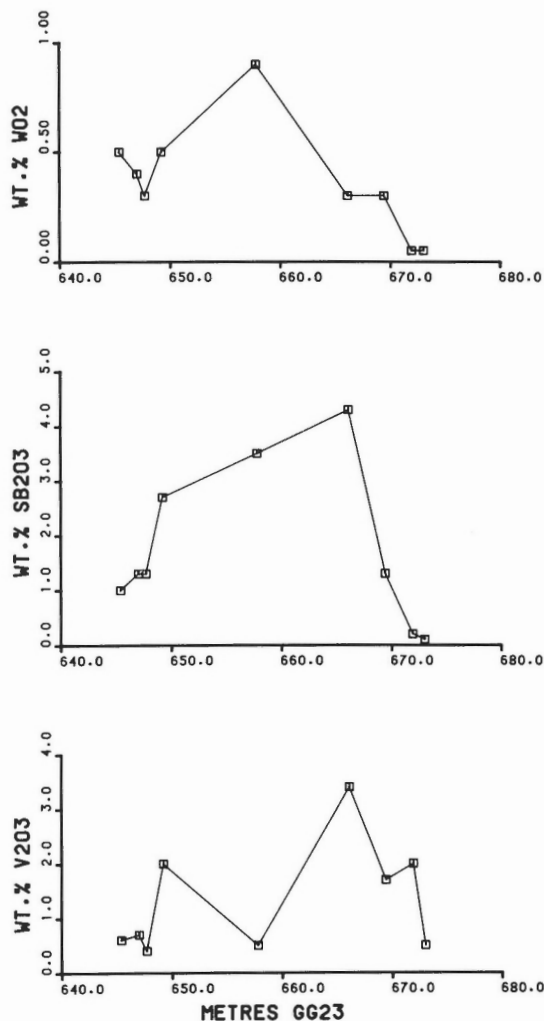


Figure 29. Plot of V₂O₃, Sb₂O₃ and WO₂ contents of rutile across the ore zone within drill hole GG23.

analyses of rutile grains (Fig. 32) reveal that only those within the main ore zone down to 880 m, and the mineralized zone at 934 m, contain V, Sb and W.

Drill hole GG20 is 200m in a northwest down-dip direction from drill hole GG14W and represents some of the thickest ore in the Golden Giant orebody. The hole intersects the main ore zone at 851.3 to 892.7 m, across a true

width of 30.4 m, and a lower mineralized zone at 930 to 950 m that contains anomalous gold values. Specimens of the drill core were included in a geochemical study by Cameron and Hattori (1985); 76 polished sections and 25 polished thin sections were prepared and compositions of the mica, rutile and feldspar were determined with the electron microprobe throughout the width of the main ore zone as

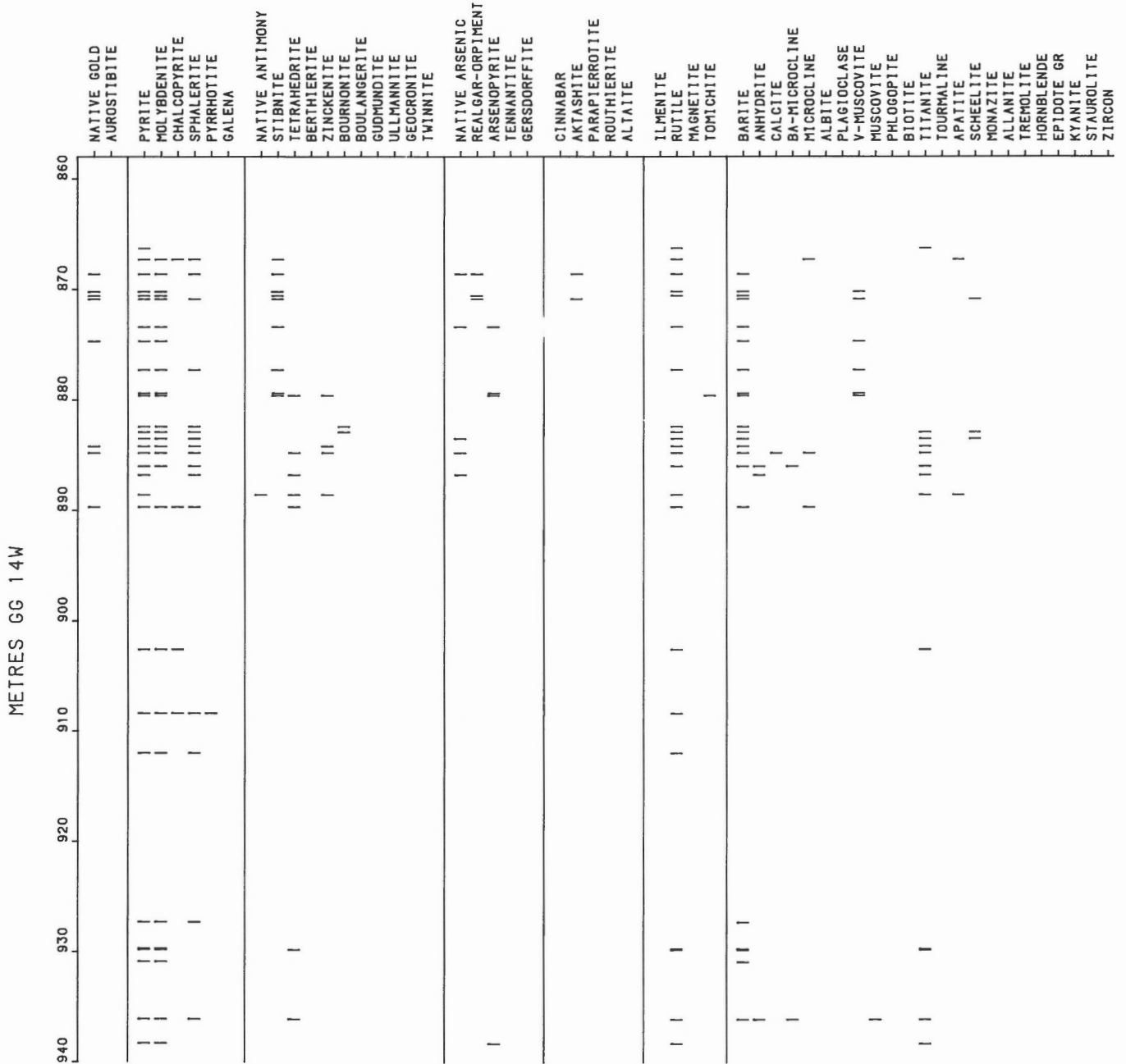


Figure 30. Plot of mineral distribution versus depth across the ore zone within drill hole GG14W.

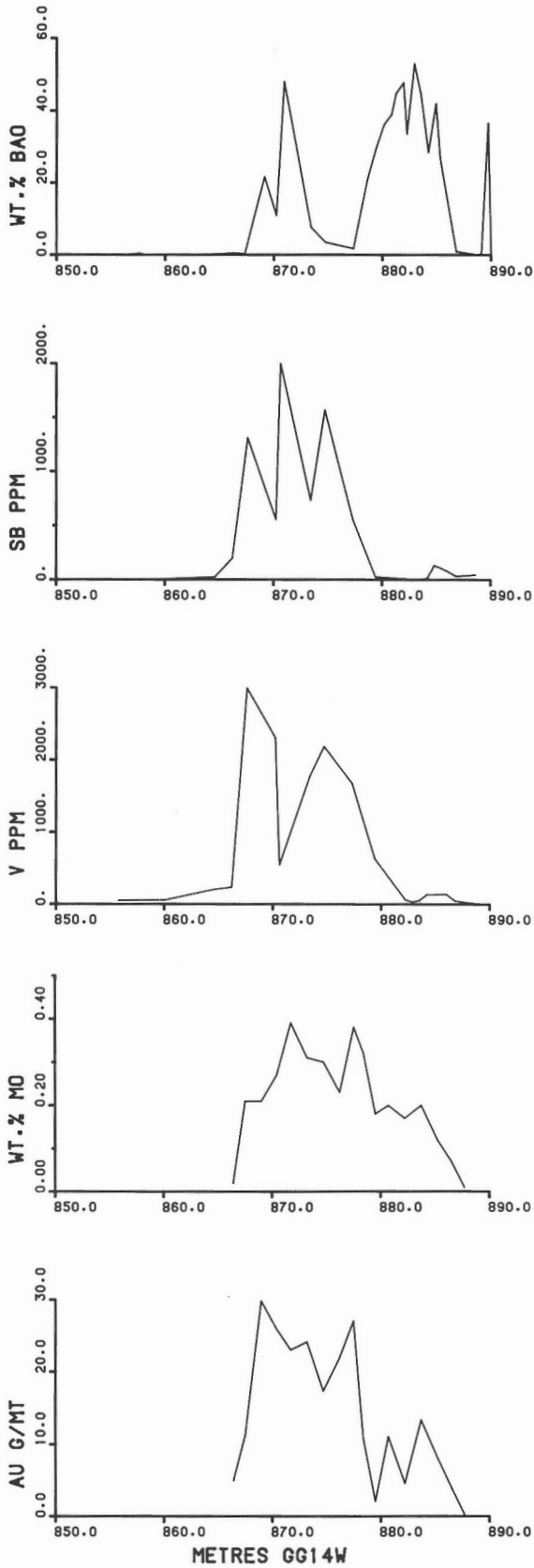


Figure 31. Geochemical profiles of Au, Mo, V, Sb and BaO across the ore zone within drill hole GG14W.

well as across the lower mineralized zone. The minerals present and their distribution are shown in Figure 33, the geochemical profiles of Au, Mo, Ba, V, Hg, Sb and As in Figure 34, the Fe, V, and Ba contents of the micas in Figure 35, the V, Sb and W contents of rutile in Figure 36 and the Ba contents of the microcline in Figure 37. The mineral distribution plot (Fig. 33) shows that within the hanging wall at 850 m, or 7 m above the gold-bearing zone, the mineral assemblage consists predominantly of kyanite, biotite, plagioclase (An₅₀), muscovite, pyrite, pyrrhotite and chalcopyrite. The hanging wall in contact with the ore zone consists of biotite-phlogopite, muscovite, plagioclase (An₅₈), barian microcline, calcite, arsenopyrite, pyrrhotite, pyrite, chalcopyrite and magnetite. The magnetite occurs as an alteration of pyrite. The gold-bearing zone starting at 857 m is

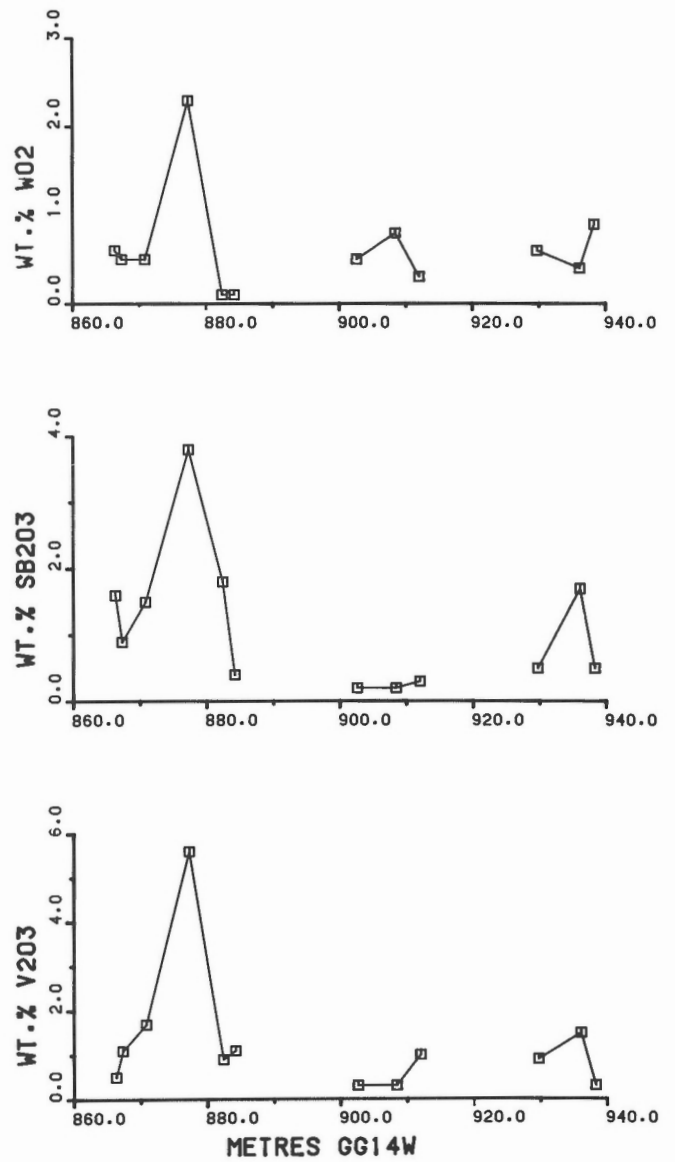


Figure 32. Plot of V₂O₃, Sb₂O₃ and WO₂ of rutile across the ore zone within drill hole GG14W.

characterized by the presence of molybdenite. A short distance into the ore zone at 861 m, the mineral assemblage consists of stibnite, tetrahedrite and native arsenic, and this assemblage appears to define an interval 4 m wide in which barite is also present. The next interval from 865 to 870 m is defined by nil to low gold values (Fig. 34), the absence of antimony-bearing minerals, the presence of trace amounts of arsenopyrite and molybdenite with barite, albite, vanadian muscovite and barian microcline. The next 17 m of the ore zone contains the highest gold grades. This section contains several antimony minerals, of which stibnite is the most common; of the arsenic-bearing minerals native arsenic, realgar and some arsenopyrite predominate; cinnabar and aktashite are the mercury minerals and routhierite is the most common thallium mineral. Barian tomichite is also relatively abundant in this interval. Barite is a major gangue mineral, with only the last few metres of the zone being devoid of it. This lower portion also contains boudinaged quartz veins with which arsenic, antimony, mercury and thallium-bearing

minerals are associated. Figure 34 illustrates the geochemical profiles of Au, Mo, Ba, V, Hg, Sb and As, and these show that the high Mo values do not necessarily correspond to high Au values. However, these elements all show a definite correlation with the gold-bearing zone. The major barium minerals are barite and barian microcline, with as much as 60 per cent barite being present in the lower portion of the ore zone, whereas in other lower-barium portions of the ore zone, barian microcline is the principal barium mineral. The barium contents in the microcline are shown in Figure 37. The principal vanadium-bearing mineral is muscovite. There is a strong correlation between vanadium and gold and, like molybdenite, dark-grass-green vanadian muscovite is an indicator of the ore zone. Systematic microprobe analyses of the Fe, V and Ba contents of the micas from the hanging wall down to and including the lower mineralized zone are shown in Figure 35. The complete analyses are listed in Table A.13. These data show that the mica in the hanging wall is biotite. At 858 m, at the start of the ore zone, the mica is muscovite and its vanadium contents increase from near zero at 863

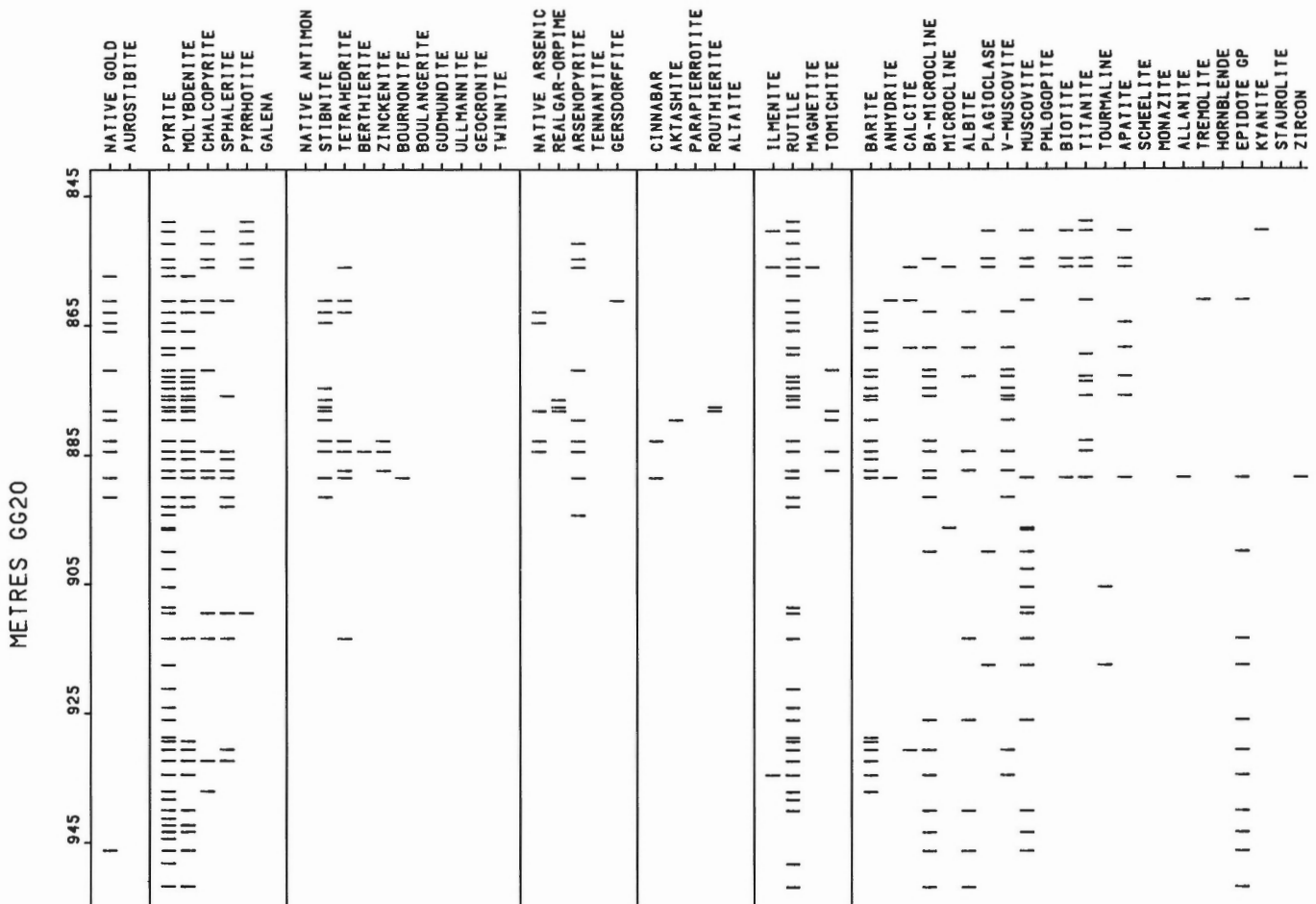


Figure 33. Plot of mineral distribution versus depth across the ore zone within drill hole GG20.

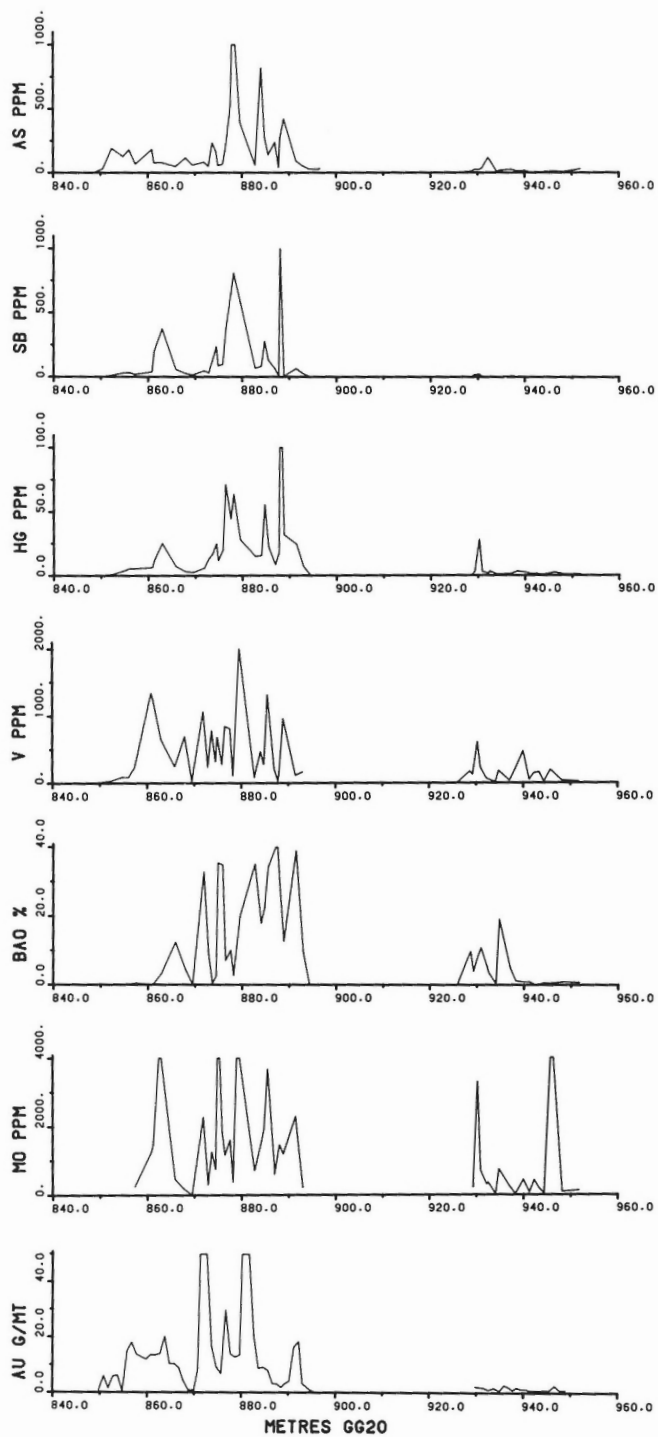


Figure 34. Geochemical profiles of Au, Mo, BaO, V, Hg, Sb and As across the ore zone within drill hole GG20.

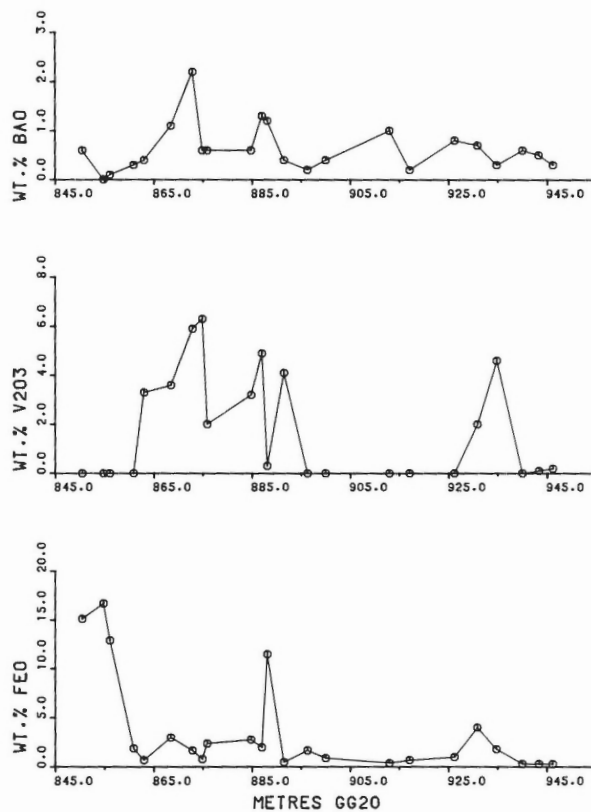


Figure 35. Plot of FeO, V₂O₃ and BaO contents of mica across the ore zone within drill hole GG20.

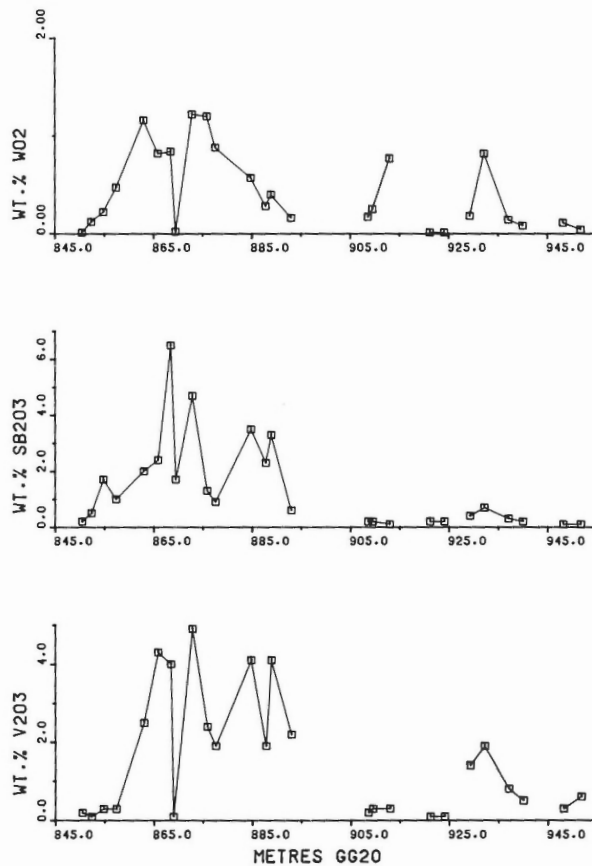


Figure 36. Plot of V₂O₃, Sb₂O₃ and WO₂ contents of rutile across the ore zone within drill hole GG20.

m to 6.5 wt. % V_2O_3 in the ore zone, and decrease back to zero in the footwall at 892.7 m. The lower mineralized zone shows a similar trend in the vanadium contents of the muscovite. Barium contents in the mica are relatively low, seldom exceeding 1 per cent. The second most important vanadium-bearing mineral is rutile, which is widespread, but as a minor constituent. In addition to vanadium, rutile contains significant amounts of antimony and trace amounts of tungsten. The substitution of these elements in rutile is shown in Figure 36 and, as for the micas, the rutile compositions indicate the presence of the gold-bearing zone with a sharp increase in V, Sb and W from 863 m to the footwall at 892.7 m. The lower mineralized zone shows a similar trend, but to a lesser extent.

Drill hole GG21 is west of drill hole GG20, adjacent to the Page-Williams orebody and separated from drill hole GG20 by a diabase dyke. The ore zone extends from 820 to 866 m for a true width of 36.1 m, which is one of the greatest ore widths in the Golden Giant mine. The minerals and their distribution are presented in Figure 38 and the gold

assay data are plotted in Figure 39. Detailed study of the drill core reveals the following; at 819.8 m, which is the hanging wall contact, the rock is a fine grained biotite schist

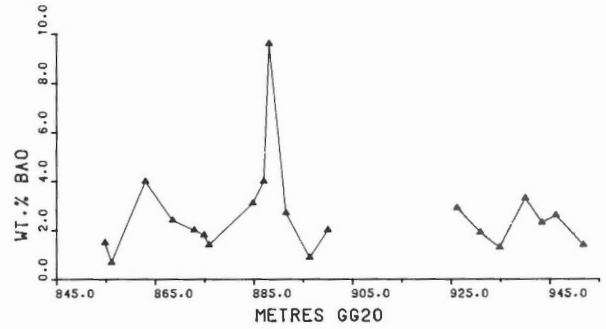


Figure 37. Plot of BaO contents of microcline across the ore zone within drill hole GG20.

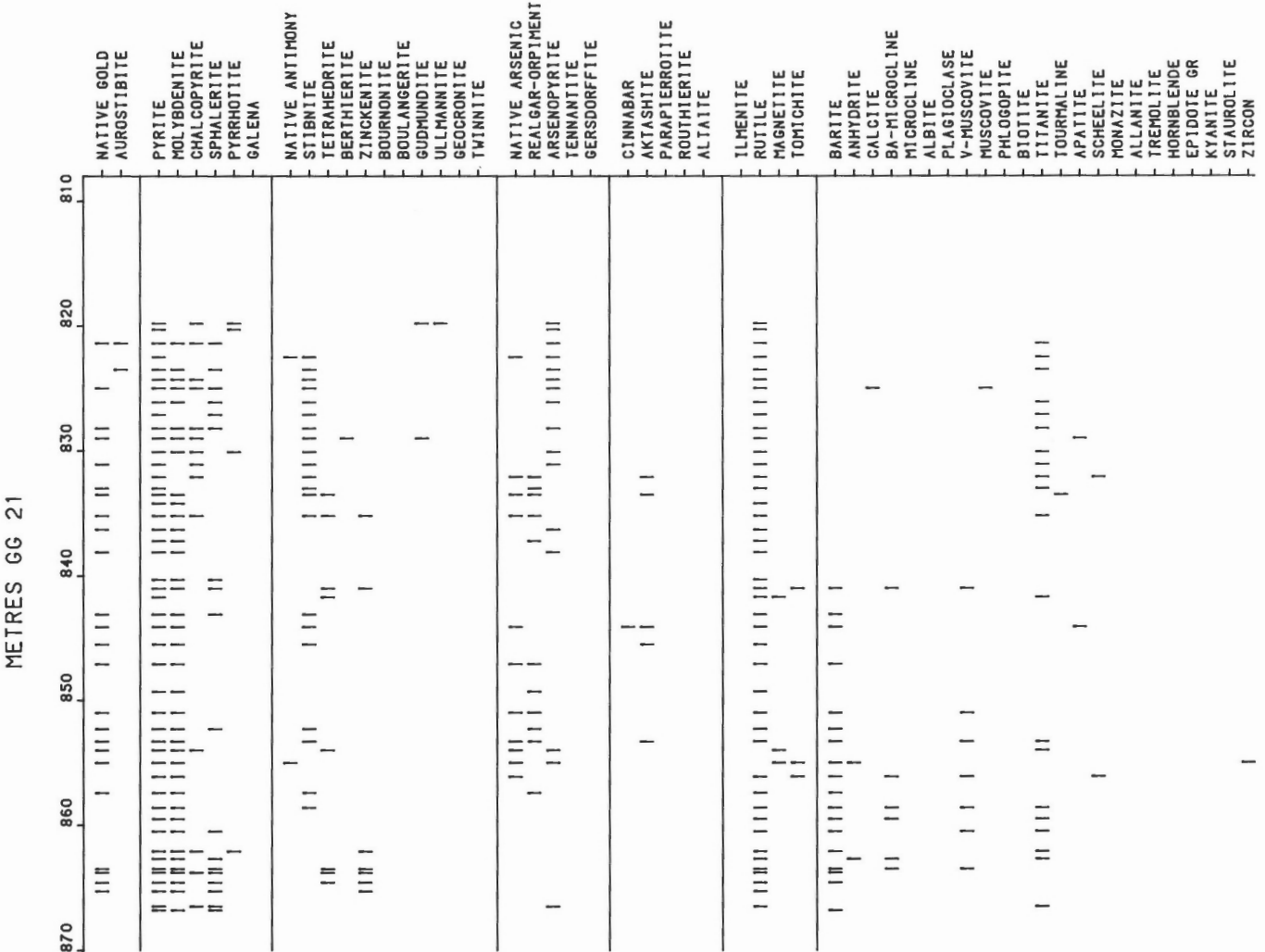


Figure 38. Plot of mineral distribution versus depth across the ore zone within drill hole GG21.

that contains pyrite and trace amounts of pyrrhotite, chalcopyrite, arsenopyrite, gudmundite and ullmannite. Immediately within the ore zone at 820 m, the rock is a well foliated muscovite-pyrite schist that continues to a depth of 840.3 m. A number of distinct ore mineral assemblages are present within this portion of the ore zone. The interval 820 to 822 m is characterized by aurostibite, native gold, native antimony, native arsenic, stibnite and arsenopyrite. The interval 822 to 832.1 m contains stibnite, minor to trace amounts of chalcopyrite, sphalerite and arsenopyrite. The interval 832.1 to 837.2 m, contains realgar, native arsenic, tetrahedrite and aktashite. From 837.2 to 840.3 m the ore is pyrite-rich and has a low gold content with some molybdenite. From 840.3 to 844.0 m the host rock is fragmental to granular and has some schistose layers that contain green vanadian muscovite and the first barite. From 844 m to the footwall at 866 m, barite is a major gangue mineral and the rock has a layered texture due to concentrations of pyrite. Within this lower barite-rich zone are two biotite-rich zones located at 841.7 m and 855.0 m. The ore minerals from 844 to 857.4 m are realgar, native arsenic, native gold, minor stibnite and rare aktashite and cinnabar. The next interval from 857.4 to 863.5 m contains sparse ore minerals. From 863.5 to the footwall at 866 m, the ore minerals are essentially sphalerite, chalcopyrite, zinkenite and tetrahedrite. Barian tomichite was identified within the two narrow biotite-rich zones at 841.7 m and from 855.0 to 856.1 m, and the only established occurrence of cafarsite in the deposit is at 865.3 m. Barian microcline and vanadian muscovite occur principally within the lower part of the ore zone, but more study would be required to determine whether they are present throughout the width of the ore. Microprobe analyses of the rutile are presented in Figure 40, and show that the rutile in the top 11 m from 820 to 831.0 m contains only trace amounts of V, Sb and W, whereas that in the bottom portion of the ore zone to 866.0 m contains significant V, Sb and W.

Drill hole GG45 is approximately 150 m down-dip from hole GG20, near the projected lower limits of the deposit.

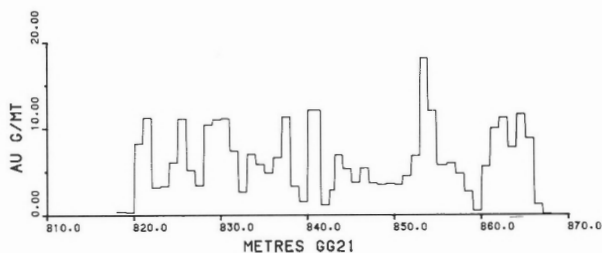


Figure 39. Profile of gold assay data across the ore zone within drill hole GG21.

The main ore zone is at 1105.2 to 1112.4 m and has a true width of 6.10 m. A lower gold-bearing zone with anomalous gold values at 1156.7 to 1159.0 m is probably the extension of the lower mineralized zone in drill hole GG20. The minerals present and their distribution are presented in Figure 41. Samples collected at 1103.7 m, which is 1.5 m above the gold-bearing zone, consist of muscovite schist that contains euhedral arsenopyrite and pyrite with minor native arsenic, native antimony, berthierite, stibnite and tetrahedrite. This assemblage of minerals is unusual without economic gold values. The start of the ore zone at 1105.2 m is characterized by the presence of molybdenite with realgar, stibnite, tetrahedrite, zinkenite, native arsenic, chalcopyrite, sphalerite and aktashite in a muscovite schist with traces of phlogopite and tremolite. At 1106.2 m some barite is present in association with realgar-rich quartz veins. At 1107.6 m the ore has a fragmental appearance and contains major barite and pyrite-rich layers. Between 1108 and 1109 m the gold grades are less than 1 g/t and coarse pyrite and magnetite are the major opaque minerals, with trace amounts of tetrahedrite and bournonite. From 1109 to 1112.4 m the ore is barite-rich with minor tetrahedrite, zinkenite, chalcopyrite and sphalerite. Pyrite-rich layers occur throughout the zone and give a distinct banding to the ore. The lower limit of the ore zone at 1112.4 m is at the contact with muscovite

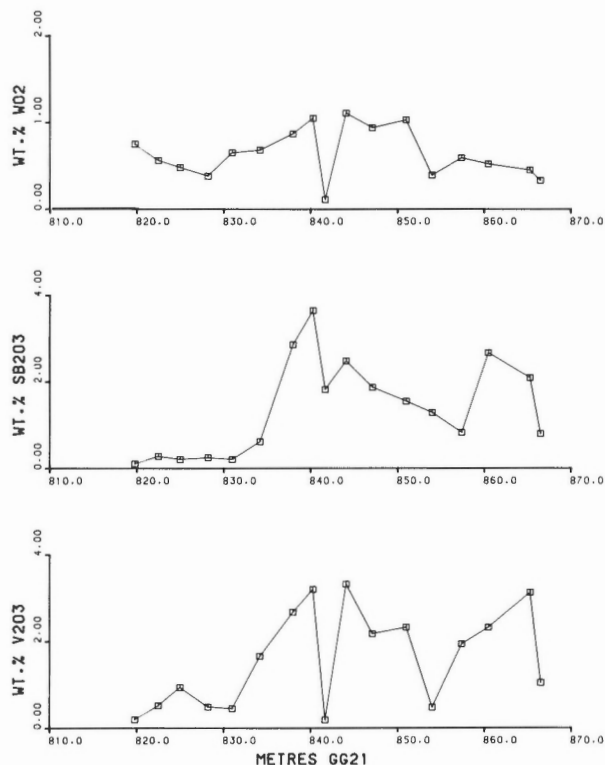


Figure 40. Plot of V_2O_3 , Sb_2O_3 and WO_2 contents of rutile across the ore zone within drill hole GG21.

METRES GG 45

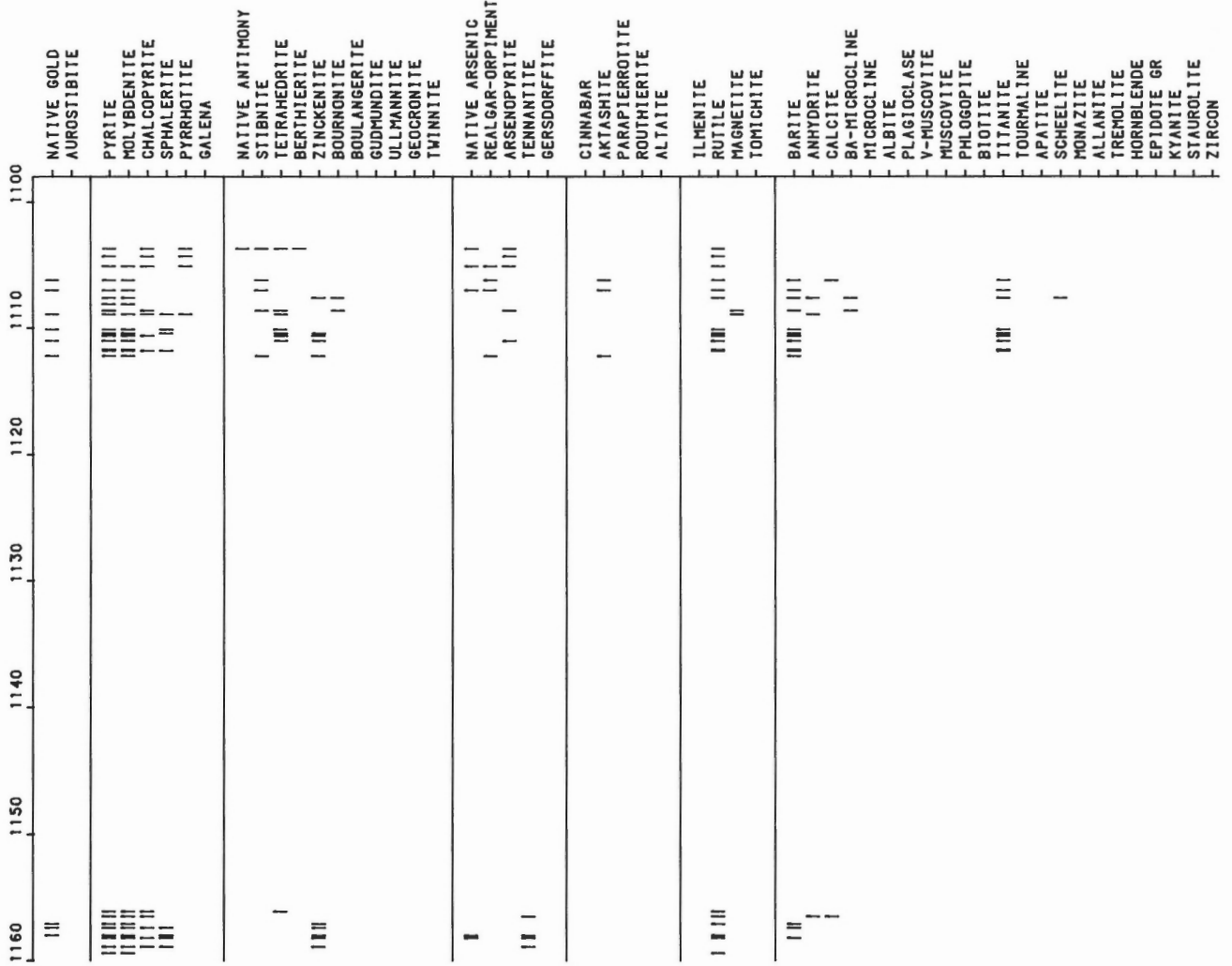


Figure 41. Plot of mineral distribution versus depth across the ore zone within drill hole GG45.

METRES GG 37Y

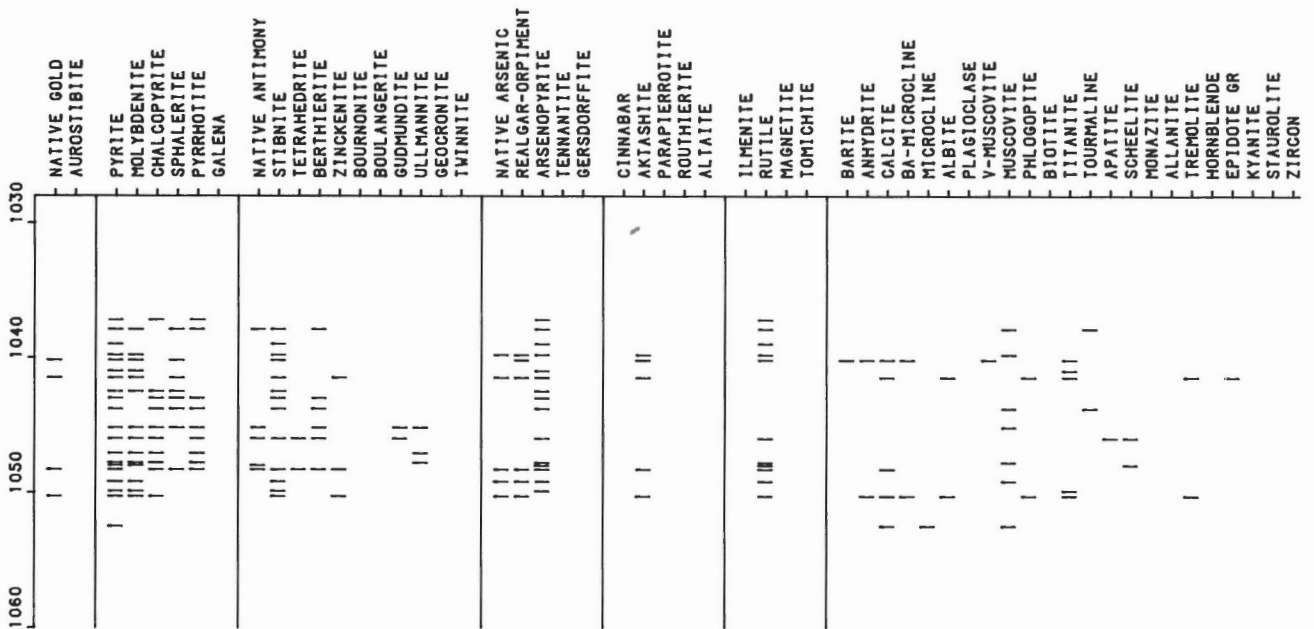


Figure 42. Plot of mineral distribution versus depth across the ore zone within drill hole GG37Y.

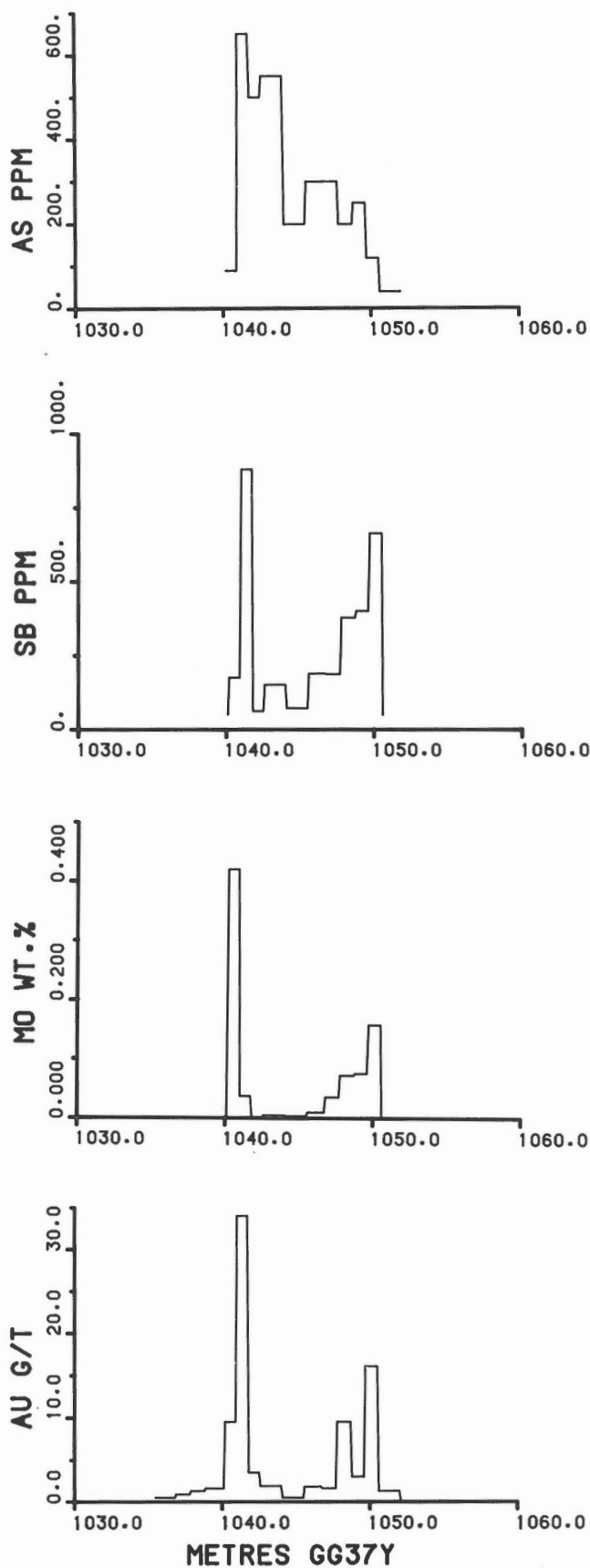


Figure 43. Geochemical profiles of Au, Mo, Sb and As across the ore zone within drill hole GG37Y.

schist with pyrite-rich bands. The lower ore zone at 1156.1 to 1159.4 m has maximum gold grades of 6 g/t and contains molybdenite with chalcopyrite, sphalerite, zinkenite, native arsenic and arsenopyrite. The rock has a granular texture and contains minor muscovite and barite.

Drill hole GG37Y is near the projected lower limits of the orebody close to Golden Giant's mine shaft. The orebody consists of two gold-bearing zones that together extend from 1040.1 to 1050.55 m for a combined true width of 9.49 m. The minerals present and their distribution are presented in Figure 42 and the geochemical profiles of the elements Au, Mo, Sb and As in Figure 43. The mineralogy of the two gold-rich zones is almost identical and the textural features are very similar, suggesting that the two zones may represent the limbs of a tight isoclinal fold and that the true primary ore thickness was 2 to 3 metres. The upper zone from 1040.10 to 1042.55 m contains boudinaged quartz veins rich in realgar, native arsenic, tetrahedrite and aktashite. At 1041.6 m the quartz veins are enclosed in a brecciated coarse tremolite-phlogopite schist that also contains green muscovite, orange calcite and zoisite. The lower zone from 1048.75 to 1050.55 m contains almost identical boudinaged quartz veins, with realgar and coarse stibnite, but no phlogopite. The gold-bearing, but low-grade, intermediate zone from 1042.6 to 1047.7 m consists mainly of quartz-muscovite schist with minor narrow phlogopite and pyrite layers. The footwall rock is a quartz-eye muscovite schist. Traces of barite occur in the two gold-rich zones, but the principal barium mineral is a strongly zoned barian microcline (Fig. 7) with as much as 15.5 wt.% BaO. The highest content of vanadium detected in vanadian muscovite in this drill hole, 6.1 wt.% V_2O_3 , occurs at 1040.2 m. Most of the rutile grains have been altered to titanite, but some were analyzed for V, Sb and W with results as follows:

Microprobe Analyses of Rutile in Drill Hole GG37Y

Sample	V_2O_3	Sb_2O_3	WO_2
1037.9	1.0	0.1	1.2
1040.2	2.8	1.2	1.7
1048.0	1.5	0.3	1.3
1049.2	0.4	0.2	0.0

The Page-Williams mine

The Page-Williams mine constitutes the western portion of the deposit and contains the largest tonnage of ore. The gold-bearing zones on the property have been referred to as the "A", "B" and "C" orebodies. The "A" orebody extends from surface to a vertical depth of 320 m where, on crossing the claim boundaries, it becomes the Golden Giant orebody. The orebody plunges to the northwest at approximately 45 degrees and below the 9975 level* on the property it is called the "B" orebody. The "B" orebody continues down-dip to the northwest to a vertical depth of approximately 1300 m. It has true ore thicknesses as great as 45 m, is more barite-rich, and contains very little of the biotite-rich fragmental rock that forms the ore in most of the zone in the Golden Giant mine to the east. The "C" orebody is located at the west end of the property in felsic rocks and the mineralization

* Designation of the mining levels in the Page-Williams mine are 5000+ the equivalent level in the Golden Giant and David Bell mines.

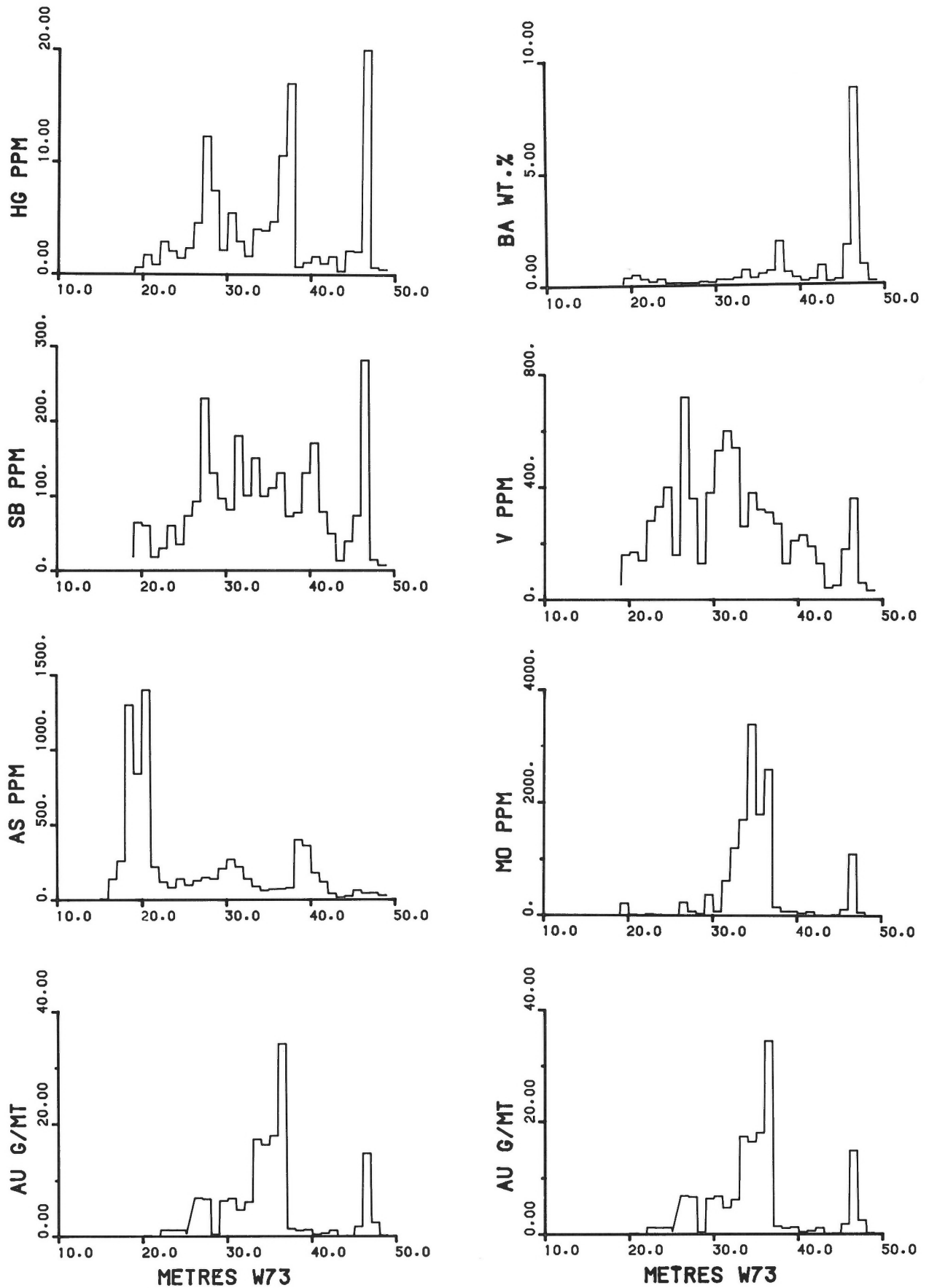


Figure 44(a). Geochemical profiles for Au, As, Sb and Hg across the ore zone within drill hole W73.
(b). Geochemical profiles for Au, Mo, V and Ba across the ore zone within drill hole W73.

is different from that within the main orebody in that the gold occurs as native gold, calaverite, and petzite in association with molybdenite, altaite, hessite, coloradoite, frobergite, chalcopyrite, sphalerite and tennantite in thin fractures within felsic rocks that have a porphyritic texture.

Mining of the ore on the Page-Williams property commenced with an open pit operation on the "A" orebody. Most of the gold-bearing zones within the "A" orebody are in fine-grained, in places siliceous, rock composed primarily of microcline and of plagioclase that has been invariably altered to sericite. Parts of the muscovite-sericite schist are rich in molybdenite, cinnabar and stibnite that occur along the foliation planes and these minerals impart a distinct bluish to reddish colour to the surface of the rock. Within the schist are well-developed boudinaged quartz veins as much as 30 cm in width that are in places extremely rich in the assemblage realgar-cinnabar-stibnite. The "A" orebody comprises a hanging wall ore zone separated from a footwall ore zone by waste. Along the northwest plunging axis, the two ore zones can be mined together to give the greatest mineable thickness (25 m); in plan, the orebody has an "H" configuration (Walford et al., 1986). Near the surface the bulk of the ore is in the hanging wall ore zone, whereas on the lower levels the footwall ore zone constitutes the bulk of the ore.

The hanging wall ore zone, both near surface and at depth, pinches out over short distances to the west but extends approximately 200 m to the east nearly to the David Bell property boundary.

Drill hole W73 is located near surface on the eastern portion of the "A" orebody. The ore in this part of the deposit was mined in 1986 by the open pit operation. As shown by the gold assays in Figure 44(a,b), the gold is concentrated in two zones that form the limbs of the "H" configuration. The hanging wall ore zone extends from 26 to 37 m and a narrow footwall ore zone extends from 46 to 47 m. The bulk of the ore is in the hanging wall ore zone. The minerals present and their distribution are shown in Figure 45. These data show that the rocks at 12.7 to 18.3, or 8 m above the ore zone, are characterized by a staurolite-biotite schist that represents the metasedimentary rocks. Next in the sequence, at 19.6 m, the rocks consist of a kyanite-muscovite schist that changes to a muscovite-phlogopite-biotite schist towards the ore zone at approximately 26 m. The hanging wall rocks contain anomalous gold values and trace amounts of molybdenite. Sphalerite containing 9.0 wt. % Hg is present at 22.4 m. The principal ore minerals are pyrite and arsenopyrite, with minor associated pyrrhotite. The host rock to the hanging wall ore zone is a quartz-microcline rock with trace

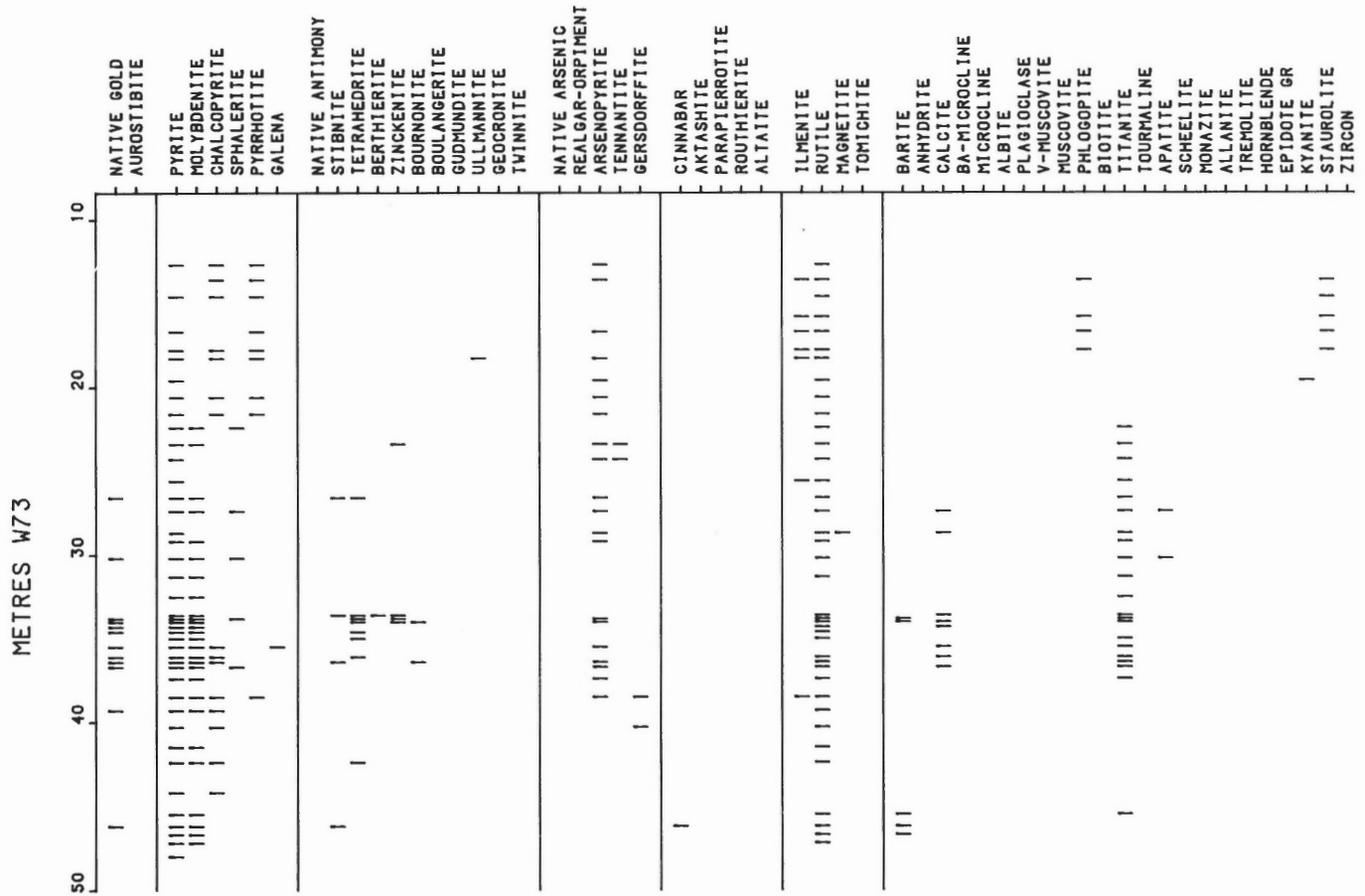


Figure 45. Plot of mineral distribution versus depth across the ore zone within drill hole W73.

amounts of green vanadian muscovite. The ore minerals are native gold, associated principally with stibnite, and minor tetrahedrite and sulphosalts. At 34 m the ore is very vuggy and contains fine acicular crystals of stibnite, flakes of molybdenite and visible native gold along fractures and within the vugs. The two ore zones are separated by waste that consists of a quartz-feldspar rock similar to the hanging wall ore host, layers of muscovite schist, a quartz-feldspar porphyry sill and rocks rich in epidote, chlorite, carbonate and biotite with some vugs. Minor barite occurs in the hanging wall ore zone, in the waste rock between the zones and within the footwall ore zone. The mineralization in the footwall ore zone is sparse, but native gold and trace amounts of cinnabar

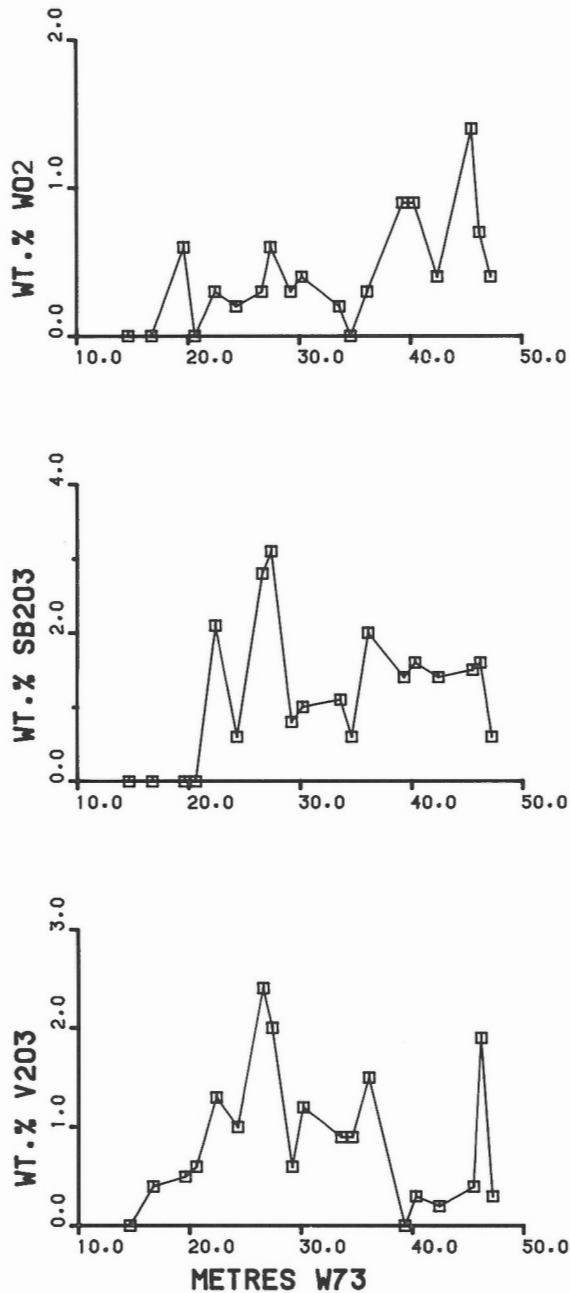


Figure 46. Plot of V_2O_3 , Sb_2O_3 and WO_2 contents of rutile across the ore zone within drill hole W73.

were observed. At its footwall this ore zone is in contact with a muscovite-phlogopite schist containing some tourmaline. Trace element geochemical profiles of V, Sb, and Ba (Fig. 44a,b) show that alteration extends from 20 to 47 m. This includes 6 m of barren rock above the hanging wall ore zone, in which trace amounts of molybdenite and mercury-bearing sphalerite were identified, the hanging wall ore zone, the barren waste rock and is terminated at the footwall contact at 47 m. Rutile grains that contain significant V, Sb and W

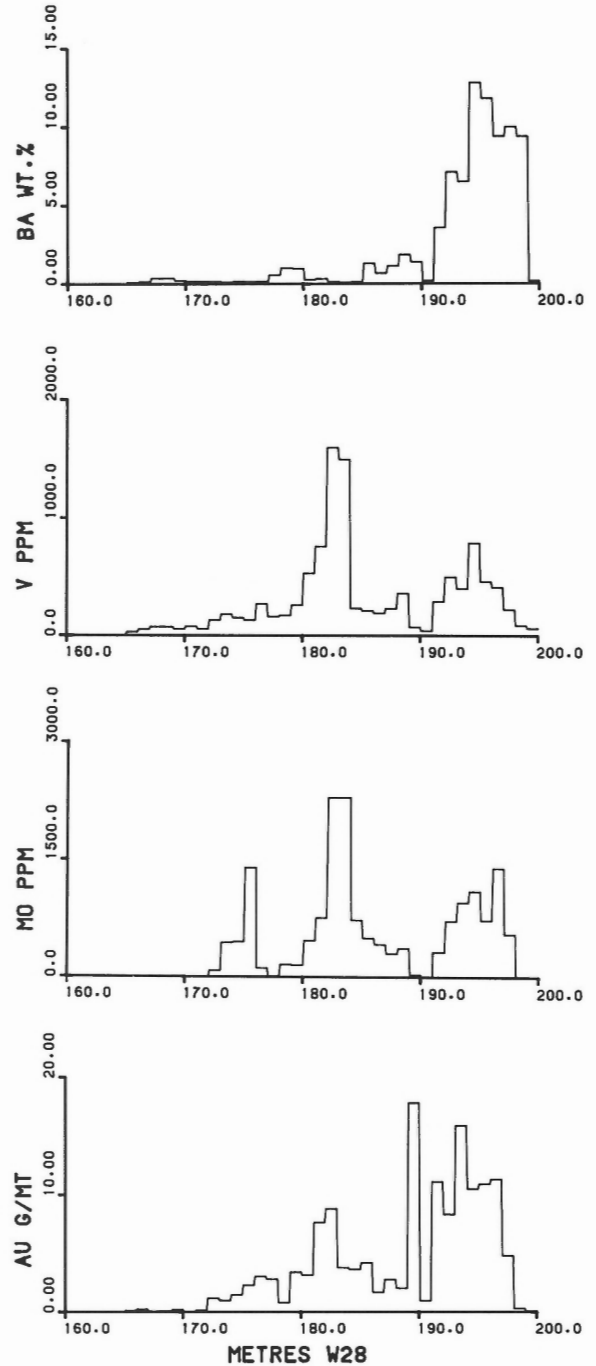


Figure 47. Geochemical profiles of Au, Mo, V and Ba across the ore zone within drill hole W28.

contents (Fig. 46) are distributed throughout the full width of altered rock and not restricted to the two economic gold-bearing portions. The potential mining width of the ore zone at this location should be considered to extend from 20 to 47 m, even though economic gold values only occur in two zones, because along strike to the west towards the centre of the "A" orebody and down-dip, economic gold values occur throughout the total width of the orebody.

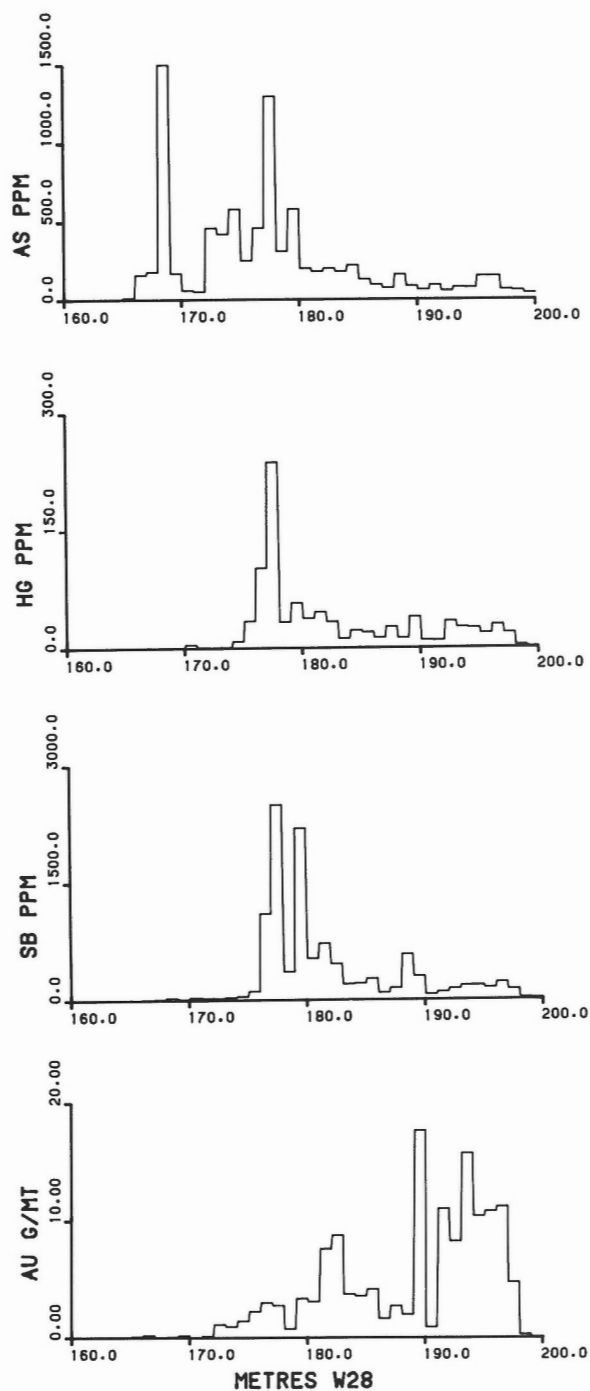


Figure 48. Geochemical profiles of Au, Sb, Hg and As across the ore zone within drill hole W28.

Drill hole W28 is located at a vertical depth of 250 m from surface in the central portion of the "A" orebody and 70 m above the property boundary of the Golden Giant orebody. The ore zone extends from 172 to 198 m or an uncorrected width of 26 m. Geochemical profiles of the elements Au, Mo, V, Ba, Sb, Hg and As are shown in Figures 47 and 48. The minerals and their distribution are shown in Figure 49 and the V, Sb and W contents of rutile in Figure 50. The host rock for the ore in this part of the deposit is mainly feldspathic, with included layers of sericite schist and seams of pale green muscovite, both of which frequently contain coarse pyrite lenses and molybdenite. Pale yellow sphalerite occurs throughout most of the ore zone and microprobe analyses (Table A.1) show that the mineral contains up to 24.4 wt. % Hg, with the higher mercury contents occurring within the centre of the ore zone. In places, stibnite-realgar- and cinnabar-bearing quartz veins, sometimes with coarse pale brown tourmaline at their margins, occur within the ore. At 189.7 m the ore is very vuggy and contains visible native gold, olive green vesuvianite and brownish yellow lewisite. The lower portion of the ore zone is barium-rich with barite, the principal barium mineral, occurring as much as 1.5 m below the ore zone. The lower limits of the ore zone are not easy to recognize because the footwall does not coincide with the characteristic quartz-eye muscovite schist as found in other parts of the deposit.

Drill hole W104 represents the western limits of the down-dip portion of the "A" orebody. The zone extends from 251 to 266 m and, as shown by the gold assays in Figure 51, the ore consists of hanging wall and footwall ore zones, with the bulk of the ore in the footwall ore zone in contrast to drill hole W73 where the bulk of the ore occurs in the hanging wall ore zone. Gold values occur throughout most of the total width, except for a quartz-feldspar porphyry sill 2 m thick at 259 to 261 m. Sampling of the hole commenced at 243.4 m or 7.4 m above the hanging wall ore zone. The minerals and their distribution are shown in Figure 52 and the V, Sb and W contents of the rutile in Figure 53. The country rock from 243.4 to 247.8 m consists of a well foliated biotite-phlogopite to muscovite schist with sparse coarse lenses of pyrite. Associated with the pyrite are minor chalcopyrite, pyrrhotite and arsenopyrite. At 248.7 to 249.5 m the rock consists of a kyanite-bearing muscovite schist that contains stibnite, arsenopyrite, sphalerite, native arsenic, realgar, tetrahedrite and cinnabar. The textural relationships of these minerals with the kyanite indicate that they are later and therefore probably formed after the metamorphism that produced the kyanite (Fig. 54). From 249.5 to 252.3 m the host rock is muscovite schist, similar in appearance to the kyanite-muscovite schist that contains quartz-rich lenses with major stibnite and associated cinnabar, realgar, native arsenic, arsenopyrite, aktashite, tetrahedrite and zinkenite. Native gold was first observed at 252.3 m, which coincides with the presence of molybdenite. Trace amounts of barite occur in the hanging wall ore zone, but barite is more abundant in the feldspathic footwall ore zone that also contains minor to trace amounts of green vanadian muscovite. Microprobe analyses of the rutile grains (Fig. 53) show that those containing significant V, Sb and W occur principally within the feldspathic footwall ore zone.

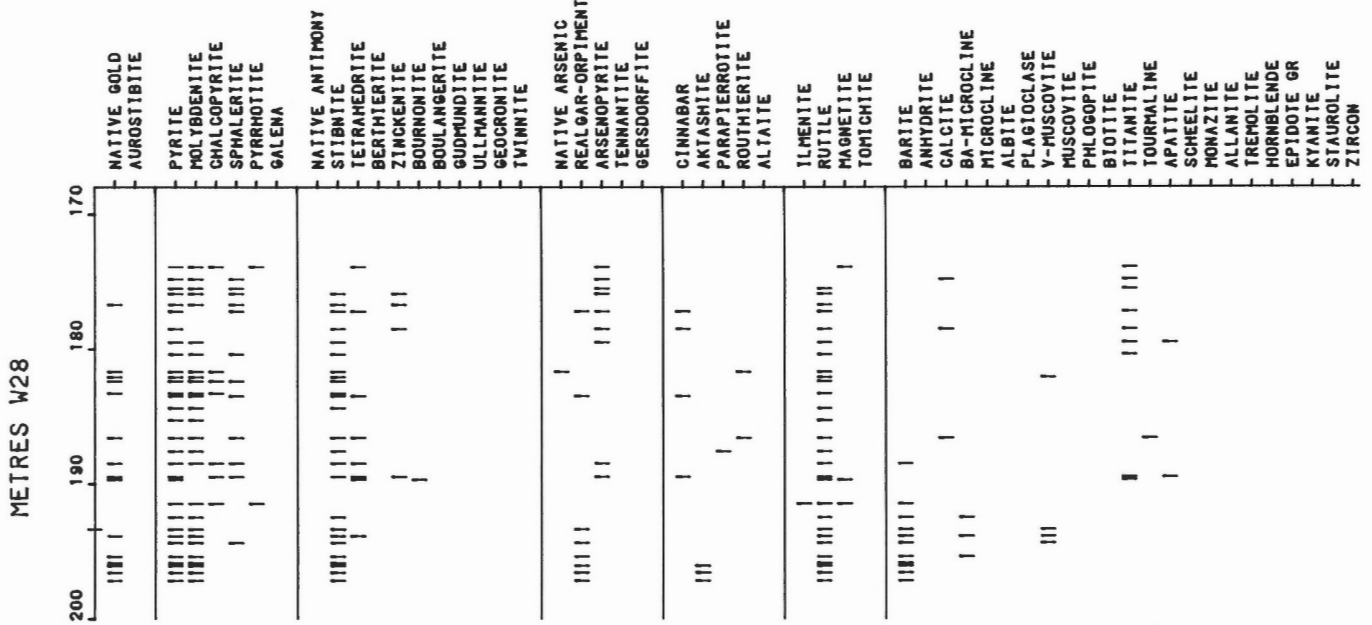


Figure 49. Plot of mineral distribution versus depth across the ore zone within drill hole W28.

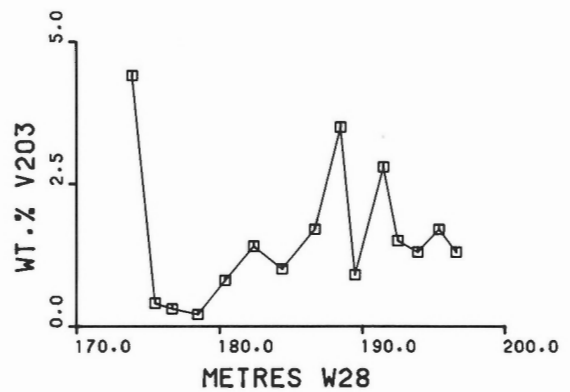
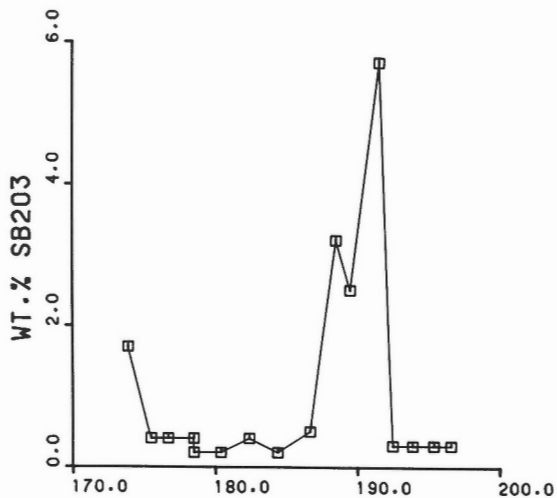
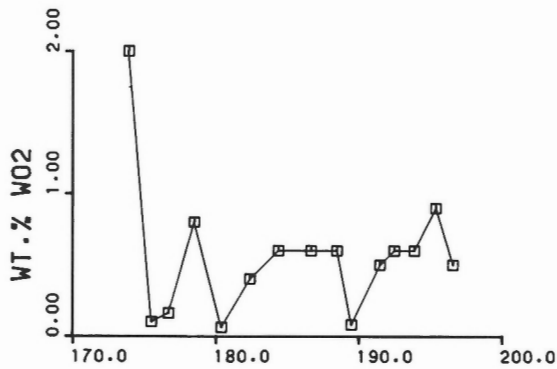


Figure 50. Plot of V_2O_3 , Sb_2O_3 and WO_2 contents of rutile across the ore zone within drill hole W28.

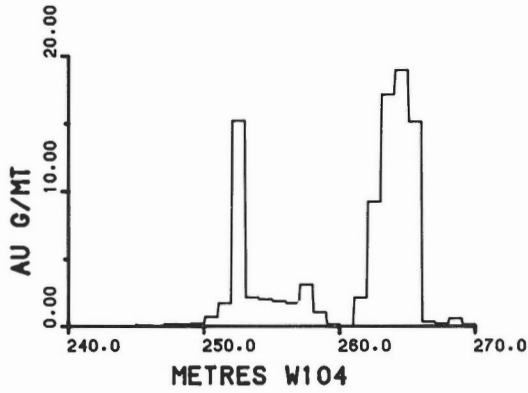


Figure 51. Profile of gold assay data across the ore zone within drill hole W104.

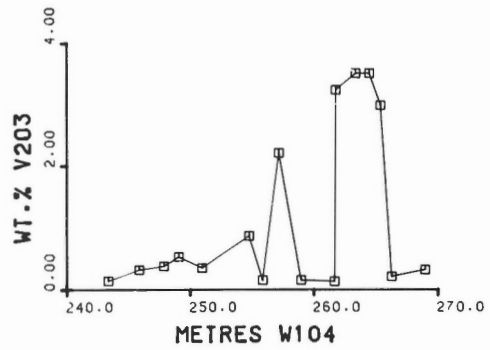
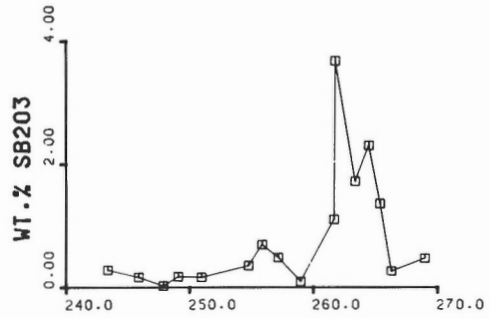
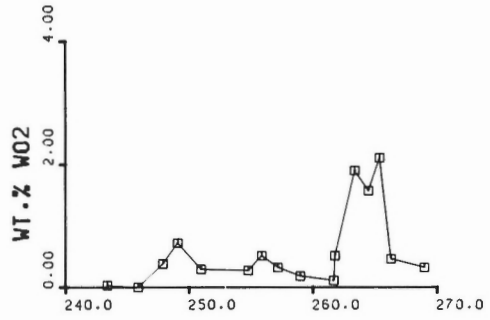


Figure 53. Plot of V_2O_3 , Sb_2O_3 and WO_2 contents of rutile across the ore zone within drill hole W104.

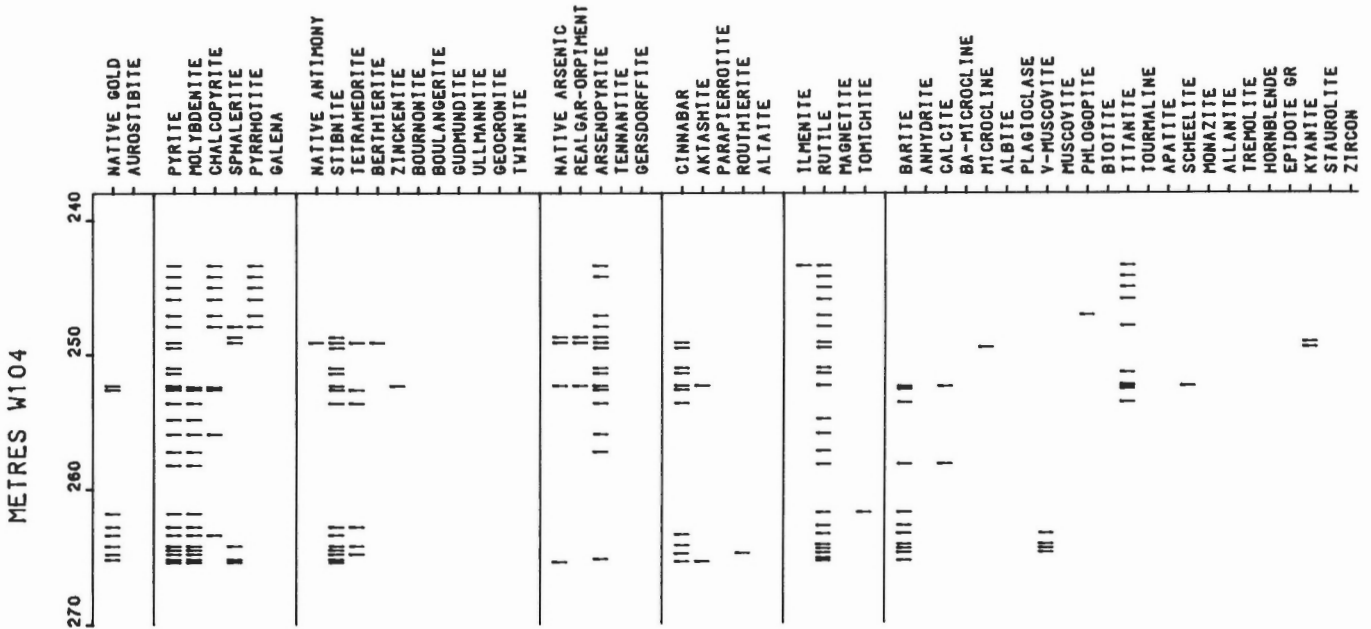


Figure 52. Plot of mineral distribution versus depth across the ore zone within drill hole W104.

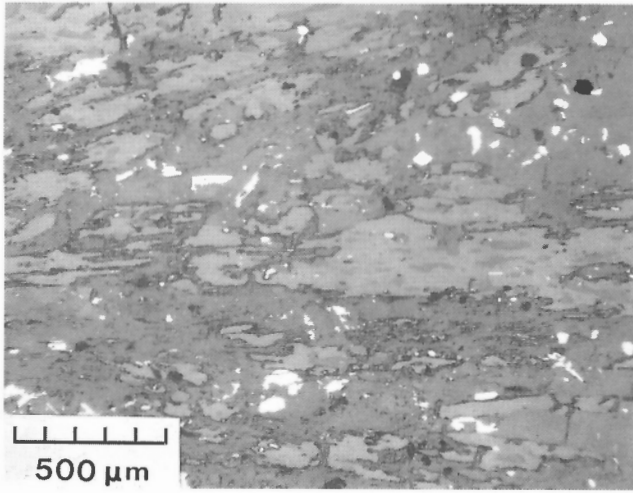


Figure 54. Photomicrograph of poikiloblastic kyanite, partially altered to sericite, with quartz. Interstitial to the kyanite are stibnite, pyrite, sphalerite, arsenopyrite and rutile. W104, 249.5m.

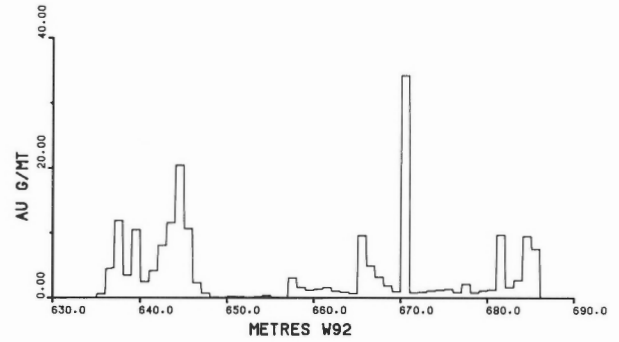


Figure 55. Profile of gold assay data across the ore zone within drill hole W92.

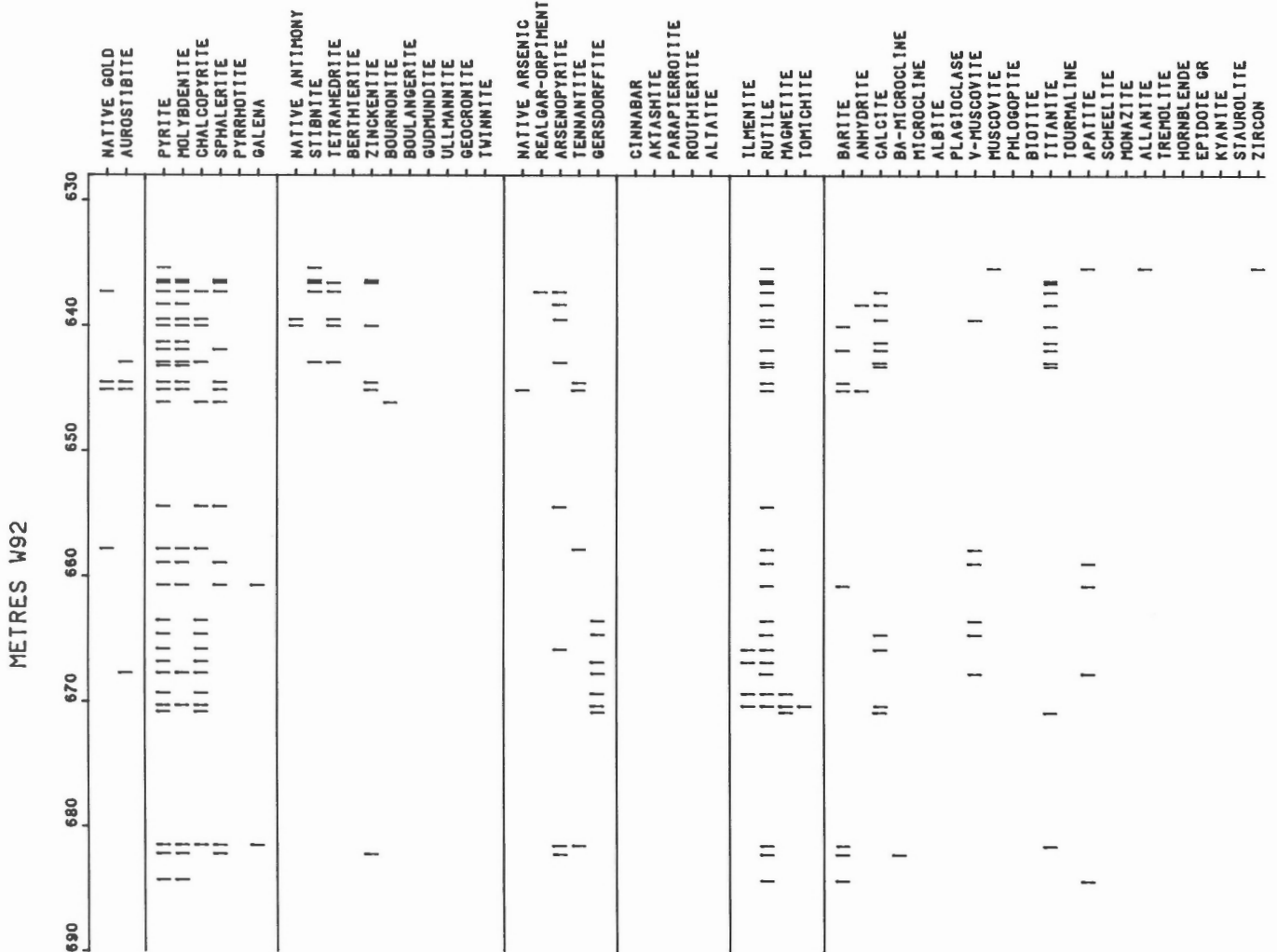


Figure 56. Plot of mineral distribution versus depth across the ore zone within drill hole W92.

Drill hole W69 is located down-dip close to the western limits of the upper portions of the "B" orebody. The ore zone is approximately 4 m wide with gold contents up to 35 g/t across a one-metre width. Only a few samples were selected from the drill hole and those examined contained very sparse native gold, with major pyrite, molybdenite and trace amounts of arsenopyrite, chalcopyrite, tetrahedrite, pyrrhotite and magnetite.

Drill hole W92 is approximately 650 m in vertical depth from surface within the "B" orebody and towards the western limits of the deposit. The orebody consists of two zones (Fig. 55), the upper ore zone from 636 to 648 m (uncorrected for drill hole inclination) and a lower ore zone from 657 to 686 m that consists of two distinct gold-rich portions. The upper and lower ore zones are separated by 9 m of barren rock that resembles a feldspar porphyry. The minerals and their distribution are presented in Figure 56. The ore minerals within the upper ore zone are native gold, austrostitite, molybdenite, and various antimony and arsenic minerals, but mercury minerals are absent. The host rock ranges from a feldspathic to a muscovite schist, with some barite and calcite throughout the zone. Trace amounts of green vanadian muscovite occur in thin seams. The lower ore zone is different in appearance in that, although it has a feldspathic character, it contains layers of bright green mica, coarse biotite layers and other layers that are baritic. The gold values are erratic, with some 1 m core intersections containing as much as 43 g/t Au. The different nature

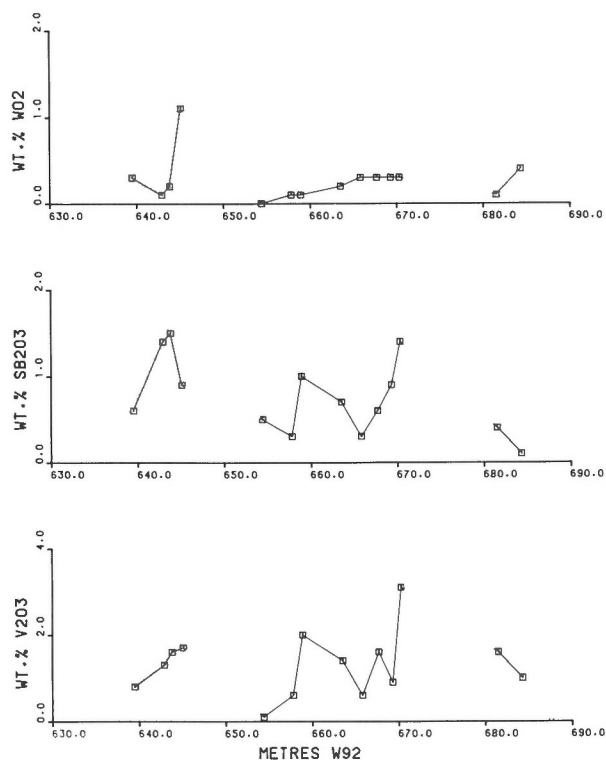


Figure 57. Plot of V_2O_3 , Sb_2O_3 and WO_2 contents of rutile across the ore zone within drill hole W92.

of this zone is reflected in its mineralogy, with sparse molybdenite present, no antimony minerals, gersdorffite as the common arsenic mineral, and ilmenite, chromite and rutile as the principal oxide minerals. The chromite occurs within the thin seams of green mica in which neither vanadium nor chromium were detected. Visible native gold with low mercury contents and mercury-free sphalerite also occur in this zone. The footwall portion of the lower zone contains two narrow gold-bearing layers, containing as much as 9 g/t Au within a pyrite-rich feldspathic rock with seams of coarse barite and some barian microcline. These layers are very similar in appearance to those within the upper barite-rich zone. The ore minerals are molybdenite, coarse pyrite, minor sphalerite and trace amounts of galena, tennantite and zinkenite. Microprobe analyses of the rutile are shown in Figure 57 and, although the vanadium and antimony contents are variable, the rutiles in both the upper and lower zones show similar compositions.

Drill hole W70 represents the heart of the Hemlo gold deposit. The drill hole is located at a vertical depth of 750 m adjacent to the boundary of the Golden Giant orebody to the east. The ore is about 45 m thick, which is the greatest thickness attained by the Hemlo deposit. Because of the inclination of the drill hole, the gold zone in the drill core extends from 709 to 781 m. Sampling of the drill core commenced in the hanging wall at 701.3 m and continued into the footwall at 781 m; 124 samples were collected. A polished section was prepared for each and polished thin sections for more than half of the samples. The minerals and their distribution are presented in Figure 58, the Fe, V, and Ba contents of the micas are shown in Figure 59 and the complete analyses for these micas are listed in Table A.13, the V, Sb, and W contents of the rutiles in Figure 60, and the barium contents of the microclines in Figure 61. Whole rock geochemical analyses were obtained on the samples collected in this study and some of these results were reported by Cameron and Hattori (1985); additional geochemical analyses were also provided by LAC Minerals. Geochemical profiles of eight elements are presented in Figures 62 and 63. The mineralogical studies show the following:

1. In the hanging wall at 701.3 m or 8 m above the gold-bearing zone, the metasedimentary rock consists of biotite that contains 14 wt. % FeO (Fig. 59), staurolite, kyanite, tourmaline, and andesine plagioclase with some calcite, titanite, apatite, pyrite, chalcopyrite, sphalerite, pyrrhotite, ilmenite and rutile.

2. Next, in the hanging wall at 705.2 m, immediately above the gold-bearing zone, the rock is a biotite schist with 18 wt. % FeO in the mica, andesine plagioclase, minor calcite, tourmaline, titanite and barian microcline with as much as 7 wt. % BaO (Fig. 61). At 707.2 m the iron content in the mica drops to 5.6 wt. %, plagioclase is An_{93} , and minor calcite, tourmaline, titanite, pyrite, ilmenite, magnetite, rutile, arsenopyrite, pyrrhotite and chalcopyrite are present. The hangingwall rutile contains no detectable V, Sb or W.

3. The ore zone commences at 710 m with the host rock consisting of muscovite schist containing microcline, some titanite and tourmaline. The presence of molybdenite in hand

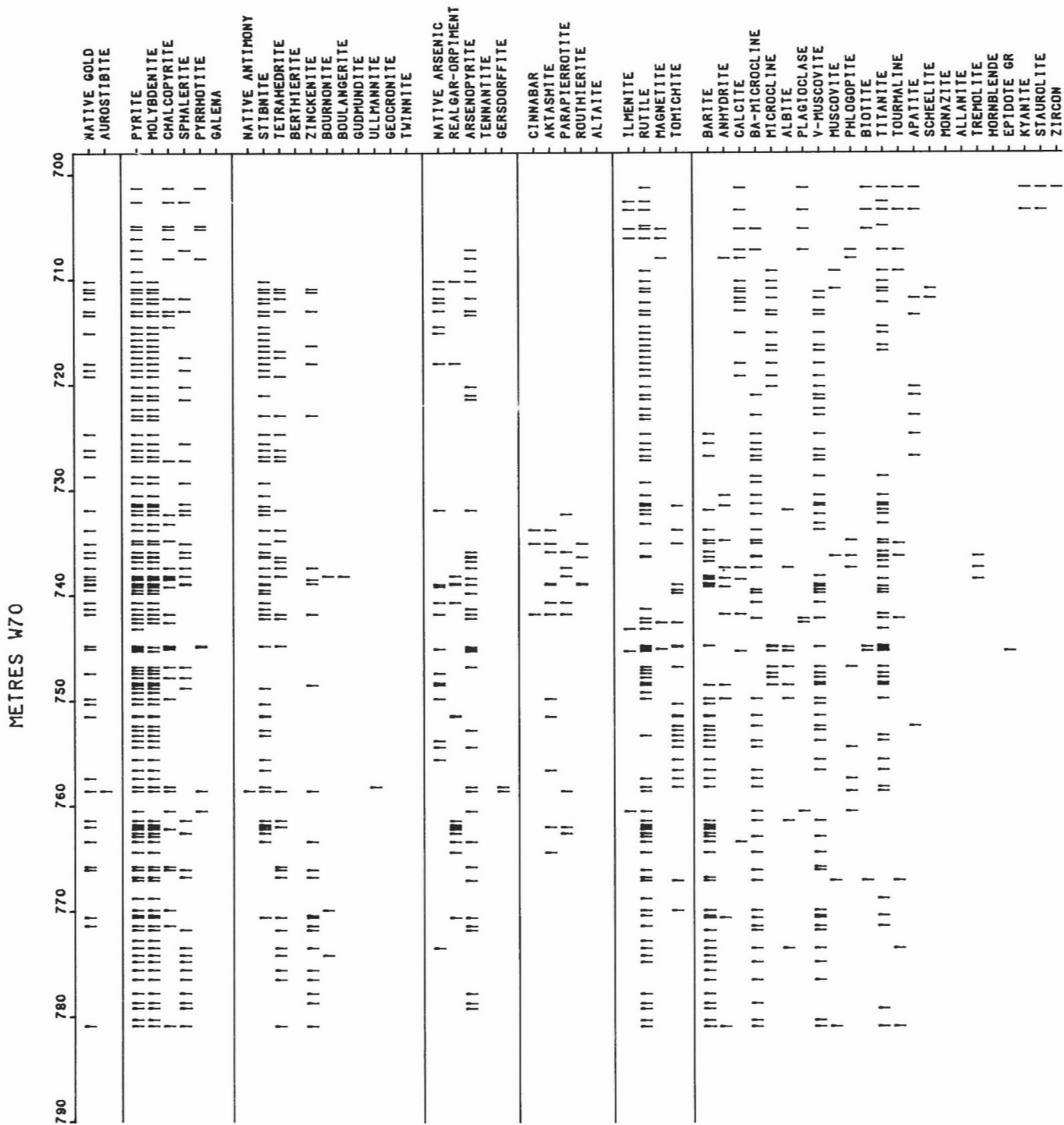


Figure 58. Plot of mineral distribution versus depth across the ore zone within drill hole W70.

specimen, as well as the associated stibnite, tetrahedrite, zinkenite, native arsenic and realgar, permits recognition of the gold-bearing zone. Some of the muscovite is pale green indicating the presence of vanadium, as confirmed by the microprobe analyses (Fig. 59). No significant differences were observed in the next 14 m of drill core.

4. At 724.7 m where barite appears, rutile shows a sharp increase in V and Sb, microcline contains barium and muscovite shows an increase in V and Ba. The only difference in the ore minerals is the absence of arsenic-bearing phases.

5. At 731 m mercury and thallium minerals appear in the ore zone, with stibnite as the major antimony mineral, realgar as the principal arsenic mineral, and barian tomichite and some biotite present. In places the ore zone is barite-rich. A zone of similar mineralization extends down to about 765 m. Within this zone there are also tremolite-bearing

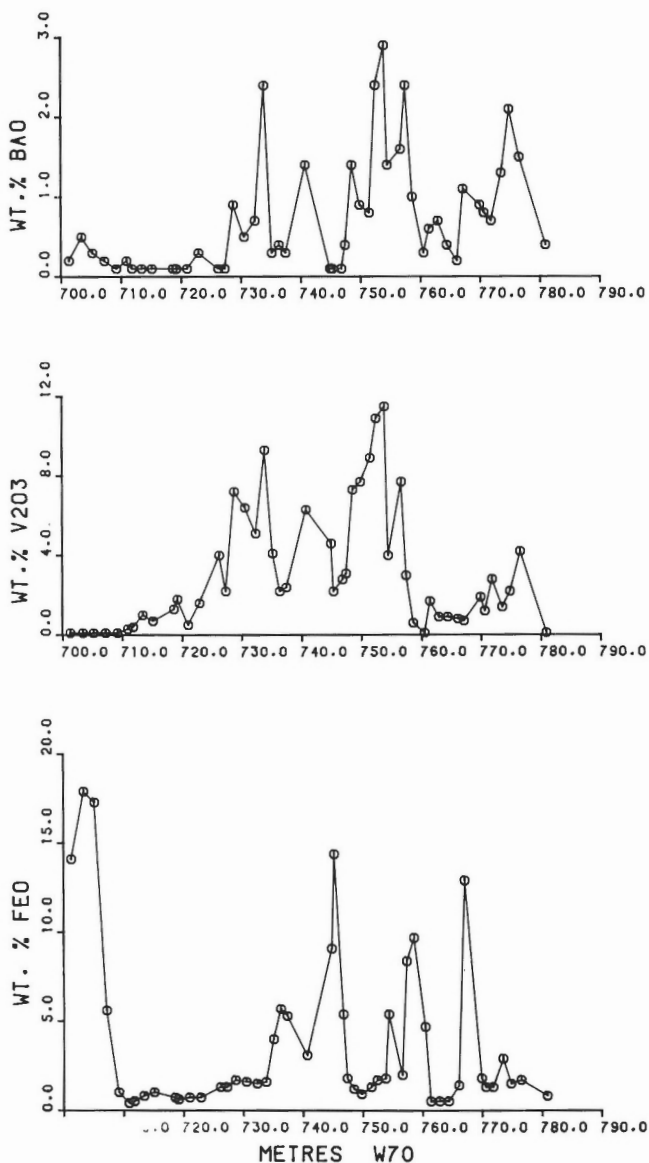


Figure 59. Plot of FeO, V₂O₃ and BaO contents of mica across the ore zone within drill hole W70.

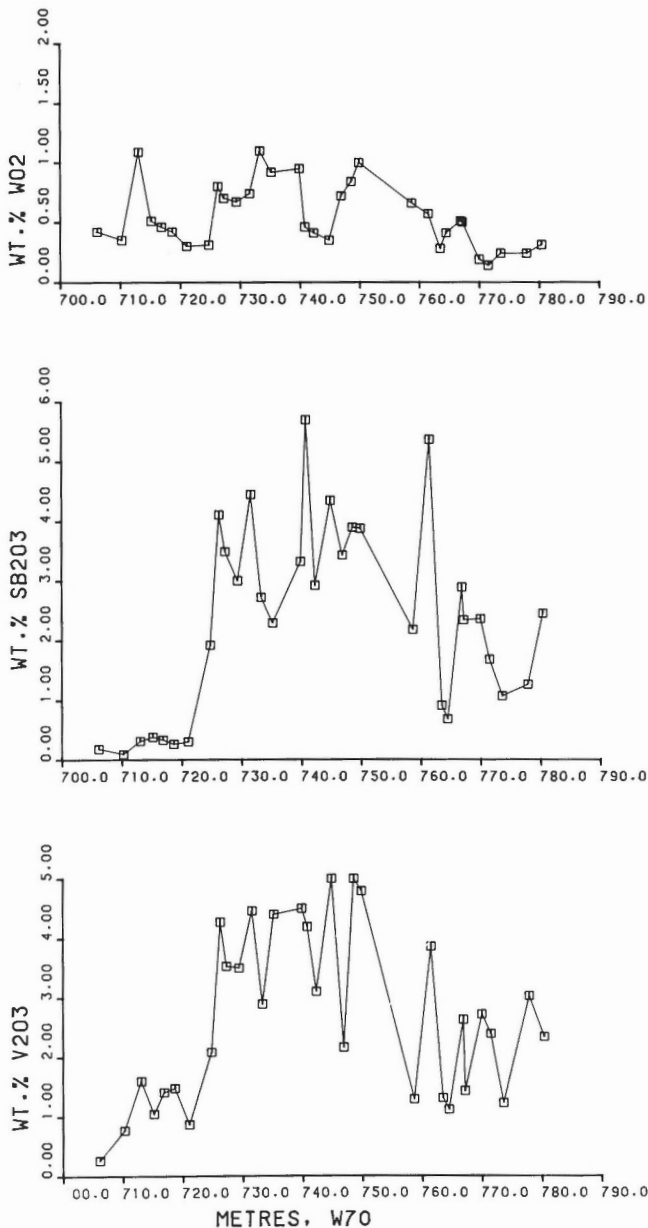


Figure 60. Plot of V₂O₃, Sb₂O₃ and WO₂ of rutile across the ore zone within drill hole W70.

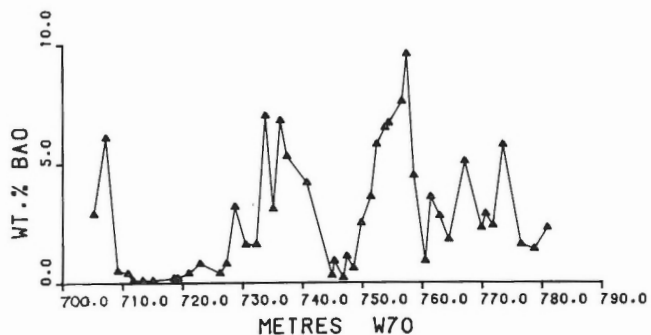


Figure 61. Plot of BaO contents of microcline across the ore zone within drill hole W70.

layers that contain high gold values, boudinaged quartz veins that contain realgar, sphalerite, stibnite, cinnabar, and thallium minerals, as well as numerous other rare minerals. The muscovite contains significant vanadium down to 760 m, and V-Sb-bearing rutile and barian microcline continue below this zone.

This drill hole is the only one in the deposit that contains sphalerite throughout the ore zone so that the variation of its mercury content could be determined in a reasonably continuous manner across the zone. The microprobe analyses are plotted in Figure 10, and the results show an increase

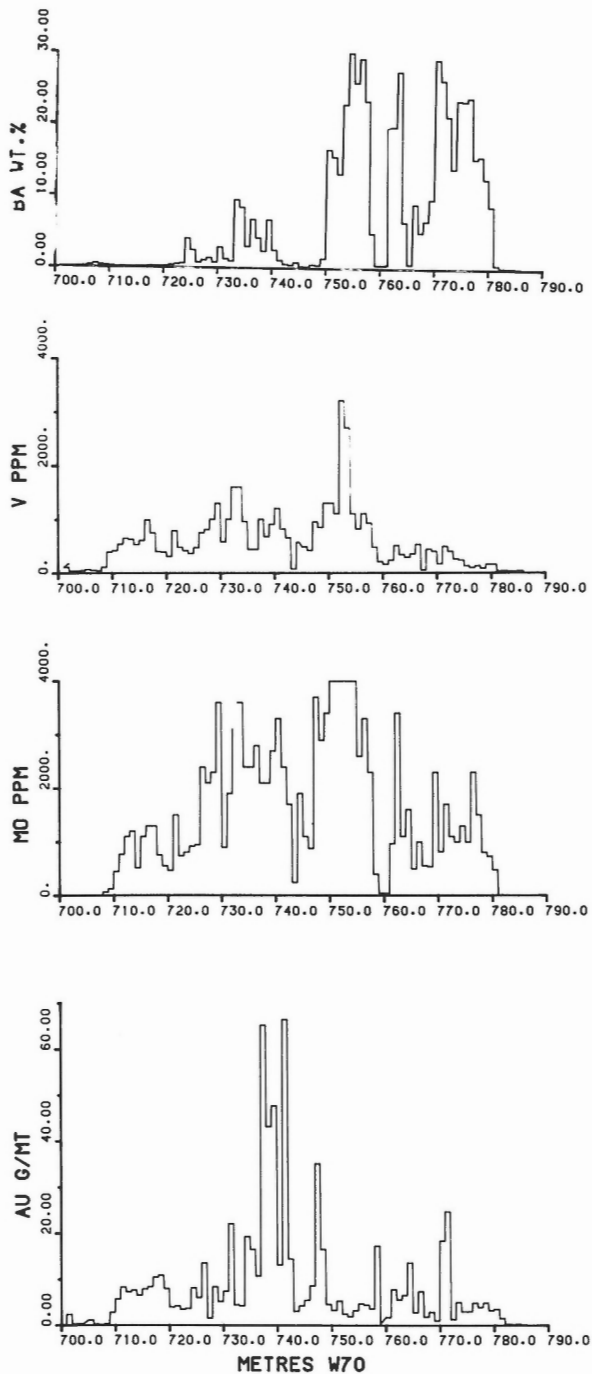


Figure 62. Geochemical profiles of Au, Mo, V and Ba across the ore zone within drill hole W70.

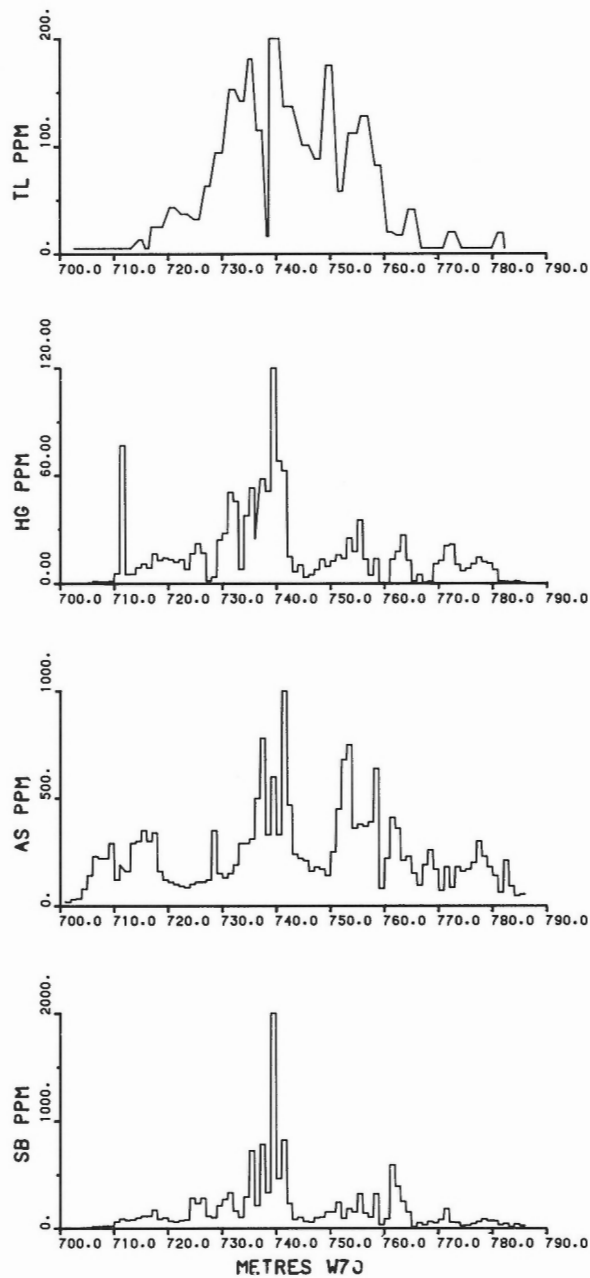


Figure 63. Geochemical profiles of Sb, As, Hg and Tl across the ore zone within drill hole W70.

from the hanging wall at 710 down to 760 m. This increase may be fortuitous, but the sharp drop at 760 m correlates with a sharp decrease in the vanadium content of the muscovite and also closely corresponds with the disappearance of mercury and thallium minerals and stibnite.

6. The lower portion of the ore zone to the footwall at 781 m contains rutile with lower Sb contents, is sphalerite-rich with low mercury contents, contains sparse slightly-vanadian muscovite, and the gangue minerals are chiefly quartz, barite and barian microcline.

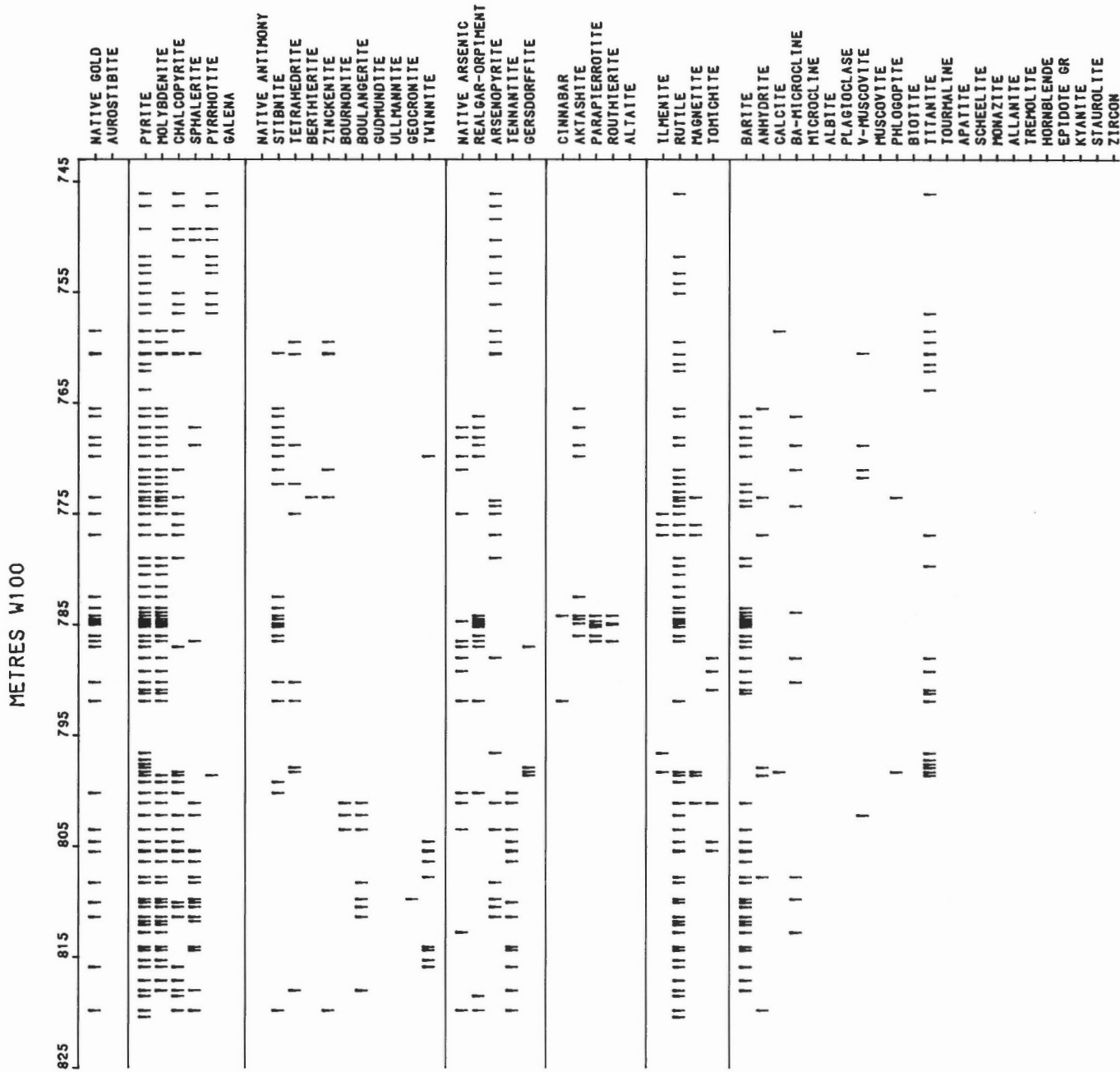


Figure 64. Plot of mineral distribution versus depth across the ore zone within drill hole W100.

Figure 65. Plot of V_2O_5 , Sb_2O_3 and WO_2 of rutile across the ore zone within drill hole W100.

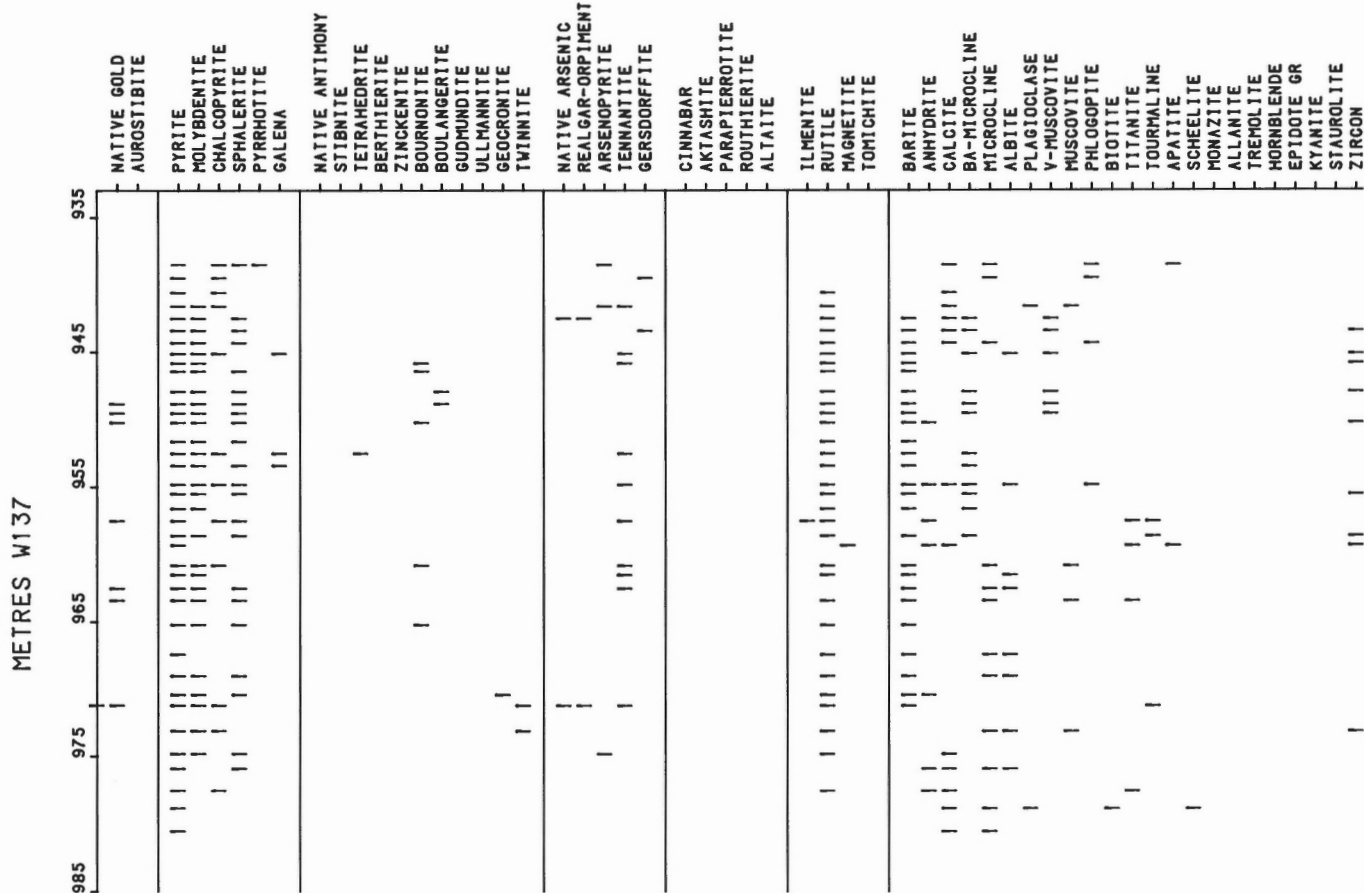
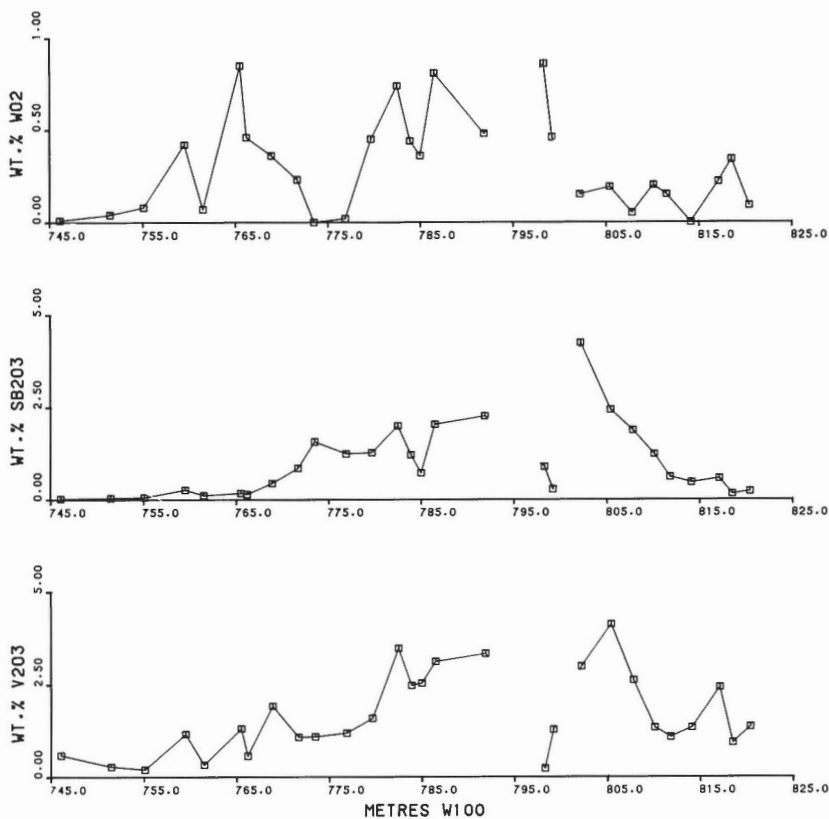


Figure 66. Plot of mineral distribution versus depth across the ore zone within drill hole W137.

Drill hole W100 is approximately 150 m west of drill hole W70, also within the heart of the Hemlo gold deposit. The ore extends from 758 m to 820 m or 62 m uncorrected for drill hole inclination. The true width is approximately 45 m. The minerals present and their distribution are presented in Figure 64. Sampling of the drill core commenced at 746 m. The rock in the hanging wall consists of fine grained biotite schist that grades to muscovite schist with layers of biotite at 749 m, to well foliated pyrite-rich muscovite schist at 753 m, and to fine grained biotite schist in contact with the ore zone at 758 m. The ore minerals in the hanging wall are pyrite, pyrrhotite, arsenopyrite, and minor to trace amounts of chalcopyrite and sphalerite. The host rock of the ore is feldspathic with thin layers of muscovite, some of which is a pale green. The principal ore minerals, other than pyrite, in the top 3 m of the ore zone are molybdenite, stibnite, tetrahedrite, zinkenite and arsenopyrite. The ore zone from

761 to 765 m is mainly muscovite-phlogopite-pyrite schist with low gold values. At 765 m the ore is baritic and at 768 m it has a distinct brecciated appearance with barite as fracture fillings and surrounding the host rock fragments. The host rock is feldspathic with seams of green vanadian muscovite, finely disseminated realgar, some tourmaline and, in places, is pyrite-rich. Stibnite is the principal antimony mineral, with native arsenic, realgar and aktashite also present. This assemblage of minerals ends at 775 m. From 775 to 783 m, the gold values range from 1 to 10 g/t, the rock is fine grained and feldspathic with some biotite layers, no antimony or mercury minerals, arsenopyrite as the arsenic mineral, traces of barite, and some magnetite and ilmenite. From 783 to 793 m the ore zone is barite-rich with as much as 39 wt.% Ba, and contains a series of realgar-rich boudinaged quartz veins with stibnite, native arsenic, cinnabar, aktashite and the thallium minerals parapirotite and routhierite. The lower portion of this zone contains barian tomichite that appears to have formed in place of rutile, which is absent. A feldspar porphyry sill is present from 795 to 796 m. From 796 to 799 m the rock consists of biotite schist with narrow quartz veins and is extremely rich in gold, with values as great as 156 g/t Au for 1 m intervals. Ore microscope studies reveal no native gold, molybdenite or other common ore minerals in the schist itself, suggesting that the quartz veins are the host for the gold. Generally within the Hemlo deposit these narrow white quartz veins are barren of gold, although visible gold has been observed in some veins. The lower portion of the ore zone from 799 to 820 m consists of rocks similar to other parts of the deposit, with major barite that has a fragmental nature, layers of coarse

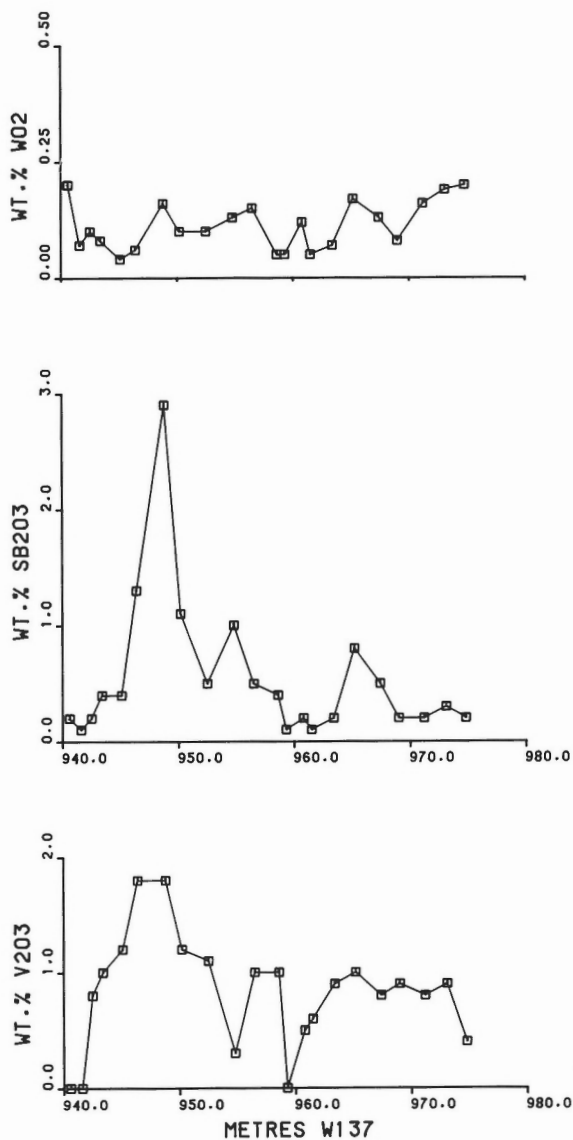


Figure 67. Plot of V_2O_3 , Sb_2O_3 and WO_2 contents of rutile across the ore zone within drill hole W137.

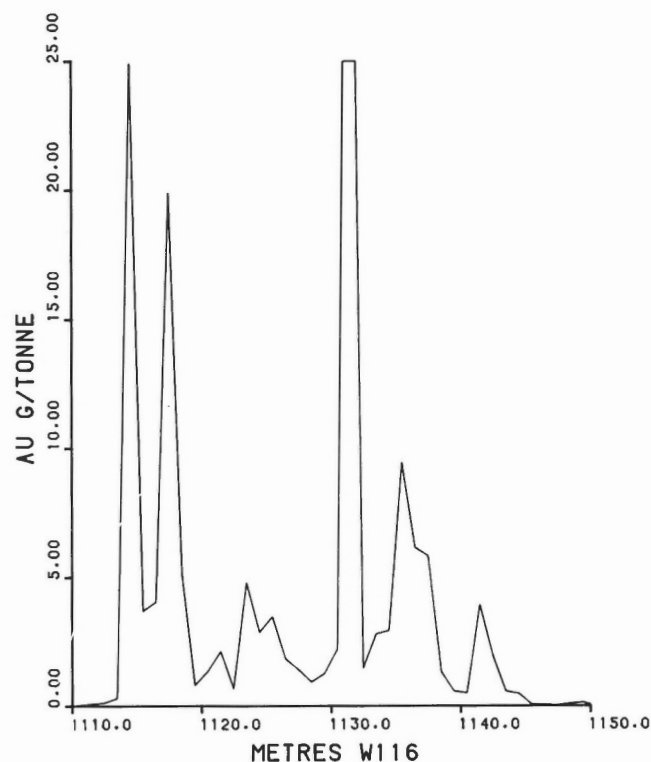


Figure 68. Profile of gold assay data across the ore zone within drill hole W116.

pyrite and thin layers or seams of green vanadian muscovite. However, the ore minerals within this zone are different. The antimony minerals consist of bournonite and twinnite, both with high arsenic contents and with one analysis of the bournonite-type mineral yielding arsenic in excess of antimony in atomic proportions, which means the mineral is seligmannite. Other arsenic minerals are tennantite, minor arsenopyrite and native arsenic. No mercury minerals occur within this zone. Sphalerite is moderately common and it contains from not detected (less than 0.4 wt. %) to 4.0 wt. % Hg (Table A.1). Some barian tomichite was noted in the upper portion of this zone. The footwall contact at 820 m is with a quartz-eye muscovite schist. Microprobe analyses of rutile (Fig. 65) reveal significant substitution of V, Sb and W for Ti throughout the width of the ore zone, whereas the rutile in the hanging wall from 746 to 758 m contains undetectable to low values of V. The increase in concentration of these elements in rutile at 758 m defines the start of the ore zone and they gradually increase in abundance in the rutile to the contact with the feldspar porphyry sill at 796 m. Below the sill to 799 m, where biotite schist containing gold-bearing quartz veins is present, the rutile grains are low in V, Sb and W; this correlates with the lack of ore minerals within this sequence, which probably indicates that the biotite schist was not as intensely altered or mineralized by the ore forming solutions. The lower portion of the ore zone contains rutile grains with high V and Sb contents and the abundance of these elements in rutile gradually decreases to the footwall at 820 m.

Drill hole W137 is approximately 300 m along the north-west down-plunge extension of the orebody from drill hole

W100. The minerals present and their distribution are illustrated in Figure 66 and the V, Sb and W contents of the rutile in Figure 67. The ore zone extends from 942 to 976 m in drill core or for a true width of approximately 25 m. The minerals present within this portion of the deposit are similar to those encountered in the lower portion of drill hole W100. In this hole sphalerite with low contents of mercury (Table A.1) occurs throughout most of the ore zone, bournonite is the principal antimony mineral, tennantite is the principal arsenic mineral, mercury minerals are absent, and galena is sparse. Barite is a principal gangue mineral throughout most of the ore zone and from 945 to 954 m it has a distinct fragmental nature. At 957.5 m a narrow biotite-rich layer is present that is similar to the hanging wall metasedimentary rocks. Above the hanging wall contact of this layer is a muscovite schist with scattered small tourmaline crystals. At 971.2 m a rare zone of telluride minerals was encountered. The minerals occur within a thin seam and consist of calaverite (AuTe₂), hessite (Ag₂Te), coloradoite (HgTe) and an unnamed phase (AgSbTe₂), associated with native arsenic, native gold, tennantite, twinnite, geocronite, sphalerite, molybdenite and pyrite. This is the first documented occurrence of significant amounts of telluride minerals within the Hemlo deposit.

Drill hole W116 is approximately 200 m down-dip from drill hole W137. The ore zone extends from 1114 to 1143 m (29 m, uncorrected for inclination) and has an average gold grade of 5.26 g/t (Fig. 68). The minerals present and their distribution are shown in Figure 69, the mica compositions are shown in Figure 70 and the barium contents of the microcline

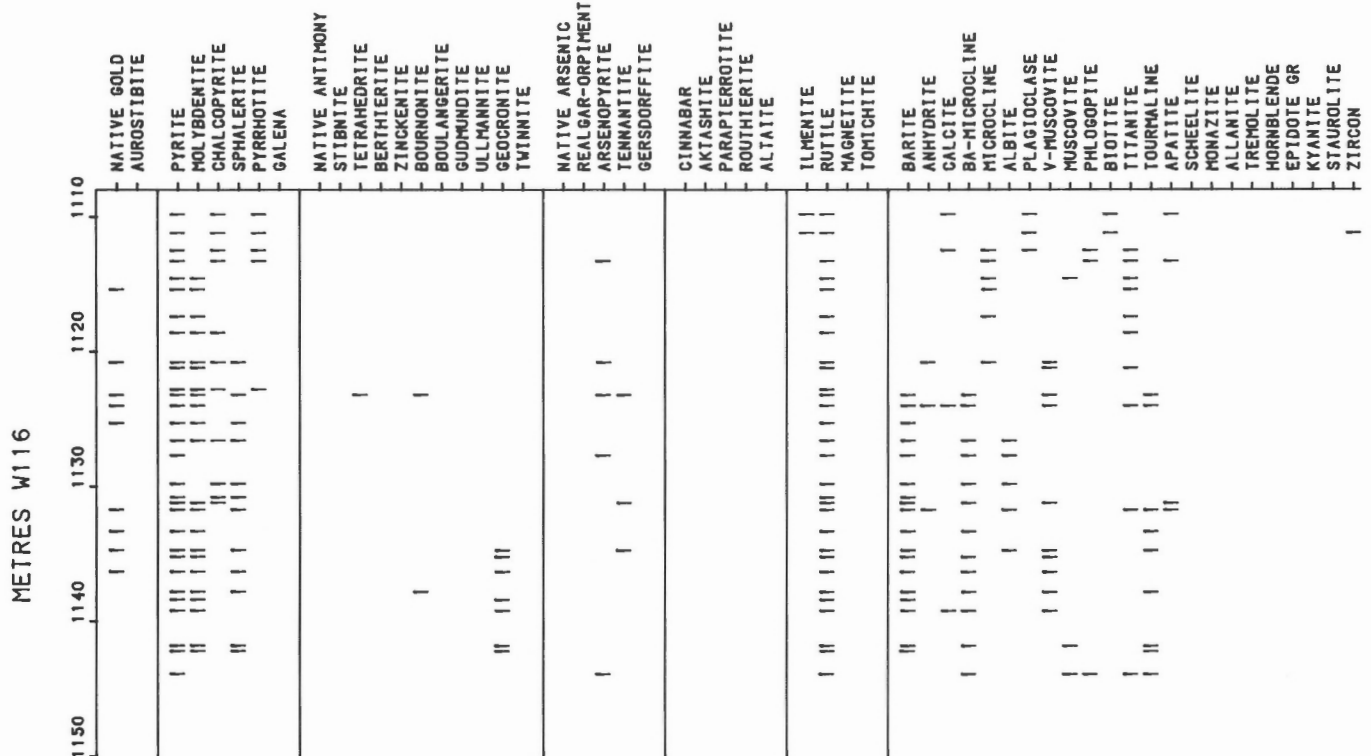


Figure 69. Plot of mineral distribution versus depth across the ore zone within drill hole W116.

are shown in Figure 72. In this part of the deposit, the hanging wall consists of dark to light coloured, fine grained biotite schist with some ilmenite, with pyrrhotite generally in excess of pyrite, and with trace amounts of chalcopyrite and arsenopyrite. Within one metre of the ore zone, the rock is a well foliated muscovite schist with some barian microcline and this lithology continues into the ore zone with increasing amounts of pyrite defining the contact. The V and Sb contents of rutile (Fig. 71) clearly define the hanging wall contact of the ore zone and the Fe and V contents of the micas reflect the change from biotite in the hanging wall to muscovite and vanadian muscovite in the ore zone. Barite occurs from 1123 to 1142 m, and within this interval it is a major gangue mineral and has a fragmental nature. The significant increase in the barium contents of the microcline (Fig. 72) correlate very closely with the presence of barite at 1123 m, although this may be fortuitous. The ore minerals form less complex assemblages and consist of pyrite, molybdenite and sphalerite, sparse antimony minerals with geocronite in the lower portion, sparse arsenopyrite and tennantite and no mercury minerals. The mercury contents of the sphalerite (Table A.1) are very low (0.2 - 1.4 wt. % Hg). The foot-wall contact at 1143 m is not well defined, due to a diabase dyke from 1145 to 1149 m. Below the dyke, gold values are almost nil.

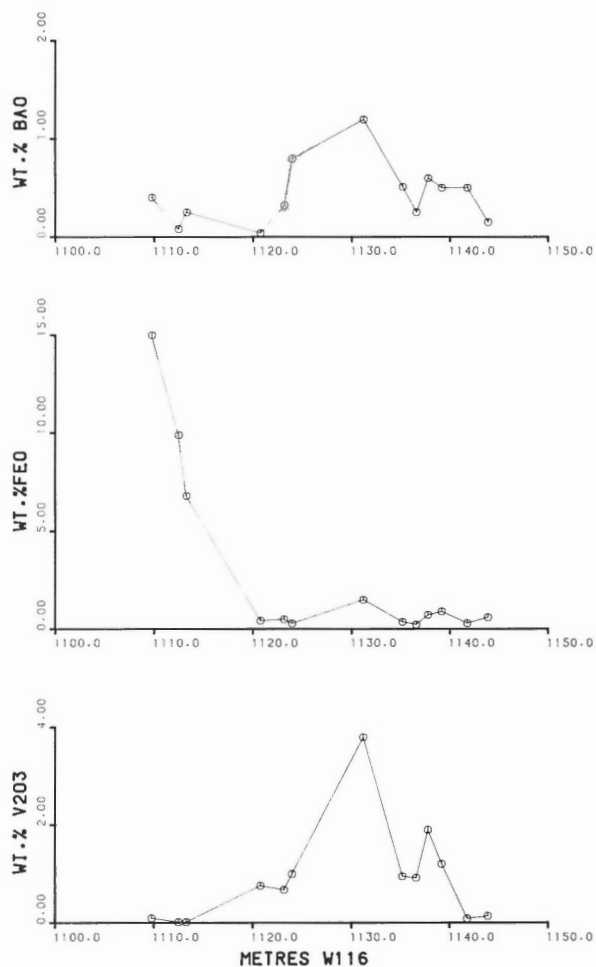


Figure 70. Plot of V_2O_3 , FeO and BaO contents of mica across the ore zone within drill hole W116.

Drill hole W135 is near the bottom of the Page-Williams' main shaft and is the most westerly down-plunge drill hole examined in this study. The ore zone extends from 1173 to 1201 m, contains variable gold values from 0.3 to 8.7 g/t, and is barite-rich and has a fragmental nature in places. The ore minerals and their distribution (Fig. 73) indicate that a distinct assemblage is present consisting of sphalerite (undetectable Hg), galena and altaite as the common minerals. Trace amounts of tetrahedrite occur in the upper portion of the zone and trace amounts of tennantite in the lower portion. Rare tellurides are coloradoite and melonite. Analyses of the native gold (Table A.2) show no mercury. Rutile analyses (Fig. 74) indicate 1 to 2 wt. % V_2O_3 with undetectable to low antimony and tungsten contents. Pale green muscovite occurs in thin seams, but was not analyzed. Microprobe analyses of barite yielded strontium values of 0.6 to 1.4 wt. % SrO.

Drill hole W129 is the deepest hole examined in the deposit at a vertical depth of approximately 1350 m. The ore occurs in two zones, the upper or an extension of the main zone at 1377 to 1384 m and a lower zone at 1422 to 1451 m (Fig. 75). The upper zone contains gold values of less than 1 g/t. Native gold was not identified, but other ore minerals include realgar, native arsenic, arsenopyrite,

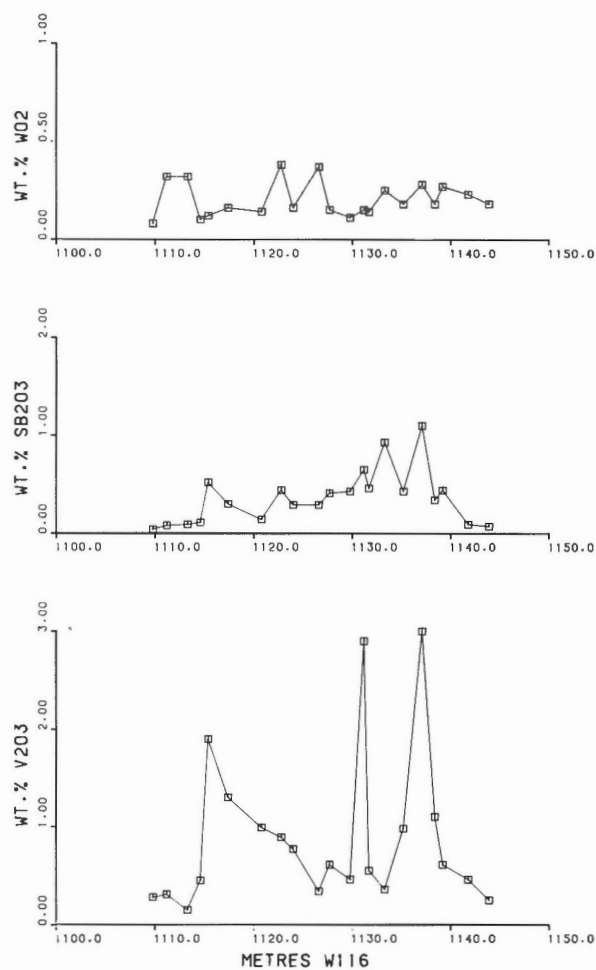


Figure 71. Plot of V_2O_3 , Sb_2O_3 and WO_2 contents of rutile across the ore zone within drill hole W116.

optical properties with colours of bronze to red, is strongly birefractant with very strong anisotropism varying from brilliant yellow to fiery orange to reddish. Microprobe analyses show that the mineral has a variable composition and contains Fe (0.3-3.5), Ag (2.1-2.6), Pb (4.0-7.0), Te (8.6-13.5), Au (64.4-71.2). A mineral of similar optical properties was reported by Harris et al. (1983) from the Ashley gold deposit, Ontario where it occurs replacing calaverite. This unidentified phase could be identical to one of the minerals bilibinskite or bezsmertnovite. These minerals were first described as intermetallic gold compounds with the formula $Au_5Cu_3(Te,Pb)_5$ and $Au_4Cu(Te,Pb)$, respectively. However, recent studies by Bocek et al. (1982) have shown that they are unequivocally new hydrid minerals of the intermetallic compound-oxide type with the general formula $(Au,Cu,Ag,Pb)_n(TeO_2)$, where $n \approx 0.3$ for bilibinskite and 0.07 for bezsmertnovite. The strong optical anisotropism reported for these minerals is similar to that observed for the unidentified gold-bearing phase.

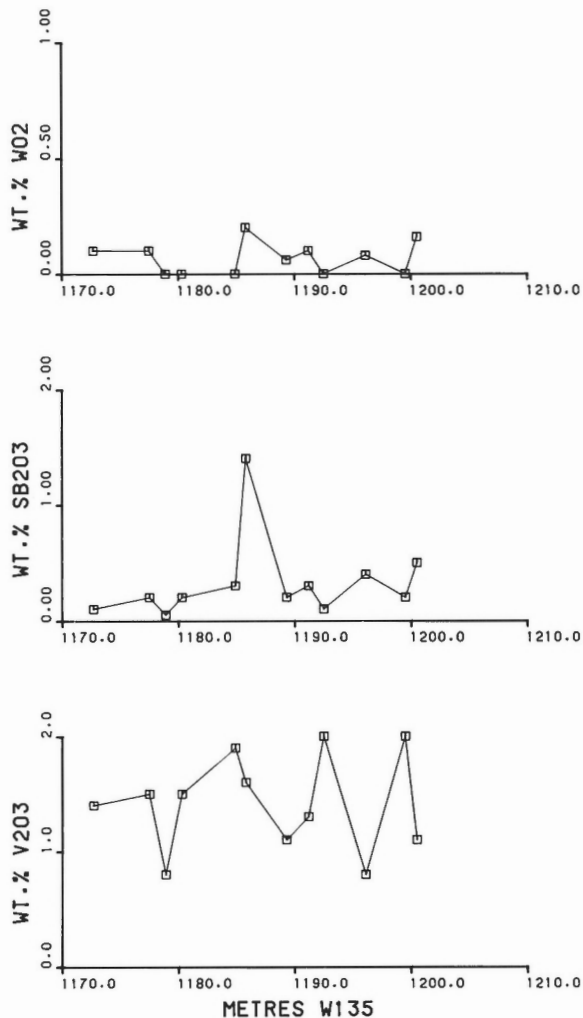


Figure 74. Plot of V_2O_3 , Sb_2O_3 and WO_2 contents of rutile across the ore zone within drill hole W135.

The Golden Sceptre Resources Property

Golden Sceptre Resources Limited has a block of claims in which Noranda holds an interest, adjacent to the Page-Williams "C" zone. A trench 120 m west of the Golden Sceptre/Page-Williams claim boundary, provides a stratigraphic section across the lower two-thirds of the sequence of felsic pyroclastic rocks of the Moose Lake Formation. Altered stratigraphic equivalents of these rocks host the main Hemlo orebody, some 1-2 km to the east. The north end of the trench encroaches on a broad area of erratic Au-Mo mineralization referred to as the "South Zone" that does not appear to be stratabound, as well as crossing the stratabound "North Zone" of siliceous tuffs that carries Au and Mo and is located approximately 200 m to the north. A trench sample labelled as the fracture zone that assayed 148 oz/t Au, and probably is from the "South Zone", was obtained from G. Patterson. The fracture zone is "hosted" in quartz veins which cut a quartz porphyry (Patterson, 1986). Ore microscopic study of the sample shows that the mineralization consists of native gold of variable compositions ranging from 69.4 to 85.2 wt. % Au, 13.9 to 28.0 wt. % Ag and 0.0 to 4.0 wt. % Hg, pyrite, chalcopyrite, sphalerite, molybdenite, petzite, hessite, altaite, coloradoite, tetrahedrite, rare galena and calaverite. An unidentified phase with a formula $AgFeS_2$ occurs in one of the polished sections. The sample shows the effect of surface weathering with formation of goethite after pyrite and lead sulphate after galena and lead tellurate after altaite. An unusual textural feature of some of the gold-hessite grains is the presence of filaments or veinlets of native gold in hessite (Fig. 78). Identical gold-hessite textures have been observed in gold samples from

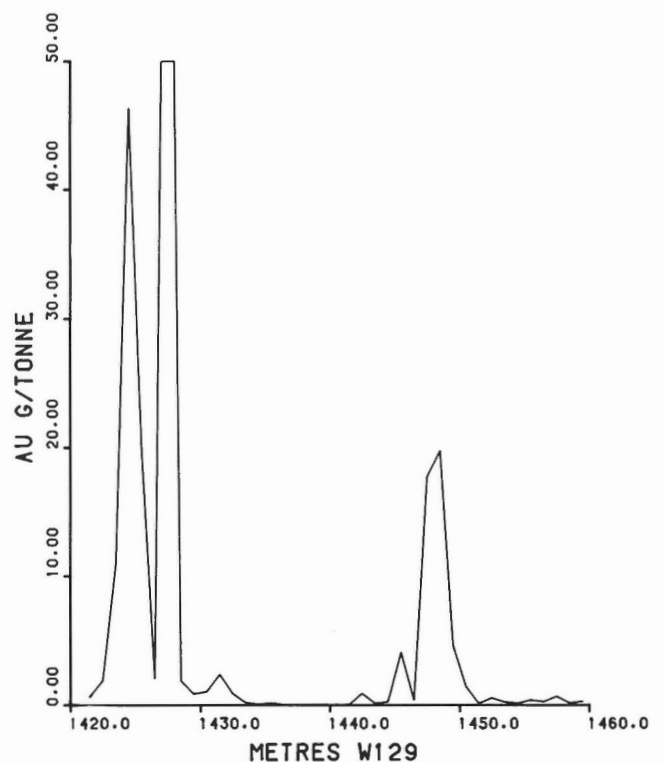


Figure 75. Profile of gold assay data across the ore zone within drill hole W129.

near-surface gold occurrences in the Atlin area, B.C.; from the Bessie G epithermal gold telluride deposit in the La Plata Mountains, Colorado, U.S.A. (Saunders and May, 1986), and Lebedeva (1986) reported filamentous veinlets of native gold in hessite from a near-surface gold-silver deposit in Central Kamchatka. The origin of this texture is unclear, but generally the filaments of native gold in the hessite have a higher fineness than native gold in gangue in the same sections.

ALTERATION

Walford et al. (1986) have identified three types of alteration associated with the Page-Williams orebody and adjacent rocks; calc-silicate alteration which has affected the enclosing sedimentary rocks; pervasive potassic alteration that is reflected by microcline formation in the felsic rocks and adjacent sedimentary rocks; and muscovite alteration that has affected the orebodies and surrounding rocks. Detailed study of the Golden Giant orebody by Kuhns (1986) has shown the existence of a symmetrical mineral zonation which may represent an alteration halo enveloping the Main Ore Zone. Burk et al. (1986) reported that metasomatic alteration related to the David Bell mine of Teck-Corona is seldom obvious in the wall rocks, whereas microcline and white mica schists display a spatial correlation with most of the ore zones, indicating that extensive potassic alteration was an integral part of the ore-forming processes. On the Page-Williams property the most spectacular aspect of the felsic rocks that form the footwall to the deposit and extend to the east beneath the Golden Giant orebody is the abundance of a bright pink potassium feldspar rock. On the 10115 level (5115 level

Fig. 4) and other levels, the red, altered rock passes gradationally either directly into a quartz-eye muscovite schist or into a grey quartz-eye, microcline-bearing rock. Beneath the "A" zone, this rock contains molybdenite as fracture controlled wisps, interstitial grains and streaks, together with visible native gold of 970 fineness, pyrite and rutile in a matrix of finely disseminated barite interstitial to barian microcline (1.5 to 6.3 wt. % BaO) and quartz (Fig. 79). Although the bulk of the thicker ore is hosted in the feldspathic rocks at depth on the Page-Williams property, this rock passes transitionally into a muscovite schist near surface and to a biotite schist both to the east and west. To the east on the Golden Giant property the biotite schist is the host to most of the ore on the upper levels.

This study has shown that most of the microcline reported by other workers in the main ore zone is a barium-containing variety and, although mainly restricted to the ore zone, this barian microcline also occurs within the altered metasedimentary hanging wall rocks and the red potassic footwall unit. The Ba-rich hydrothermal fluids that formed the barian microcline also were enriched in Mo, Au, Hg, Sb, As, V and this accounts for the deposition of the large number of minerals in the deposit, in particular the characteristic V-Sb-W-bearing rutiles and vanadian muscovite that are closely associated with the gold-molybdenite mineralization.

ORIGIN OF MINERALIZATION

Various genetic models have been suggested for the origin of the mineralization at the Hemlo gold deposit. Most research prior to 1986 suggested either a syndimentary or

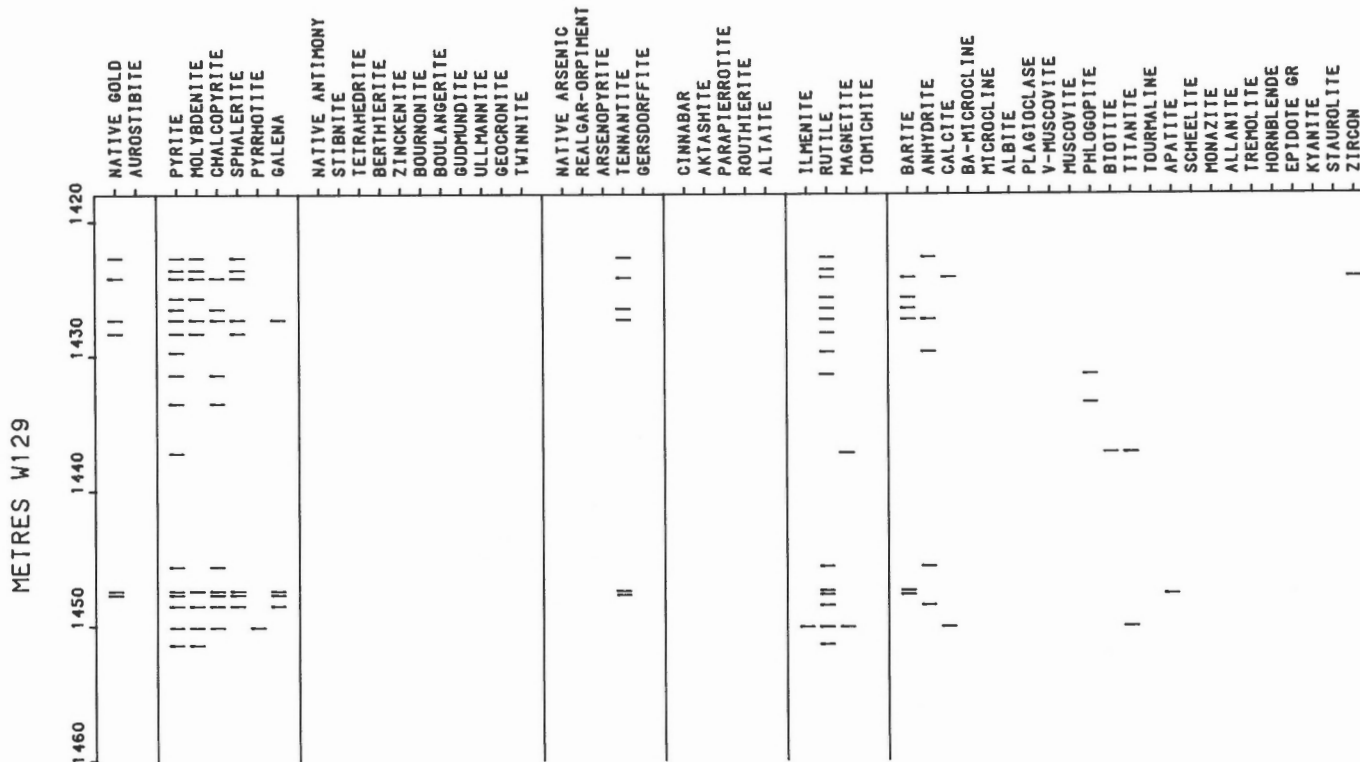


Figure 76. Plot of mineral distribution versus depth across the ore zone within drill hole W129.

synvolcanic origin for the main orebody. Quartermain (1985) reported that in the David Bell mine (formerly Teck-Corona), sericitic alteration associated with the mineralization is developed in the hanging wall and more extensively in the footwall. From the west to east across the property, there is a thinning of the footwall felsic volcanics from 30 to 3 m, a corresponding thinning of the ore zone and a decrease in grade. The felsic volcanics, ore zone and sericitic alteration all terminate at the east end of the property. Quartermain recognized that these observations could be used to support either a syngenetic or epigenetic origin for the mineralization, but he concluded that the consistent distribution of gold in the east end of the orebody and almost complete lack of visible gold were not typical of structurally controlled epigenetic gold deposits. Further, in drill hole 240 at 722.5 m, an "ore clast" is present in the reworked felsic pyroclastic unit above the ore zone that contains molybdenite and a 1 mm speck of visible gold. It was interpreted that the fragment originated from the mineralized horizon and on this basis, a syngenetic origin was proposed for the mineralization.

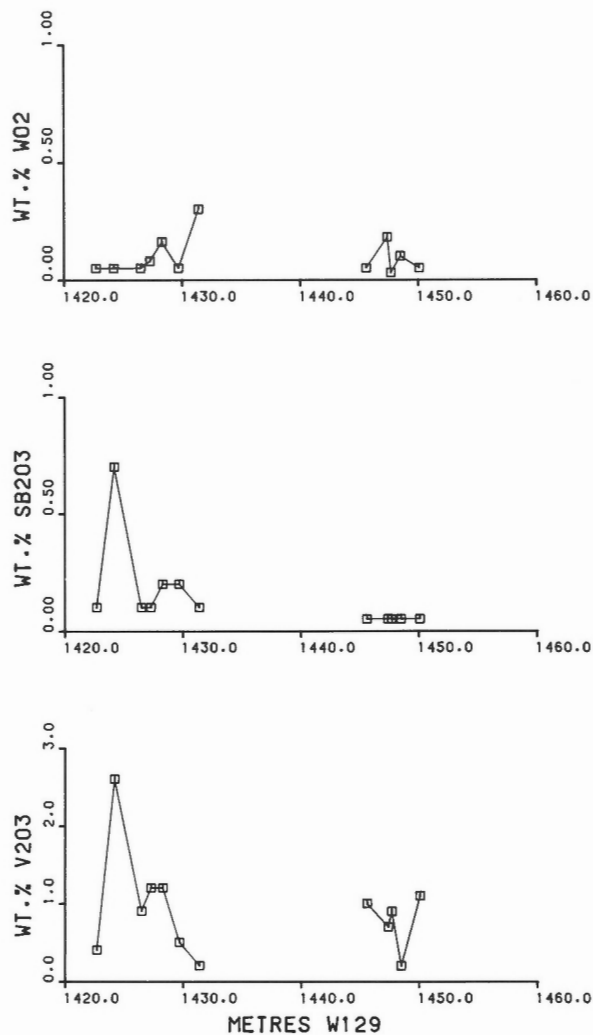


Figure 77. Plot of V₂O₃, Sb₂O₃ and WO₂ contents of rutile across the ore zone within drill hole W129.

Valliant (1985) suggested that the stratiform nature of the Page-Williams orebody at the contact between footwall felsic rocks and overlying sedimentary rocks indicates that the ore was deposited during a quiescent stage following a period of felsic volcanism. Intercalation of felsic volcanic and sedimentary lithologies in the ore is evidence for episodic influx of tuff and clastic sedimentary debris during ore deposition. The preservation of fine compositional layering in ore and the presence of rock deformation fabrics in ore similar to those of enclosing volcanic and sedimentary rocks support the interpretation that ore was deposited as a sediment and subsequently deformed during later orogenic events. The intimate association of gold, pyrite, molybdenite, barite and other metallic minerals indicates that all components of ore

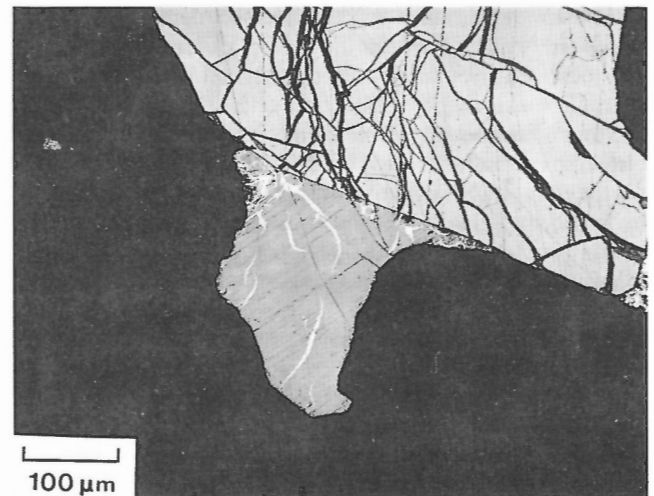


Figure 78. Photomicrograph of filaments or veinlets of native gold in hessite (Ag₂Te) in contact with fractured pyrite. Golden Sceptre Resources trench sample.

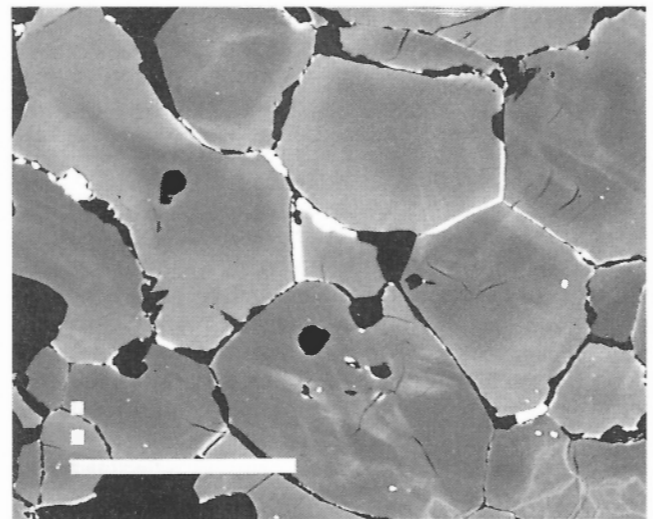


Figure 79. Electron backscattered image of barian microcline showing also fine inclusions of barite and pyrite interstitial to the microcline grains. The black areas are quartz. The scale bar is 100 μ m. Sample from the Page-Williams 10115 level.

were deposited consanguinously as a chemical sediment. The regionally extensive muscovite-rich rock and the occurrence of aluminous minerals such as andalusite, kyanite, garnet, staurolite and chloritoid near ore reflect hydrothermal alteration of tuff and sediment during ore deposition. More recently, Valliant and Bradbrook (1986) presented information on the relationship between stratigraphy, faults and the ore zone within the Page-Williams mine and illustrated with schematic cross-section diagrams an evolutionary model for gold deposition. They concluded that the orebodies and their enclosing rocks were deposited in second order basins, separated by a growth fault and forming on the edge of a larger sedimentary basin to the east. The environment to the west of the growth fault was close to a volcanic source and coarser grained volcanic and volcanoclastic rocks were deposited rapidly and greater thicknesses accumulated here than to the east, where fine grained volcanic and sedimentary rocks were deposited. Faulting within the second order basins initiated and localized circulation of hydrothermal fluids through the volcanic rocks which resulted in the leaching of Au, Fe, Ba, Mo and other metals. These metals were deposited in structural traps or basins created by the faulting. West of the major northeast fault (NEF) active volcanism resulted in ascending hydrothermal fluids depositing numerous lenses of gold-bearing rock, each of which was possibly formed during an hiatus in volcanism. These lenses of ore now represent the "C" zone. East of the NEF, quiescence allowed deposition of large quantities of gold-bearing rock on the sea floor. The hydrothermal system was sealed rapidly in the west by deposition of volcanoclastic rocks, whilst slower deposition in the east allowed continued hydrothermal activity that resulted in development of the aluminous compositions of the upper sedimentary rocks, ultimately producing garnet, staurolite and kyanite. Continued deposition of the sedimentary rocks eventually sealed the hydrothermal system in the east, although continued gold deposition within the deposits may have persisted below the surface. Host rock and gold ore were rapidly tilted and subjected to shear deformation in a broad tectonic zone of strike-slip motion separating an active volcanic centre to the west and a growing sedimentary basin to the east. Subsequently, granodiorite plutons were intruded into the volcanic and sedimentary sequence and faults and fractures were filled by diabase and lamprophyre dykes.

Goldie (1985) noted that the main Hemlo orebody has many similarities with sinters formed by two New Zealand hot springs, the Ohaki and Champagne pools. Both Hemlo and the sinters are enriched in gold, sulphur, arsenic, antimony, mercury and thallium and are not enriched in copper and zinc. Both occur as tabular zones conformable with the host rocks, and in both cases the host rocks are volcanic and sedimentary. The rocks underlying the New Zealand sinters have been altered to an argillic assemblage, whereas the rocks hosting the Hemlo main ore zone are cut by a quartz-white mica stockwork, probably reflecting argillic alteration. On this evidence, Goldie suggested that the gold at Hemlo was transported to the surface as a thio-complex in neutral waters of low salinity and precipitated subaerially along with silica, sulphur, arsenic, antimony, mercury and thallium as a result of one or more of the following: boiling, oxidation, cooling, acidification and adsorption onto sols. Some differences between Hemlo and the sinters were noted,

particularly the presence of barite and molybdenite as major constituents at Hemlo and their absence from the sinters. However, the presence of barite at Hemlo was not considered an argument against a subaerial origin, since barite is common in other subaerial sinters. The molybdenite could be used as an argument against a subaerial origin, because molybdenite is usually precipitated at depth, adjacent to or in plutons of intermediate to felsic composition, although a sinter at Waimangu contains 500 ppm, a concentration comparable to that at Hemlo.

A geochemical and isotopic study by Cameron and Hattori (1985) showed that the Sr isotopic composition of barite from the main orebody is similar to that of the sedimentary barite west of Hemlo and to initial ratios of contemporaneous volcanic rocks. They showed that sulphur in the pyrite from the ore is unusually strongly fractionated and that the ore contains sulphide that is more strongly depleted in ^{34}S than any sulphide of Archean age recorded to date. The study showed a close correlation between the isotopic composition of pyrite in the deposit and Au assays that suggests that both had a common genetic link and were deposited contemporaneously. Further, since sulphide of this composition could only have formed by equilibration with oxidized sulphur species, the sulphate forming the barite must be linked genetically and temporally with the sulphide, and hence also with the gold. Therefore, a syngenetic depositional model seemed to most readily accommodate the low $^{87}\text{Sr}/^{86}\text{Sr}$ isotopic data for barite, the asymmetrical distribution of sulphur species and isotopic values within the deposit, and the continuity in these distribution patterns from section to section.

Structural field studies by Hugon (1984) demonstrated the Hemlo deposit is contained within a major dextral ductile shear zone, with the ore zone itself described as the Lake Superior shear zone, and is situated at the boundary between felsic metavolcanics and metasedimentary rocks. The metamorphic fabric of the rock indicated that the shear zone was active during the peak of metamorphism. Hugon (1986) concluded that the structural field evidence demonstrates that the auriferous mineralized rocks at Hemlo occupy the most intensely deformed, central portion of a large scale, wide ductile zone of oblique thrusting. Petrofabric analysis supports the hypothesis that the mineralizing event occurred subsequent to the attainment of peak amphibolite metamorphism.

Walford et al. (1986) presented evidence to support the view that the gold and other metallic minerals were not deposited as a syngenetic deposit for the following reasons:

1. gold and metallic minerals are related to microcline alteration;
2. the microcline alteration, although strongest in the felsic rocks, is also developed in the sedimentary rocks adjacent to the orebody;
3. muscovite-tourmaline alteration occurred subsequent to microcline alteration, as is common in magmatic-hydrothermal environments;
4. the "A" zone orebody includes microcline- and muscovite-altered felsic rocks, and altered sediments with gradational contacts.

5. many geological features of the orebody and surrounding rocks appear to be structurally controlled.

Based on this evidence, Walford et al. (1986) favoured a hydrothermal origin with alteration and mineralization controlled in part by deformation along the Lake Superior shear zone.

Detailed studies by Kuhns et al. (1986) on the Golden Giant orebody, which represents one-third of the Hemlo deposit, shows that:

1. alteration consists of an interior potassic zone grading outward into a sericitic/phyllitic zone, and finally, in places, into an outer argillic zone.

2. the main ore zone is stratiform, but not stratabound (i.e. Walford et al. (1986) have shown that the zone transgresses lithologic units along strike).

3. ore is hosted within amphibolite facies metamorphic rocks, and mineralization preceded peak metamorphism.

4. ore is hosted in, and in some places cuts across, a variety of lithological units. Protoliths are represented by mudstone and siltstone of turbidite sequence, and by felsic and mafic volcanic and volcanoclastic rocks.

5. ore has been faulted and only limited remobilization of the gold and molybdenum occurred subsequent to faulting.

6. the mineralization is spatially associated with granitoid sills (in the footwall) and stocks.

Due to post-mineralization metamorphism and tectonism, Kuhns et al. (1986) concluded that there is no consistent genetic model for the Golden Giant orebody.

Burk et al. (1986) presented a descriptive overview of the geology of the David Bell mine (Teck-Corona) and their main conclusions were as follows:

1. The Hemlo gold deposit is spatially associated with the eastern portion of a lenticular, quartz-porphyritic, rhyolitic body of probable volcanic origin, which occurs in a sequence of fine grained wackes, mudstones and conglomerates.

2. Progressive deformation in the area has involved initial isoclinal folding followed by the development of at least two localized, planar zones of high strain.

3. One of the high strain zones contains the main David Bell (Teck-Corona) ore zone, and the other, the Barren Sulphide Zone.

4. Progressive metamorphism involved an initial phase of high pressure, moderate temperature mineral growth which possibly developed through tectonic thickening, followed by a lower pressure, moderate temperature phase of mineral growth associated with erosional unroofing. The dominant planar fabric within the high strain deformation zones developed during the second phase of metamorphism.

5. the main ore zone is an elongate body with a plunge of approximately 45° towards the northwest and transgresses the contacts of adjacent rocks. Muir and Elliot (1987) noted that the plunge is parallel to F₂-fold axes and L₂ lineations

which are contained in rocks near the up-dip projection of the mineralized zone, and within the Hemlo fault. The F₂ folds appear to have a geometric, and possibly genetic, relationship to Au-Mo mineralization.

6. The dominant type of mineralization is a laminated, microcline-rich, quartzofeldspathic rock containing laminae of green vanadian muscovite, 5-10% pyrite, up to about 0.5% molybdenite and approximately 12 g/t Au. Less important are mineralized, highly strained, conglomerate and baritic ores.

7. Alteration is reflected in the abundance of microcline and muscovite, especially green muscovite, in the ore and spatially associated rocks.

8. The texture of the ore and associated altered rocks indicates the gold deposition predated much of the deformation and amphibolite facies metamorphic recrystallization in the high strain zones. Quartz veins containing stibnite and realgar, and rarely molybdenite and gold, cut across the fabric in the ore zone, and are probably a product of retrograde metamorphic remobilization.

9. The Hemlo gold ores were deposited from hydrothermal fluids in zones of intense strain prior to the final phase of regional amphibolite facies metamorphism. Barite, however, may have been deposited in the original volcanic and sedimentary environment.

As shown above, more recent research and evidence based on detailed surface mapping, drill core logging, and work in three mines has led to recognition of major lithological, structural, and alteration features which tend not to favour the earlier syngenetic origin, but favour deposition of the ore by hydrothermal fluids within or in the proximity of a ductile shear zone. Evidence that supports this model includes:

1. Gold and associated ore minerals are closely related to microcline alteration. This microcline alteration, although strongest in the felsic rocks, is also developed in the sedimentary rocks adjacent to the orebody. The alteration is most dominant in the Page-Williams orebody. This study shows that the microcline is principally a barian variety.

2. Barite is a major gangue mineral in the Page-Williams orebody, and in parts of the Golden Giant orebody, whereas it is nearly absent in the eastern portion of the David Bell orebody (Fig. 5). The absence of native gold grains, and of most other ore minerals in the barite suggests that the barite is later than the formation of the ore. The barite appears to act as a dilutant since those portions of the deposit with the greatest width contain the highest amounts of barite and are generally of lower grade. In places, angular fragments of ore are contained within the barite matrix and only where sufficient ore fragments are present is the rock of ore grade.

3. The extreme strain conditions that the ore has undergone render it unlikely that a syngenetic mineral deposit would retain the primary features that have been interpreted to be present by the proponents for such an origin. Thus the overwhelming evidence from structural analysis is that the mineralizing event is syntectonic.

4. The metasomatic nature of the barian microcline, the vanadian muscovite and the V-, Sb- and W-bearing rutile, all of which help define the ore zone as a "lithological" unit, seem to favour an epigenetic hydrothermal origin.

5. The timing of the mineralization relative to the metamorphic events is unresolved. The presence of kyanite and sillimanite in the sedimentary rocks adjacent to the ore zone has led some researchers (i.e. Kuhns et al., 1986 and Burk et al., 1986) to propose that the mineralization preceded peak amphibolite grade metamorphism. If the gold mineralizing event occurred after peak metamorphic conditions were established, then the hydrothermal alteration mineral assemblage would overgrow and perhaps replace the metamorphic mineral assemblage. Within the Page-Williams orebody, these conditions were noted in hanging wall sedimentary rocks where the calc-silicate alteration has resulted in replacement of biotite, amphibole and plagioclase by calcite, tremolite-actinolite, epidote and titanite, and by the clear replacement of kyanite and staurolite by zoisite and also by skarn-like assemblages of grossular garnet, epidote, calcite and tremolite (Walford et al., 1986). The pervasive potassic alteration and accompanying deposition of ore minerals was noted in this study in drill hole W104. The minerals present in drill hole W104, in the kyanite-muscovite schist are stibnite, arsenopyrite, sphalerite, native arsenic, realgar, tetrahedrite and cinnabar, and microscopic study reveals that the ore minerals are interstitial to the poikiloblastic, partially altered, kyanite (Fig. 53). Muir and Elliot (1987) felt that the disagreement as to the timing of the mineralization might be resolved in part by the recognition of more than one deformation event. They reported that third- and fourth-generation structures do overprint the orebody, and the main mineralized zone appears to be a zone of intense dextral shear. However, other zones of dextral shear are not mineralized.

6. The stibnite-realgar-cinnabar-rich boudinaged quartz veins with native gold that occur principally in the central portion of the deposit (the zone of mercury minerals) and cut across the fabric in the ore zone may represent the final stages of hydrothermal activity. These veins are highly deformed, and it is unlikely that the low temperature minerals cinnabar and realgar could survive the amphibolite facies of metamorphism.

7. The mineralogical and chemical similarities between the "lower mineralized zone" and the main ore zone, particularly in the Golden Giant mine, indicates a common genetic origin.

8. The aurostibite-native antimony-berthierite-gudmundite assemblages found in the biotite-rich portions of the Golden Giant orebody are indicative of conditions of low sulphur activities (Barton, 1971) at the time the ore formed.

9. The increased presence of the base metal minerals galena, chalcopyrite and sphalerite, and the near absence of mercury, in the northwest down-plunge extension of the Page-Williams orebody may be indicative of higher temperature deposition and perhaps indicates the direction from which the ore fluids ascended, or, alternatively, it may be the result of a change in the chemistry of the fluids.

10. The extreme mineralogical and geochemical diversities of the Hemlo deposit are similar to, but much more complex than those of any known hot-spring-type deposit reported to date.

11. The fact that molybdenite is a principal ore mineral that paragenetically was the first to be formed and is directly correlated with gold, has been suggested to indicate a relationship to a porphyry system.

12. The overwhelming evidence from structural analysis by Hugon (1986) is that the mineralizing event is syntectonic and occurred after peak metamorphic conditions were established.

ACKNOWLEDGMENTS

The author gratefully acknowledges the cooperation of R. Quartermain, Teck Explorations Limited; G. Pierce, R. Kusins, D. Carson, R. Cooper and W. Hogg of Noranda's exploration and mining staff of the Golden Giant mine; R. Valliant and P. Walford of LAC Minerals Limited exploration and mining staff of the Page-Williams' mine. The large number of polished sections were prepared by J.J.Y. Bourgoin, CANMET and by R. Burke, GSC. X-ray identifications were done by A.C. Roberts, GSC. R. Lancaster and K. Nguyen, GSC drafted the longitudinal sections of the deposit. G. Patterson, Ontario Ministry of Northern Development and Mines, Thunder Bay, provided the trench sample from the Golden Sceptre Resources property and the photographs for Figures 1 and 2. T. Muir, Ontario Geological Survey provided the black and white print of the regional geology in Figure 3. E. Cameron, GSC, provided drill core samples and geochemical data from his study of the deposit. Both E. Cameron and R. Thorpe, GSC critically reviewed the paper and made numerous constructive comments.

REFERENCES

- Barbanson, L., Saulas, D. and Touray, J.-C.
1985: Les blends mercurifères de la région de Cabezon de la Sal (Santander, Espagne); *Bulletin Mineralogique*, v. 108, p.483-486.
- Barton, P.B.Jr.
1971: The Fe-Sb-S system; *Economic Geology*, v.66, p.121-132.
- Bochek, L.I., Malinovskiy, Yu.A., Sandomirskaya, S.M. and Chuvikina, N.G.
1982: Bilibinskite and bessmertnovite, new hybrid minerals of the intermetallic compound-oxide type rather than intermetallic compounds of gold; *Doklady Earth Sciences Sections*, v.267, Nov.-Dec. issue, p.145-148.
- Botinelly, T., Neuerburg, G.J. and Conklin, N.M.
1973: Galkhaite, (Hg,Cu,Tl,Zn)(As,Sb)₂ from the Getchell mine, Humboldt County, Nevada; *in Journal of Research, U.S. Geological Survey*, 1, p.515-517.
- Brown, P., Carson, D., Cooper, P., Farr, E., Gibson, J., Harvey, J., Hogg, W., MacIsaac, N., Mackie, B., Nash, W. and Pierce, G.
1985: Golden Giant joint venture properties — Hemlo: *in Gold and Copper — Zinc Metallogeny within metamorphosed greenstone terrain, Hemlo-Manitouawadge-Winston Lake, Ontario, Canada*. R.H. McMillan and D.J. Robinson (eds.); Joint publication Geological Association of Canada and the Canadian Institute of Mining and Metallurgy, p.58-65.

- Burk, R., Hodgson, C.J. and Quartermain, R.A.**
1986: The Geological Setting of the Teck-Corona Au—Mo—Ba Deposit, Hemlo, Ontario, Canada; *in* Macdonald, A.J. ed.; Proceedings of Gold '86, an International Symposium on the Geology of Gold; Toronto, 1986, p.311-326.
- Cameron, E.M. and Garrels, R.M.**
1980: Geochemical compositions of some Precambrian shales from the Canadian Shield; *Chemical Geology*, v.28, p.181-197.
- Cameron, E.M. and Hattori, K.**
1985: The Hemlo gold deposit, Ontario: A geochemical and isotopic study; *Geochimica et Cosmochimica Acta*, v.49, p.2041-2050.
- Chen, T.T. and Szymanski, J.T.**
1981: The structure and chemistry of galkhaite, a mercury sulfosalt containing Cs and Tl; *Canadian Mineralogist*, v. 19, p.571-581.
1982: A comparison of galkhaite from Nevada and from the type locality, Khaydarkan, Kirgizia, U.S.S.R.; *Canadian Mineralogist*, v. 20, p.575-577.
- Craig, J.R. and Barton, P.B., Jr.**
1973: Thermochemical approximations for sulfosalts; *Economic Geology*, v. 68, p. 493-506.
- Edenharter, Von A., Nowacki, W. and Weibel, M.**
1977: Zur struktur und zusammensetzung von cafarsit. *Schweizerische Mineralogische und Petrographische Mitteilungen*, v. 57, p.1-16.
- Fleischer, M.**
1987: Glossary of mineral species 1987. 5th edition: The Mineralogical Record Inc., Tucson.
- Goldie, R.**
1985: The sinters of the Ohaki and Champagne pools, New Zealand: Possible modern analogues of the Hemlo gold deposit, Northern Ontario; *Geoscience Canada*, v.12, pt.2, p.60-64.
- Graeser, S.**
1966: Asbecasit and cafarsit, zwei neue mineralien aus dem Binnatal (Kt. Wallis); *Schweizerische Mineralogische und Petrographische Mitteilungen*, v. 46/2, p.367-375.
- Graeser, S. and Roggiani, A.G.**
1976: Occurrence and genesis of rare arsenate and phosphate minerals around Pizzo Cervandone, Italy/Switzerland; *Societa Italiana di Mineralogia e Petrologia Rendicanti*, v. XXXII (1), p.279-288.
- Grey, I.E., Madsen, I.C. and Harris, D.C.**
1987: Barian tomichite, Ba_{0.5}(As₂)_{0.5}Ti₂(V,Fe)5O₁₃(OH), its crystal structure and relationship to derbylite and tomichite; *American Mineralogist*, v. 72, p.201-208.
- Gruzdev, V.S.**
1975: Isomorphism of zinc and mercury in natural sphalerite and metacinnabarite; *Doklady Earth Sciences Sections*, v.225, Nov.-Dec. issue, p.114-117.
- Gruzdev, V.S., Chernitsova, N.M. and Skumkova, N.G.**
1972a: Aktashite: Cu₆Hg₃As₅S₁₂ — new data; *Akademiya Nauk. S.S.S.R. Doklady*, v. 206, p.127-130.
- Gruzdev, V.S., Stepanov, V.I., Shumkova, N.G., Chernitsova, N.M., Yudin, R.N. and Bryzgalov, I.A.**
1972b: Galkhaite (HgAsS₂), a new mineral from arsenic-antimony-mercury deposits of the U.S.S.R.; *Akademiya Nauk. S.S.S.R. Doklady*, v. 205, p.1194-1197.
- Harris, D.C., Sinclair, W.D. and Thorpe, R.I.**
1983: Telluride minerals from the Ashley deposit, Bannockburn Township, Ontario; *Canadian Mineralogist*, v. 21, p.137-143.
- Harris, D.C.**
1984: Mineralogy of the International Corona and Golden Giant gold deposits, Hemlo area, Ontario: Program with abstracts; Geological Association of Canada and the Mineralogical Association of Canada. London, Ontario.
1986a: The minerals in the main Hemlo gold deposit, Ontario; *in* Current Research, Part A, Geological Survey of Canada, Paper 86-1A, p.49-54.
1986b: Mineralogy of the main Hemlo gold deposit; *in* Harris, D.C. (ed.) 1986. The Hemlo gold deposits, Ontario; Geological Association of Canada, Mineralogical Association of Canada, Canadian Geophysical Union, Joint Annual Meeting, Ottawa '86, Field Trip 4: Guidebook, 74p; *also in* Pirie, J. and Downes, M.J., (eds.), Gold '86 Excursion Guidebook: Toronto, 1986, p.158-165.
1986c: Mineralogy and geochemistry of the main Hemlo gold deposit, Hemlo, Ontario, Canada; *in* Macdonald, A.J., ed. Proceedings of Gold '86, an International Symposium on the Geology of Gold; Toronto, 1986, p.297-310.
- Harris, D.C., Roberts, A.C., LaFlamme, J.H. Gilles and Stanley, C.J.**
1988: Criddleite (TlAg₂Au₃Sb₁₀S₁₀), a new gold-bearing mineral from Hemlo, Ontario, Canada; *Mineralogical Magazine*, v. 52, p.691-697.
- Harris, D.C., Roberts, A.C. and Criddle, A.J.**
1989: Vaughanite (TlHgSb₄S₇), a new mineral from the Hemlo gold deposit, Hemlo, Ontario, Canada; *Mineralogical Magazine* v. 53, 79-83.
- Harris, D.C., Hoskins, B., Grey, I.E., Criddle, A.J. and Stanley, C.J.**
1989: Hemloite, a new mineral from the Hemlo gold deposit, Hemlo, Ontario, Canada; *Canadian Mineralogist*. (in press)
- Healy, R.E. and Petruk, W.**
1989: Compositional and textural variation in Au—Ag—Hg alloy from the Trout Lake deposit, Flin Flon, Manitoba, Canada; *Canadian Mineralogist*. (in prep).
- Heinrich, E.Wm. and Levinson, A.A.**
1955: Studies in the mica group; X-ray data on roscoelite and barium — muscovite; *American Journal of Science*, v. 253, p.39-43.
- Hugon, H.**
1984: The Hemlo deposit: Gold mineralization within a dextral shear zone; *in* Summary of Fieldwork 1984, Ontario Geological Survey, Miscellaneous Paper 119, p.212-217.
1986: The Hemlo gold deposit, Ontario, Canada: A central portion of a large scale, wide zone of heterogeneous ductile shear; *in* Macdonald, A.J., ed., Proceedings of Gold '86, an International Symposium on the Geology of Gold; Toronto, 1986, p.379-387.
- Ivanov, T.**
1963: Zonal distribution of elements and minerals in the Allchar Deposit (in Russian); *in* Symposium "Problems of postmagmatic ore deposits", 1, p.186, Prague.
- Johan, Z., Mantiene, J., and Picot, P.**
1974: La routhierite, TlHgAsS₃, et la laffittite, AgHgAsS₃, deux nouvelles especes minerales; *Bulletin de Societe Francaise Mineralogie et Cristallographie*, v. 97, p.48-53.
- Johan, Z., Picot, P., Hak, J. and Kvacsek, M.**
1975: La parapirotite, un nouveau mineral thallifere d'Allchar (Yougoslavie); *Tschermaks Mineralogische Petrographische Mitteilungen*, v. 22, p.200-210.
- Kuhns, R.J.**
1986: Alteration styles and trace elements dispersion associated with the Golden Giant deposit, Hemlo, Ontario, Canada; *in* Macdonald, A.J., ed., Proceedings of Gold '86, an International Symposium on the Geology of Gold; Toronto, 1986, p.340-354.
- Kuhns, R.J., Kennedy, P., Cooper, P., Brown, P., Mackie, B., Kusins, R. and Friesen, R.**
1986: Geology and mineralization associated with the Golden Giant deposit, Hemlo, Ontario, Canada; *in* Macdonald, A.J., ed., Proceedings of Gold '86, an International Symposium on the Geology of Gold; Toronto, 1986, p.327-339.
- Lebedeva, N.V.**
1986: Natural and synthetic tellurides of gold and silver; *Vestnik Moskovskogo Universiteta Geologiya*, v. 41, no. 2, p.89-92.
- Mantiene, J.**
1974: La mineralisation thallifere de Jas Roux (Hautes-Alpes); These, Docteur de L'Universite de Paris.

- McIlveen, D.G.**
1983: Petrology and geochemistry of the tuffaceous footwall rocks of the Williams ore zone, Hemlo area, Ontario; unpublished B.Sc. Thesis, McMaster University.
- Muir, T.L.**
1982a: Geology of the Heron Bay Area, District of Thunder Bay; Ontario Geological Survey, Report 218, 89p., accompanied by Map 2439, scale 1:31,000.
1982b: Geology of the Hemlo Area, District of Thunder Bay; Ontario Geological Survey, Report 217, 65p., accompanied by Map 2452, scale 1:31,680.
1983: Geology of the Hemlo-Heron Bay Area; p.230-239 in *Geology of Gold in Ontario*, ed. A.C. Colvine, Ontario Geological Survey, Miscellaneous Paper 110, 278p.
1985: Geology of the Hemlo-Heron Bay area; p.30-38 in *Gold and Copper-Zinc Metallogeny: Hemlo-Manitouwadge-Winston Lake, Ontario*, A Compendium edited by R.H. McMillan and D.J. Robinson; A Joint Publication of Minerals Deposits Division, Geological Association of Canada, and Geology Division, the Canadian Institute of Mining Metallurgy, 91p.
1986: Hemlo Tectono-Stratigraphic Study; p.95-106 in *Summary of Field Work and Other Activities 1986*, by the Ontario Geological Survey, edited by P.C. Thurston, Owen L. White, R.B. Barlow, M.E. Cherry, and A.C. Colvine; Ontario Geological Survey, Miscellaneous Paper 132, 435p.
- Muir, T.L. and Elliot, C.G.**
1987: Hemlo Tectono-Stratigraphic Study, District of Thunder Bay; p.117-129 in *Summary of Field work and Other Activities 1987*, by the Ontario Geological Survey, edited by R.B. Barlow, M.E. Cherry, A.C. Colvine, Burkhard O. Dressier, and Owen L. White, Ontario Geological Survey, Miscellaneous Paper 137, 429p.
- Naz'mova, G.N. and Spiridonov, E.M.**
1979: Mercury-rich gold; *Doklady Earth Sciences Sections*, v. 246, p.138-141.
- Nickel, E.H.**
1977: Mineralogy of the "green leader" gold ore at Kalgoorlie, Western Australia; *Australasian Institute of Mining and Metallurgy Proceedings*, v.263, p.9-13.
- Nickel, E.H. and Grey, I.E.**
1979: Tomichite, a new oxide mineral from Western Australia; *Mineralogical Magazine*, v.43, p.469-471.
- Nysten, P.**
1986: Gold in the volcanogenic mercury-rich sulfide deposit Langsele, Skellefte ore district, northern Sweden; *Mineralium Deposita*, v.21, p.116-120.
- Oberthur, T. and Saager, R.**
1986: Silver and mercury in gold particles from the Proterozoic Witwatersrand placer deposits of South Africa. Metallogenic and geochemical implications; *Economic Geology*, v. 81, p.20-31.
- Patterson, G.C.**
1986: Regional Field Guide to the Hemlo Area; Harris, D.C. (ed.) 1986. The Hemlo gold deposits, Ontario; Geological Association of Canada, Mineralogical Association of Canada, Canadian Geophysical Union, Joint Annual Meeting, Ottawa '86, Field Trip 4: Guidebook, 74p.
- Quartermain, R.**
1985: Road guide to the geology of the Teck-Corona mine at Hemlo, Ontario; in *Gold and Copper-Zinc Metallogeny within metamorphosed greenstone terrain Hemlo-Manitouwadge-Winston Lake, Ontario, Canada*; R.H. Mcmillan and D.J. Robinson (eds.); Joint publication Geological Association of Canada and the Canadian Institute of Mining and Metallurgy, p.39-46.
- Radtke, A.S., Taylor, C.M., Erd, R.C. and Dickson, F.W.**
1974: Occurrence of lorandite, $TlAsS_2$, at the Carlin gold deposit, Nevada; *Economic Geology*, v. 69, p.121-124.
- Radtke, A.S. and Dickson, F.W.**
1975: Carlinite, Tl_2S , a new mineral from Nevada; *American Mineralogist*, v. 60, p.559-565.
- Roberts, A.C., Ansell, H.G. and Bonardi, M.**
1980: Pararealgar, a new polymorph of AsS , from British Columbia; *Canadian Mineralogist*, v. 18, p.525-527.
- Rogers, A.F.**
1912: Lorandite from the Rambler mine, Wyoming; *American Journal of Science*, 4th ser., v. 33, p.105-106.
- Saunders, J.A. and May, E.R.**
1986: Bessie G: A high-grade epithermal gold telluride deposit, La Plata County, Colorado, U.S.A.; in *Macdonald, A.J., ed., Proceedings of Gold '86, an International Symposium on the Geology of Gold*. Toronto, 1986, p.436-444.
- Shikazono, N. and Shimizu, M.**
1988: Mercurian gold from the Tsugu gold-antimony vein deposit in Japan; *Canadian Mineralogist*, v.26, p.423-428.
- Spiridonov, E.M., Krapiva, L.Ya., Stepanov, V.I. and Chvileva, T.N.**
1983: Antimony auktashite from the Chauvay mercury deposit, Soviet Central Asia; *Doklady Earth Science Series*, 261, p.171-175.
- Tauson, V.L. and Abramovich, M.G.**
1980: Hydrothermal study of the ZnS-HgS system; *Geochemistry International* v.17, p.117-128.
- Tintor, N.**
1986: Who really knows?: The Northern Miner Magazine, #1 Issue, p.39-43.
- Thorpe, R.I. and Harris, D.C.**
1973: Mattagamite and tellurantimony, two new telluride minerals from Mattagami Lake mine, Matagami area, Quebec; *Canadian Mineralogist*, v. 12, p.55-60.
- Valliant, R.**
1985: The Lac discoveries; *Canadian Mining Journal*, May Issue, p.39-47.
- Valliant, R.I. and Bradbrook, C.J.**
1986: Relationship between stratigraphy, faults and gold deposits, Page-Williams Mine, Hemlo, Ontario, Canada; in *Macdonald, A.J., ed., Proceedings of Gold '86, an International Symposium on the Geology of Gold*; Toronto, 1986, p.355-361.
- Vasil'ev, V.I.**
1968: New ore minerals of the mercury deposits of Cornyi Altai and their parageneses; in *problems of the Metallogeny of Mercury* Izdat. "Nauka" Moscow, p.111-129 (in Russian); *Abstract American Mineralogist*, v. 56, 1971, p.358.
- Vasil'yev, V.I. and Lavrent'yev, Yu.G.**
1969: A new mercury-bearing species of sphalerite; *Akademiya Nauk SSSR Doklady*, v.186, p.137-139.
- Vershkovskaya, O.V., Sandomirskaya, S.M. and Gorshkov, Ye. N.**
1984: Mercury-rich gold from one mercury-antimony deposit in Soviet Central Asia; *Doklady Earth Sciences Sections*, v.278, p. 171-174.
- Walford, P., Stephens, J., Skrecky, G. and Barnett, R.**
1986: The Geology of the "A" zone, Page-Williams Mine, Hemlo, Ontario, Canada; in *Macdonald, A.J., ed., Proceedings of Gold '86, an International Symposium on the Geology of Gold*; Toronto, 1986, p.362-378.
- Weissberg, B.G.**
1969: Gold-silver ore-grade precipitates from New Zealand thermal waters; *Economic Geology*, v. 64, p.95-108.

APPENDIX A

Microprobe analyses of minerals in the Hemlo Gold deposit

Table A.1: Microprobe Analyses of Sphalerite

DDH	Metres	Zn	Hg	Fe	S	
TC236	685.9	46.9	24.1	0.0	27.6	
TC220W	923.45	58.0	10.4	0.0	31.6	
	923.8	46.4	26.4	0.0	27.2	
	"	44.7	29.5	0.0	26.8	
TC218W	774.25	47.2	27.5	0.0	28.2	
	774.5	47.0	25.4	0.0	28.3	
NTC9W	583.3	63.7	3.5	0.0	33.0	
	584.3	51.0	17.1	0.5	30.6	
	584.8	52.0	17.3	0.0	29.9	
GG14W	867.3	63.1	4.6	0.0	32.0	
	870.9	52.3	17.9	0.0	30.1	
	884.2	66.0	1.3	0.0	33.0	
	884.8	65.9	1.0	0.0	32.7	
GG20	854.8	61.6	2.0	0.7	32.6	
	861.3	59.4	5.7	0.6	31.6	
	884.8	64.2	3.4	0.1	32.3	
	887.0	63.7	3.8	0.2	32.3	
	891.5	64.1	1.7	0.5	32.7	
	930.3	65.6	0.7	0.3	32.6	
	932.5	65.5	0.6	0.7	32.5	
GG21	863.5	64.1	2.0	0.2	32.9	
GG23	651.6	64.2	1.0	0.3	32.7	
GG37Y	1041.4	63.5	6.1	0.0	30.0	
GG45	1110.6	63.7	3.1	0.0	32.3	
W28	174.8	63.4	1.8	1.3	32.7	
	175.5	61.4	2.9	0.9	32.7	
	176.7	56.6	10.8	0.7	31.7	
	177.2	46.4	24.4	0.3	29.4	
	180.4	51.9	17.8	0.2	30.3	
	181.7	54.3	14.7	0.3	30.7	
	182.4	53.2	18.6	0.0	30.4	
	183.6	50.7	20.6	0.0	29.9	
	186.6	56.2	13.1	0.0	30.9	
	189.5	54.4	14.7	0.0	30.9	
	197.2	60.3	6.8	0.0	31.7	
	W70	711.8	64.9	2.2	0.3	32.6
		717.4	62.5	3.9	0.5	32.0
725.6		60.1	8.4	0.6	31.4	
731.9		60.5	6.4	0.3	31.8	
732.3		58.0	8.9	1.9	31.4	
735.1		55.3	13.5	0.1	30.3	
"		61.5	6.9	0.0	32.1	
735.9		53.2	13.1	0.1	30.2	
737.4		62.0	6.3	0.4	31.4	
738.9		56.9	10.3	0.0	31.0	
739.2		56.9	12.8	1.0	30.4	
741.8		54.3	15.8	0.4	29.9	
747.8		58.4	10.6	0.4	30.8	
748.8		55.8	13.6	0.5	30.6	
758.6		56.9	10.2	1.2	30.6	
761.4		63.8	2.5	0.0	31.8	
763.4		64.9	2.6	0.0	32.0	
764.4		64.8	0.2	0.3	32.0	
766.8		64.7	1.7	0.5	31.9	
771.8		65.0	1.6	0.1	32.5	
773.5		65.3	1.1	0.2	32.3	
775.6		64.5	1.6	1.1	32.5	
777.8		65.5	1.2	0.2	32.8	
779.2		64.2	1.3	0.2	32.7	
780.9		64.9	0.4	0.9	32.6	

Table A.1: continued

DDH	Metres	Zn	Hg	Fe	S
W73	22.4	57.4	9.0	0.9	32.0
	30.2	58.2	8.7	0.4	32.0
W92	636.6	56.6	5.8	1.6	31.0
	644.5	62.3	2.4	0.0	32.9
	645.1	61.9	3.9	0.3	32.9
	658.9	65.7	0.0	0.3	33.2
	681.5	66.1	0.0	0.3	33.4
W100	786.5	60.3	7.0	0.2	32.0
	801.1	64.6	2.4	0.0	32.5
	805.4	62.9	4.0	0.0	32.6
	805.5	62.8	3.5	0.5	32.6
	808.3	65.2	0.0	0.2	33.5
	809.8	65.4	0.0	0.0	33.0
	811.4	66.1	0.0	0.0	33.6
	811.5	64.5	0.5	0.0	33.2
	811.8	64.7	0.2	0.2	33.2
	814.1	63.9	0.0	0.0	33.4
	818.0	65.9	1.3	0.2	32.9
819.8	63.1	1.1	0.0	33.0	
W104	248.7	46.4	24.3	0.0	29.3
	264.2	46.3	24.3	0.0	29.3
	265.4	50.0	19.4	0.0	30.2
W116	1120.8	64.5	0.5	0.2	33.2
	1123.2	64.7	0.5	0.1	33.5
	1125.3	64.8	0.2	0.2	33.2
	1129.8	63.3	0.5	0.3	33.5
	1134.7	64.2	0.5	0.1	33.1
	1136.3	65.2	0.2	0.2	33.2
	1137.1	64.3	0.5	0.2	33.4
1142.2	63.6	1.4	0.1	33.3	
W129	1378.9	64.4	0.3	0.5	33.7
	1383.9	64.7	0.0	0.7	33.3
	1424.2	66.0	0.0	0.4	33.6
	1427.3	66.3	0.0	0.2	33.4
	1447.4	66.1	0.0	0.4	33.4
	1447.7	65.9	0.0	0.4	33.2
W135	1180.3	64.8	0.0	0.5	32.6
	1183.3	64.5	0.0	0.0	32.5
	1184.9	64.0	0.0	0.6	32.2
	1187.9	65.7	0.0	0.2	32.5
	1191.2	65.9	0.0	0.1	32.1
W137	938.5	60.7	0.0	3.0	33.3
	942.5	65.8	1.0	0.0	33.3
	943.4	66.3	0.6	0.2	32.8
	948.8	66.3	0.7	0.2	32.9
	950.2	66.0	1.6	0.2	32.9
	955.5	64.6	1.5	0.3	33.0
	962.5	66.3	0.6	0.1	33.4
	963.4	66.5	0.6	0.1	33.3
	965.2	66.7	0.6	0.2	33.2
	970.4	65.1	0.2	0.7	33.6
	974.8	66.4	1.0	0.1	33.1
975.9	66.0	0.6	0.3	33.2	

Table A.2: Microprobe Analyses of Native Gold

DDH	Metres	Au	Hg	Ag
TC216	877.2	89.5	1.4	4.3
TC234	902.5	86.8	3.3	8.0
TC220W	923.8	67.8	26.9	3.7
TC218W	767.5	70.7	16.3	17.4
	772.9	88.2	8.1	2.9
	773.7	81.0	17.2	3.2
	774.25	82.8	14.8	2.9
	"	78.6	19.3	2.9
	"	79.4	17.6	3.6
	"	92.2	6.9	1.0
	"	78.1	16.6	4.8
	"	94.1	1.4	4.7
NTC9W	563.1	97.5	0.8	-
GG25	336.4	86.1	14.6	0.3
	343.7	87.3	11.2	2.2
	348.2	91.2	5.5	3.5
GG23	651.6	79.3	7.8	12.2
	668.5	85.5	9.2	6.1
GG14W	868.6	91.2	3.2	2.8
		97.2	0.0	1.3
GG20	857.4	88.5	12.4	0.3
	864.6	90.1	4.6	2.5
	879.6	83.3	8.6	7.4
GG21	825.0	92.0	3.5	3.2
	853.3	94.1	5.5	0.3
	863.5	91.2	2.7	6.5
GG37Y	1041.4	86.3	9.0	4.4
GG45	1106.2	93.6	0.5	5.6
W73	30.2	97.4	0.7	-
	36.4	77.0	11.5	11.5
	"	88.5	6.5	4.6
	"	86.6	8.0	6.4
	"	97.0	1.8	0.7
	46.2	93.9	4.7	1.3
	"	76.9	20.6	1.2
W28	176.7	88.3	7.7	1.1
	186.6	86.3	10.0	3.8
	189.5	92.0	4.5	2.8
	197.2	85.8	8.4	4.3
W104	252.6	88.2	10.0	2.1
	264.2	90.9	6.6	3.0
	264.8	78.1	12.8	6.9
W70	713.0	95.1	--	1.4
	718.0	86.6	2.8	7.6
	726.8	84.9	5.8	6.9
	728.7	96.0	1.4	--
	731.9	82.7	7.9	7.1
	735.1	86.8	4.7	7.1
	738.2	80.4	9.5	7.9
	738.5	80.9	9.1	7.5
	739.5	88.8	7.1	0.9
	741.3	78.4	11.1	6.4
	741.8	81.5	12.1	4.8
	745.1	93.0	3.8	1.7
	758.6	69.8	16.3	11.6
	761.4	96.4	--	1.3
	765.8	79.0	6.5	12.7
	766.1	82.5	1.8	14.1

Table A.2: continued

DDH	Metres	Au	Hg	Ag
W100	766.2	86.7	6.4	6.8
	768.8	85.4	7.2	7.2
	769.8	89.6	6.8	3.6
	776.9	90.3	8.2	2.0
	784.2	98.8	--	1.2
	784.9	88.6	6.3	5.1
	790.2	83.2	6.9	4.4
	791.9	79.7	13.6	6.4
	803.5	72.9	5.5	19.7
	805.5	72.9	9.5	16.4
	815.9	86.1	2.6	10.1
W92	644.5	58.7	20.3	19.4
	"	63.1	22.1	13.7
	645.1	90.0	5.4	5.9
	657.8	78.0	3.4	19.2
W137	957.5	79.4	5.8	9.2
	962.5	88.3	--	3.5
	971.2	95.4	--	3.5
W116	1123.2	79.0	1.6	13.6
	1131.7	94.7	--	3.9
	1136.3	92.8	--	6.6
W129	1427.3	80.0	0.3	18.1
	"	90.2	--	10.5
	"	80.1	1.0	18.6
	1447.7	71.3	0.2	28.8
	"	71.4	0.2	29.1
	"	85.9	0.0	14.9
W135	1177.5	82.5	1.0	13.1
	1183.3	94.9	1.2	0.8
	1187.9	91.1	0.2	6.1
	1191.2	91.7	0.2	6.7
	1196.1	90.3	--	5.7

Table A.3: Microprobe Analyses of Stibnite

DDH	Metres	Sb	As	S
TC220W	923.8	69.4	2.8	28.2
W28	176.7	71.0	2.0	28.3
	177.2	69.9	2.7	28.2
	181.7	67.4	4.8	28.2
	189.5	70.9	0.0	28.0
W92	636.6	70.7	0.3	27.7
W70	735.9	69.3	1.1	27.9
	737.4	70.4	0.3	27.8
	738.9	68.2	1.8	27.7
	741.8	69.7	0.3	27.4
	758.6	70.0	0.0	27.5
W100	769.8	67.9	3.3	27.9
	784.9	70.9	0.4	27.2
	791.9	65.9	1.8	27.2
	800.2	69.4	1.4	27.9
	819.8	67.8	2.2	28.2
W104	248.7	71.4	0.0	28.2

Table A.4: Microprobe Analyses of Tetrahedrite-Tennantite*

DDH	Metres	Cu	Ag	Hg	Fe	Zn	Sb	As	S	
TC236	689.9	37.1	--	--	7.7	6.1	28.4	--	27.0	
TC220W	926.3	37.2	-	2.0	3.4	2.8	28.3	0.6	24.9	
	"	33.0	5.8	-	3.1	3.4	28.8	-	24.1	
	"	36.9	1.2	0.9	3.9	2.5	28.0	0.8	24.8	
	926.8	28.4	10.9	8.1	0.4	3.3	25.2	-	21.8	
		39.3	-	-	5.3	1.5	11.9	12.2	27.2*	
TC218W	767.5	36.7	2.9	5.3	1.9	3.3	17.1	7.3	25.1	
NTC9W	576.2	40.6	0.4	0.0	3.8	3.2	2.8	18.4	28.3*	
	577.4	39.2	0.0	0.0	3.9	3.3	17.2	8.5	26.5	
	"	38.0	0.0	0.0	1.9	5.6	19.4	1.9	26.2	
	582.4	27.1	0.0	10.3	4.6	3.0	2.7	19.8	29.1*	
	583.3	39.5	0.9	1.5	3.3	3.9	3.7	17.9	28.0*	
		40.0	0.5	2.4	0.8	6.5	5.3	16.6	27.7*	
GG14W	884.8	39.2	1.3	1.1	0.3	7.2	5.5	16.4	27.7*	
GG20	882.8	32.2	4.4	13.1	0.6	2.2	18.1	5.5	23.5	
GG21	832.1	39.5	--	4.2	0.5	5.9	6.3	14.6	28.1*	
	863.5	40.2	2.1	2.5	0.8	6.4	7.0	15.1	26.2*	
GG23	651.6	38.8	1.0	1.0	1.5	5.6	19.8	6.9	25.9	
	668.5	37.4	2.8	4.5	1.3	4.8	16.5	8.4	26.0	
GG45	1158.2	42.4	0.7	1.0	0.9	6.9	3.6	17.9	27.9*	
W73	24.3	40.3	--	--	4.3	2.7	11.9	12.0	27.3*	
	26.6	37.1	0.7	3.2	2.3	3.7	16.4	8.0	26.2	
	34.6	36.4	1.3	--	2.3	4.5	27.8	0.7	24.9	
	36.1	36.2	0.7	--	4.6	1.8	28.8	--	25.3	
W28	183.6	34.8	0.3	8.8	2.5	1.5	22.2	4.5	24.8	
	186.6	34.3	0.5	2.5	4.1	1.8	27.1	1.7	24.5	
	189.5	33.9	1.0	12.4	0.7	2.6	25.9	1.0	23.6	
	189.7	34.3	0.9	12.4	0.3	2.7	25.0	1.5	23.4	
W104	252.6	35.3	--	13.3	0.4	2.4	19.1	5.1	24.4	
	264.2	35.0	0.9	15.2	1.3	1.7	11.2	10.3	25.0*	
	264.8	32.3	1.8	18.6	0.4	0.7	19.9	4.1	23.0	
W70	734.8	35.4	1.0	7.6	1.3	3.8	22.5	4.2	24.3	
	737.4	34.9	1.6	9.0	0.5	4.4	23.1	3.0	24.2	
	738.2	33.8	3.2	7.3	0.7	4.5	24.4	2.9	24.0	
	741.8	34.6	1.0	12.3	0.5	3.0	21.6	3.6	23.8	
	758.6	32.7	4.4	7.2	1.6	2.8	26.8	0.6	23.6	
W100	773.5	35.7	2.0	7.7	2.4	2.2	16.1	8.1	25.0	
	790.2	32.6	0.4	16.1	1.5	1.7	23.0	2.3	23.3	
	791.9	32.7	0.7	13.7	0.9	1.7	19.3	4.8	23.6	
	"	31.1	1.4	13.1	0.6	2.5	23.4	0.6	21.9	
	800.2	39.7	1.4	4.3	0.9	5.8	6.5	14.8	27.1*	
	801.1	41.1	0.7	1.0	4.7	2.3	8.9	13.6	27.4*	
	803.5	38.7	2.3	2.7	2.0	4.9	11.5	11.4	26.4*	
	804.6	38.8	1.2	5.8	1.4	5.0	10.3	11.8	26.4*	
	805.4	37.2	2.4	5.7	2.1	5.0	9.2	12.4	26.5*	
	805.5	37.5	2.8	2.3	3.0	3.2	8.4	14.0	27.2*	
	811.4	39.7	2.1	--	0.4	7.4	4.0	16.8	28.0*	
	814.1	40.9	1.8	--	0.9	7.3	5.7	15.7	27.9*	
	815.9	40.3	1.9	0.6	2.5	4.8	4.7	16.4	28.2*	
	818.0	35.1	8.3	1.4	0.7	6.9	12.2	10.9	26.0*	
	"	38.8	3.6	1.0	0.9	8.2	5.5	16.0	27.5*	
	"	33.7	8.9	1.4	0.5	7.0	16.5	7.9	25.5*	
	"	40.6	2.1	0.9	0.9	7.0	4.5	16.9	27.7*	
	819.8	40.4	0.9	1.2	0.4	7.3	5.3	16.1	27.7*	
	W92	636.6	35.9	1.4	5.6	1.8	3.5	20.0	5.7	25.0
		640.0	34.8	2.0	5.5	1.4	4.0	23.3	3.1	24.7
642.9		35.7	1.2	9.8	1.5	2.4	15.9	7.8	25.1	
644.5		37.7	0.6	6.9	0.3	5.1	8.8	13.0	26.5*	
645.1		38.3	0.9	5.5	1.8	3.9	8.3	13.5	27.1*	
657.8		40.8	--	-	1.9	5.9	9.0	14.2	27.7*	
681.5		40.5	0.5	-	2.9	4.8	7.0	15.4	28.0*	
W135	1177.5	37.6	0.2	-	1.4	6.1	25.7	2.0	25.2	
	1184.9	38.9	0.8	-	2.4	5.3	14.1	9.8	26.2*	
	1191.2	40.0	1.5	-	0.8	7.0	6.8	15.2	26.5*	
W129	1377.9	41.6	0.4	-	1.6	7.2	17.0	3.0	28.4	
	1378.9	40.5	0.5	2.0	1.5	6.8	15.4	4.3	27.6	
	1381.6	41.6	0.5	0.4	2.5	5.4	16.1	3.2	28.3	
	1424.2	39.3	2.2	-	2.4	6.9	2.7	14.1	28.1*	
	1426.5	40.6	-	-	1.4	6.9	4.3	17.3	28.0*	
	1427.3	37.8	3.3	-	1.7	6.1	11.5	10.6	26.5*	
	1447.4	40.0	-	-	2.0	5.9	9.1	13.8	27.5*	
	1447.7	40.2	-	-	2.8	4.9	11.8	9.5	26.9*	
W69	437.5	39.9	-	-	2.4	5.0	18.4	8.0	26.2	
W116	1120.8	36.7	1.4	-	2.9	5.4	28.6	1.8	25.0	
	1123.2	40.5	-	-	2.5	5.0	2.8	18.1	28.6*	
	1131.2	39.9	-	-	3.4	4.7	10.8	12.6	28.0*	
	1134.7	39.0	1.6	0.5	1.1	6.7	7.9	14.4	27.6*	
	1136.3	38.5	1.0	-	0.8	6.6	11.3	12.3	27.0*	
W137	941.6	40.9	-	-	5.7	1.4	2.9	17.8	28.6*	
	942.5	40.3	0.5	0.2	0.8	7.2	3.1	18.0	28.4*	
	945.1	40.9	0.7	1.0	1.7	6.2	6.2	15.3	27.5*	
	945.8	39.9	0.2	0.2	0.5	7.3	3.2	17.5	28.0*	
	952.5	39.6	0.3	0.6	2.5	5.6	14.0	10.1	26.8*	
	"	39.7	0.5	0.9	2.3	5.3	16.0	9.7	27.3	
	"	41.0	-	1.0	2.6	5.1	9.3	13.3	27.8*	
	954.8	41.7	0.2	0.4	2.9	5.0	4.2	16.8	28.0*	
	960.8	40.0	-	0.7	2.1	6.7	8.8	13.6	27.9*	
	962.5	40.8	0.9	0.5	1.2	6.8	6.0	15.5	28.0*	
	971.2	41.4	0.2	1.0	-	8.0	3.6	17.1	28.1*	

* = tennantite

Table A.5: Microprobe Analyses of Aktashite

DDH	Metres	Cu	Hg	Fe	Zn	Sb	As	S
TC218W	774.25	23.0	34.2	0.0	0.3	1.8	12.7	24.4
	"	22.3	34.5	0.0	0.4	2.1	12.8	24.6
TC220W	923.45	21.6	29.7	0.5	1.1	3.8	15.1	25.3
NTC9W	584.3	21.8	33.2	0.3	0.3	3.0	15.6	25.1
GG21	832.1	24.3	29.4	0.3	1.5	2.3	17.7	26.4
GG25	324.9	22.9	35.3	0.0	0.4	1.1	16.4	24.9
GG37Y	1040.3	22.5	33.2	0.0	0.0	2.8	17.3	25.8
	1041.4	23.3	30.5	0.0	1.6	4.2	16.9	25.7
GG45	1106.2	23.4	31.9	0.2	1.1	2.3	18.0	26.2
W28	197.2	25.2	31.0	0.2	1.3	1.4	17.0	25.0
W70	735.1	22.7	33.9	0.0	0.4	2.6	15.7	24.7
	"	22.8	31.6	0.0	0.9	6.2	10.6	24.2
	"	23.0	32.5	0.0	0.9	6.3	10.4	24.5
	"	22.6	33.6	0.4	0.4	4.2	14.8	24.6
	735.9	22.8	35.0	0.0	0.4	3.7	14.5	24.7
	"	22.9	34.8	0.4	0.4	2.6	15.8	24.7
	738.9	23.6	32.9	0.0	0.4	3.3	15.5	25.0
W100	768.8	23.1	33.0	0.0	0.4	1.5	16.9	25.4
	769.8	23.6	34.3	0.0	0.7	1.2	17.3	25.3
	784.2	23.6	34.2	0.0	0.7	1.1	16.6	25.3
	"	23.5	33.1	0.0	0.9	1.1	15.7	25.1
	"	23.4	33.6	0.0	0.7	1.1	15.9	24.9
	784.9	22.3	34.7	0.0	0.4	1.0	16.9	25.1
W104	252.3	23.3	33.2	0.0	0.5	3.5	15.4	25.1
	265.4	23.2	29.6	1.9	0.0	3.7	16.0	26.1

Table A.6: Microprobe Analyses of Parapierrrotite

DDH	Metres	Tl	Sb	As	S
NTC9W	584.8	19.0	56.8	0.0	24.2
GG25	324.9	18.4	55.7	1.1	23.8
GG23	651.6	19.8	60.0	-	24.6
W70	735.1	19.6	54.6	1.6	23.8
	735.9	18.8	55.6	1.4	24.0
	741.8	18.2	55.5-	-	23.1
	758.6	18.4	56.3	-	23.6

Table A.7: Microprobe Analyses of Routhierite

DDH	Metres	Cu	Zn	Tl	Hg	As	Sb	S	Total wt. %
TC218W	770.3	5.8	0.6	19.3	37.5	9.2	6.3	19.3	98.0
GG25	324.9	5.8	0.5	18.2	39.4	8.5	9.0	19.6	101.0
W70	735.1	5.6	0.9	19.5	38.6	9.2	6.6	19.9	100.3
"	"	5.6	0.3	19.6	36.8	5.4	12.9	18.9	99.5
"	"	5.7	-	19.6	38.6	7.7	9.6	19.4	100.6
"	"	6.1	-	19.6	37.6	6.3	11.3	18.8	99.7
"	"	5.8	-	19.8	37.7	5.3	12.7	19.0	100.3
"	738.9	6.0	0.6	19.8	37.6	8.2	9.1	19.1	100.4
"	"	5.1	0.6	18.5	40.3	10.2	5.8	20.2	100.7
W100	784.2	5.6	1.3	18.7	39.4	11.9	2.3	20.3	99.5
"	791.9	5.8	-	19.3	36.9	2.8	17.8	18.7	101.3
"	"	6.0	0.4	19.3	37.3	8.3	9.0	19.3	99.6
W28	181.7	5.6	0.5	16.0	40.4	9.3	8.6	20.5	100.9
"	186.6	5.5	0.6	15.3	39.9	8.8	9.8	20.4	100.3
Atomic Proportions Total = 12									
TC218W	770.3	0.94	0.10	0.98	1.94	1.28	0.54	6.22	
GG25	324.9	0.92	0.08	0.90	2.00	1.14	0.74	6.22	
W70	735.1	0.89	0.14	0.96	1.95	1.25	0.54	6.27	
"	"	0.92	0.06	1.00	1.92	0.76	1.12	6.22*	
"	"	0.92	-	0.98	1.98	1.06	0.82	6.24	
"	"	1.00	-	1.00	1.98	0.88	0.98	6.16*	
"	"	0.96	-	1.02	1.98	0.74	1.10	6.20*	
"	738.9	0.96	0.10	1.00	1.92	1.12	0.76	6.14	
"	"	0.84	0.08	0.94	2.04	1.56	0.24	6.30	
W100	784.2	0.88	0.20	0.92	1.96	1.58	0.18	6.28	
"	791.9	0.96	-	1.00	1.94	0.38	1.54	6.18*	
"	"	0.98	0.08	0.96	1.94	1.14	0.76	6.14	
W28	181.7	0.88	0.08	0.78	2.00	1.22	0.70	6.34	
"	186.6	0.86	0.09	0.75	1.99	1.17	0.80	6.34	

*antimony-rich routhierite

Table A.8: Microprobe Analyses of Lead Sulphantimonide Minerals

DDH	Metres	Weight %				Atomic %			Mineral
		Pb	Sb	As	S	Pb	Sb	As	
GG14W	884.2	36.0	24.8	12.5	24.6	31.9	37.4	30.7	Zink*
GG20	882.8	31.2	42.3	1.8	22.8	28.9	66.5	4.6	Zink*
GG21	863.5	35.8	25.6	11.6	24.7	32.1	39.2	28.6	Zink*
W28	176.7	32.1	44.5	1.2	22.8	28.8	68.0	3.2	Zink
"	189.5	31.3	44.6	0.5	22.6	28.9	69.9	1.2	Zink
W92	636.6	31.1	43.3	1.1	22.5	28.8	68.3	2.9	Zink
"	640.0	31.4	44.2	0.5	22.6	29.1	69.8	1.1	Zink
"	645.1	31.8	35.1	6.3	23.5	29.2	54.8	16.0	Zink
W70	738.2	35.7	38.7	1.6	20.8	33.7	62.2	4.1	Twin
"	738.9	30.2	40.4	3.2	23.0	28.0	63.9	8.1	Zink*
"	741.8	30.7	42.3	1.1	22.4	29.0	68.0	3.0	Zink
"	758.6	30.3	44.4	0.0	22.4	28.4	71.7	0.5	Zink
W100	769.8	24.8	25.8	11.7	23.8	31.3	39.5	29.2	Twin
"	801.1	55.4	23.1	1.1	18.5	56.5	40.1	3.4	Boul
"	804.6	34.8	35.1	4.9	23.2	32.1	55.3	12.5	Twin
"	805.4	37.9	27.6	9.7	23.8	33.9	42.0	24.1	Twin
"	"	27.1	27.6	9.4	23.5	33.7	42.8	23.5	Twin
"	805.5	37.4	26.5	10.4	23.8	33.7	40.4	25.9	Twin*
"	808.3	68.3	9.5	4.0	17.5	71.4	17.1	11.4	Geo
"	"	55.7	21.5	2.4	19.2	56.2	37.1	6.7	Boul
"	811.8	48.2	14.5	12.9	22.3	44.4	22.7	32.9	Baum*
"	814.1	38.5	24.0	12.0	23.8	34.2	36.3	29.5	Twin
"	"	38.3	23.7	12.2	24.1	34.1	35.8	30.0	Twin
"	815.9	38.4	21.5	13.4	24.2	34.4	32.6	33.0	Twin
"	818.0	47.8	15.8	12.4	22.6	44.0	24.7	31.3	Baum*
"	"	57.2	16.2	5.8	19.3	56.8	27.3	15.9	Boul
"	"	53.4	13.6	10.4	21.1	50.8	21.8	27.4	Duf
"	819.8	31.0	30.5	10.6	24.6	27.6	46.1	26.2	Zink
W137	942.5	51.0	25.8	0.9	19.0	68.7	29.6	1.7	Geo
"	947.9	54.9	21.7	2.3	18.9	56.0	37.7	6.4	Boul
"	948.8	51.2	22.1	2.7	19.4	48.3	35.3	16.4	
"	970.4	63.1	13.1	3.6	17.6	66.3	23.3	10.4	Geo
"	971.2	30.1	29.1	11.5	24.9	27.0	44.6	28.4	Zink
"	"	29.7	29.7	11.3	24.9	26.6	45.2	28.2	Zink
"	"	36.4	20.3	14.9	24.0	32.5	30.8	36.7	Twin*
W116	1134.7	65.4	9.8	5.4	18.0	67.1	17.4	15.4	Geo
"	1135.2	67.9	8.9	4.8	17.5	70.4	15.5	14.1	Geo
"	1136.3	68.5	9.2	4.6	17.4	70.9	16.3	12.8	Geo
"	1138.4	70.2	8.3	3.9	16.7	74.1	14.8	11.1	Geo
"	1139.2	69.3	5.4	7.5	17.6	71.9	12.9	15.1	Geo
W135	1191.2	68.2	7.9	4.8	16.7	71.9	14.4	13.7	Geo*
W129	1377.9	38.6	16.6	16.3	25.0	34.5	25.2	40.3	Twin

* = X-rayed

Zink = Zinkenite; Boul = Boulangerite; Twin = Twinnite; Baum = Baumhauerite; Duf = Dufrenoyite; Geo = Geocronite.

Table A.9: Microprobe Analyses of Sulphosalts - Chalcostibite, Bournonite, Berthierite and Jamesonite.

		Chalcostibite					
DDH	Metres	Cu	Sb	S			
TC220W	926.3	24.9	48.8	25.8			
GG23	651.6	25.3	49.8	25.7			
GG25	324.9	25.2	48.5	26.1			
W73	26.6 36.1	24.8 24.9	48.9 48.7	25.8 26.1			
		Bournonite-Seligmannite					
DDH	Metres	Cu	Zn	Pb	Sb	As	S
W28	189.7	12.4	0.0	41.0	25.4	0.0	19.0
W73	36.4	12.1	0.0	41.6	25.6	0.0	19.4
W100	801.1 803.5 818.0	13.7 13.6 14.0	0.0 0.0 1.4	43.1 42.3 44.2	18.1 18.9 12.5	4.2 3.4 8.1	20.3 19.8 20.7*
W116	1123.2 1137.1	13.3 13.4	0.0 0.0	43.4 43.7	15.8 15.4	6.0 5.9	20.5 20.7
W129	1377.9	13.3	0.0	43.4	14.8	5.7	20.7
W137	950.2 965.2	13.2 13.6	0.0 0.0	41.3 43.3	24.8 14.7	0.4 6.1	19.6 20.6
* seligmannite							
		Berthierite					
DDH	Metres	Fe	Mn	Sb	As	S	
GG20	884.8	8.0	4.7	57.0	0.0	28.0	
GG25	324.9	11.8	0.4	55.9	0.0	29.8	
GG37Y	1037.9	12.5	0.0	57.5	0.0	30.4	
W100	773.5 784.2 784.5 784.7	11.3 0.0 0.0 0.0	0.0 13.4 12.5 12.4	56.9 52.1 55.0 53.7	0.0 2.4 1.8 2.2	29.1 30.1* 29.9* 30.0*	
* Mn analogue of berthierite							
		Jamesonite					
DDH	Metres	Fe	Pb	Sb	As	S	
TC220W	926.3	2.5	37.6	35.6	0.0	22.6	
GG14	composite	2.6	39.8	34.0	0.0	20.9	
W73	33.8	2.1	38.0	34.1	0.0	20.9	

Table A.10: Microprobe Analyses of Rutile in the David Bell Orebody

DDH	Metres	TiO ₂	V ₂ O ₃	Sb ₂ O ₃	WO ₂	Fe ₂ O ₃
TC232	501.6	98.6	0.5	0.8	-	-
	502.2	95.3	2.3	0.4	0.7	-
	503.0	96.5	0.8	0.5	0.5	0.5
TC236	688.4	93.5	0.7	1.1	2.5	1.6
TC216	850.0	93.2	3.3	1.7	1.4	-
	871.9	98.1	0.6	0.5	0.3	-
	874.5	98.2	0.9	0.6	0.8	0.4
	875.3	91.0	4.0	1.7	1.7	-
	876.3	95.2	2.6	1.0	1.1	-
TC220W	926.3	95.9	-	1.6	0.8	1.3
TC218W	744.5	-	-	-	-	-
	749.8	99.9	-	-	-	-
	751.8	100.2	-	-	-	-
	753.1	99.1	-	-	0.4	-
	755.5	99.5	-	-	0.3	-
	758.3	98.5	-	-	0.9	-
	759.7	99.1	0.4	0.3	0.4	-
	761.6	97.9	0.2	0.3	0.9	0.8
	764.2	95.6	1.2	1.9	0.4	0.5
	767.5	88.8	4.3	3.3	3.2	-
	769.2	92.2	3.4	1.4	3.0	-
	771.2	98.1	1.1	0.5	0.5	-
	773.7	98.1	1.2	0.5	0.6	-
	775.3	94.7	2.3	0.9	1.0	-
	776.3	98.1	0.3	0.8	0.5	0.8

Table A.11: Microprobe Analyses of Barian Tomichite

DDH	Metres	As ₂ O ₃	Sb ₂ O ₃	Al ₂ O ₃	V ₂ O ₃	Fe ₂ O ₃	SiO ₂	BaO	TiO ₂	Cr ₂ O ₃
GG14W	879.55	13.3	0.8	1.0	34.8	13.1	0.2	7.6	27.2	0.0
	879.65	12.2	1.3	0.0	36.6	10.4	0.0	6.7	25.8	0.7
GG20	871.9	10.4	5.0	0.0	23.8	13.9	0.0	3.6	37.8	0.4
	884.0	12.5	3.3	1.1	23.1	19.3	0.0	3.6	34.7	0.0
	884.1	12.5	2.9	1.2	30.3	12.9	0.0	4.4	32.6	0.0
	887.0	12.3	3.3	0.8	26.9	14.0	0.1	5.0	32.5	1.2
GG21	856.1	10.9	4.9	0.8	17.8	19.6	0.0	5.7	35.1	1.3
	"	11.6	4.3	0.8	20.3	16.8	0.0	5.1	35.9	1.6
	"	11.1	5.1	0.8	19.7	17.8	0.0	5.2	35.5	1.2
	"	11.5	4.4	0.8	23.0	15.5	0.2	5.0	31.9	4.5
AVE.	856.1	11.2	4.6	0.8	21.6	16.8	0.0	5.3	33.8	2.2
	856.1	11.2	4.6	0.8	21.6	16.8	0.0	5.3	33.8	2.2
GG23	650.4	7.4	10.0	0.8	25.6	17.1	0.2	3.6	30.8	0.9
W70	731.5	9.8	4.9	0.5	35.9	8.6	0.0	4.1	33.6	0.7
	735.1	11.2	3.5	0.5	31.3	10.0	0.2	4.6	33.7	0.9
	"	11.7	3.3	0.5	29.9	9.6	0.0	5.7	34.7	0.8
	"	12.2	2.5	0.5	33.8	7.9	0.1	6.6	31.6	1.0
	"	10.9	3.8	0.5	34.8	8.6	0.2	4.3	30.4	1.1
	739.5	11.1	2.9	0.0	41.6	6.6	0.0	4.6	27.7	0.6
	744.8	10.4	5.9	0.9	22.1	20.6	0.0	2.9	34.1	0.0
	750.3	11.4	3.0	0.0	36.1	6.8	0.0	4.0	33.8	0.6
	751.4	12.0	2.8	0.0	38.5	6.7	0.0	4.4	29.3	0.7
	752.4	12.4	1.6	0.0	39.0	7.7	0.0	6.7	26.0	0.7
	753.8	11.8	2.3	0.0	38.3	8.4	0.0	6.0	26.4	0.9
754.4	12.3	2.0	0.9	36.8	9.0	0.0	6.2	29.2	0.0	
757.4	11.8	2.5	0.0	33.6	11.6	0.0	5.8	30.0	0.6	
W100	789.2	12.8	1.2	0.2	44.8	8.7	0.0	7.3	17.8	1.4
	790.95	11.9	3.3	0.4	28.3	13.4	0.0	6.3	30.0	0.9
	791.9	12.2	3.1	0.6	22.8	16.2	0.0	6.7	34.0	0.9
	802.2	12.1	3.1	0.8	20.5	18.2	0.3	4.2	33.3	1.8

Table A.12: Microprobe Analyses of Feldspars

DDH	Metres	Na ₂ O	K ₂ O	CaO	BaO	Al ₂ O ₃	SiO ₂	Species
TC236	688.4	9.1	-	3.0	-	22.3	67.6	An15
TC216	850.0	7.8	-	5.4	-	24.8	63.4	An28
	871.9	1.8	12.9	-	0.9	19.3	67.5	BaKsp
	"	8.8	-	3.1	-	22.6	67.4	An16
	875.3	0.5	12.3	-	9.4	20.7	58.6	BaKsp
	"	0.9	12.9	-	6.6	20.1	61.3	"
	"	0.9	11.6	-	9.5	20.7	58.4	"
TC234	905.7	9.2	-	2.7	-	22.2	66.0	An14
TC220W	926.3	7.7	-	1.7	-	21.5	69.7	An11
TC218W	745.9	7.6	-	6.3	-	24.8	60.0	An32
	748.9	9.5	-	4.0	-	23.7	65.3	An19
	"	0.6	11.9	-	9.0	20.4	59.0	BaKsp
	"	1.0	8.1	-	17.0	22.9	52.6	"
	762.0	2.1	-	16.1	-	33.0	48.7	An81
	"	1.3	13.5	-	4.9	20.0	63.0	BaKsp
	768.2	0.6	14.7	-	4.3	19.1	60.8	"
	770.3	0.3	15.1	-	3.1	19.1	62.1	"
	773.7	1.0	13.7	-	6.7	20.4	61.4	"
	776.3	0.3	15.7	-	1.4	18.4	63.2	"
	"	9.5	-	3.4	-	22.6	65.0	An16
NTC9W	577.4	8.6	-	3.5	-	22.7	66.2	An18
	582.7	0.4	15.0	-	3.3	19.3	64.2	BaKsp
	584.3	0.6	12.9	-	8.5	20.4	58.9	"
GG14W	855.8	7.6	-	6.9	-	25.4	59.3	An33
	870.2	11.8	-	0.4	-	19.3	66.9	An0
	882.9	0.8	13.2	-	4.3	20.3	60.2	BaKsp
	883.5	1.0	12.0	-	3.2	19.5	59.8	"
	884.2	10.7	-	-	-	20.6	71.9	An0
	"	0.4	15.5	0.5	1.7	18.3	62.9	BaKsp
	886.0	-	13.4	-	7.9	18.2	64.2	"
GG20	850.5	5.1	-	10.4	-	29.1	54.1	An53
	854.8	4.5	-	11.4	-	29.6	52.9	An58
	"	0.4	15.2	-	0.7	18.7	64.1	Ksp
	856.1	6.3	-	8.3	-	26.8	57.4	An42
	"	5.9	-	9.2	-	27.7	56.0	An46
	863.0	-	14.0	-	4.0	19.5	62.0	BaKsp
	"	11.0	-	-	-	19.5	68.2	An0
	868.5	11.1	-	-	-	19.5	68.5	An0
	"	-	14.8	-	2.4	19.0	62.7	BaKsp
	872.9	-	14.9	-	1.6	18.8	63.4	"
	"	-	14.8	-	2.4	19.1	62.9	"
	"	11.3	-	-	-	19.3	68.0	An0
	874.9	-	15.1	-	1.9	18.7	63.1	BaKsp
	875.9	-	14.6	-	1.8	18.8	63.3	"
	884.8	-	14.8	-	2.8	19.0	62.1	"
	"	-	14.4	-	3.8	19.4	61.3	"
	887.0	-	14.3	-	2.9	18.9	63.0	"
	"	-	13.6	-	4.9	19.4	60.6	"
	"	11.0	-	-	-	19.8	67.7	An0
	888.1	-	11.1	-	10.1	21.2	57.6	BaKsp
	891.5	-	15.0	-	2.8	19.1	62.6	"
	896.3	-	15.2	-	0.9	18.4	63.4	"
	900.0	-	15.1	-	2.0	18.9	62.9	"
	"	7.6	-	6.4	-	24.7	59.2	An31
	913.0	10.4	-	1.5	-	20.6	65.3	An7
	917.1	9.0	-	3.5	-	22.4	63.2	An17
	926.2	0.6	14.2	-	3.0	19.2	62.8	BaKsp
	"	10.7	-	0.8	-	20.0	66.4	An4
	930.9	-	14.9	-	1.9	18.6	62.4	BaKsp
	934.8	-	15.3	-	1.6	18.8	63.9	"
	940.0	-	14.3	-	3.3	19.0	61.4	BaKsp
	"	11.2	-	-	-	19.4	66.8	An0
	943.4	-	14.9	-	2.5	18.7	62.1	BaKsp
	946.2	-	15.0	-	2.6	18.5	61.7	BaKsp
	"	11.5	-	-	-	19.1	67.4	An0
	951.8	-	15.4	-	1.5	18.4	63.1	BaKsp
	"	11.4	-	-	-	19.2	66.9	An0
GG23	647.0	8.7	-	4.6	-	23.6	62.2	An23
	647.7	9.6	-	2.6	-	21.8	64.9	An22
	649.2	10.2	-	1.6	-	20.7	65.8	An8
	653.6	8.7	-	4.7	-	23.1	62.8	An23
	"	11.2	-	-	-	19.3	68.6	An0
	655.0	7.4	-	6.6	-	24.9	59.6	An23
	657.8	8.7	-	4.2	-	23.0	62.6	An21
	662.3	6.4	-	8.4	-	26.8	57.1	An41
	673.0	11.5	-	-	-	19.2	67.6	An0
GG37Y	1040.2	1.0	8.3	-	14.9	23.5	54.4	BaKsp
	"	1.4	7.2	-	16.6	24.0	53.3	"
	"	11.1	-	-	-	20.0	69.2	An0
	1050.3	1.0	8.7	-	13.5	22.9	56.4	BaKsp
	"	0.9	8.2	-	15.7	23.7	54.5	"
	"	11.2	-	-	-	19.9	69.4	An0
	1052.5	0.4	15.0	-	1.2	19.4	65.4	BaKsp

Table A.12: continued

DDH	Metres	Na ₂ O	K ₂ O	CaO	BaO	Al ₂ O ₃	SiO ₂	Species
W70	701.3	7.0	-	7.4	-	26.2	58.4	An36
	703.4	7.5	-	6.4	-	25.3	59.3	An32
	705.2	7.2	-	7.2	-	25.7	58.9	An35
		0.5	13.8	-	-	2.9	19.2	BaKsp
	707.2	0.7	-	17.8	-	35.0	45.0	An93
		0.6	12.5	-	-	6.1	20.2	BaKsp
	709.2	0.4	14.9	-	-	0.5	18.7	Ksp
	710.9	0.4	14.1	-	-	0.4	17.9	"
	711.8	-	15.5	-	-	-	18.4	"
	713.4	0.5	15.6	-	-	-	18.5	"
	715.1	-	15.7	-	-	-	18.5	"
	718.6	-	15.7	-	-	-	18.5	"
	719.2	0.4	15.6	-	-	-	18.6	"
	721.0	-	15.6	-	-	0.4	18.6	"
	722.9	-	15.5	-	-	0.8	18.6	"
	726.2	-	15.6	-	-	0.4	18.5	"
	727.3	-	15.5	-	-	0.8	18.7	"
	728.7	0.4	14.2	-	-	3.2	19.3	BaKsp
	730.5	-	14.8	-	-	1.6	18.7	"
	732.3	0.4	14.9	-	-	1.6	18.9	"
	733.8	-	13.0	-	-	7.0	20.3	"
	735.1	-	14.5	-	-	3.1	19.3	"
	736.3	0.4	13.0	-	-	6.8	20.5	"
	737.4	-	12.7	-	-	5.3	20.1	"
	740.7	0.4	13.6	-	-	4.2	19.6	"
	744.9	-	15.5	-	-	0.3	18.6	Ksp
	745.3	-	15.4	-	-	0.9	18.7	"
	746.8	0.5	14.9	-	-	-	18.7	"
	747.4	0.4	15.1	-	-	1.1	18.8	BaKsp
	748.5	-	15.7	-	-	0.6	18.6	"
	749.8	-	14.9	-	-	2.5	19.0	"
	751.4	0.4	13.8	-	-	3.6	19.4	"
	752.4	0.6	13.1	-	-	5.8	20.0	"
	753.8	0.5	12.9	-	-	6.5	20.2	"
	754.4	0.6	12.6	-	-	6.7	20.5	"
	756.6	0.7	12.0	-	-	7.6	20.5	"
	757.4	1.0	10.9	-	-	9.6	20.9	"
	758.6	1.0	12.9	-	-	4.5	19.8	"
	760.5	0.5	15.0	-	-	0.9	18.6	"
	761.4	0.5	14.2	-	-	3.6	19.3	"
	762.9	0.4	14.5	-	-	2.8	19.0	"
764.4	0.3	14.9	-	-	1.8	18.6	"	
767.1	0.9	12.7	-	-	5.1	19.7	"	
769.9	0.4	14.7	-	-	2.3	18.8	"	
770.6	-	14.8	-	-	2.9	18.9	"	
771.8	-	14.9	-	-	2.4	18.7	"	
773.5	0.5	13.3	-	-	5.8	19.9	"	
776.5	-	15.6	-	-	1.6	19.1	"	
778.7	-	15.5	-	-	1.4	18.6	"	
780.9	-	15.0	-	-	2.3	18.7	"	
W137	938.5	-	15.6	-	0.5	18.2	64.1	Ksp
	940.6	-	15.1	-	0.3	18.0	64.8	"
	941.6	6.8	-	7.0	-	24.8	59.5	An36
	942.5	-	14.5	-	3.1	19.2	61.8	BaKsp
	944.3	-	14.4	-	0.3	17.1	64.6	"
	946.4	-	14.5	-	1.1	17.5	64.1	"
	947.9	-	15.1	-	2.5	19.1	63.6	"
	949.5	-	15.3	-	1.7	18.9	64.4	"
		-	14.9	-	2.8	19.3	63.3	"
	952.5	-	15.3	-	2.0	19.0	63.3	"
	954.8	11.5	-	-	-	19.4	68.6	An0
	-	14.5	-	3.6	18.9	62.3	BaKsp	
W116	1109.8	1.2	-	17.4	-	34.7	45.7	An89
	1112.5	-	15.4	-	-	18.6	65.5	Ksp
		-	-	25.5	-	25.5	46.0	An100
	1113.3	-	15.4	-	0.9	18.6	64.4	Ksp
	1115.4	-	16.0	-	-	18.5	66.3	"
	1117.4	-	16.1	-	-	18.4	64.4	"
	1120.8	-	15.8	-	-	18.3	65.1	"
	1123.2	0.4	15.6	-	0.9	18.8	64.3	"
	1124.0	0.5	14.6	-	2.6	19.3	63.1	BaKsp
	1126.6	9.6	-	-	-	19.9	70.0	An0
		-	15.5	-	1.8	19.0	63.3	BaKsp
		-	13.6	-	5.2	19.8	60.0	"
	1129.8	-	15.1	-	2.0	19.0	63.2	"
	1131.2	-	14.9	-	1.8	18.8	63.2	"
	1133.3	-	14.5	-	2.2	18.8	63.3	"
	1135.2	-	15.5	-	1.9	19.0	62.6	"
	1136.6	-	15.8	-	0.8	18.5	63.6	"
	1137.8	0.4	14.7	-	2.5	19.2	62.6	"
	1139.2	-	15.8	-	0.7	18.6	64.0	"
	1141.8	-	14.8	-	2.2	19.4	65.1	"
1143.9	-	14.7	-	1.9	19.0	63.4	"	
	-	14.9	-	0.4	18.5	64.8	"	

Table A.13: Microprobe Analyses of Micas

DDH	Metres	K ₂ O	BaO	MgO	FeO	V ₂ O ₃	Cr ₂ O ₃	Al ₂ O ₃	TiO ₂	SiO ₂	F	
TC218W	745.9	9.4	0.0	9.1	21.9	0.0	0.0	16.5	2.5	35.7	N.A	
	748.9	9.2	3.7	1.6	2.1	0.0	0.0	31.7	0.0	43.9	N.A	
	"	9.6	0.7	17.6	9.2	0.0	0.0	16.9	1.6	38.3	N.A	
	767.5	10.4	0.8	1.8	1.1	3.5	0.0	29.0	0.9	45.4	N.A	
	768.2	10.6	0.9	2.1	0.9	2.4	0.0	29.7	1.4	46.1	N.A	
	770.3	10.6	0.7	1.5	0.3	0.0	0.0	31.7	1.3	46.0	N.A	
	772.9	9.4	2.9	1.7	0.9	5.5	0.0	28.0	0.8	43.1	N.A	
	773.7	10.2	1.5	1.6	0.4	0.0	0.0	32.5	1.2	46.4	N.A	
	774.2	10.1	1.2	1.8	0.5	3.0	0.0	30.2	1.1	45.5	N.A	
	776.3	10.8	0.0	1.7	0.0	0.0	0.0	31.6	1.2	47.6	N.A	
"	10.5	0.0	19.7	7.4	0.0	0.0	16.4	1.3	40.0	N.A		
TC236	688.4	9.1	2.1	1.2	3.9	0.0	0.9	30.2	1.3	44.7	0.7	
TC216	850.0	7.7	6.9	1.7	0.8	2.8	0.0	32.0	0.6	43.8	0.0	
	875.3	9.1	2.1	2.6	1.1	1.9	0.0	31.1	1.3	50.4	0.4	
TC234	902.5	9.7	0.0	16.2	11.7	0.3	0.0	17.4	0.7	39.1	0.8	
	903.6	8.7	0.0	23.7	6.6	1.3	0.0	14.1	0.3	39.1	0.8	
	904.6	10.1	0.0	20.7	5.5	0.3	0.0	17.5	0.9	41.5	0.5	
	905.7	9.4	0.0	14.9	16.3	0.0	0.0	14.7	0.9	39.8	1.3	
TC220W	926.3	9.4	1.2	1.4	1.9	0.0	0.0	33.5	1.4	49.0	0.3	
GG14W	866.3	9.5	0.9	9.3	7.1	0.0	0.0	23.8	1.3	44.0	0.7	
	867.3	9.4	0.9	1.3	0.7	0.3	0.0	34.9	1.3	49.8	0.3	
	868.6	8.9	1.0	2.4	0.6	1.7	0.0	31.1	1.0	51.0	0.5	
	870.2	8.7	3.4	2.0	0.9	4.7	0.0	28.8	0.9	47.1	0.2	
	873.4	8.5	2.8	2.3	1.1	6.1	0.0	27.7	1.0	48.0	0.3	
	877.3	7.9	3.7	2.1	1.1	5.9	0.0	27.4	0.8	45.9	0.6	
	879.4	7.4	6.2	1.7	3.3	7.3	0.0	25.3	0.4	41.9	0.1	
	NTC9W	577.4	9.5	2.2	9.0	4.6	0.0	0.0	26.4	1.4	43.4	1.4
581.9		10.8	0.8	2.0	0.5	3.2	0.0	30.4	0.9	47.9	0.2	
582.7		9.7	0.9	2.5	0.4	1.7	0.0	32.1	1.3	50.8	0.7	
584.3		9.0	2.6	1.2	0.4	1.4	0.0	33.8	1.2	46.9	0.5	
GG20	850.5	8.9	0.6	13.4	15.1	0.0	0.0	19.6	1.5	36.8	0.6	
	"	9.5	1.3	0.8	2.0	0.0	0.0	34.7	0.8	44.8	0.0	
	854.8	9.5	0.0	13.6	16.7	0.0	0.0	17.3	1.7	37.8	0.2	
	"	10.5	0.7	1.7	3.0	0.0	0.0	31.6	0.8	46.6	0.1	
	856.1	10.6	0.4	1.8	3.5	0.0	0.0	31.4	0.7	46.3	0.0	
	"	9.7	0.1	12.9	17.7	0.1	0.0	17.1	2.1	37.5	0.5	
	860.9	10.9	0.3	1.9	1.3	0.0	0.0	33.1	0.0	47.7	0.2	
	"	10.8	0.4	2.6	1.4	0.6	0.0	31.0	0.2	47.2	0.0	
	863.0	10.4	0.4	2.2	0.8	3.3	0.1	29.2	1.2	46.3	0.3	
	868.5	10.2	1.1	2.5	3.0	3.6	0.0	27.1	0.6	46.4	0.3	
	872.9	9.9	2.2	2.1	1.7	5.9	0.2	27.5	0.9	45.1	2.8	
	874.9	10.3	0.5	2.5	0.9	6.4	0.1	26.1	1.3	45.7	0.1	
	875.9	10.4	0.5	2.4	0.6	1.7	0.0	30.0	1.4	47.3	0.3	
	GG23	884.8	10.0	0.6	20.5	2.9	3.0	0.2	15.6	1.1	40.2	2.2
		"	9.9	1.0	2.3	1.1	6.6	0.3	25.6	0.9	44.4	0.2
		"	10.2	0.7	22.5	2.1	2.2	0.1	15.4	1.0	40.0	2.2
		887.0	10.2	1.2	3.9	2.0	4.3	0.0	25.4	0.8	45.4	0.2
		"	9.9	1.5	1.9	2.1	5.0	0.0	28.2	0.7	45.5	0.1
		888.1	9.3	1.2	15.6	11.5	0.3	0.0	17.2	2.0	37.7	1.0
		"	9.5	2.9	1.8	3.0	0.6	0.0	31.2	0.9	44.2	0.1
		891.5	10.7	0.4	1.7	0.9	0.0	0.0	32.7	0.7	46.3	0.2
		913.0	8.7	1.2	0.4	0.5	0.0	0.0	35.5	0.7	45.3	0.3
		917.1	10.6	0.3	1.8	0.7	0.0	0.0	32.8	0.9	47.0	0.0
		926.2	10.5	0.8	1.6	1.1	0.0	0.0	32.8	0.8	46.2	0.1
		930.9	10.6	0.9	2.6	3.8	2.9	0.0	25.3	0.7	46.7	0.5
		934.8	10.5	0.3	2.7	1.8	4.6	0.1	26.3	0.4	46.2	0.3
		940.0	10.4	0.6	1.3	0.3	0.0	0.0	33.3	1.2	46.2	0.3
		943.4	10.5	0.4	1.8	0.4	0.1	0.0	32.7	0.7	47.0	0.4
		946.2	10.5	0.3	2.3	0.3	0.3	0.0	31.3	0.8	47.7	0.6
	GG23	643.5	9.4	0.0	13.5	17.4	0.0	0.0	16.2	1.5	37.4	0.3
		645.4	9.8	0.0	17.1	9.6	0.0	0.0	17.8	1.4	38.9	0.5
		647.0	9.5	0.9	16.8	9.4	0.0	0.0	18.0	1.5	38.1	0.5
"		9.6	3.1	2.2	2.5	0.0	0.0	31.4	0.8	45.4	0.2	
647.7		9.4	2.8	2.1	1.1	0.0	0.0	31.6	1.2	46.5	0.0	
649.2		9.6	2.1	1.5	1.6	0.6	0.0	32.6	1.3	45.3	0.0	
650.4		9.2	3.7	1.7	3.1	6.1	0.0	27.6	0.6	43.3	0.2	
"		9.0	2.0	15.0	11.2	1.5	0.0	16.7	1.6	37.3	1.1	
653.6		9.4	0.7	11.9	16.4	0.0	0.0	15.7	2.2	37.4	0.3	
655.0		9.0	1.0	16.1	11.0	0.0	0.0	16.2	1.8	37.7	0.3	
657.8		9.0	1.6	11.7	5	0.0	0.0	18.1	2.6	35.8	0.0	
"		8.7	3.9	1.3	2.9	0.0	0.0	32.6	0.6	43.6	0.0	
662.3		9.4	0.9	16.2	11.1	0.0	0.0	17.6	1.4	38.6	0.4	
"		9.9	2.7	1.9	2.9	0.0	0.0	31.1	0.6	45.2	0.0	
666.1		10.2	1.7	2.5	2.9	1.6	0.0	29.3	0.8	45.9	0.0	
667.4		9.9	2.2	1.9	2.8	1.0	0.0	30.1	0.6	45.1	0.0	
669.4		10.1	1.1	1.9	1.1	1.1	0.0	30.4	1.3	46.0	0.3	
670.8		10.8	0.5	4.6	0.0	2.2	0.0	26.4	0.8	48.5	0.8	
671.9		10.6	0.4	1.9	0.0	1.0	0.0	31.1	1.4	46.8	0.2	
673.0		9.9	1.6	0.8	0.2	0.0	0.0	35.0	1.3	45.3	0.0	
675.7		10.4	0.6	1.5	0.5	0.0	0.0	33.3	0.6	46.3	0.2	

Table A.13: continued

DDH	Metres	K ₂ O	BaO	MgO	FeO	V ₂ O ₃	Cr ₂ O ₃	Al ₂ O ₃	TiO ₂	SiO ₂	F	
W70	701.3	8.6	0.2	13.6	14.1	0.0	0.0	18.8	1.9	37.2	0.4	
	703.4	8.3	0.5	11.1	17.9	0.0	0.0	19.1	1.6	36.9	0.2	
	705.2	9.5	0.2	12.4	16.9	0.0	0.0	17.6	2.0	37.2	0.7	
	707.2	8.8	0.2	17.8	5.6	0.0	0.0	18.4	1.3	40.3	0.3	
	709.2	9.5	0.2	2.0	1.0	0.0	0.0	32.0	1.5	47.5	0.4	
	710.9	10.6	0.2	0.6	0.4	0.3	0.0	34.9	1.3	46.2	0.0	
	711.8	10.6	0.0	0.8	0.5	0.4	0.0	34.0	1.4	46.2	0.1	
	713.4	10.5	0.0	0.9	0.8	1.0	0.0	33.7	1.3	46.8	0.2	
	715.1	10.7	0.0	1.1	1.0	0.7	0.0	32.9	1.4	46.2	0.3	
	718.6	10.8	0.0	1.4	0.7	1.3	0.0	32.3	1.4	46.6	0.3	
	719.2	10.9	0.0	1.4	0.6	1.8	0.0	32.0	1.4	46.3	0.2	
	721.0	10.9	0.0	1.5	0.7	0.5	0.0	32.4	1.4	46.8	0.2	
	722.9	10.8	0.3	2.3	0.7	1.6	0.0	30.4	1.3	47.8	0.2	
	726.2	10.5	0.0	2.1	1.3	4.0	0.1	27.8	1.3	46.3	0.2	
	727.3	10.6	0.2	1.8	1.3	2.2	0.0	30.3	1.2	46.9	0.2	
	728.7	10.5	0.9	2.0	1.5	2.4	0.0	29.8	1.2	46.3	0.0	
	730.5	10.3	0.5	2.2	1.6	6.4	0.2	26.6	0.9	45.1	0.1	
	732.3	10.3	0.7	2.2	1.5	5.1	0.2	26.9	1.4	46.2	0.9	
	733.8	9.6	2.4	3.5	1.6	9.3	0.3	23.0	0.7	44.3	0.1	
	736.3	9.6	0.4	20.2	5.7	2.2	0.1	14.8	1.3	40.2	0.6	
	737.4	9.6	0.3	20.2	5.3	2.4	0.2	15.5	0.8	40.1	0.6	
	740.7	9.7	1.4	10.8	3.0	6.3	0.2	19.8	1.5	41.9	0.3	
	744.9	9.9	0.1	7.0	9.1	4.6	0.2	20.5	1.2	41.4	0.5	
	745.3	9.6	0.1	12.3	14.4	2.2	0.0	16.4	2.5	37.9	1.2	
	746.8	10.0	0.0	4.9	5.4	2.8	0.1	25.4	1.4	43.7	0.4	
	747.8	10.3	0.4	2.2	1.8	3.1	0.0	28.4	1.3	46.7	0.4	
	748.5	9.9	1.4	2.7	1.2	7.3	0.2	25.1	1.2	45.0	0.3	
	749.8	10.1	0.9	3.2	0.9	7.7	0.2	23.7	0.9	46.3	0.4	
	751.4	7.4	0.8	2.9	1.3	8.9	0.2	24.5	0.7	48.6	0.5	
	752.4	9.4	2.4	3.1	1.7	10.9	0.3	21.6	0.7	43.3	0.2	
	753.8	9.4	2.9	2.6	1.8	11.5	0.3	21.9	0.6	43.3	0.4	
	754.4	9.6	1.4	18.0	5.4	4.0	0.1	15.2	0.9	39.0	1.7	
	756.6	9.9	1.6	2.5	2.0	7.7	0.2	25.2	0.5	43.9	0.1	
	757.4	8.9	2.4	15.3	8.4	3.0	0.1	16.8	1.3	37.7	0.7	
	758.6	9.6	0.9	9.4	9.7	0.6	0.6	21.0	1.5	39.7	0.4	
	760.5	10.3	0.3	1.1	4.7	0.0	0.1	30.3	0.3	44.9	0.2	
	761.4	10.6	0.6	2.7	0.5	1.7	0.2	30.2	0.6	46.5	0.1	
	762.9	10.3	0.7	0.8	0.5	0.9	0.0	33.5	1.2	45.5	0.2	
	764.4	10.5	0.4	1.7	0.5	0.9	0.0	31.8	1.3	47.0	0.2	
	766.?	10.6	0.2	1.5	1.4	0.8	0.0	31.7	1.3	46.4	0.4	
	767.1	9.3	1.1	13.8	13.0	0.7	0.3	16.7	1.8	36.8	1.1	
	769.9	10.2	0.9	2.1	1.7	1.9	0.1	29.5	1.1	45.8	0.3	
	770.6	10.2	0.8	2.0	1.2	1.2	0.1	31.3	1.2	46.5	0.3	
	771.8	10.2	0.7	2.2	1.3	2.8	0.1	28.8	1.2	45.8	0.3	
	773.5	9.8	1.3	10.6	2.9	1.4	0.2	23.6	1.3	41.9	1.3	
	774.8	9.6	2.1	2.0	1.5	2.2	0.2	30.1	1.3	45.2	0.3	
	776.5	10.0	1.5	2.2	1.7	4.2	0.4	27.6	1.3	44.4	0.3	
	780.9	10.6	0.4	1.8	0.7	0.1	0.0	32.2	0.7	46.3	0.4	
	W116	1109.8	8.1	0.4	13.1	15.0	0.0	0.0	19.6	1.7	37.4	0.2
		1112.5	8.7	0.0	18.1	9.9	0.0	0.0	17.6	0.3	40.5	0.6
		1113.3	10.0	0.4	2.0	1.8	0.0	0.0	32.1	1.0	47.0	0.0
			9.7	0.0	15.9	11.9	0.0	0.0	18.4	1.7	37.7	0.3
		1120.8	9.5	0.1	1.6	0.4	0.8	0.0	35.4	1.2	51.9	0.5
		1123.2	8.9	0.3	1.9	0.5	0.8	0.0	33.2	1.3	49.9	0.6
		1124.0	8.3	0.8	2.4	0.3	1.0	0.2	31.9	1.2	50.6	0.4
1131.2		7.6	1.2	2.0	1.5	3.8	0.2	31.4	0.8	50.6	0.0	
1135.2		9.5	0.6	2.1	0.4	0.8	0.0	33.0	1.3	48.9	0.2	
		9.4	0.4	2.0	0.4	1.1	0.0	34.7	1.2	51.1	0.2	
1136.6		9.4	0.1	1.8	0.2	1.0	0.0	32.5	1.4	47.4	0.3	
1137.8		9.3	0.7	2.0	0.6	1.3	0.0	34.2	0.8	50.8	0.0	
1139.2		9.0	0.5	2.0	0.9	1.2	0.0	33.9	1.2	50.6	0.3	
1141.8		9.1	0.6	1.1	0.3	0.0	0.0	36.1	0.6	49.9	0.2	
1143.9		8.4	0.0	1.7	0.6	0.0	0.0	31.5	1.3	45.9	0.0	
		9.7	0.0	20.8	3.2	0.0	0.0	17.8	1.3	39.6	0.8	

N.A. not analyzed

Table A.14: Microprobe Analyses of Titanite

DDH	Metres	CaO	Al ₂ O ₃	SiO ₂	FeO	TiO ₂	V ₂ O ₃
TC234	902.5	26.6	2.3	31.3	0.5	33.2	0.4
	904.6	26.5	1.5	31.2	0.2	31.1	3.3
GG20	854.8	27.0	1.6	30.2	0.4	33.7	0.3
	856.1	27.6	1.8	30.3	0.5	36.9	-
	860.9	27.8	1.6	30.4	0.2	33.3	4.2
	888.1	27.9	1.2	30.2	0.3	37.2	0.6
	926.2	26.4	4.1	29.9	0.7	32.1	0.5
GG23	643.5	28.2	1.2	30.2	0.8	37.4	-
	655.0	28.1	1.3	30.1	0.6	37.5	-
	662.3	27.4	1.6	30.6	0.3	37.2	-
GG37Y	1040.2	28.0	1.7	30.0	-	32.7	5.3
	1041.4	27.8	1.7	29.8	-	34.6	3.0
	1041.6	27.9	1.9	29.7	0.2	34.4	3.0
	1050.3	27.9	3.0	30.4	-	32.7	3.2
W70	707.2	27.7	1.5	30.2	0.2	35.0	-
	709.2	27.3	1.9	30.5	-	34.4	-
	710.9	27.0	1.8	30.4	34.4	-	-
	728.7	27.4	0.9	30.0	-	34.9	1.0
	730.5	27.0	3.4	30.6	1.6	22.3	8.5 XR
	732.3	27.4	1.2	30.2	0.2	31.1	4.6
	735.1	26.8	0.4	29.9	-	30.8	5.2
	736.3	26.9	0.7	29.7	0.2	25.9	10.1
	748.5	27.6	2.7	30.7	0.2	23.9	9.2
	749.8	27.6	2.0	30.0	-	20.0	14.2

Table A.15: Microprobe Analyses of Tourmaline

DDH	Metres	Al ₂ O ₃	SiO ₂	CaO	Na ₂ O	MgO	FeO
GG14W	888.6	33.8	38.9	2.0	2.2	11.7	0.8
GG20	917.1	31.3	37.5	1.3	2.0	11.0	1.3
GG23	647.7	33.0	38.5	-	2.3	9.7	1.6
GG37Y	1037.9	35.3	39.4	0.6	1.8	9.6	0.4
	1045.2	33.6	38.7	0.6	1.5	9.8	1.3
W70	701.3	33.0	38.4	1.1	1.5	8.0	5.0
	703.4	33.8	37.0	1.1	1.6	7.6	5.9
	758.6	30.9	36.9	0.7	2.1	8.1	4.2
	760.5	30.3	36.5	1.2	1.8	8.3	4.1
W116	1143.9	32.8	38.2	1.7	1.6	11.2	0.7

Table A.16: Microprobe Analyses of Zoisite/Clinzoisite

DDH	Metres	Al ₂ O ₃	V ₂ O ₃	CaO	SiO ₂	FeO
TC234	902.5	26.3	0.4	22.0	39.5	9.8
	904.6	27.5	0.2	21.9	39.3	8.1
	905.7	23.1	-	21.5	39.0	14.4
GG14W	888.6	31.8	-	25.3	40.0	-
GG20	860.9	30.5	-	23.2	39.1	3.6
	888.1	23.4	-	22.4	38.0	11.9
	"	21.4	1.5	21.5	37.1	11.9
	900.0	25.1	-	22.0	37.6	9.1
	913.0	25.1	-	22.0	37.6	9.1
	917.1	25.0	-	22.9	38.5	9.9
	926.2	21.7	-	19.6	35.6	10.7
	930.9	23.2	1.9	22.6	37.7	9.7
	934.8	18.7	6.6	20.4	36.1	7.9
	943.4	21.8	-	22.4	37.5	13.0
	946.2	23.3	-	22.7	38.0	11.2
951.8	23.2	-	22.4	37.7	11.7	
GG23	643.5	23.9	-	21.8	38.5	12.0
	657.8	22.3	-	21.3	37.9	13.8
	"	23.7	-	22.4	38.2	11.7
GG37Y	1041.4	33.5	-	22.8	40.6	1.2
W70	745.3	21.7	1.3	20.4	37.4	13.4
	"	18.6	4.0	19.9	36.3	13.2

APPENDIX B

Location of drill core specimens collected from the Hemlo deposit

Diamond drill holes and depths (metres) of samples examined from the main Hemlo gold deposit.
A polished section was made from each sample and a polished thin section from those marked *.

TC232	486.5, 487.4, 488.3, 489.0, 500.0, 501.6, 502.2, 502.3, 503.0.
TC236	660.7, 664.1, 665.7, 668.0, 671.0, 673.1, 673.8, 673.9, 675.3, 677.0, 678.5, 680.0, 681.5, 682.8, 685.2, 685.9, 686.7, 688.4, 689.9, 690.0, 691.5, 693.0, 694.7, 696.6, 698.0, 699.0, 704.0, 705.6.
TC216	849.2, 849.7, 850.0, 850.5, 851.1, 851.5, 852.0, 871.9, 873.4, 873.8, 874.5, 875.3, 875.6, 876.3, 877.2.
TC234	902.5*, 902.9, 903.6*, 903.8, 904.2, 904.6*, 905.2, 905.4, 905.7*, 906.1, 906.6*.
TC220W	923.2, 923.45, 923.8, 924.3, 925.1, 925.7, 926.3, 926.8.
TC218W	744.5, 745.9*, 748.9*, 749.3, 749.8, 750.2, 751.2, 751.8, 752.4, 753.1, 753.3, 753.5, 753.6, 754.0, 754.4, 755.0, 756.8, 758.3, 758.5, 759.0, 759.5, 759.7, 760.4, 761.6, 761.8, 762.0*, 764.2, 766.5, 767.5*, 768.2, 769.2, 770.3*, 771.3, 771.4, 771.7, 772.9*, 773.7*, 774.25*, 775.3, 776.3*.
NTC9W	563.1, 564.1, 565.1, 565.9, 566.9, 568.8, 570.2, 572.2, 573.1, 574.4, 576.2, 577.4, 579.2, 580.5, 581.4, 581.9, 582.4, 582.7, 583.3, 584.3, 584.8, 585.6.
GG25	322.6, 322.9, 323.4, 324.0, 324.2, 324.9, 324.95, 325.0, 325.1, 325.3, 325.7, 326.5, 327.0, 327.7, 328.0, 328.2, 328.6, 329.2, 330.0, 330.6, 331.5, 332.5, 333.1, 333.9, 334.4, 335.2, 336.1, 336.4, 336.9, 337.8, 338.6, 339.0, 339.7, 341.2, 342.3, 342.9, 343.7, 344.2, 345.9, 346.9, 347.6, 348.2, 348.9, 349.7, 350.3, 351.0, 351.9, 352.8, 353.8, 354.3, 354.55, 355.2, 356.0, 356.9, 357.6.
GG23	642.5, 643.5*, 644.5, 645.4*, 646.4, 647.0*, 647.7*, 648.4, 649.2*, 649.8, 650.4*, 651.6, 652.1, 653.6*, 654.3, 655.0*, 656.5, 657.8*, 659.1, 661.0, 662.3*, 662.5, 663.4, 664.1, 664.9, 665.4, 666.1*, 666.9, 667.4*, 667.8, 668.5, 669.4*, 670.3, 670.8*, 671.3, 671.9*, 672.1, 673.0*, 674.0, 675.1*.
GG14W	870.2, 870.8, 871.0, 879.45, 879.5, 879.65, 879.7.
GG20	849.0, 850.5*, 852.4, 854.8*, 856.1, 857.4, 860.9*, 861.3, 863.0*, 864.6, 865.9, 868.5*, 869.5, 871.9, 872.9*, 873.7, 874.5, 874.9*, 875.9*, 876.5, 877.6, 877.9, 878.2, 879.1, 879.4, 879.5, 879.6*, 881.4, 882.8, 884.0, 884.1, 884.7, 884.8*, 885.6, 886.8, 886.9, 887.0*, 887.8, 888.1*, 888.9, 891.5*, 893.0, 894.3, 896.3*, 896.6, 900.0*, 902.7, 905.5, 908.6, 909.5, 913.0*, 913.9, 917.1*, 917.9, 921.2, 924.1, 926.0, 926.2*, 928.7, 929.3, 930.3, 930.*, 932.2, 932.5, 934.1, 934.8*, 937.1, 938.3, 940.0*, 941.3, 942.3, 943.4*, 944.4, 946.2*, 948.2, 951.8*.
GG21	819.8, 820.3, 821.45, 822.5, 823.5, 824.3, 825.0, 826.1, 827.1, 828.2, 829.0, 830.1, 831.05, 832.1, 833.0, 833.5, 834.2, 835.2, 836.3, 837.2, 838.05, 839.2, 840.3, 841.0, 841.7, 843.1, 844.1, 845.45, 847.1, 849.3, 851.0, 852.3, 853.3, 854.0, 855.0, 856.1, 856.2, 857.4, 858.6, 859.5, 860.5, 862.1, 862.7, 863.5, 863.7, 863.8, 864.6, 865.3, 866.5, 866.8.
GG37Y	1037.2, 1037.9*, 1039.0, 1039.8*, 1040.2*, 1040.3, 1041.0, 1041.4*, 1041.6*, 1042.5, 1043.0, 1043.8*, 1045.2*, 1046.0, 1047.1, 1047.8*, 1048.0*, 1048.25, 1048.3, 1048.4, 1049.2*, 1049.9, 1050.3*, 1052.5*.
GG45	1103.7, 1104.3, 1105.1, 1106.2, 1107.0, 1107.6, 1108.1, 1108.6, 1108.9, 1110.1, 1110.4, 1110.6, 1111.0, 1111.7, 1111.8, 1112.2, 1115.1, 1116.5, 1117.1, 1117.4, 1118.0, 1118.2, 1118.9, 1119.4.
W73	12.7, 13.6, 14.6, 15.8, 16.7, 17.8, 19.6, 20.6, 21.6, 22.4, 23.4, 24.3, 25.6, 26.6, 27.4, 28.7, 29.2, 29.6, 30.2, 31.3, 32.5, 33.6, 33.8, 34.0, 34.3, 34.6, 35.0, 35.5, 36.1, 36.4, 36.7, 37.4, 38.5, 39.3, 40.3, 41.5, 42.4, 44.2, 45.5, 46.2, 46.7, 47.2, 48.0.
W28	173.9, 174.8, 175.5, 176.7, 177.2, 178.5, 179.5, 180.4, 181.7, 182.1, 182.4, 183.3, 183.5, 183.6, 184.4, 185.3, 186.6, 186.7, 187.6, 188.5, 188.9, 189.0, 189.5, 189.7, 191.5, 192.5, 193.4, 193.9, 194.4, 195.4, 195.9, 196.1, 196.6, 197.2.
W104	243.4, 244.2, 245.0, 245.9, 247.1, 247.9, 248.7, 249.1, 249.5, 251.0, 251.4, 252.3, 252.4, 252.6, 253.6, 254.8, 255.9, 257.2, 258.2, 259.0, 261.7, 262.8, 263.4, 264.2, 264.5, 264.8, 265.2, 265.4, 266.3.
W69	435.9, 436.6, 437.4, 437.45, 437.5, 438.2, 439.2.
W92	635.4, 636.4, 636.6, 637.3, 638.25, 639.5, 640.0, 641.3, 641.9, 642.7, 643.2, 643.8, 644.5, 645.1, 646.1, 654.4, 657.8, 658.9, 660.7, 663.5, 664.65, 665.8, 666.8, 667.7, 669.3, 670.3, 670.8, 681.5, 682.2, 684.3.
W70	700.2, 701.3*, 702.0, 702.6*, 703.4*, 704.9, 705.2*, 706.1*, 707.2*, 708.0*, 709.2, 710.2, 710.95, 711.2*, 711.8, 712.2, 713.0*, 713.4, 714.5*, 715.1, 715.7*, 716.3, 716.8*, 717.4, 718.0, 718.6*, 719.2, 720.2*, 721.0, 721.4, 722.3*, 722.9, 723.3, 724.7*, 725.6, 726.2, 726.8*, 727.2, 727.3, 728.7*, 729.3, 730.5, 731.3*, 731.5, 731.9, 732.3, 733.2*, 733.8, 734.8*, 735.0, 735.1, 735.9, 736.3*, 736.4, 736.8, 737.4, 738.2*, 738.4, 738.5, 738.9, 739.0, 739.2*, 739.5, 739.8, 740.7, 741.3*, 741.8, 742.2, 742.6, 743.2, 743.4, 744.8*, 744.9, 745.1, 745.3, 746.8, 747.1*, 747.4, 747.8, 748.3, 748.5, 748.8, 749.2*, 749.8, 750.3, 751.4*, 751.5, 752.4, 752.8, 753.3*, 753.8, 754.4, 755.6*, 756.6, 757.4, 758.2*, 758.6, 759.5, 760.5*, 761.4, 761.8, 762.0, 762.2*, 762.6, 762.9, 763.4*, 764.4, 765.8, 766.1, 766.8*, 767.1, 768.8, 769.9*, 770.2, 770.4, 770.6, 771.4, 771.8*, 772.8, 773.5, 774.2*, 774.8, 775.6, 776.5*, 777.8, 778.7*, 779.2, 780.3, 780.9*.
W100	746.1, 747.2, 748.4, 749.3, 750.3, 751.8, 752.6, 753.3, 754.2, 755.1, 756.1, 756.9, 758.5, 759.5, 760.5, 760.6, 761.5, 762.1, 763.8, 765.5, 766.2, 767.2, 768.1, 768.9, 769.8, 771.0, 771.7, 772.3, 773.5, 773.8, 774.3, 775.0, 776.0, 776.9, 779.0, 779.7, 780.5, 781.6, 782.0, 782.5, 783.5, 783.8, 783.9, 784.2, 784.3, 784.5, 784.9, 785.0, 785.2, 786.0, 786.5, 787.0, 788.0, 789.2, 790.2, 790.75, 791.2, 791.9, 794.5, 796.6, 796.9, 797.2, 797.6, 797.9, 798.3, 798.6, 799.2, 800.2, 801.1, 802.2, 803.0, 803.5, 804.6, 805.4, 805.5, 806.4, 807.8, 808.3, 809.9, 910.1, 810.5, 811.4, 811.8, 812.1, 812.8, 814.1, 814.4, 815.3, 815.9, 817.1, 818.0, 818.5, 819.8, 820.4.
W137	938.5, 939.5, 940.6, 941.6, 942.5, 943.4, 944.3, 945.1, 945.8, 946.4, 947.9, 948.8, 949.5, 950.2, 951.6, 952.5, 953.4, 954.8, 955.5, 956.5, 957.5, 958.6, 959.3, 960.8, 961.5, 962.5, 963.4, 965.2, 967.4, 969.0, 970.4, 971.2, 973.1, 974.8, 975.9, 977.5, 978.8, 980.5.
W116	1109.8, 1111.2, 1112.5, 1113.3, 1114.6, 1114.9, 1115.4, 1117.5, 1118.6, 1120.8, 1121.2, 1122.8, 1123.2, 1124.0, 1125.3, 1126.6, 1127.7, 1129.8, 1130.8, 1131.2, 1131.5, 1131.7, 1133.3, 1134.7, 1135.2, 1136.3, 1136.6, 1137.1, 1137.8, 1138.4, 1139.2, 1141.8, 1142.2, 1143.9.
W135	1172.7, 1173.4, 1174.1, 1175.25, 1176.3, 1177.5, 1178.9, 1180.3, 1181.9, 1182.6, 1183.3, 1184.9, 1184.95, 1185.5, 1185.85, 1186.6, 1187.95, 1188.5, 1189.3, 1190.6, 1191.2, 1191.85, 1192.5, 1193.5, 1194.4, 1196.1, 1197.5, 1199.5, 1200.5.
W129	1422.7, 1423.65, 1424.2, 1425.7, 1426.5, 1427.3, 1428.3, 1429.7, 1431.4, 1433.5, 1437.2, 1445.6, 1447.45, 1447.7, 1448.5, 1450.1, 1451.4.

INT-HOLE	V ppm	Cr ppm	Co ppm	Ni ppm	Cu ppm	Zn ppm	As ppm	Rb ppm	Sr ppm	Mo ppm	Ag ppm	Sb ppm	Hg ppb	Pb ppm
745.9-218	133	20	17	8	90	132	8.5	70	1750	1	0.1	0.3	120	7
748.9-218	39	30	15	24	9	97	137.1	20	365	11	0.1	2.8	924	1
750.2-218	29	40	15	28	35	49	166.7	30	720	4	0.1	3.8	216	8
753.3-218	26	50	15	42	3	215	99.8	20	370	8	0.1	1.9	1080	1
754.4-218	139	20	26	6	45	71	102.3	70	540	1	0.1	5.7	408	9
756.8-218	88	10	12	2	3	27	31.7	110	265	1	0.1	1.9	180	16
758.5-218	95	20	16	7	53	71	152.3	90	360	9	0.1	1.9	204	18
762.0-218	62	10	15	5	16	86	127.1	70	290	1	0.1	8.5	300	8
764.2-218	610	30	9	3	24	116	65.0	50	74	1670	4.8	1624.0	145200	10
766.5-218	2620	90	7	1	3	12	29.6	50	18	6380	3.6	143.7	7131	9
767.5-218	545	80	11	9	5	31	38.3	50	111	3290	1.6	38.8	13980	8
768.2-218	1170	60	8	16	3	12	40.4	30	13	2320	2.0	38.8	6900	1
769.2-218	520	5	22	5	7	7	33.9	10	345	10000	3.8	257.9	16020	12
770.3-218	50	5	17	5	1	9	49.1	10	275	2770	0.4	304.1	16200	1
771.3-218	27	5	38	4	1	1	8.5	10	415	320	0.6	60.7	3222	4
772.9-218	965	5	21	7	13	24	84.9	10	270	1700	1.6	6456.4	47820	1
773.7-218	910	30	15	8	7	14	94.8	60	131	1460	2.8	336.7	70080	7
775.3-218	90	5	14	10	1	10	25.4	80	330	670	1.4	69.1	7440	15
776.3-218	65	10	10	4	1	52	14.8	90	425	20	0.1	6.1	2160	40
778.9-218	4	10	3	1	1	21	23.2	80	480	2	0.1	5.7	576	94
780.5-218	1	10	2	1	1	20	10.6	90	520	1	0.1	7.6	1866	22
784.6-218	5	10	2	1	2	16	36.1	60	520	3	0.1	5.7	372	18
786.5-218	4	5	2	1	1	28	29.6	100	475	2	0.1	4.7	624	17
660.7-236	68	60	14	15	16	58	21.1	40	640	16	0.1	1.9	144	9
664.1-236	65	30	9	14	10	21	29.6	50	530	20	0.1	5.7	20	11
665.7-236	44	30	12	20	9	66	6.3	40	825	17	0.1	3.8	20	10
668.0-236	81	150	13	39	17	70	8.5	40	605	70	0.1	2.8	78	10
671.0-236	111	60	22	28	52	130	25.4	10	550	3	0.1	3.8	20	18
673.1-236	75	20	11	16	17	230	235.6	60	430	38	2.0	301.3	858	47
673.8-236	80	20	11	4	3	23	349.2	30	445	101	0.1	109.1	408	8
673.9-236	265	40	14	20	34	74	336.9	30	395	550	0.8	205.0	540	7
675.3-236	54	30	14	25	22	114	27.5	50	375	20	0.1	5.7	312	4
677.0-236	535	40	19	14	23	73	178.2	50	740	455	1.0	1624.0	16860	16
678.5-236	108	20	16	8	38	89	53.5	40	680	1	0.1	14.2	1320	15
680.0-236	56	30	11	27	310	170	16.9	10	410	9	0.6	5.7	1140	7
681.5-236	129	30	24	11	35	64	82.4	10	775	1	0.1	11.4	462	10
682.8-236	148	30	52	21	48	16	172.4	30	830	1	0.1	15.2	450	1
685.9-236	670	5	76	7	15	192	19.0	60	3920	840	0.1	1324.0	131760	21
686.7-236	755	20	31	7	12	75	27.5	70	1230	570	0.8	46.6	11940	5
688.4-236	240	710	29	112	78	70	8.5	50	575	40	0.4	13.3	2682	1
690.0-236	79	60	16	52	1	43	10.6	70	590	104	0.4	5.7	1368	12
691.5-236	90	380	27	88	63	58		70	630	37	1.2			4
693.0-236	102	60	20	67	13	36	53.5	60	470	195	0.6	10.4	1584	8
694.7-236	39	40	14	23	12	30	12.7	30	875	66	0.6	1.9	1590	12
696.6-236	38	40	12	26	20	61	19.0	40	985	88	0.6	11.4	790	23
698.0-236	21	20	9	8	1	45	14.8	40	1030	51	0.4	0.3	642	14
699.0-236	23	10	9	9	1	74	10.6	70	1330	2	0.1	0.3	390	16
704.0-236	89	70	16	30	130	42	31.7	50	610	127	1.8	3.8	2160	14
705.6-236	57	100	24	63	1	20	38.3	60	405	12	0.4	2.8	114	8
853.7-14W	70	20	17	9	41	30	3246.1	90	745	1	0.4	32.2	180	8
854.2-14W	68	20	16	11	54	33	1580.6	10	795	6	0.2	20.7	318	20
855.8-14W	48	30	13	24	77	47	252.9	30	605	7	0.4	2.8	156	84
857.6-14W	47	20	11	5	42	56	612.0	50	455	3	0.2	7.6	600	20
858.3-14W	27	40	36	39	137	28	762.0	10	260	19	0.2	9.5	180	1
858.5-14W	15	40	87	96	240	7	612.0	10	157	25	0.6	9.5	180	1
860.0-14W	49	30	11	13	17	40	144.5	50	450	1	0.4	4.7	642	40
862.3-14W	141	20	75	322	77	159	104.8	10	119	12	0.2	3.8	420	10
866.2-14W		150					264.4	90	114.1	7320				
866.3-14W	180	280	30	74	11	200	169.5	90	133	37	0.4	71.7	3180	23
867.3-14W	510	70	15	12	8	52	117.2	80	50	935	0.4	53.0	8304	1
867.6-14W	3130	90	29	32	25	195	112.2	60	49	6680	0.4	1924.0	19920	28
869.1-14W	156	5	3	3	7	6	51.3	10	198	240	0.2	504.1	14280	6
870.2-14W	2340	60	12	26	23	50	195.4	10	26	3460	1.0	569.1	15960	4
870.6-14W	625	20	14	6	35	68	564.6	40	53	2470	4.0	3124.0	100920	30
870.9-14W	295	5	20	1	9	5	553.3	10	405	1410	1.2	2324.0	76920	1
873.4-14W	2030	40	4	3	28	23	198.3	20	102	2800	4.8	975.6	27780	14
874.7-14W	2060	60	11	18	24	24	252.9	40	55	10000	1.4	3024.0	8760	4
877.3-14W	1540	60	15	32	50	305	206.9	20	25	2960	3.2	650.4	70200	6
879.4-14W	708	5	3	18	12	43	471.0	10	40	1550	0.2	35.3	3852	2
879.6-14W	355	5	159	13	5	4	202.3	10	980	1100	0.4	33.9	2940	25
880.1-14W	295	5	27	27	11	205	86.9	10	450	880	1.0	62.8	23460	2
880.8-14W	219	5	2	8	1	186	40.6	10	220	1400	0.2	24.5	9960	4
881.2-14W	143	5	6	29	20	754	40.6	20	169	1700	1.2	29.1	34560	4
881.6-14W	240	5	3	29	17	315	26.2	10	143	2080	1.0	30.0	16320	4
882.2-14W	72	5	11	10	7	213	24.0	30	159	815	0.2	9.3	5520	12
882.5-14W	69	5	8	21	23	882	26.2	30	103	627	0.4	23.6	12480	13
882.9-14W	35	5	4	14	18	740	17.4	10	169	1340	1.0	12.4	14340	16
883.5-14W	64	5	2	7	10	415	17.4	20	122	2000	0.4	7.2	7860	4
884.2-14W	142	5	15	29	27	2730	113.2	40	105	2590	3.6	276.2	58200	38
884.8-14W	148	5	11	10	82	1240	139.5	20	130	3540	6.0	228.7	34020	48
884.9-14W	88	5	26	9	41	600	129.0	10	182	1530	3.4	223.3	21840	54
885.3-14W	85	5	16	4	41	3220	86.9	40	186	820	1.2	108.4	140880	38
886.8-14W	44	10	11	5	11	37	35.6	100	94	6	0.2	35.2	4500	18
888.4-14W	10	10	4	1	1	42	26.2	90	60	1	0.4	35.2	4200	14
888.5-14W	26	10	7	6	11	53	33.1	80	76	7	0.2	33.9	4020	18
888.6-14W	14	5	8	4	15	46	38.1	70	125	2	0.2	139.3	5640	32
889.1-14W	13	10	4	1	1	37	13.1	110	44	1	0.1	28.2	2460	17

INT-HOLE	SiO ₂ %	TiO ₂ %	Al ₂ O ₃ %	Fe ₂ O ₃ %	MnO%	MgO%	CaO%	Na ₂ O%	K ₂ O%	BaO%	P ₂ O ₅ %	H ₂ O%	CO ₂ %	S%
889.7-14W	38.60	0.19	0.99	1.26	0.01	0.06	0.11	0.65	0.38	38.95	0.02	0.3	0.1	9.26
890.6-14W	68.40	0.27	17.50	1.99	0.01	0.88	0.51	1.50	4.80	0.29	0.03	1.3	0.1	1.14
891.3-14W	71.80	0.20	15.30	0.50	0.01	0.69	1.61	4.63	3.47	0.11	0.09	0.7	0.6	0.16
892.6-14W	72.60	0.18	14.30	0.72	0.01	0.54	1.90	4.55	2.74	0.08	0.08	0.5	0.6	0.68
895.2-14W	68.80	0.21	15.60	0.86	0.01	0.70	1.61	4.10	5.34	0.42	0.09	0.4	0.6	0.16
899.2-14W	70.40	0.23	16.70	0.58	0.01	0.73	1.30	1.92	4.93	0.18	0.09	0.8	0.1	0.41
902.6-14W	58.90	0.59	14.50	10.10	0.03	0.90	0.91	0.88	5.20	1.28	0.10	0.8	0.1	6.47
905.4-14W	78.00	0.18	13.70	0.55	0.01	0.24	0.13	0.41	3.76	0.08	0.07	0.9	0.1	0.30
908.4-14W	57.10	1.09	18.20	7.17	0.01	1.11	2.88	2.89	3.73	0.25	0.38	1.1	0.1	3.76
910.6-14W	57.90	1.21	21.10	2.52	0.01	1.01	4.71	5.71	1.93	0.17	0.33	0.6	0.4	1.18
912.0-14W	53.70	0.19	9.20	18.30	0.01	0.46	1.78	2.76	1.15	0.79	0.06	0.6	0.3	14.40
913.4-14W	68.90	0.25	17.00	1.06	0.01	0.67	1.38	4.87	3.00	0.15	0.06	0.6	0.5	0.77
916.8-14W	71.50	0.21	15.90	0.57	0.01	0.59	1.40	5.48	2.52	0.16	0.09	0.4	0.4	0.54
920.0-14W	67.90	0.28	16.70	2.03	0.01	1.02	2.22	6.34	1.85	0.17	0.27	0.4	0.4	1.46
924.2-14W	64.10	0.27	20.90	0.96	0.01	1.05	1.91	5.15	3.25	0.21	0.11	0.4	0.2	0.33
927.2-14W	63.90	0.28	21.20	0.74	0.01	0.94	1.67	4.56	4.07	0.13	0.11	0.8	0.2	0.34
927.3-14W	43.40	0.22	2.65	8.82	0.01	0.18	0.05	0.58	0.69	23.32	0.03	0.8	0.2	12.80
929.7-14W	26.40	0.42	8.59	24.20	0.01	0.46	0.22	0.84	3.17	14.06	0.02	1.9	0.2	
929.8-14W	15.70	0.37	5.83	8.91	0.01	0.35	0.17	0.82	1.84	41.18	0.03	1.0	0.1	15.80
930.9-14W	31.50	0.20	2.01	3.48	0.01	0.11	0.05	0.62	0.37	37.61	0.02	0.4	0.2	11.80
931.8-14W	69.10	0.33	16.20	1.85	0.03	0.91	1.74	1.18	5.27	0.55	0.11	1.0	0.2	0.64
933.1-14W	61.80	0.78	20.30	2.95	0.02	1.02	0.48	0.55	6.56	0.80	0.32	1.1	0.2	1.56
936.1-14W	48.50	0.48	13.70	1.83	0.01	0.77	0.64	0.70	5.37	15.62	0.08	1.3	0.2	4.42
937.6-14W	44.90	0.59	15.80	7.44	0.07	0.84	4.69	4.30	2.93	5.28	0.16	3.7		
938.3-14W	44.80	0.39	10.60	22.90	0.01	0.85	0.37	0.68	3.40	0.65	0.13	0.9	0.1	
939.1-14W	58.60	0.43	17.70	4.66	0.09	2.20	4.31	1.82	4.74	0.90	0.12	1.4	0.4	1.80
942.7-14W	75.50	0.15	8.00	7.05	0.03	1.05	1.92	1.40	0.88	0.04	0.05	0.7	0.2	3.95
849.0-20	74.90	0.32	15.50	0.79	0.01	0.55	2.03	1.61	2.34	0.16	0.08	0.7	0.3	0.04
850.5-20	71.50	0.30	15.80	1.92	0.04	1.68	3.85	2.21	1.26	0.10	0.09	0.9	0.3	0.07
852.4-20	67.90	0.37	16.10	2.86	0.03	1.73	2.44	0.93	3.62	0.13	0.16	1.4	0.4	0.48
854.8-20	59.90	0.62	15.90	5.82	0.08	2.23	4.63	1.12	5.30	0.13	0.34	1.2	0.9	1.52
856.1-20	58.50	0.60	16.60	6.58	0.07	2.19	4.12	2.05	5.32	0.17	0.34	0.8	0.7	1.56
857.4-20	56.80	0.70	18.40	4.80	0.02	1.73	1.95	0.71	8.74	0.44	0.37	1.2	0.4	2.28
860.9-20	57.80	0.36	9.06	11.50	0.05	4.06	5.81	0.11	3.18	0.09	0.18	0.9	1.5	7.76
861.3-20	73.60	0.38	10.30	3.02	0.01	0.43	0.42	0.46	6.96	0.26	0.18	0.6	0.2	1.96
863.0-20	59.30	0.38	8.43	11.60	0.01	0.19	0.27	0.75	5.95	3.41	0.13	0.6	0.3	9.24
865.9-20	52.30	0.41	9.08	8.23	0.01	0.11	0.56	0.97	6.29	11.27	0.18	0.4	0.3	8.12
868.0-20	45.30	0.42	8.66	20.60	0.01	0.22	0.39	1.02	5.96	4.45	0.15	0.9	0.2	15.20
869.5-20	68.00	0.35	15.40	2.07	0.02	1.26	2.49	5.80	1.74	0.15	0.14	1.0	0.6	0.09
871.9-20	41.70	0.19	1.48	3.58	0.01	0.08	0.29	0.61	0.83	43.52	0.04	0.3	0.3	8.46
872.9-20	66.30	0.29	8.43	3.19	0.06	0.13	0.21	0.90	6.10	8.62	0.16	0.3	0.3	3.40
873.7-20	28.80	0.12	2.89	39.70	0.01	0.35	0.19	0.30	2.06	0.44	0.02	0.7	0.1	27.94
874.5-20	42.50	0.29	5.36	30.20	0.01	0.17	0.12	0.50	4.06	2.49	0.02	0.6	0.2	14.43
874.9-20	28.70	0.22	1.73	7.21	0.01	0.12	0.05	0.71	1.00	35.49	0.02	0.2	0.2	13.20
875.9-20	31.60	0.29	3.97	3.01	0.01	0.11	0.13	0.79	2.73	37.05	0.07	0.2	0.2	9.92
876.5-20	59.50	0.38	11.20	8.38	0.06	0.39	0.19	0.72	6.71	6.35	0.17	0.9	0.0	6.83
877.6-20	51.80	0.40	9.20	10.40	0.01	0.27	0.13	0.72	5.81	9.82	0.03	0.3	0.1	9.24
878.2-20	55.30	0.39	8.97	16.10	0.01	0.11	0.27	0.75	6.53	2.76	0.02	0.4	0.2	12.40
879.6-20	18.00	0.19	1.74	31.60	0.01	0.25	0.47	0.58	0.56	20.31	0.03	0.9	0.1	24.90
882.8-20	36.00	0.33	5.01	0.80	0.01	0.08	0.05	0.78	3.85	36.05	0.02	0.1	0.8	7.46
884.1-20	52.70	0.31	5.89	4.92	0.01	0.12	0.83	0.71	3.84	16.96	0.02	0.4	0.2	7.40
884.8-20	42.90	0.26	3.75	11.60	0.01	0.10	0.05	0.73	2.49	21.20	0.02	0.4	0.2	13.00
885.6-20	33.00	0.18	0.83	6.72	0.01	0.11	0.05	0.60	0.25	34.15	0.02	0.4	0.1	12.70
887.0-20	19.50	0.24	1.07	6.68	0.01	0.08	0.11	0.69	0.58	43.41	0.01	0.3	0.2	14.20
887.8-20	24.30	0.30	3.28	2.81	0.01	0.12	0.12	0.97	2.03	42.07	0.02	0.2	0.2	11.20
888.1-20	42.60	0.35	5.11	2.75	0.02	1.06	1.61	0.75	2.44	25.33	0.12	0.6	0.1	7.24
888.9-20	44.30	0.34	6.96	15.50	0.01	0.28	0.20	0.79	4.97	10.27	0.02	0.7	0.2	13.70
891.5-20	20.70	0.21	1.32	8.06	0.01	0.08	0.05	0.76	0.76	42.63	0.02	0.2	0.3	14.80
893.0-20	61.40	0.31	11.80	0.40	0.01	0.06	0.05	0.82	9.38	8.68	0.02	0.2	0.1	2.02
894.3-20	68.10	0.22	16.60	1.19	0.01	0.52	0.82	1.32	7.27	0.25	0.11	2.4	0.2	1.10
896.3-20	68.60	0.27	18.50	1.26	0.01	0.89	0.18	0.49	6.52	0.28	0.04	1.1	0.2	0.42
896.6-20	63.90	0.25	18.20	3.33	0.01	0.88	0.49	1.17	6.01	0.52	0.10	1.3	0.2	
900.0-20	70.70	0.22	16.30	0.47	0.01	0.78	1.76	1.99	4.15	0.29	0.08	0.9	0.3	0.36
902.7-20	72.10	0.22	16.30	0.57	0.01	0.67	0.82	1.61	4.71	0.32	0.09	0.7	0.3	0.29
905.5-20	69.10	0.25	18.30	1.58	0.01	1.05	0.40	0.71	5.08	0.18	0.12	1.0	0.4	0.63
909.5-20	37.40	1.36	20.80	18.10	0.01	1.19	0.90	2.11	4.59	0.23	0.25	1.2	0.1	12.10
913.0-20	50.40	0.15	5.08	26.70	0.01	0.15	0.17	0.58	1.07	0.16	0.02	0.6	0.1	18.10
913.9-20	60.20	0.95	18.70	5.28	0.02	0.80	0.88	2.16	4.26	1.19	0.32	1.1	0.2	3.06
917.1-20	67.40	0.24	18.20	1.48	0.01	0.93	1.03	3.30	3.91	0.15	0.11	0.9	0.1	0.72
917.9-20	72.00	0.23	17.00	0.66	0.01	0.62	0.68	2.99	3.68	0.15	0.09	0.7	0.1	0.32
921.2-20	70.10	0.22	16.00	1.68	0.01	0.95	1.44	4.16	2.50	0.20	0.10	0.7	0.1	0.62
924.1-20	69.60	0.23	17.10	1.36	0.01	0.57	0.76	4.08	3.76	0.23	0.10	0.8	0.1	0.61
926.0-20	68.30	0.22	16.30	2.26	0.01	1.22	1.16	3.99	2.93	0.29	0.09	0.8	0.1	1.25
926.2-20	68.40	0.23	16.40	2.00	0.01	0.48	0.64	1.97	5.79	1.22	0.09	0.7	0.1	1.23
928.7-20	56.60	1.00	16.00	2.02	0.01	0.75	0.82	0.99	5.88	8.25	0.40	2.1	0.1	2.93
929.3-20	61.80	0.81	13.30	3.91	0.01	0.33	1.18	1.36	8.33	3.38	0.35	0.2	0.1	3.42
930.3-20	52.30	0.65	10.30	9.56	0.01	0.25	0.60	0.77	7.68	7.59	0.10	0.5	0.1	9.43
930.9-20	35.10	0.54	10.20	17.30	0.06	0.30	0.44	0.84	6.96	9.87	0.16	0.5	0.1	18.98
932.2-20	34.60	0.60	7.67	28.40	0.01	0.14	0.41	0.69	6.14	4.73	0.15	0.7	0.1	21.90
932.5-20	33.60	0.68	9.08	30.20	0.01	0.11	0.55	0.62	7.13	3.55	0.15	0.5	0.1	20.90
934.1-20	69.30	0.25	15.50	1.59	0.01	0.85	1.94	5.18	3.16	0.30	0.10	0.6	0.1	0.07
934.8-20	44.10	0.34	10.20	3.49	0.09	0.24	0.73	1.48	6.82	18.75	0.28	0.2	0.1	7.41
938.3-20	46.90	2.05	28.80	4.35	0.01	0.80	0.66	1.01	8.66	1.15	0.03	1.8	0.1	2.36
940.0-20	50.10	1.65	26.40	3.75	0.01	0.91	0.97	0.91	7.97	0.85	0.25	2.2	0.1	2.91
941.3-2														

INT-HOLE	V ppm	Cr ppm	Co ppm	Ni ppm	Cu ppm	Zn ppm	As ppm	Rb ppm	Sr ppm	Mo ppm	Ag ppm	Sb ppm	Hg ppb	Pb ppm
889.7-14W	101	5	25	3	1	34	8.7	10	235	1190	1.0	8.3	4140	2
890.6-14W	49	10	12	8	20	226	15.3	100	348	34	0.2	29.1	9720	42
891.3-14W	9	10	2	1	1	27	10.9	80	455	1	0.4	2.1	540	13
892.6-14W	22	10	12	11	8	607	17.4	50	585	4	0.2	2.1	4260	30
895.2-14W	25	5	4	1	2	182	17.4	110	245	22	1.0	5.2	2520	21
899.2-14W	9	20	5	1	9	15	4.4	100	565	1	0.1	0.3	300	26
902.6-14W	98	20	19	12	16	90	17.4	110	590	182	0.6	3.1	1320	64
905.4-14W	10	10	1	1	1	1	0.3	70	159	1	0.1	0.3	300	11
908.4-14W	163	30	31	9	15	29	21.8	90	235	3	0.1	2.1	48	14
910.6-14W	171	20	18	2	36	74	45.6	60	535	9	0.1	6.2	1020	53
912.0-14W	34	20	11	12	14	122	21.8	40	1240	230	0.6	4.1	5280	26
913.4-14W	11	10	2	1	1	31	0.3	90	555	1	0.1	2.1	1080	8
916.8-14W	13	10	3	1	1	31	0.3	70	720	1	0.1	0.3	540	11
920.0-14W	17	20	5	3	4	38	13.1	50	490	3	0.1	0.3	420	13
924.2-14W	8	10	6	1	1	51	0.3	100	575	1	0.1	2.1	300	23
927.2-14W	8	10	5	1	1	65	0.3	110	345	1	1.2	2.1	600	23
927.3-14W	725	10	44	29	6	20	50.6	20	325	8380	1.0	23.6	3900	8
929.7-14W	360	30	61	31	18	6	35.6	20	955	555	2.0	25.5	2820	12
929.8-14W	1850	20	150	10	18	85	35.9	30	1440	8130	2.0	33.9	8160	31
930.9-14W	530	5	44	7	8	115	28.1	10	455	6680	2.4	25.5	9180	9
931.8-14W	36	20	9	5	1	60	22.5	120	115	20	0.8	4.1	1620	20
933.1-14W	134	30	19	7	1	41	28.1	160	59	5	0.6	3.1	720	10
936.1-14W	280	5	99	6	81	1280	22.5	60	1890	2510	5.2	45.7	43200	92
937.6-14W	122	10	47	15	12	255	53.4	40	1220	765	0.8	14.5	14760	61
938.3-14W	78	50	15	11	5	66	205.3	60	92	21	0.4	6.2	1320	1
939.1-14W	54	30	14	20	28	45	14.1	130	197	3	0.6	3.1	492	7
942.7-14W	20	20	33	48	12	59	11.3	30	85	30	0.6	0.3	228	7
849.0-20	19	20	4	1	1	11	5.6	50	535	1	0.4	0.3	120	3
850.5-20	13	10	5	1	1	43	28.1	50	545	1	118.0	0.3	252	23
852.4-20	31	20	11	20	16	85	188.9	80	260	1	12.6	14.5	852	95
854.8-20	88	10	15	6	21	98	125.8	100	415	1	0.4	30.0	3480	15
856.1-20	83	10	18	10	24	74	177.9	100	465	1	0.6	33.9	5340	12
857.4-20	230	5	21	3	1	61	64.1	150	265	240	2.2	18.2	5340	13
860.9-20	1340	50	14	39	18	108	180.6	80	44	1250	1.0	39.2	6060	6
861.3-20	1240	40	13	26	19	45	76.5	70	39	1470	3.0	196.4	11520	1
863.0-20	650	30	18	28	58	210	76.5	70	110	10000	6.8	371.3	24900	21
865.9-20	245	5	42	9	60	20	45.9	60	425	450	3.2	56.2	6720	27
868.0-20	695	30	24	35	8	32	113.5	10	76	145	1.0	23.6	2700	1
869.5-20	23	20	9	6	1	50	58.4	40	910	3	0.4	14.5	2160	10
871.9-20	1060	5	27	6	20	4	79.6	10	670	2260	1.8	47.1	5580	2
872.9-20	235	5	39	4	15	16	48.4	60	290	295	2.0	29.1	12960	9
873.7-20	780	50	6	21	19	7	235.5	10	23	1250	2.0	126.0	16740	1
874.5-20	320	30	14	17	27	11	161.4	50	63	740	2.4	234.1	24660	1
874.9-20	685	5	24	8	8	24	53.4	20	250	7360	1.4	84.9	11400	1
875.9-20	275	5	28	5	3	19	64.1	20	350	1850	200.0	96.6	19620	2
876.5-20	845	10	53	28	16	200	183.4	90	220	1160	1.4	349.7	70560	7
877.6-20	810	20	33	17	21	30	531.4	60	163	1600	1.0	645.6	44340	6
878.2-20	105	10	23	16	14	9	2022.9	80	73	365	1.4	807.1	63120	1
879.6-20	2830	50	56	45	24	8	394.2	10	285	8660	2.0	582.4	27840	3
882.8-20	78	5	27	4	5	1	58.4	30	290	700	2.4	66.7	14760	12
884.1-20	470	5	40	3	8	18	816.0	30	240	1450	1.0	81.9	15540	28
884.8-20	275	5	41	18	9	790	282.2	30	170	1900	0.6	277.1	55260	13
885.6-20	1310	5	39	10	8	122	138.2	20	335	3670	0.4	130.4	22140	6
887.0-20	200	5	33	17	4	102	238.3	10	220	785	0.1	62.8	8340	4
887.8-20	29	5	28	20	1	405	38.4	20	255	590	0.8	7.2	17100	7
888.1-20	189	5	131	26	890	115	271.2	10	1210	1460	48.0	1119.3	456000	88
888.9-20	960	40	47	42	16	1220	421.6	60	285	1190	1.6	4.1	31500	14
891.5-20	111	5	27	13	33	700	88.8	10	175	2280	2.0	65.4	24420	18
893.0-20	161	10	57	24	2	700	48.4	90	420	205	0.6	23.6	6780	50
894.3-20	11	5	6	1	1	23	25.3	100	117	2	0.1	2.1	840	375
896.3-20	15	5	5	1	1	88	25.3	100	85	2	0.4	3.1	684	140
896.6-20	15	10	7	1	1	181	30.9	110	270	1	0.1	4.1	588	58
900.0-20	13	10	4	1	1	9	5.6	90	250	1	0.1	2.1	300	155
902.7-20	11	10	5	1	1	26	0.3	100	190	1	0.1	0.3	324	16
905.5-20	12	20	3	1	1	29	11.3	110	118	1	0.4	0.3	120	13
909.5-20	188	30	49	6	12	63	88.8	130	197	6	0.4	6.2	768	23
913.0-20	16	30	7	22	20	128	53.4	50	107	11	0.4	8.3	348	30
913.9-20	153	130	43	72	8	62	27.3	100	166	27	0.6	6.2	1200	16
917.1-20	12	10	6	1	1	33		110	205	1	0.4			18
917.9-20	7	10	4	1	1	23	0.3	80	192	1	0.4	0.3	120	13
921.2-20	8	10	5	1	1	22	0.3	90	365	1	0.1	0.3	180	12
924.1-20	9	10	5	4	1	19	0.3	70	300	1	0.4	0.3	20	13
926.0-20	12	10	7	1	1	25	0.3	50	230	1	0.4	0.3	480	10
926.2-20	13	10	10	1	1	29	0.3	100	315	1	0.1	0.3	420	15
928.7-20	170	10	59	10	1	30	11.3	90	815	4	0.1	0.3	240	12
929.3-20	121	10	30	7	17	14	22.5	110	320	200	1.0	18.2	2640	23
930.3-20	610	10	53	17	34	1570	22.5	90	385	3290	5.0	21.8	27720	42
930.9-20	230	5	49	7	11	8	33.4	80	365	695	1.4	4.1	2520	28
932.2-20	60	10	18	5	11	36	116.6	10	141	295	1.4	3.1	1320	20
932.5-20	57	20	16	2	27	250	101.1	40	134	350	0.8	4.1	3120	4
934.1-20	10	10	6	1	1	47	5.6	70	765	1	0.1	2.1	540	53
934.8-20	179	5	67	6	5	22	16.9	80	610	740	0.6	4.1	660	28
938.3-20	200	20	48	8	32	48	11.3	140	80	16	0.1	3.1	3000	11
940.0-20	475	30	47	12	2	37	14.1	150	44	430	0.6	2.1	2220	20
941.3-20	43	5	8	1	1	21	0.3	130	71	59	0.4	0.3	960	21
942.3-20	146	20	59	12	1	8	5.6	40	179	425	0.6	2.1	1200	6
943.4-20	159	20	5	1	1	3	0.3	50	300	168	0.4	0.3	420	4
944.4-20	17	10	5	5	1	1	8.4	70	66	32	0.4	0.3	780	2
946.2-20	193	20	8	15	1	12	11.3	70	123	6500	1.4	3.1	2340	12
948.2-20	33	30	22	10	1	4	5.6	90	146	80	0.1	2.1	600	7
951.8-20	17	20	26	36	2	1	28.1	100	142	125	0.4	2.1	600	1

OXIDE/ELEMENT	ANALYTICAL METHOD	DETECTION LIMIT
SiO ₂ %	XRF	N/A
TiO ₂ %	XRF	N/A
Al ₂ O ₃ %	XRF	N/A
Fe ₂ O ₃ %	XRF	N/A
MnO%	XRF	N/A
MgO%	XRF	N/A
CaO%	XRF	N/A
Na ₂ O%	XRF	N/A
K ₂ O%	XRF	N/A
BaO%	XRF	N/A
P ₂ O ₅ %	XRF	N/A
H ₂ O%	WET CHEMICAL	0.2
CO ₂ %	LECO FURNACE	0.2
S%	LECO FURNACE	0.02
V ppm	EMISSION-ICP	2
Cr ppm	XRF	10
Co ppm	EMISSION-ICP	1
Ni ppm	EMISSION-ICP	1
Cu ppm	EMISSION-ICP	1
Zn ppm	EMISSION-ICP	1
As ppm	HYDRIDE-AAS	0.5
Rb ppm	XRF	10
Sr ppm	EMISSION-ICP	N/A
Mo ppm	EMISSION-ICP	1
Ag ppm	AAS	0.1
Sb ppm	HYDRIDE-AAS	0.5
Hg ppb	HYDRIDE-AAS	40
Pb ppm	EMISSION-ICP	1

ABBREVIATIONS:
XRF X-ray Fluorescence Spectrometry
ICP Inductively-coupled Plasma Spectrometry
AAS Atomic Absorption Spectrometry

NOTES:
In the table, all values below the detection limit are shown as 0.5 x detection limit.